

# **The Joint Probability of Waves and Water Levels: JOIN-SEA**

**A rigorous but practical new  
approach**

**Report SR 537  
November 1998**

**(Re-issued with minor amendments May 2000)**

**LANCASTER  
UNIVERSITY**



# **The Joint Probability of Waves and Water Levels: JOIN-SEA**

**A rigorous but practical new approach**

**Report SR 537  
November 1998**

**(Re-issued with minor amendments May 2000)**



**Address and Registered Office: HR Wallingford Ltd. Howbery Park, Wallingford, OXON OX10 8BA  
Tel: +44 (0) 1491 835381 Fax: +44 (0) 1491 832233**

**Registered in England No. 2582099. HR Wallingford is a wholly owned subsidiary of HR Wallingford Group Ltd.**



## Contract

This report describes work funded by the Ministry of Agriculture, Fisheries and Food under Commission FD0202 (predicting waves at or near the coastline). Publication implies no endorsement by the Ministry of Agriculture, Fisheries and Food of the report's conclusions or recommendations.

The HR Wallingford Job Number was CCS14W. The work at HR Wallingford was carried out by Dr Peter Hawkes, Mr Ben Gouldby and Mr Andy Yarde. The work at Lancaster University was carried out by Prof Jonathan Tawn and Miss Paola Bortot. Mr Michael Owen was chairman of the advisory group for the project. The Project Manager was Dr Hawkes. The Ministry's Nominated Project Officer was originally Mr A C Polson, and then Mr J R Goudie. HR's Nominated Project Officer was Dr S W Huntington.

Prepared by Peter J. Hawkes  
.....  
(name)

Project Manager  
.....  
(Title)

Approved by KAPowell  
.....  
(name)

Director  
.....  
(Title)

Date 10 May 2000  
.....

© Ministry of Agriculture, Fisheries and Food, Copyright 2000



# Summary

The Joint Probability of Waves and Water Levels: JOIN-SEA

A rigorous but practical new approach

Report SR 537

November 1998

(Re-issued with minor amendments May 2000)

A common application of joint probability in coastal engineering is to the simultaneous occurrence of a large wave height and a high still water level, and its consequent effect on sea defences. If two or more variables are either completely independent or completely dependent, then the joint probability calculations are relatively easy: however, this is rarely a good approximation in practice. In the past, the fitting and extrapolation of the dependence function between large wave heights and high water levels has involved complicated and/or subjective approaches unsuitable for use by non-specialists.

We present a new approach to the joint probability of large wave heights and high water levels which:

- removes most of the subjectivity from the present methods;
- allows the distribution of wave period to be included in calculations, by treating wave steepness as a third variable partially dependent upon wave height;
- allows long-term simulation of the combined wave height, wave period and water level variables, in turn allowing more accurate calculation of the effects on sea defences.

This research was funded by the Ministry of Agriculture, Fisheries and Food, and was undertaken jointly by HR Wallingford and Lancaster University. The first part of the report, written by HR Wallingford, summarises the new developments and their range of applicability, and tests them against a number of field data sets. The second and longer part, written by Lancaster University, gives full technical details of the new methods and a more rigorous comparison of alternative approaches based on synthetic sea state data. A shorter companion report (HR, 2000) is intended for day-to-day application as a user manual for the associated JOIN-SEA joint probability software. A paper on the development and testing of the new methods was presented at the MAFF Conference of River and Coastal Engineers (Owen, 1997).

## Availability of programs and reports

In principle, the methods, reports and programs are freely available, since they were developed entirely with MAFF funding. However, adoption of the methods and programs requires some familiarity with numerical modelling and joint probability methods, and there are costs in terms of training, follow-up advice, software library licences and copying of documentation (and of course the time series wave and water level data required as input). MAFF funded an initial

## ***Summary continued***

distribution of the programs to industry specialists for beta-testing, in the form of a briefing workshop in February 2000, at which the issues relating to dissemination were clarified.

For further information on this report and the associated computer programs please contact Dr Peter Hawkes of the Coastal Department at HR Wallingford.

# Contents

<i>Title page</i>	<i>i</i>
<i>Contract</i>	<i>iii</i>
<i>Summary</i>	<i>v</i>
<i>Contents</i>	<i>vii</i>

## Part I HR Wallingford Report

1.	Introduction .....	1
1.1	Background.....	1
1.2	Definitions used in joint probability analysis .....	2
1.3	Dependence .....	3
1.4	Review of alternative methods .....	5
1.5	Outline of the new method .....	7
1.6	Research outputs.....	7
2.	The new approach.....	8
2.1	Input data requirements .....	8
2.2	Fitting of statistical distributions to the marginal variables.....	9
2.3	Statistical models for dependence .....	10
2.4	Long-term simulation .....	10
2.5	Analysis of joint exceedance extremes and structural response functions .....	11
2.6	Software implementation.....	11
3.	Applications.....	12
3.1	Example applications to synthetic data.....	13
3.2	Case studies using field data.....	16
3.3	Example application using both inshore and offshore wave data	20
3.4	Issues raised during analysis of other data sets.....	24
4.	Discussion.....	26
4.1	Past practice for use of results in design.....	26
4.2	Advantages of the new approach .....	27
4.3	New possibilities based on long-term simulation .....	28
4.4	Recommended options for joint probability analysis .....	29
4.5	Performance of the various techniques.....	31
4.6	Availability of methods and staff time involved .....	33
4.7	Future developments.....	34
5.	References .....	35

### Tables

Table 1	Direct hindcasting and extrapolation of overtopping rate, applied to data set Sim1 .....	15
Table 2	Direct hindcasting and extrapolation of overtopping rate, applied to data set Sim2 .....	15
Table 3	Direct hindcasting and extrapolation of overtopping rate, applied to data set Sim3 .....	16
Table 4	Direct hindcasting and extrapolation of overtopping rate, applied to data set Sim4 .....	16

## Contents continued

Table 5	Direct hindcasting and extrapolation of overtopping rate, applied to data set Sim5 .....	16
Table 6	Comparison between overtopping rates ( $m^3/s/m$ ) for different analysis methods at Christchurch .....	18
Table 7	Comparison between overtopping rates ( $m^3/s/m$ ) for different analysis methods at Dover.....	18
Table 8	Comparison between overtopping rates ( $m^3/s/m$ ) for different analysis methods at Dowsing .....	19
Table 9	Comparison between overtopping rates ( $m^3/s/m$ ) for different analysis methods at Cardiff (0-190°N) .....	19
Table 10	Comparison between overtopping rates ( $m^3/s/m$ ) for different analysis methods at Cardiff (190-360°N) .....	19
Table 11	Comparison between overtopping rates ( $m^3/s/m$ ) for different analysis methods at North Wales.....	20
Table 12	100 year overtopping rates ( $m^3/s/m$ ) for Somerset (no limit on wave steepness).....	22
Table 13	100 year armour size (m) for Somerset (no limit on wave steepness).....	22
Table 14	Overtopping rates ( $m^3/s/m$ ) for Somerset (minimum wave steepness of 0.020) .....	23

### Figures

Figure 1	Joint exceedance and joint structural probabilities .....	3
Figure 2	Probability density contours showing negative dependence between surge and wave height (off Hythe) .....	4
Figure 3	Probability density contours showing positive dependence between surge and wave height (Christchurch Bay).....	5
Figure 4	Joint exceedance contours of $H_s$ (m) and water level (mOD) for a site with very low dependence.....	13
Figure 5	Joint exceedance contours of $H_s$ (m) and water level (mCD) for a site with high dependence .....	14

### Appendices

Appendix 1	Comparisons between joint exceedance extremes for different analysis methods	
------------	--	--

## Part II Lancaster University Report

# ***Part I HR Wallingford Report***



# 1. INTRODUCTION

## 1.1 Background

### Meaning of joint probability

Joint probability typically refers to two or more partially related environmental variables occurring simultaneously to produce a response of interest. Examples are:

- large wave heights and high water levels;
- large river flows and high sea levels;
- large surges and high astronomical tidal levels.

### Importance of joint probability

Damage to sea defences is often associated with times when large wave heights and high water levels occur simultaneously, even if neither one is exceptional in its own right: hence it is necessary to estimate their joint probability. There are a range of techniques available: from an intelligent choice of a single water level to use with established wave conditions, to a rigorous joint probability assessment using long time series data; from a general offshore study which might be valid over a wide area, to a site-specific prediction of overtopping volumes. MAFF has been funding research on this topic for several years (HR, 1994; Coles and Tawn, 1994; POL, 1997) and is increasingly expecting the results to be applied in scheme assessment.

### Prediction of joint probability

Compared with other types of oceanographic variable, there is a large volume of high quality tide data around the UK. This, together with the fact that spatial variations in tide are smooth in some areas such as the east coast of Britain, means that extreme water levels can be predicted quite reliably for much of the UK. Conversely, the lack of long-term wave measurements in many cases, and the variability of wave conditions in coastal waters, mean that prediction of extreme wave conditions is more difficult and uncertain. Meanwhile, estimates of the level of service of UK coastal defences can be nearly as sensitive to uncertainties about the dependence between large waves and high water levels as they are to uncertainties about extreme wave heights. HR (1994) includes an example calculation for a location with a small positive dependence between waves and water levels, and deep water at the structure toe. The assumption of complete dependence between wave heights and water levels could lead to a sea wall crest level up to two metres too high. Conversely, the assumption of independence could lead to a crest level half a metre or so too low. It therefore seems reasonable to put about the same amount of effort into assessing this dependence as into assessing wave conditions.

### The Start-up Workshop

In August 1994, MAFF hosted a Workshop on joint probability (MAFF, 1995) at which Messrs Hawkes, Owen and Tawn presented their own preferred approaches. As a result of the Workshop, MAFF agreed to fund a two-year joint research project at HR Wallingford and Lancaster University. The intention was to combine the best of the existing methods, and to develop, test and eventually disseminate a rigorous and practical approach to the joint probability of large wave heights and high water levels.

### The present project

MAFF provided funding for the development and testing of new joint probability methods from April 1995 to March 1997, although in practice development continued until September 1998. Most of the development and validation of the methods and computer programs was carried out at Lancaster University, but the process continued when program code was transferred to HR Wallingford in April 1996. In principle, the computer programs and reports are freely available, since they were developed entirely with MAFF funding. However, in practice there are additional costs associated with training, follow-up advice, NAG licences and copying of documentation.

## 1.2 Definitions used in joint probability analysis

### Marginal probability and return period

Marginal probability refers to the distribution of a single variable, for example wave height or water level. Return period refers to the average period of time between occurrences of a particular high value of that variable. So, for example the 100 year return period still water level is the level equalled or exceeded once, on average, in each period of 100 years.

### Record interval and event duration

Usually, in the context of sea defences, only conditions at high water are of interest, and typically peak surges and wave conditions persist for less than half a day. Therefore, each high water (706 per year) can conveniently be taken as an independent 'record', which is assumed to persist over the duration of high water. Therefore, 1 year and 100 year return period 'events', for example, have probabilities of occurrence of  $1/706$  and  $1/(100 \times 706)$  and are assumed to persist over the duration of high water.

### Joint structural probability and return period

Joint probability refers to the chance of two or more partially related variables ( $x, y$ ) occurring simultaneously. The joint *structural* probability refers to the occurrence of a particular response (such as overtopping) which in turn depends on the joint occurrence of those variables. The blue and red curves in Figure 1 illustrate the typical shape of contours of equal response, with the shaded areas above the curves indicating the outcomes which give occurrence of the two responses. Different types of response may occupy different parts of the wave and water level distribution. In this example, the equal overtopping curve lies towards the bottom right of the diagram where the water level is higher, whilst the equal force curve lies towards the top left where the wave height is higher. If the response value(s) is/are chosen to correspond to structural failure, then the probability (or risk) of failure is obtained by summing the probabilities of all the outcomes of the response which give structural failure, i.e. summing the probabilities of  $(x = x_0, y = y_0)$  for all  $(x_0, y_0)$  in the appropriate shaded region. Therefore, in determining probabilities of structural failure in this way it is necessary to estimate the joint probability density  $(x = x_0, y = y_0)$  for extreme values of  $(x_0, y_0)$  for the two variables. This may be either in the form of an extrapolated probability distribution or a long-term simulation.

### Joint exceedance probability and return period

Joint exceedance probability combinations of wave heights and water levels with a given chance of occurrence are defined in terms of sea conditions in which a given wave height is exceeded at the same time as a given water level being exceeded ( $x > x_0$  and  $y > y_0$ ). The black curve in Figure 1 illustrates a contour of equal joint exceedance probability for wave heights and water levels, with the brown points indicating particular examples which might be tested in design. The green and yellow areas illustrate ranges of wave height and water level with the given joint exceedance probability. These areas, and the probability they represent, provide an approximation to the red and blue failure regions shown in Figure 1 and the probabilities they represent.

### The discrepancy between joint exceedance and joint structural probabilities

In current practice, a number of combinations of waves and water levels are derived with a given joint exceedance return period (these are represented by the brown dots in Figure 1). Only one of these will be a worst case in terms of structural response, and it may not be the same one for each response (these 'worst cases' are represented by ringed brown dots in Figure 1). The probability of occurrence of the structural response function (eg overtopping or force) calculated from the worst case combination of wave height and water level will be higher than the joint exceedance probability. In other words, joint exceedance return period sea conditions will tend to under-predict responses if the responses are assumed to have the same return period. This is because the same structural response function value might be obtained by other sea conditions in which only one or other of wave height and water level takes a very high value. This is illustrated in Figure 1 by the difference between the green and red areas and between the blue and yellow areas. In current practice, a small margin of safety is added to the joint exceedance probability predictions to try to offset this discrepancy with the return period of the response. The new method, conversely, works in terms of the joint

probability *density* of the two variables and calculates the return periods of the structural response function(s) (where known).

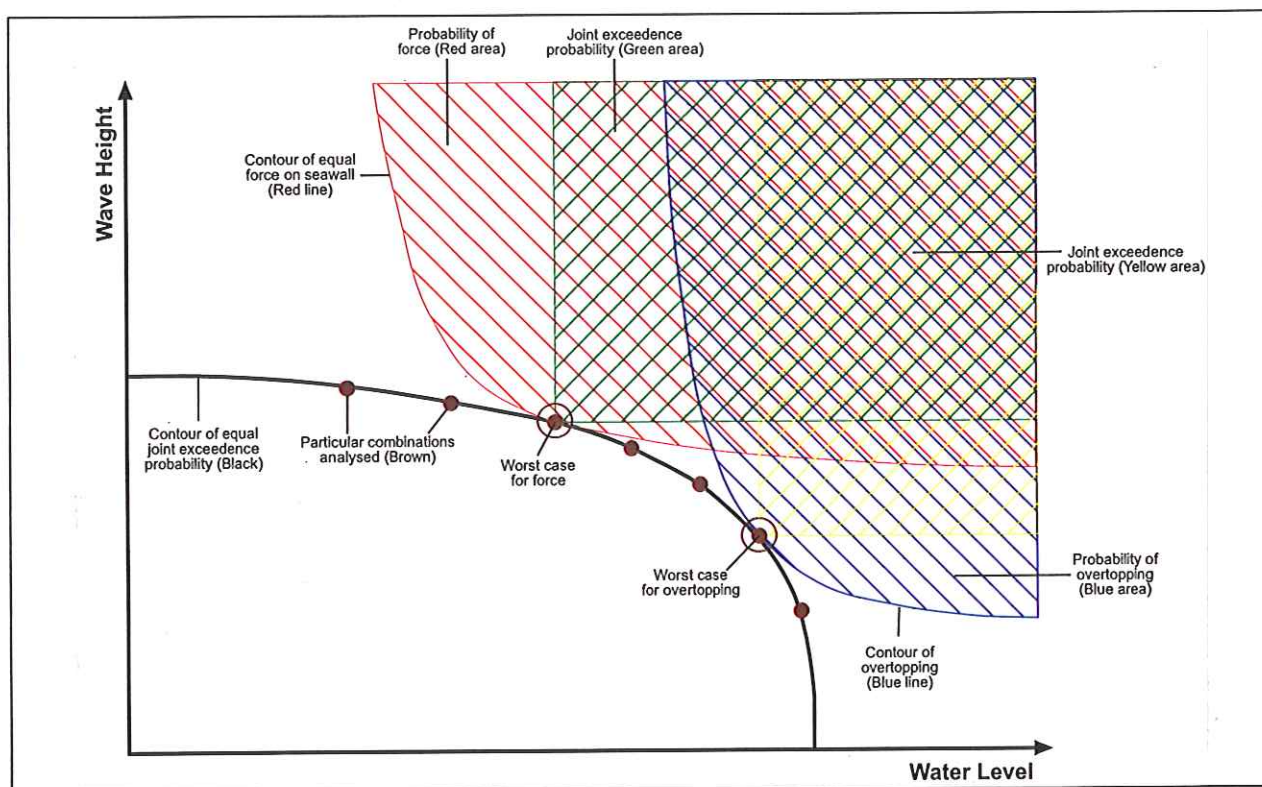


Figure 1 Joint exceedance and joint structural probabilities

### 1.3 Dependence

#### Simple example of independence

A simple example of two independent variables contributing to produce a combined result is the overall total score recorded by independently throwing a pair of dice. The chance of one die scoring four or more is  $\frac{1}{2}$ . The joint exceedance probability of both dice scoring four or more is the product of the two marginal probabilities, i.e.  $\frac{1}{2} \times \frac{1}{2} = \frac{1}{4}$ . However, this calculation does not represent the overall 'risk' (or joint structural probability) of scoring eight or more since it excludes the additional 5&3, 6&2 and 6&3 combinations, so the probability of scoring eight or more is  $\frac{1}{4} + \frac{6}{36} = \frac{15}{36}$ .

#### Simple example of complete dependence

A simple example of two fully dependent variables is two dice fixed together, such that if one shows a six then the other will also show a six. The probabilities of a six on one die, a six on the other die and a combined total of twelve, are all equal. In this case the only possible outcomes which give a total score of eight or more are (4, 4), (5, 5) and (6, 6), each with probability  $\frac{1}{6}$ , so the probability of this event is  $\frac{1}{2}$ . A similar hypothetical situation in coastal engineering might be where the only time that very high waves and very high water levels occur is during rare hurricane events, where high values of each variable always occur together.

#### Degree of dependence between waves and water levels

In reality, wave heights and surges are usually partially dependent (since both are related to the local weather conditions) to an extent which depends on a number of factors. It is possible to estimate the degree of dependence based on judgement and on previous studies in the same area, and it may ultimately be possible to produce design guidelines, but at present the dependence is best determined using simultaneous data on the two variables. For example, on the east coast of Britain, strong northerly winds will produce both surges and high waves. There are some locations (eg Dover) where surges are associated with winds from one direction (south-west at Dover), whilst the highest waves are associated with winds from a different direction (south and

south-east at Dover). In this situation there may be a very low or even negative dependence between high surges and large wave heights. However, this dependence (which may not be particularly high to begin with) is masked in consideration of wave heights and *total* water levels, because the astronomical tidal component is unrelated to the weather conditions. This leads to the bulk of wave and water level data being very modestly dependent (and perhaps suggests a future approach in which the dependence between waves and *surges* is assessed and extrapolated, before adding in deterministic tides). However, the most extreme conditions (usually including a high surge component) will tend to be more dependent, particularly where the surge to tide ratio is larger.

Scatter diagrams to illustrate the degree of dependence

An easy way of demonstrating the approximate degree of dependence between two variables is by means of a scatter plot. Many pairs of values of Variables A and B are shown as points on a diagram which has Variable A on its x-axis and Variable B on its y-axis. Well scattered points are indicative of low dependence. Points lying approximately on a line with a positive slope are indicative of a strong positive dependence. Points lying approximately on a line with a negative slope are indicative of a strong negative dependence. In the case of waves and water levels, any dependence is usually modest and typically shows itself as a slight upward (or occasionally downward) trend in the scatter. To illustrate the idea and to emphasise the dependence, Figures 2 and 3 are scatter diagrams of wave height against *surge*. Figure 2 contains data for a site demonstrating negative dependence between wave height and surge, whilst Figure 3 shows data for a site with positive dependence. Different types of dependence and degrees of correlation are also illustrated in Section 3.3.1 of the Lancaster University part of this report.

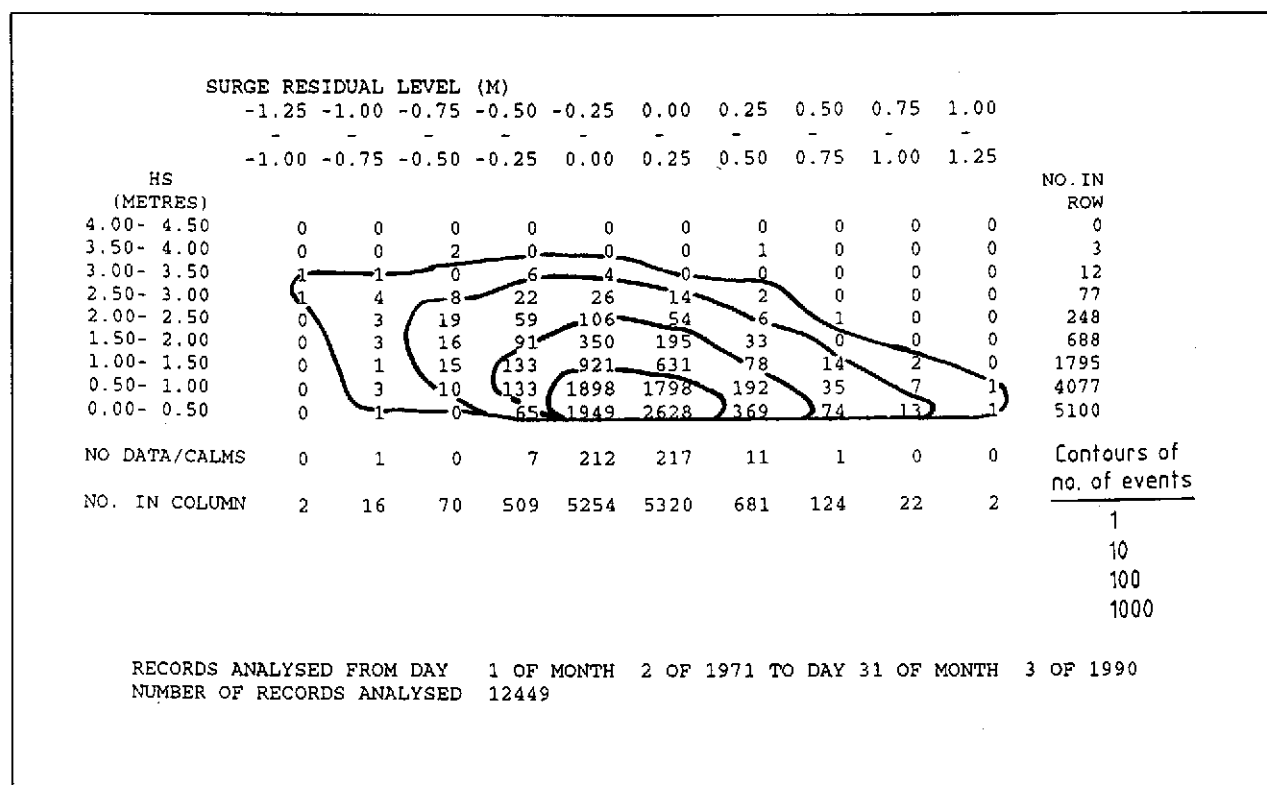


**Figure 2 Probability density contours showing negative dependence between surge and wave height (off Hythe)**

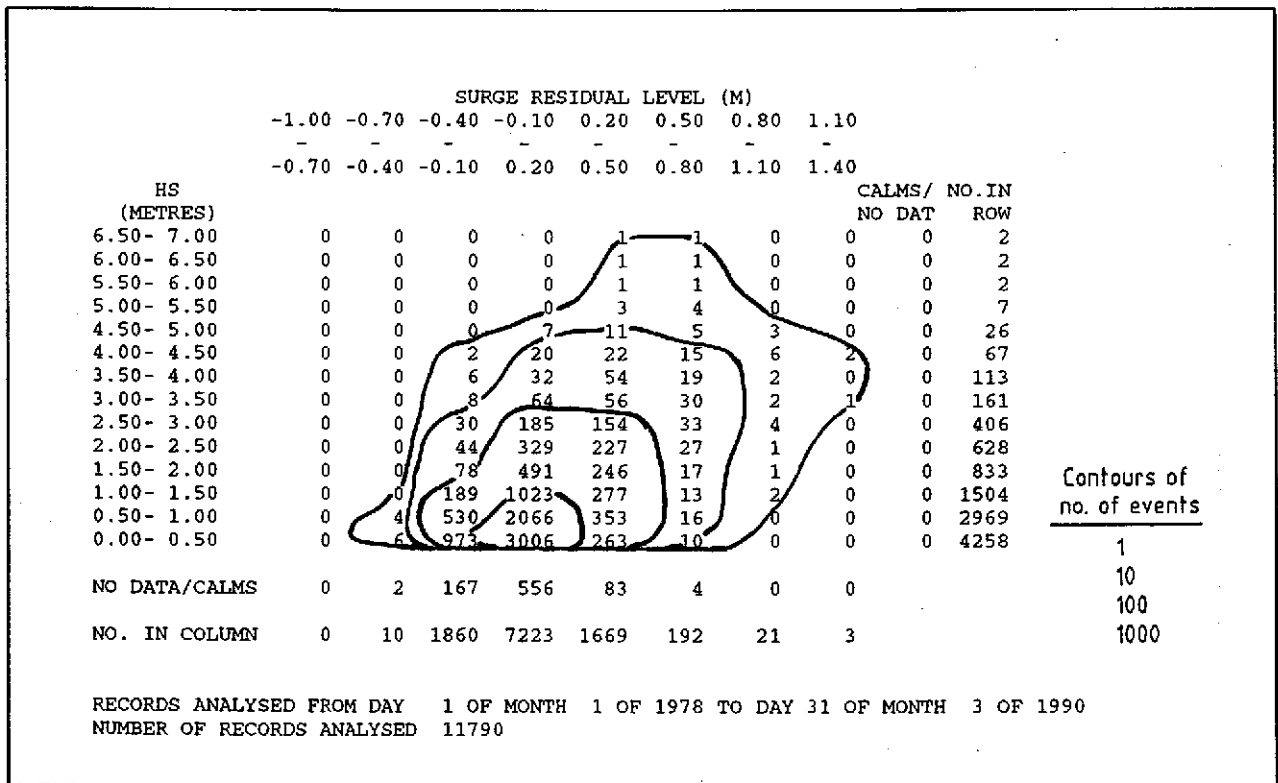


**Figure 3 Probability density contours showing positive dependence between surge and wave height (Christchurch Bay)**

### 1.4 Review of alternative methods

#### Scope of the review

There are several joint probability analysis methods available, depending upon time, budget and amount of field data available, and upon the end purpose of the calculations. Even when it is not considered explicitly, and the structural response is primarily dependent upon the incident wave conditions, a representative high water level will often be required for calculations. In principle, any number of partially dependent variables can be analysed, although in practice both the calculations and the results become too unwieldy when more than three are used. There are several methods of presenting the results, depending upon the end purpose and the end user. Most of the assessment methods are compatible with most of the presentation methods. A more detailed review and testing of the earlier methods is given in HR (1994).

#### Independent and dependent cases

The dependent case is trivial, assuming that the statistics of waves alone and of water levels alone are known, since one only has to combine waves and water levels each with the same marginal probabilities as the response. The independent case is easy when working with joint exceedance probability (which provides an approximation to the response with the same probability) as it is just the product of the two marginal probabilities. As the independent and dependent cases are simple to calculate, it may be worth deriving them early in any project. Treating these as the 'most optimistic' and 'most pessimistic' scenarios, respectively, may help in judging the value of any more detailed joint probability analysis.

#### Intuitive joint probability assessment

The simplest method for assessment of dependence is an intuitive one based on general experience and the shape and size of the sea area around the prediction point. The assessment may conclude that there is a modest dependence, and for example, that high waves and high water levels with a 100 year joint exceedance return period are 10 to 100 times more likely to occur together than the assumption of independence would suggest. It may conclude that there is a strong dependence, and for example, that high waves and high water levels with a 100 year joint exceedance return period are only 10 to 100 times less likely to occur than the assumption of dependence would suggest. (The probability ratio between the independent and dependent

cases is 706 x 100.) This is the basis of a joint probability method described in the *Beach management manual* (CIRIA, 1996, Section 3.5.3).

#### Full analysis of dependence and joint probabilities

A better approach, if constraints on time, budget and data permit, is to examine several years of simultaneous wave and water level data in order to assess dependence and to derive joint probability extremes. This allows the analysis to be performed in a similar objective scientific manner to that which would be applied to the separate wave and water level predictions. The dependence is determined by analysis of pairs of values of wave height and water level at each high water over a period of several years. Before JOIN-SEA became available, extremes were determined by extrapolating wave heights for successively rarer water levels, and water levels for successively rarer wave heights. By combining these extrapolations, contours were constructed joining combinations of wave height and water level with equal joint exceedance return periods. The normal way of incorporating wave direction was to undertake a series of 'conditional' analyses, one for each direction sector of interest. The normal way of incorporating wave period was to assume that it is completely dependent upon wave height, and could be determined from an assumed wave steepness.

#### Extrapolation of joint probability density

Joint probability density can be visualised as a three-dimensional histogram, in which the vertical axis shows the likelihood of occurrence of combinations of the variables shown on the two horizontal axes. If a bi-variate probability distribution model can be fitted to the observed joint density, then the fitted distribution can be extrapolated to extremes. In the past, the main difficulty with this approach was in representation of the dependence between the variables in the fitted distribution (although as stated earlier, the independent and dependent cases would be trivial). An alternative way of calculating extreme densities, which has been used in the past, involves numerical differentiation between previously calculated contours of joint exceedance return period (see previous paragraph). Extrapolation of probability density is perhaps the most flexible method for presentation of extremes predictions, and permits a direct estimation of the probability of a given response or structure variable such as failure due to high overtopping. This concept is a fundamental aspect of the JOIN-SEA method.

#### Direct hindcasting of design variables

An alternative approach can be used where a very specific local result is required, for example, run-up or overtopping of a particular short stretch of sea defence. Site-specific shallow water wave data directly at the point of interest, together with sequential water level data, could be used in a site-specific run-up or overtopping formula to hindcast long-term run-up or overtopping conditions. The resulting single variable data could then be extrapolated directly to extremes, avoiding the complications of a true joint probability approach in which waves and water levels are kept separate throughout. This single variable approach has the advantage of using all the available information on individual wave conditions, for example including the wave period, which is important for run-up and overtopping. However, it relies on the extrapolated variable being of the same form as within the body of the distribution. It would not be applicable, for example, where wave overtopping is expected to give way to weir overtopping or to structural failure at higher levels. The advantages of this approach are available within the JOIN-SEA analysis method, with the added advantage that it can be applied to a long-term simulation of wave and water level data.

#### Offshore and inshore extremes

Joint probability extremes can be calculated and presented either offshore or inshore. Offshore results are more generally applicable over a larger area, but may need to be transformed inshore before further use. Inshore results are more site-specific, and can take better account of any hydraulic interactions, but may be applicable only in one small area. Wave predictions and joint probabilities are often calculated as a function of direction. This is important, since general exposure to waves, the relationship between high waves and high water levels, and transformation inshore, may all be dependent upon storm direction.

#### Depth-limited conditions

In coastal engineering applications, wave heights may be depth-limited. For example, there may be only a few metres of water at the toe of a structure even in extreme conditions, so that the full force of the waves

may not impact directly upon the structure. In extreme cases of these circumstances, only the highest water levels need to be considered. A possible general approach for depth limitation is to determine the extreme water levels, and then to check the probability that the depth-limited wave height could occur at the same time. However, it is worth noting in this situation that swell waves, which do not usually have the largest wave heights, may be a worse case for structural design than depth limited wind waves.

#### Presentation of results

Joint exceedance results are normally calculated and presented as 'contours' of combinations of wave heights and water levels with given joint exceedance return periods, from which a 'worst case' can be determined as and when required for any particular situation. The same information might be shown in the form of a table of pairs of values of wave height and water level (drawn from the 'contours'). This approach would allow the 'worst case' to be identified in terms of run-up (or other design variables) at the site of interest, but usually requires that several potential 'worst cases' be tested. Alternatively, results can be presented as extrapolated probability densities, in which 'contours' indicate the likelihood of occurrence of particular combinations of wave heights and water levels. This approach is useful for risk analysis, where the total risk is found by integrating probabilities over a wide range of wave conditions and water levels in which 'failure' may occur. Either results format can be converted to other relevant variables, for example run-up, overtopping or force on a coastal structure. Please note that although the joint density approach can provide a direct estimation of the return period of *the response*, the joint exceedance extremes contours can provide only an approximation to this probability.

### **1.5 Outline of the new method**

#### Main elements

The new method consists of the five main elements listed below and described in more detail in Sections 2.1-2.5.

1. Preparation of input data, consisting of many independent records of wave height, wave period and water level.
2. Fitting of statistical distributions separately to the wave heights, the water levels and the wave steepnesses.
3. Fitting the dependence between wave heights and water levels, and between wave heights and steepnesses.
4. Simulation of a large sample of wave height, wave period and water level data, using the fitted distributions.
5. Extremes analysis of a range of response variables based on the simulated data.

#### Main developments

The main developments of the new method and its applications are in elements 2 to 5. It is more objective, particularly in its modelling of dependence, than most existing approaches to joint probability assessment, and allows wave period (or wave steepness) to be included as a variable. With careful use its *long-term simulation* approach can deliver more accurate predictions of joint extreme values and structural response function values (eg overtopping, run-up, force) than methods already in common use. It will also assist in a gradual move towards risk-based design of sea defences.

### **1.6 Research outputs**

#### Products

There are three main types of output from this research project, namely reports, computer programs and workshops, plus of course improved joint probability analysis in consultancy studies.

### JOIN-SEA software

The software consists of FORTRAN computer programs, incorporating numerical statistical subroutines (in NAG). The programs are research-based and have not been tested to normal commercial standards, but are available, initially on a trial basis, to appropriate users.

### JOIN-SEA reports

The first part of this document gives a brief description of the new approach and its application in coastal engineering. The accompanying statistical methodology and further case studies are given in the technical report which forms the second part of this document. A companion user manual (HR, 2000) describing inputs, outputs and options available to the user is intended for day-to-day use with the new programs.

### Workshops and dissemination

A specialist workshop was held at HR Wallingford on 3 December 1998, at which this report and the associated user manual were released in draft form. The workshop was attended by those directly involved in the research and by a number of invited coastal engineers familiar with joint probability applications. It was hoped that the workshop discussion would guide future dissemination, usage and continued development of joint probability methods, and ultimately MAFF policy in regard to their use. A subsequent briefing workshop was held at HR Wallingford on 4 February 2000. This was attended by about a dozen industry specialists interested in receiving copies of the programs and training in their use. It is hoped that the subsequent beta-testing programme will yield useful feedback on continued development and usage of the methods.

## **2. THE NEW APPROACH**

### **2.1 Input data requirements**

#### Preparation of the input data

The first of the five stages involves preparation of the input data. Generation and pre-processing of the input wave and water level data is probably the most time-consuming part of the joint probability analysis procedure. Each input record consists of a wave height, a wave period and a water level (or alternatively a surge) preferably using identical measurement or prediction locations for both waves and water levels. The data can come from measurements or hindcasts, but for each record the values should represent conditions at a particular point and time. A convenient way of satisfying the requirement for the records to be both temporally independent, and relevant, is to use only those records representing conditions at the peak of each tidal cycle (ie one record every 12 or 13 hours). At least three years of data, not necessarily continuous but representative of the type of sea states of interest, are needed to justify the effort involved in applying the new approach.

#### Stages in data pre-processing

Typically the following pre-processing of the data would be carried out:

- combining of the separate wave and water level data into a single sequential data file;
- extraction and retention of only one record, closest to high water, per tidal cycle;
- optionally, division of the data into two or three separate populations (data sets) corresponding (for example) to different wave direction sectors or seasons, or to wind-sea and swell;
- removal of
  - obviously faulty data, and
  - (optionally) records with zero wave height and records with very low wave steepness (although both of these are automatically trapped by the programs since they cause problems in the later analysis and long-term simulation of wave steepness);

- running of the preliminary diagnostic program *TESTDATA* to assess the type of dependence and whether independence or dependence would be adequate assumptions.

### The *TESTDATA* diagnostic program

It is assumed that users will make their own arrangements for any pre-processing considered necessary: in terms of the computer programs required, only the *TESTDATA* program forms part of the JOIN-SEA package. The purpose of this program, which can be run immediately before the joint probability analysis, is to provide guidance on the degree of dependence within the data, and whether it changes with exceedance threshold. For example, it may indicate that complete dependence or complete independence would be a reasonable assumption, or that dependence needs to be modelled carefully. The test statistic,  $T(z)$ , is derived from the conditional probability of the second variable exceeding the marginal  $T$  year level for that variable given that the first variable exceeds its own marginal  $T$  year return level. Here  $z$  is related to  $T$  by  $z = -1/\log(1 - 1/706T)$  and a range of  $T$  values are considered. It is defined in Section 3.3.2 of the Lancaster University part of this report, with examples and advice on interpretation of the results being given in Section 7.1.2. The rate of change of  $T(z)$  with  $\log(z)$  should be  $(1-\rho)/(1+\rho)$ , where  $\rho$  is the correlation coefficient for that threshold. A constant rate of change is indicative of a constant level of dependence, with a constant  $T(z)$  value of zero indicating complete dependence and a gradient of one indicating independence. A varying rate of change of  $T(z)$  with  $\log(z)$  would indicate that dependence varies with threshold.

## **2.2 Fitting of statistical distributions to the marginal variables**

### Statistical models for the marginal variables

The second stage involves the fitting of statistical models to wave heights, water levels and wave steepnesses. Generalised Pareto Distributions are fitted to the top few percent of the primary marginal variables, ie wave heights and water levels; and the distribution of wave steepness is modelled through a combination of its empirical distribution and a regression relationship with high wave heights. For each of the three marginal distributions, a threshold, specified in terms of the proportion of data less than, is used for fitting. Below the threshold, the distribution is represented empirically, and above the threshold by the fitted distribution. Details are given in Chapters 3 and 4 of the Lancaster University part of this report and a brief summary is given below.

### The Generalised Pareto Distribution (GPD)

The GPD is described in Section 3.1 of the Lancaster University part of this report. Although in practice the GPD is fitted only above a chosen threshold, a feature of the distribution is that (if it is a good fit to the data) it is invariant to the threshold. Another feature of the distribution is that, unlike the Weibull distribution for example, it does not necessarily increase roughly in proportion to the log of the return period. Instead it can also either increase more rapidly in the tail or it can level off towards an absolute maximum value. Numerical tests carried out using several of the project data sets suggest that extremes predictions are not sensitive to the threshold chosen, and that 0.95 is usually a reasonable value to use, so that the GPD is fitted to the top 5% of the data.

### Importance of wave period

In some situations wave period can be as important as wave height in calculating effects at the coast such as overtopping or armour damage, especially when wave heights are depth-limited at a sea wall. Although good information on extreme water levels and extreme wave heights will usually be obtained or derived during a coastal modelling study, the marginal distribution of wave period is rarely considered beyond the estimation of a representative wave steepness. However, in the JOIN-SEA and structure variable methods the distribution of wave periods is built in through respectively a model for the distribution of wave steepness and empirically.

### Incorporation of improved predictions of marginal extremes

Joint probability analysis is based on simultaneous information on the variables of interest. It is quite likely that there will be additional non-simultaneous data on at least one of the variables, with which to

refine the extremes predictions for that one variable. For example, there may be 20 years of water level data but only 10 years of wave data; accurate extreme values for one or other variable may have already been established (eg from spatial analysis of water levels (POL, 1997)); or there may be anecdotal evidence of severe sea conditions outside the period of the measurements. Good joint probability analysis uses this additional information. This might involve modification of the parameters of the fitted distribution(s) or scaling of the predicted extremes to achieve better agreement with the refined marginal predictions. The present method incorporates any refinements by scaling during the long-term simulation of data, thus permanently building this information into the synthesised sea state data to be used in subsequent structural analysis.

## 2.3 Statistical models for dependence

### The modelling procedure

The third stage involves conversion to Normal scales, and fitting of a dependence function to the bulk of the wave height and water level data. Simple diagnostic tests have been developed to assess whether full dependence or independence models are adequate approximations. For situations when these simplifications cannot be made, two alternative partial dependence statistical models have been developed to represent the dependence between wave heights and water levels. These consist of a single Bi-Variate Normal (BVN) Distribution and a mixture of two BVN's. These models were chosen, since the dependence and extremes characteristics of the BVN are well understood, and together these two models are considered to provide a sufficiently flexible family of models.

### Selection of statistical model

The choice between one and two BVN's is determined by the relative goodness of fit to the data, which can be assessed with reference to the varying degree of correlation, expressed as a function of exceedance level. The single BVN may be adequate for a location at which all the wave conditions belong to a single population, although frequently the correlation will increase rapidly towards the tail and the mixture model will be needed. However, where the wave conditions belong to more than one population, for example wind-sea and swell, the mixture model is always likely to be needed to capture the different dependences in the two populations.

### User input

In this and in the previous stages the user retains some control over the process, primarily by having the choice of selected dependence model, and secondarily by being able to select both the thresholds above which the fitting will be applied, and the starting values for optimisation of the fits: this is assisted by reference to diagnostics to assess the fits.

## 2.4 Long-term simulation

### The simulation procedure

The fourth stage involves simulation of a large sample of synthetic records of  $H_s$ ,  $T_m$  and water level, based on the fitted distributions, and with the same statistical characteristics as the input data. At this stage it is possible to re-scale the marginal extreme distributions to more established values, if they are known. For example, concurrent wave and water level data may be available for a period of ten years, and by extrapolation of this data the marginal distributions of the two variables are calculated within the joint probability software. However, if either or both of the data sets extends beyond the concurrent period of ten years, it is preferable to use the additional information contained within the extra data. Therefore the marginal distribution can be derived from the longer data set and incorporated into the data simulation process through the use of the re-scaling option. This is achieved by altering individual affected wave heights and water levels from one scale to the other between simulation from the fitted distributions and writing permanently to an output file. Thus, based on all available data, thousands of years worth of sea conditions can be simulated with fitted distributions, extremes and dependences for wave height, water level and wave period. This provides greater flexibility in the subsequent analysis of the sea state data.

### The simulation product

Output from this stage details the number of events per year, the number of records in the file, as well as the individual sea state records and the marginal extremes. Checks can be made on the return period marginal conditions that are within the time span of the input data. For example, if the input data consisted of a time span of five years, the 1 year marginal extreme should be approximately equal to the fifth highest record in the input file.

## **2.5 Analysis of joint exceedance extremes and structural response functions**

### Analysis of the simulated data

The fifth stage involves analysis of the large simulated sample of data to produce extreme values for use in design and assessment of sea defences. These can take the form of extreme wave heights (and associated periods), extreme water levels, or extreme combinations of the two. In addition, any structural response function (eg overtopping, run-up, force) which can be defined in terms of constants (eg wall slope, toe depth, crest elevation etc) and variables  $H_s$ ,  $T_m$  and water level, can be synthesised directly for every record in the simulated data sample. Direct analysis of the distribution and extremes of the structural response variable is then relatively easy.

### The 'count-back' extremes analysis method

Rather than fitting probability distributions to the synthesised data, extreme values are estimated from the appropriate empirical exceedance probability in the synthesised data. This is achieved by 'counting back' through the highest values within the simulated data, a method based on the literal definition of return period and best described by means of an example. If, for a 2000 year simulation, the 100 year return period value (ie the level equalled or exceeded on average once every hundred years) is required, then this is given by 'counting back' to the  $2000/100 = 20$ th highest value, which is then assigned a return period of 100 years. Joint exceedance extremes are determined in a similar way, for example by 'counting back' through the highest wave heights, but only considering those records above a certain threshold of water level. This intuitive approach is reliable for return periods up to about one quarter of the simulation length. Hence it is necessary to synthesise at least four times as much data as the highest return period of interest, and in practice ten times would be a more typical ratio.

### Direct analysis of structural response variables

At present, as well as marginal and joint exceedance extremes, four simplified structural response variables are included in the computer programs for demonstration purposes, for which more details of the formulae used and the input variables are given in the user manual (HR, 2000):

- overtopping rate on a smooth slope;
- run-up on a smooth slope;
- force on a vertical wall;
- armour size for a sea wall.

### Analysis of more complex variables

More complex variables, for example the simultaneous occurrence of a high force and a high overtopping rate, which would have been difficult to assess previously, can now be routinely studied. Sensitivity and alternative designs can also be assessed relatively easily, by making appropriate changes to the structural response function(s) analysed without the need for additional statistical analysis of dependence or marginal variables or a new long-term simulation.

## **2.6 Software implementation**

### Introduction

This section briefly describes the software package and the functions of the five main programs for the joint probability analysis: *BVN*, *MIX*, *SIMBVN*, *SIMMIX* and *ANALYSIS*. For a more detailed description and instructions on the use of the programs, a companion manual (HR, 2000) is available. In normal use in

consultancy studies, the user would need to write some additional programs to carry out the necessary pre-processing of the input data, and to compute actual site-specific structural response variable(s).

#### Fitting of statistical models (BVN and MIX)

Two programs are used to fit statistical models to samples of data, one based on a single Bi-Variate Normal distribution (*BVN*) and one based on a mixture of two Bi-Variate Normal's (*MIX*). Both programs also fit the marginal distributions of wave height, of water level, and of wave steepness, each above a threshold selected by the user. Input data to the two programs, in file *datafile*, consists of a large number of records of wave height, water level and wave period. Output from *BVN* consists of three files: *rhovalues*, *diagnostic* and *transfer*. *Rhovalues* and *diagnostic* provide information on the fitting of the distributions and the correlation at different probability thresholds, whilst *transfer* is used to input this information into the subsequent *SIMBVN* program. The next step is to run either *MIX* or *SIMBVN*, dependent on the information on correlation detailed in the *diagnostic* and *rhovalues* files. Essentially *MIX* performs the same task as *BVN* but will provide a better fit to data where there is a large variation in correlation with probability threshold. Output from *MIX* consists of a *diagnostic* file and a *transfer* file that perform the same function as the output from *BVN*.

#### Simulation of long data samples (SIMBVN and SIMMIX)

Two programs, *SIMBVN* and *SIMMIX*, are used to synthesise much longer samples of data based on the two alternative fitted distributions. *SIMBVN* is run subsequent to *BVN*, and *SIMMIX* is run subsequent to *MIX*. Although the two programs perform the same function, the input *transfer* files (output from *BVN* or *MIX*) differ. An option of re-scaling the marginal extremes, if more established values are known, is available in both programs. The output files (*simdata*) from *SIMBVN* and *SIMMIX* are identical in form and consist of a large number of individual wave height, water level and wave period records. 'Importance sampling' can be applied at this stage, such that only the higher records are retained, so as to reduce the eventual size of the *simdata* file.

#### Extremes from the simulated data (ANALYSIS)

The last program, *ANALYSIS*, is used to derive marginal extremes, joint exceedance extremes and extreme values of demonstration structure variable(s) from the *simdata* file. Threshold wave heights are specified for which extreme water levels are derived, and vice versa, thus joint exceedance combinations are obtained. For the structure variables it is necessary to specify parameters such as toe depth, wall slope and crest level for individual structures.

#### User input

The procedure is largely automated, but requires quite substantial computer time, memory and storage capacity. Although there is a large number of questions put to the user during operation of the programs, the majority can be answered by accepting the default values. The user should be prepared to check for mixed populations or faulty records in the original data, and to re-run parts of the procedure if indicated to do so by the diagnostic information. It is sometimes necessary to take a view on the importance of one, two or three outliers, that is records of severe sea states with apparently high dependence between wave height and water level in an otherwise uncorrelated data set. As in any joint probability analysis method, the eventual results can be quite sensitive to the importance given to these records, and it may be worth checking the validity of the individual records concerned. More specific advice is given in the JOIN-SEA user manual (HR, 2000).

### **3. APPLICATIONS**

#### The test data sets

During validation and comparison of results with alternative joint probability methods several test data sets were assembled. Some were based on measured and hindcast wave and water level data - these had the advantages of not coming from pre-determined statistical distributions and of being representative of data sets to be used in consultancy studies; some were synthesised using specified probability distributions loosely based on measured data - these had the advantage that the 'true' extremes and joint probabilities were known.

### 3.1 Example applications to synthetic data

#### The simulated data sets

Five sets of wave and water level data with known statistical distributions, but broadly representative of actual conditions at different points around the coast of England and Wales, were synthesised. Details of the derivation of these data sets are given in Chapter 5 of the Lancaster University part of this report.

#### Comparisons made by Lancaster University

Combinations of wave heights and water levels with given joint exceedance return periods were calculated using HR Wallingford's existing JOINPROB software (HR, 1994) and also using the new methods. The results were compared with the 'true' joint exceedance extremes for return periods of 10 years (equal to the length of the original data set) and 1000 years. Two of the comparisons are shown in Figures 4 and 5 (which are typical of the wider range of comparisons given in Chapters 8 and 9 of the Lancaster University part of this report). In these diagrams the joint exceedance extremes predictions have been adjusted to give marginal extremes in agreement with target values, so as to highlight the modelling and extrapolation of dependence. In both figures, the 'Simulation Model' lines represent the target (or 'true') values. The 'Estimated Model' lines show results from the new method, with marginal extremes predictions scaled to give exact agreement with target values. The 'HR Estimates' lines show results from HR Wallingford's JOINPROB method, here with marginal extremes predictions scaled to agree with earlier slightly different target marginal extremes. As expected, both methods perform well for a joint return period equal to the length of the data set, but the new method gives more robust predictions at much higher return periods.

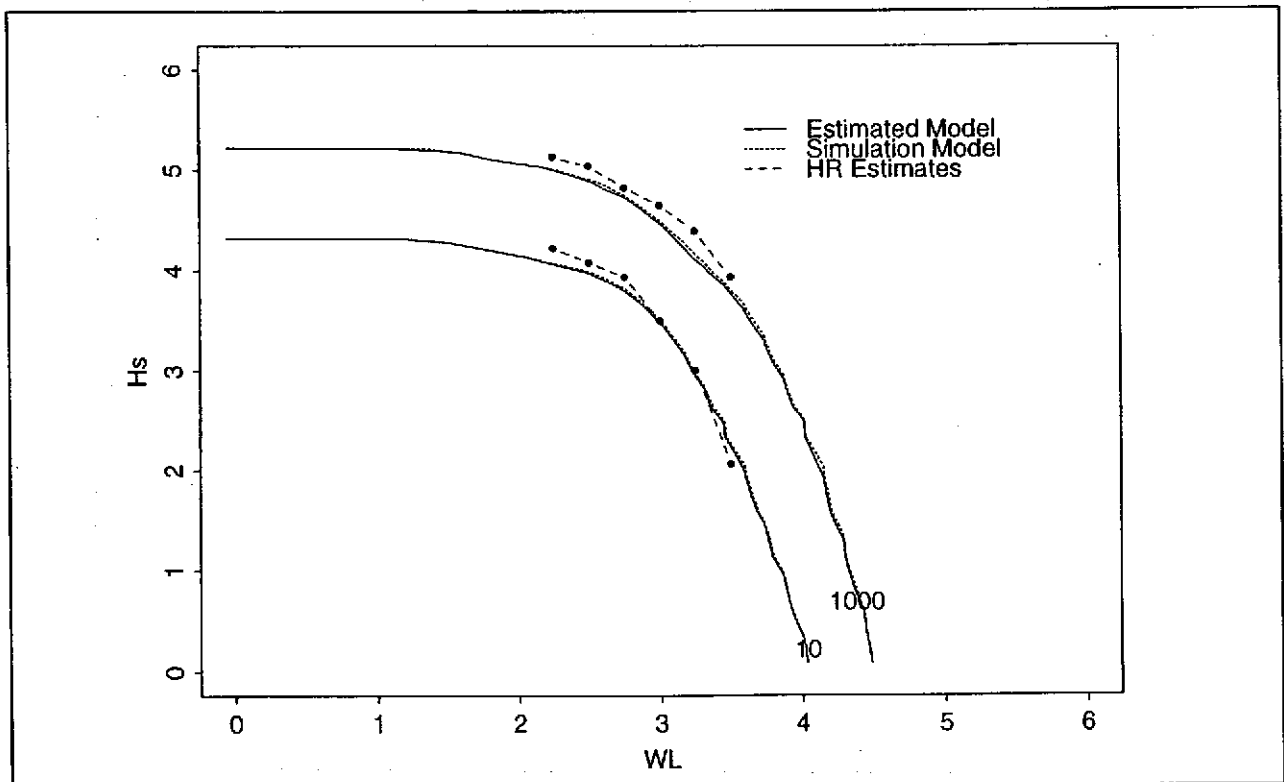
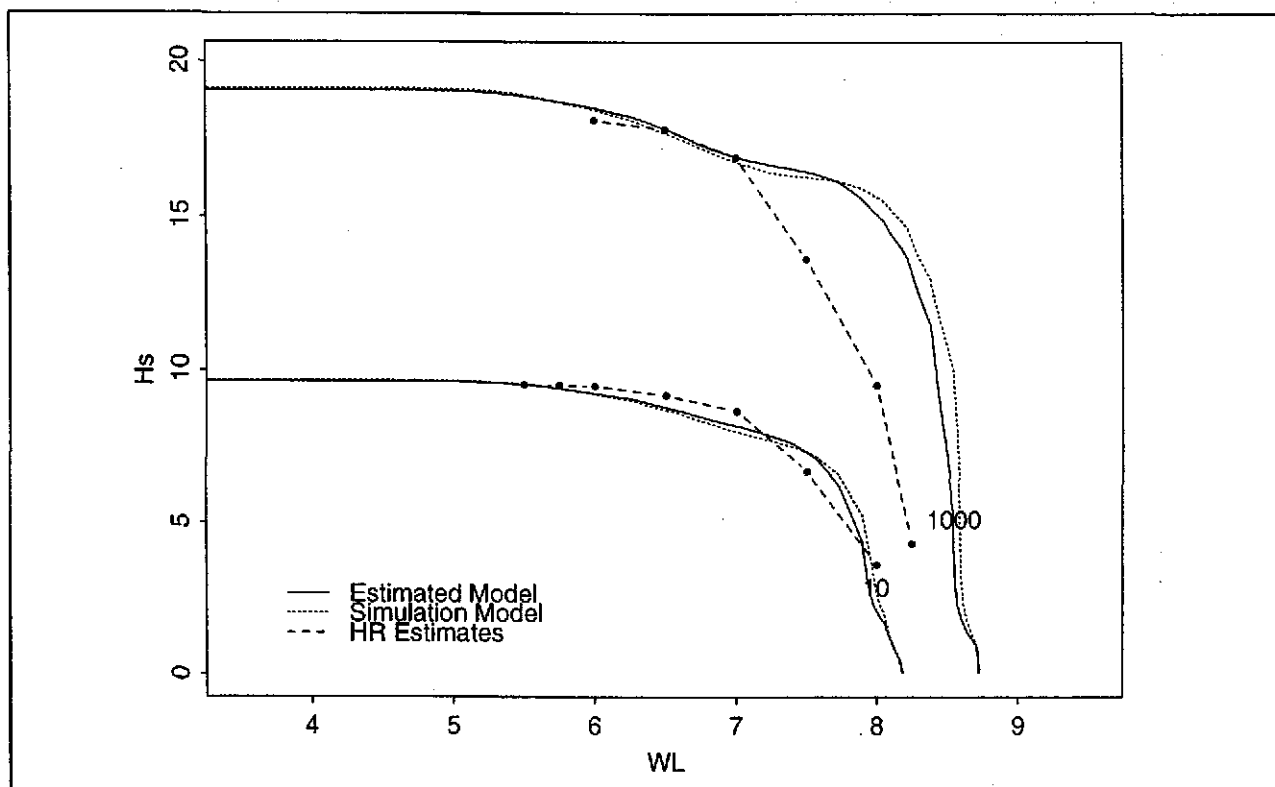


Figure 4 Joint exceedance contours of  $H_s$  (m) and water level (mOD) for a site with very low dependence



**Figure 5 Joint exceedance contours of  $H_s$  (m) and water level (mCD) for a site with high dependence**

#### Some conclusions from the Lancaster University comparisons

Overall, the comparisons presented in the Lancaster University part of this report suggest that the new approach, working directly in terms of the structural response function, is more consistent and reliable than alternative methods. The importance of wave period is shown in several ways: the use of wave periods which are too low (perhaps due to using a constant wave steepness which is too high) does not affect the joint exceedance extremes directly but it does lead to an under prediction of overtopping rate; the use of a variable wave steepness, rather than a constant wave steepness, tends to increase overtopping predictions. The return periods of structural response variables calculated (as has usually been done in the past) from joint exceedance extremes tend to be about half the size of the return periods of the joint extremes themselves. The new long-term simulation approach allows a direct and accurate assessment of the 'risk' with a given return period, without resort to the fairly arbitrary small margins of conservatism currently used in consultancy studies.

#### Additional comparisons using direct hindcasting

One further analysis method was applied to the simulated data sets after completion of the Lancaster University (LU) part of the report, to illustrate an analysis method used satisfactorily by HR Wallingford several times in the past. The remainder of this section effectively forms a post-script to LU's Chapter 9. It involves direct hindcasting and extrapolation of overtopping, applied in the way that has been used in previous HR consultancy studies. This is comparable with LU's 'SVM applied to  $Q_c$ ', referring to the Structure Variable Method applied to overtopping rate, which suggested that the method was flawed due to its great sensitivity to threshold, but that the SVM applied to  $\log(Q_c)$  was reasonable.

Extremes analysis using direct hindcasting

For each of the simulated data sets (Sim1-Sim5) in turn, each record of wave height, water level and wave steepness was converted to an equivalent rate of overtopping using the same formulae and parameter values as described in LU's Chapter 9 (although obviously the vast majority of the values were zero). For each data set an empirical distribution of overtopping rate ( $Q_c$ ) was assembled for extrapolation to extreme values using HR's standard methods. This involved fitting a three parameter Weibull distribution (see LU's Section 4.1.2), not to individual overtopping records but to equally spaced thresholds of overtopping. In other words, the information used in fitting the Weibull probability model consisted of, for example, the percentages of data less than  $Q_c$  ( $m^3/s/m$ ) = 0.005, 0.010, 0.015..., or 0.010, 0.015... Several different thresholds were tested for each data set, and the predicted 1, 10 and 100 year overtopping rates were compared with the 'true' values (not available for the 1 year return period) from the simulation model (see LU's Chapter 9).

Results and conclusions from direct hindcasting

The extreme overtopping rate predictions given in the Tables 1-5 below do not show much sensitivity to threshold and are quite close to target values. To put these results into the context of the comparisons made in Chapter 9 of the Lancaster University part of the report, take average predictions for each column in Tables 1-5 and convert to equivalent 'true' return periods. The accuracy of the direct hindcasting approach is comparable with that of the JOINPROB analysis: a little better than JOINPROB at the 10 year return period (within the data) but less reliable at the 100 year return period. This suggests that HR's current implementation of the structure variable method is sound in this application, although some care is required in preparation of the data and checking of the results, particularly for data sets containing just one or two high overtopping results. Given the simplicity of the approach, and the fact that it is not subject to the uncertainties associated with the fitting and extrapolation of dependence, the method could be retained for use in prediction of specific response variables where several years of input data are available.

**Table 1 Direct hindcasting and extrapolation of overtopping rate, applied to data set Sim1**

Threshold (ie the proportion of data ignored in fitting the distribution)	Predicted extreme overtopping rate $Q_c$ ( $m^3/s/m$ )		
	1 year return	10 year return	100 year return
0.00000	0.00064	0.0059	0.034
0.99800	0.00063	0.0065	0.021
0.99860	0.00082	0.0065	0.030
0.99914	0.00103	0.0063	0.037
'True' values	Not available	0.0075	0.030

**Table 2 Direct hindcasting and extrapolation of overtopping rate, applied to data set Sim2**

Threshold (ie the proportion of data ignored in fitting the distribution)	Predicted extreme overtopping rate $Q_c$ ( $m^3/s/m$ )		
	1 year return	10 year return	100 year return
0.00000	0.56	1.23	2.24
0.97240	0.61	1.12	1.67
0.98800	0.61	1.12	1.63
0.99390	0.61	1.11	1.63
0.99643	0.62	1.11	1.57
0.99814	0.67	1.08	1.45
0.99829	0.71	1.07	1.38
'True' values	Not available	1.15	1.87

**Table 3 Direct hindcasting and extrapolation of overtopping rate, applied to data set Sim3**

Threshold (ie the proportion of data ignored in fitting the distribution)	Predicted extreme overtopping rate $Q_e$ ( $m^3/s/m$ )		
	1 year return	10 year return	100 year return
0.00000	0.62	1.77	4.0
0.97910	0.64	1.75	3.5
0.99130	0.63	1.77	3.6
0.99510	0.62	1.78	3.9
0.99670	0.63	1.79	4.4
0.99757	0.63	1.79	4.5
0.99829	0.54	1.81	3.8
'True' values	Not available	1.41	2.6

**Table 4 Direct hindcasting and extrapolation of overtopping rate, applied to data set Sim4**

Threshold (ie the proportion of data ignored in fitting the distribution)	Predicted extreme overtopping rate $Q_e$ ( $m^3/s/m$ )		
	1 year return	10 year return	100 year return
0.00000	3.6	9.2	18.8
0.97900	4.1	7.6	11.2
0.99110	4.1	7.5	11.0
0.99370	4.1	7.5	10.8
0.99600	4.2	7.4	10.5
0.99730	4.3	7.3	10.1
0.99800	4.5	7.3	9.8
'True' values	Not available	11.7	27.2

**Table 5 Direct hindcasting and extrapolation of overtopping rate, applied to data set Sim5**

Threshold (ie the proportion of data ignored in fitting the distribution)	Predicted extreme overtopping rate $Q_e$ ( $m^3/s/m$ )		
	1 year return	10 year return	100 year return
0.00000	2.5	6.7	14.1
0.98120	3.0	5.7	8.5
0.99130	3.0	5.7	8.5
0.99390	3.0	5.7	8.4
0.99560	3.0	5.7	8.4
0.99714	3.0	5.6	8.2
0.99771	3.0	5.6	8.2
'True' values	Not available	8.3	19.5

### 3.2 Case studies using field data

#### The field data sets

The comparisons between methods described in the Lancaster University part of this report are based on five simulated data sets, loosely based on five sets of field data from different parts of England and Wales, namely Christchurch, Dover, Dowsing, Cardiff and North Wales. This section of the report describes equivalent comparative analyses between JOINPROB and JOIN-SEA using the original long time series field data sets underlying the synthetic data sets. (The word 'field' is perhaps a little misleading since in each case the wave

data came from a numerical hindcasting model, but the sequential wind and water level data are from actual measurements.) Details of the data sets are given in Table 5.1 of the Lancaster University part of the report.

#### Two data populations for Cardiff

The 28-year Cardiff data set contained two distinct populations of wave conditions: swell waves with an offshore direction between 190 and 360°N and locally generated waves with an offshore direction between 0 and 190°N. The two populations were separated at the data preparation stage and were treated as two separate 28-year data sets during the subsequent analysis even though each contained only about half as many records as the original combined set. The direction-dependent marginal and joint extremes were then defined such that there will be one extreme occurrence, on average, in each direction sector in each return period.

#### The structural response function

For the purposes of this study the same structural response function was used as in the Lancaster University comparisons, namely sea wall overtopping. Idealised sea walls were devised and the overtopping discharge was calculated using the formulae of HR (1980) at each of the sites. Further details of the formulae and the sea wall parameters can be found in Table 9.1 of the Lancaster University part of this report. However, it is not so much the values of overtopping calculated that are of interest, more the comparison between the different methods. Tables 6-11 give overtopping discharge rates using the different analysis methods described below. All discharges in the tables below are given in  $\text{m}^3/\text{s}/\text{m}$ , but please note that the idealised sea walls used in the tests do not correspond to the actual sea defences at any of the five sites.

#### JOINPROB analysis

The JOINPROB combinations column in Tables 6-11 refers to the existing HR analysis method whereby different combinations of wave height and water level, with the same joint exceedance return period, are extracted from a joint exceedance probability contour plot. These combinations are then applied to the structural response function and the 'worst case' is found. The wave steepness is calculated for the top few percent of wave conditions and is assumed to have a constant value, which is then applied to the extreme conditions to calculate the wave period.

#### JOIN-SEA analysis

The new joint probability methods were applied in three different ways in order to test different aspects of the procedure. Two involved the joint exceedance combinations approach for comparison with earlier methods and one involved direct simulation of the structural response function. The mean wave period ( $T_m$ ) for the JOIN-SEA analysis was calculated in three ways:

- 1 Assuming the same steepness (HR steepness) as used for the JOINPROB calculations in assigning a wave period to each wave height and water level combination.
- 2 Using the average steepness noted by the JOIN-SEA model for the top 5% of wave heights (not necessarily the same as the HR steepness, which was determined manually) in assigning wave periods.
- 3 Allowing a natural variation in steepness during the simulation of the long time series data set, as in the normal operation of JOIN-SEA.

#### Empirical extremes

Column 6 in each of Tables 6-11 gives extreme values derived directly from the original data. Each record, in terms of significant wave height, mean wave period and water level, was converted to an equivalent rate of overtopping. The 1 year return period extreme value was determined for each location using the 'count-back' method described in Section 2.5 (so, for example, in a 28 year data set, the required value would be the twenty-eighth largest overtopping value). This is perhaps the most accurate extreme

value estimate in each table. The 10 year, and in some cases the 20 year return period values, were also estimated from the data, but these are subject to great uncertainty.

**Comparison between JOINPROB and JOIN-SEA joint exceedance extremes**

Method 1 allows a direct comparison between the traditional sea state combinations (JOINPROB) method and the new JOIN-SEA method, applied so as to obtain design sea states defined by specific wave heights and water levels. (NB: the calculation of overtopping using the HR steepness in the JOIN-SEA model is for comparison purposes only and is not a routine practice). If both methods worked perfectly then the results in Columns 2 and 3 of the tables should be identical. Discrepancies are due to differences in marginal extremes predictions as well as to the representation of dependence.

**Comparison between joint exceedance extremes and simulation approaches**

JOIN-SEA analysis methods, numbered 2 and 3 above, give a direct comparison between the traditional method of applying design sea state combinations, and the new method of structural response simulation. Differences here highlight the discrepancy between estimating extreme values of structural response from joint exceedance probabilities (without applying the usual small margin of conservatism) and from joint structural probabilities.

**Table 6 Comparison between overtopping rates (m<sup>3</sup>/s/m) for different analysis methods at Christchurch**

Return period (years)	JOINPROB joint exceedance (HR steepness of 0.06)	JOIN-SEA joint exceedance (HR steepness of 0.06)	JOIN-SEA joint exceedance (model steepness of 0.053)	JOIN-SEA structural response simulation	Empirical (directly from original data)
1	1.13	1.23	1.45	1.81	1.68
10	2.29	2.67	3.07	3.55	2.75
20	2.63	3.40	3.88	4.20	Not available
100	Not available		4.85	5.49	
200	Not available		5.31	5.75	

**Table 7 Comparison between overtopping rates (m<sup>3</sup>/s/m) for different analysis methods at Dover**

Return period (years)	JOINPROB joint exceedance (HR steepness of 0.06)	JOIN-SEA joint exceedance (HR steepness of 0.06)	JOIN-SEA joint exceedance (model steepness of 0.045)	JOIN-SEA structural response simulation	Empirical (directly from original data)
1	0.17	0.20	0.35	0.53	0.46
10	0.51	0.48	0.75	0.99	1.1±0.4
20	0.67	0.56	0.86	1.14	Not available
100	Not available		1.32	1.66	
200	Not available		1.86	1.96	

**Table 8 Comparison between overtopping rates ( $m^3/s/m$ ) for different analysis methods at Dowsing**

Return period (years)	JOINPROB joint exceedance (HR steepness of 0.06)	JOIN-SEA joint exceedance (HR steepness of 0.06)	JOIN-SEA joint exceedance (model steepness of 0.053)	JOIN-SEA structural response simulation	Empirical (directly from original data)
1	1.14	0.99	1.19	2.20	2.6
10	3.40	3.35	3.83	5.76	7.3±2.2
20	4.85	4.26	4.84	7.19	Not available
100	Not available		8.31	10.9	
200	Not available		9.84	12.5	

**Table 9 Comparison between overtopping rates ( $m^3/s/m$ ) for different analysis methods at Cardiff (0-190°N)**

Return period (years)	JOINPROB joint exceedance (HR steepness of 0.05)	JOIN-SEA joint exceedance (HR steepness of 0.05)	JOIN-SEA joint exceedance (model steepness of 0.06)	JOIN-SEA structural response simulation	Empirical (directly from original data)
1	0.000003	0.000006	0.000003	0.00005	0.000015
10	0.0011	0.00033	0.00019	0.0013	0.0013
20	0.0067	0.00075	0.00045	0.0037	0.002±0.0005
100	Not available		0.0026	0.011	Not available
200	Not available		0.0083	0.017	

**Table 10 Comparison between overtopping rates ( $m^3/s/m$ ) for different analysis methods at Cardiff (190-360°N)**

Return period (years)	JOINPROB joint exceedance (HR steepness of 0.01)	JOIN-SEA joint exceedance (HR steepness of 0.01)	JOIN-SEA joint exceedance (model steepness of 0.039)	JOIN-SEA structural response simulation	Empirical (directly from original data)
1	0.0001	0.00025	0.00000008	0.000008	0.00014
10	0.016	0.0081	0.00006	0.00089	0.0027
20	0.049	0.016	0.00018	0.0023	0.0056±0.0012
100	Not available		0.0032	0.024	Not available
200	Not available		0.0077	0.089	

**Table 11 Comparison between overtopping rates ( $m^3/s/m$ ) for different analysis methods at North Wales**

Return period (years)	JOINPROB joint exceedance (HR steepness of 0.06)	JOIN-SEA joint exceedance (HR steepness of 0.06)	JOIN-SEA joint exceedance (model steepness of 0.047)	JOIN-SEA structural response simulation	Empirical (directly from original data)
1	0.26	0.38	0.57	1.04	0.82
10	1.26	1.43	1.86	2.59	1.55
20	2.04	1.89	2.44	3.22	Not available
100	Not available		3.85	4.42	
200	Not available		4.56	5.28	

Discussion of the direct comparison between JOINPROB and JOIN-SEA

The comparison in columns 2 and 3 of Tables 6-11, between JOINPROB (HR steepness) and JOIN-SEA (HR steepness) using the joint exceedance method of determining the worst case overtopping event and assuming the same value of wave steepness, shows good agreement at all sites. This suggests that the method of marginal extrapolation at varying thresholds, for both variables, to construct contours of equal joint exceedance return period, gives similar results to those derived from the extrapolated joint probability density obtained from JOIN-SEA. This is borne out by plots in Appendix 1 showing contours of equal joint exceedance return period (irrespective of wave steepness) for each of the test sites, derived by the JOINPROB and JOIN-SEA methods respectively.

Discussion of the sensitivity to assumed fixed wave steepness

Comparison of the two JOIN-SEA combinations columns gives insight into the potential errors of manually calculating the mean steepness for the top 5% of wave conditions, as opposed to the more rigorous calculation of steepness carried out routinely in the model. The results show the difference in discharge rates to be slightly higher (no more than a factor of two, in terms of return period) using the model steepness, for all sites, with the exception of Cardiff. The difference of the results at Cardiff is probably explained by the separation of wave conditions by direction as opposed to steepness. Some longer wave period (lower steepness) wave conditions were present in the 0-190°N (higher steepness locally generated wave conditions) data, and vice versa.

Discussion of differences between the joint exceedance extremes and joint probability density approaches

The simulation of the structural response function gives overtopping discharges that are a factor of 2-3 times greater, in terms of the return period, than those calculated using the combinations of marginal values (JOIN-SEA (model steepness)). This is as previously expected and is explained by the fact that the joint exceedance method does not account for the entire range of combinations that can contribute to the structural response value for a given return period.

Comparison with empirical extremes

With the exception of the very low overtopping rates (less than  $0.002m^3/s/m$ ) predicted for some return periods for the Cardiff data set, the JOIN-SEA results listed in Columns 4 and 5 of the tables agree well with the empirical values. The discrepancy in the low overtopping rates for Cardiff is thought to be due to the difficulty in representing the distribution of wave period correctly, as can be seen in the spread of results across each of the rows in Tables 9 and 10.

**3.3 Example application using both inshore and offshore wave data**

Reasons for choosing the Somerset site

In addition to comparing results from different analysis methods, it is interesting to compare results from i) offshore and nearshore (ie after wave transformation modelling) input wave data, and ii) depth-limited and

deep water conditions at the structure. To illustrate the differences an example study was carried out for a hypothetical site on the Somerset coast. This location was chosen for a number of reasons: it has a high tidal range; it is exposed to a mixture of locally generated waves and waves arriving from the Atlantic; wave refraction effects cause a significant increase in  $T_m$  as the waves propagate from offshore to nearshore; there is increasing dependence between wave heights and water levels as wave height increases; and 28 years of simultaneous measured water level data and hindcast wave data were available.

#### The input wave and water level data

Input water level data were derived from hourly measurements at Avonmouth over a period of 28 years, transformed for use at the study site. Input wave data was derived from a site-specific wave hindcasting model driven by hourly wind measurements at Cardiff Airport over the same period of 28 years. After pre-processing of the data as described in Section 2.1, about 20,000 records of  $H_s$ ,  $T_m$  and high water level remained as input to the joint probability analysis. Two alternative types of wave data were used:

- offshore wave data representative of conditions several kilometres away from the coast in about 20m water depth;
- nearshore wave data (after transformation using a wave refraction model) just outside the breaker zone at high water level.

#### The analysis methods

The mixture of locally generated and swell waves at the site suggested that the mixture of BVN's would be a more appropriate probability model than the single BVN. Therefore the mixture model was run to produce both joint exceedance (JE) probability sea states and direct predictions of the structure variable (SV). The BVN model was also run for comparison purposes, but was used only for direct predictions of the structure variable. HR's existing JOINPROB method was used to produce joint exceedance probability sea states. To summarise, four alternative joint probability analyses were used:

- JOINPROB\_JE analysis (HR, 1994) as used in consultancy studies in recent years - this produces multiple combinations of wave condition (with a fixed wave steepness) and water level, with a given joint exceedance probability, which can then be converted to structural response variable predictions;
- MIX\_JE analysis using two fitted BVN's - i) producing multiple combinations of wave condition (again with a fixed wave steepness for comparison with JOINPROB\_JE) and water level, with a given joint exceedance probability, which can then be converted to structural response variable predictions;
- MIX\_SV analysis using two fitted BVN's - ii) working directly in terms of the structural response variable, and now using a variable wave steepness derived from the original data;
- BVN\_SV analysis using a single BVN - working directly in terms of the structural response variable, and using a variable wave steepness derived from the original data.

#### The coastal structures

Two hypothetical structures were tested:

- a plain sea wall with a crest level 2.8m above MHWS and deep water at the toe of the wall;
- a plain sea wall with a crest level 2.8m above MHWS and a toe elevation 2.7m below MHWS.

### The structural response variables

Two structural response variables were tested:

- overtopping rate using the SWALLOW equations in HR (1980) for a wall slope of 1:4;
- armour size using equations (5.44) to (5.46) in CIRIA/CUR (1991) for a wall slope of 1:2.

### Note on wave steepness

For illustrative purposes, no upper and lower cut-offs were applied to wave steepness during the initial long-term simulation used to derive the results shown in Tables 12 and 13 for a return period of 100 years. For the offshore wave data, this made little difference. However, for the nearshore wave data, which contained a wider range of lower wave steepnesses, this had the effect of producing a small number of quite high waves with much longer mean periods than in the original sample. For this example application, the longer period waves demonstrate the importance of wave period and the sensitivity of overtopping rate to uncertainties therein. In a subsequent simulation, a lower limit of 0.020 was imposed on wave steepness, as would be done in a consultancy study. The new extreme overtopping predictions, for a wider range of return periods, are given in Table 14.

### The effect of correlation coefficient

For illustrative purposes, two additional series of BVN\_SV results are shown in Table 14. Whilst the 'Best' sub-column contains overtopping rate predictions for the best estimate of correlation directly from the data, the ' $\rho = 0$ ' and ' $\rho = 1$ ' sub-columns show equivalent results assuming independence and complete dependence, respectively.

**Table 12 100 year overtopping rates ( $m^3/s/m$ ) for Somerset (no limit on wave steepness)**

Wave data	Sea wall	JOINPROB_JE	MIX_JE	MIX_SV	BVN_SV
Offshore (steepness of 0.050 for JE)	Deep at toe	1.10	0.72	0.85	0.69
	Depth limited at toe	0.46	0.30	0.42	0.31
Nearshore (steepness of 0.029 for JE)	Deep at toe	1.34	1.08	9.0	10.7
	Depth limited at toe	1.10	0.83	8.9	9.2

**Table 13 100 year armour size (m) for Somerset (no limit on wave steepness)**

Wave data	Sea wall	JOINPROB_JE	MIX_JE	MIX_SV	BVN_SV
Offshore (steepness of 0.050 for JE)	Deep at toe	1.27	1.27	1.27	1.31
	Depth limited at toe	0.82	0.82	0.83	0.82
Nearshore (steepness of 0.029 for JE)	Deep at toe	1.45	1.45	1.43	1.37
	Depth limited at toe	0.90	0.90	0.96	0.94

**Table 14 Overtopping rates (m<sup>3</sup>/s/m) for Somerset (minimum wave steepness of 0.020)**

Wave data	Sea wall	MIX_JE	MIX_SV	BVN_SV		
		Return periods are 1, 10, 20, 100 and 200 years				
			Best estimate of $\rho$	$\rho=0$	Best	$\rho=1$
Offshore (steepness of 0.050 for JE)	Deep at toe	0.03	0.10	0.06	0.09	0.41
		0.23	0.37	0.21	0.31	0.99
		0.34	0.50	0.25	0.38	1.21
		0.72	0.85	0.47	0.69	1.81
		0.95	1.04	0.58	0.85	2.00
	Depth limited at toe	0.03	0.05	0.03	0.05	0.27
		0.15	0.19	0.10	0.16	0.57
		0.21	0.25	0.13	0.21	0.65
		0.30	0.42	0.22	0.31	0.87
		0.41	0.48	0.27	0.37	0.98
Nearshore (steepness of 0.029 for JE)	Deep at toe	0.04	0.15	0.11	0.14	0.68
		0.35	0.73	0.54	0.67	2.07
		0.51	1.01	0.77	0.90	2.45
		1.08	1.72	1.44	1.61	3.50
		1.25	2.25	1.56	1.78	4.31
	Depth limited at toe	0.04	0.11	0.07	0.09	0.67
		0.31	0.53	0.34	0.48	1.96
		0.41	0.73	0.46	0.65	2.22
		0.83	1.26	0.76	0.99	2.78
		0.91	1.78	0.84	1.32	2.94

Discussion of the Somerset case study

All of the methods appeared to work satisfactorily, but there are some interesting differences. Roughly the same armour size (which is only a little dependent upon wave period and not directly dependent on water level) was calculated whatever method was used. However, overtopping, which is dependent on  $H_s$ ,  $T_m$  and water level, was quite dependent on which method and which source of wave data was used. As with the synthetic data analysed in the Lancaster University part of this report, slightly higher values were derived directly from the structure variable than from the joint exceedance extremes. As expected, higher overtopping was predicted using the *nearshore* wave data, because of the increase in  $T_m$  in the approaches to the coast, and slightly lower armour sizes and overtopping rates were calculated in the cases of waves being depth-limited at the wall, compared to those with unlimited depth. The existing methods gave slightly higher overtopping rates than the new method, where both worked with joint exceedance extremes and an assumed constant wave steepness.

### Lower limit on wave steepness

The importance of wave period was dramatically demonstrated, in the form of much increased overtopping rates for the structure variable calculations using nearshore data where wave steepness was allowed to vary over a wide range about its mean value, based on the variability seen in the original data. To some extent this is a genuine effect, reflecting the existence of swell waves at the site, but it is over-emphasised in the results seen in Table 12. However, in practice this would be corrected by setting a lower limit on wave steepness in the synthesised data as seen in the much improved results in Table 14. The variability of the results illustrates the care that should be taken in selecting input data and methods of analysis and interpretation.

### Sensitivity to correlation coefficient

The three alternative BVN\_SV results shown in the three sub-columns on the right hand side of Table 14 illustrate the sensitivity to correlation coefficient. The lowest predictions are for ' $\rho = 0$ ', corresponding to independence between waves and water levels, and the highest are for ' $\rho = 1$ ', corresponding to complete dependence, with the best estimates being only a little higher than for independence. The independent predictions for return periods of 10 and 200 years correspond roughly to best estimate predictions for 5 and 50 year return periods, respectively. A factor of four difference in return period at this site corresponds to a difference of about a quarter of a metre in still water level, and perhaps a half a metre difference in sea defence level (allowing for the larger waves which could reach the wall at a higher water level. Conversely, the dependent predictions for return periods of 1 and 20 years correspond roughly to best estimate predictions for 10-50 and 800-3000 year return periods, respectively. This degree of overprediction for the design return period at this site would correspond to a difference of about two thirds of a metre of water level and perhaps a metre or so in sea defence level.

## **3.4 Issues raised during analysis of other data sets**

The new software has already been applied on a number of consultancy studies. This section gives an insight into some of the experience gained in applying the new methods.

### Tees Bay

The overtopping hazard was assessed at three different locations around the Tees Estuary. Wave conditions were calculated at the three locations using numerical models. Water level data from North Shields was converted to the sites of interest using factors based on differences in the tidal range. The conversion of the water level data to the Tees Estuary raised several important issues regarding wind and wave set-up.

Wind set-up is an increase in water level that occurs over a large area due to the direct effect of wind stress on the water surface. Wave set-up is a much more localised effect that causes increased water levels in the surf zone as waves break. It was thought that wind set-up would have been present in the measured water level data at North Shields, as it is a widespread phenomenon. However, the extent to which it should be included in the converted water level at the Tees Estuary was unclear. Wave set-up was thought to be excluded from the measurements, since tide gauges are generally placed with a view to excluding wave set-up.

As a result of this assessment tidal flow modelling was carried out to assess the extent of wind set-up at Tees Bay in relation to North Shields. An empirical formula was derived that allowed the water level data at Tees Bay to include the effects of wind set-up; additionally an allowance for wave set-up was made. As it transpired, the inclusion of these processes had little effect on the joint probability extremes as the wind was always from the west or south-west (ie off the land) at the time of the maximum measured water levels. However, there was a small positive correlation between large wave heights and overall water levels in the modified data, which was used in the subsequent analysis.

### Lyme Bay

JOIN-SEA was also used at a location in Lyme Bay where flood risk was to be assessed over an area comprising of several different sea defence structures. The JOIN-SEA method of extrapolating the joint

probability density and simulating a very large data set was beneficial here in treating the different risk elements in a consistent way. As in the Tees Bay study, considerable effort was concentrated on accurately assessing the water levels at the site of interest (POL, 1997, which provides extreme water level estimates for the whole of the UK was not available at the time of the study).

The nearest measured water levels to Lyme Bay (with sufficient length of data) are at Devonport, which is a considerable distance away. The tidal range changes significantly along this stretch of coastline, causing uncertainty in the interpolation of water level data to Lyme Bay. To overcome this problem, extremes at Devonport and Weymouth (to the east of Lyme Bay) were derived, and also variations in the spring range considered, before calculating factors to be applied to the measured Devonport data. The converted data was then compared to several months of measured water level data at the site of interest, which showed good agreement. However, this study highlighted the problems that can arise in 'moving' measured water levels along a stretch of coastline where the tidal range varies significantly, and reinforced the preference for having measured data directly at the site of interest.

An interesting point to make in passing is that it is not strictly necessary to 'move' the time series data, either on waves or water levels, from the measurement or prediction point to the point of application. It would be possible to determine the dependence between large waves and high water levels using data for a nearby location and then, as in the intuitive approach (see Section 1.4) to apply it at the new point of interest. However, it would still be necessary to determine the marginal extremes at the new point.

#### Korea

A consultancy project off the west coast of Korea provided a good opportunity to use the new software in environmental conditions that were considerably different to UK conditions. The wave and water level data were split into two seasons, summer and winter, and considered as two separate cases, since there is a distinct difference in climate between the two. The highest water levels were expected to occur in summer and the highest wave conditions were expected to occur in winter. The analysis for each of the two different data sets revealed a negative dependence between wave heights and water levels. This was thought to be feasible, if unexpected. However, as a conservative measure for the design calculations the relationship between the two variables was taken to be independent.

This study highlighted the requirement for a relatively long simultaneous data set. As the original three or four years of data was split into two populations, the length of the time series was effectively halved, thus creating a relatively short period of data on which to base the fitted distributions. There was therefore a greater than normal degree of uncertainty in the calculated design conditions, prompting the inclusion of a higher than average margin of safety allowance in the joint probability results.

#### Truro

Until now the only primary variables considered have been wave height and water level. However, there is no reason why JOIN-SEA cannot be used for different variables. With MAFF funding, HR Wallingford is currently involved in research into the prediction of extreme water levels in estuaries. In parts of many UK estuaries the combined effects of wave conditions, tidal surges and river discharges need to be considered. As part of the research JOIN-SEA has been used to assess the dependence between river flows and wave conditions, and river flows and tidal surges, as well as wave conditions and tidal surges.

Knowing the dependence between each pair of variables enables a three dimensional surface of combinations of wave height, tidal surge and river discharge, with a specified joint exceedance return period, to be plotted. Tests are currently under way to assess the applicability of such a method to determine extreme estuarine water levels using three-variable joint exceedance extremes.

Another method being considered, which is perhaps more in keeping with the JOIN-SEA approach, is to determine the correlation between each pair of variables and to use the results in a long-term simulation using the Tri-Variate Normal distribution. However, whichever approach is used, conversion of original

data on flow rate or wind speed to an equivalent increase in water level remains as a separate problem probably best addressed using hydraulic modelling.

### Humber Estuary

As part of a major strategy study, HR Wallingford undertook wave hindcasting at sixteen points within the Humber Estuary (based on 14 years of winds measured at Spurn Point) and a joint probability analysis based on water levels measured within the Humber. A number of interesting points are noted.

Although there are many tide gauges within the Humber, HR's client needed to undertake a spatial joint probability analysis (of tides and surges) similar to that described in POL (1997) in order to achieve the desired resolution in the water level data.

Although river flow and wind set-up will affect the water levels within the Humber, they were not explicitly accounted for in the joint probability analysis, since they would already be present in the measurements and in the spatial analysis based on those measurements.

The great majority of the records showed no dependence between wave heights and water levels, but for most of the prediction points a small handful of records showed large waves occurring simultaneously with high water levels. This rather uncertain indication of a significant correlation in the high tail of the distribution meant that some manual smoothing of the derived correlation coefficients was necessary to maintain spatial consistency between prediction points.

Analysis of extreme water levels based on over forty years of water level data in the Humber gave sufficiently different extreme values that refined values were determined by HR's client for use in re-scaling during the simulation (otherwise based on only fourteen years of data).

## **4. DISCUSSION**

### **4.1 Past practice for use of results in design**

#### Joint exceedance combinations

In the past, joint probability analysis has usually resulted in a range of combinations of wave heights and water levels, each with the same joint exceedance return period (and these 'design sea states' are a valuable output from the new method). Each combination is expected to be equalled or exceeded once, on average, in each return period. In designing or assessing a structure, one would need to ensure that it could withstand every 'design sea state' for the return period being used. In other words, for each structural response variable of interest, each combination of extreme water level and wave condition should be tested, to determine the worst case for that response variable. The return period of the value thus derived for the response variable (eg overtopping) will generally be less than the return period of the joint exceedance extremes, as illustrated in Figure 1 and discussed in the Lancaster University part of this report. This discrepancy between the two return periods is usually addressed by inclusion of a small margin of conservatism somewhere else in the assessment. A convenient method sometimes used in previous studies is to use marginal extreme wave conditions with the standard 3-hour event duration, as opposed to the 12-hour duration which is more strictly correct for extremes conditional upon being at high tide. The resulting wave conditions are then appropriately conservative.

#### Application of results at different locations

If the extremes are derived for a location other than the point at which they are to be applied, some adjustment of values may be necessary. The most obvious case is the need to modify wave conditions calculated offshore to allow for shallow water transformations prior to their arrival at coastal defences. However, where the extremes have been calculated for a large area, such as Christchurch Bay, it will also be necessary to modify the water levels from one end of the bay to another. The wave transformation may require a site-specific numerical model, but the water levels can usually be adjusted with reference to published values of tidal ranges at different locations. This remains a consideration in the new method.

### Allowance for trends and/or unrepresentative data

If the wave conditions or water levels are known to be subject to any long-term variations or if the period of measurements is known to be unrepresentative, then some allowance should be made for this. Short-term or long-term variations could be filtered out from the data before analysis begins. Alternatively, derived extremes could be adjusted to offset known unrepresentativeness. The most obvious example of long-term change is the expected rise in mean sea level due to global warming. The rate of rise is expected to be about 5mm per year for the foreseeable future, which should be incorporated into design and assessment of coastal defences. Other trends include increasing wave heights in the Atlantic, the tendency for the highest tides to occur at certain times of day and certain times of year, and the 18.6 year cycle for predicted tides. Again this remains a consideration in the new method, but one which is handled more neatly than in past approaches.

### Analysis of wave period

In the past, except where direct hindcasting of the response variable has been possible, wave period has not normally been considered as a separate partially independent variable. Any treatment of wave period has usually been based on the assumption that wave height and wave period are strongly dependent, perhaps being related by some standard wave steepness.  $(2\pi H_s/gT_m^2)$  is calculated for approximately the top one per cent of the wave data and the same steepness is assumed to be valid for the extreme wave conditions.

### Analysis of wave direction

Any treatment of wave direction is usually based on a 'conditional analysis', the condition being that the wave records analysed have directions within a particular angular sector. In other words, wave data within different direction sectors are considered as being members of different populations (perhaps with different wave steepnesses) which can be analysed separately. Ideally, the directional sectors should be chosen to correspond with the different populations of waves expected to occur at the inshore site of interest, taking account of aspects such as bathymetry, fetch lengths, headlands, dependence upon water depth etc. Each direction sector then provides separate and effectively independent sea conditions to be considered in any subsequent assessment. This approach to the use of wave direction is retained in the new method.

## **4.2 Advantages of the new approach**

### The main advantages

The new joint probability approach is potentially more objective, flexible and accurate than alternative methods currently used in consultancy studies, although preparation of the input data and assessment of the diagnostics for the statistical analysis requires experience. The new approach can provide all of the outputs available from alternative methods, eg marginal distributions and extremes, joint exceedance extremes, joint probability density, direct calculation of the distribution and extremes of structural response variables, and parameters of all fitted distributions. It can thus provide input to both 'design sea state' and 'risk-based' analyses of sea defences. Generally it performs at least as well as currently used methods, and in some tests gave significantly better estimates than existing methods, particularly at very high return periods. Specific advantages, relevant in the majority of applications, are:

1. Incorporation of the variability of wave period (or wave steepness) both in the analysis and in the simulation of long samples of data.
2. Assimilation into the analysis of improved marginal predictions based on additional (non-simultaneous) data on any of the variables.
3. More direct analysis of structural response function(s) such as run-up or overtopping, thereby addressing the risk of failure or damage more directly. Once the long-term simulation has been carried out, several

different structural response functions and/or different designs can be tested consistently and relatively easily.

#### More accurate sensitivity testing

Sensitivity to uncertainty in the environmental variables can be tested in a similar way. For example, assume that all wave heights could be under-predicted by 15% and all wave periods by 10%: sensitivity could be calculated easily and directly by repeating the structural response variable(s) calculations with suitable multipliers applied to all wave heights and periods. Uncertainty in the dependence level could be tested in a similar way. Although not so easy, the present approach would permit direct assessment of the sensitivity to a distribution of uncertainty in one or more of the input variables and/or the combined effect of uncertainties in more than one partially dependent variable.

#### Users and usage of the new approach

The methods are intended for use both by practising engineers and by researchers, although training, software and input data will be required. The amount of effort, experience and input data required is comparable with running a fairly sophisticated wave transformation model. The potential benefit of using the new joint probability approach (or something similar), as opposed to an intuitive estimate, is also comparable with the benefit of using a sophisticated wave model, as opposed to a simpler method.

#### The requirement for specialist data and programs

One disadvantage, common to all analytical approaches to joint probability, concerns the need for reliable simultaneous data on waves and water levels, the cost of which may not be justifiable in some applications. Another factor that may limit widespread adoption of the new methods is their reliance on specialist computer programs and training.

### **4.3 New possibilities based on long-term simulation**

#### The present 'design sea state' approach

A small number of design sea states for a particular location are often used in design and assessment of sea defences. These sea states might correspond to wave conditions with specified return periods or to combinations of wave conditions and water levels with given joint exceedance return periods. These design sea states may be applied to the calculation of different variables (eg overtopping, armour size etc) and to different types of sea defence. However, the same (or even higher) values of the structural response variables might occur, for example, during swell wave conditions with a lower wave height but with a longer wave period. The return periods of the calculated structural response variables will therefore not necessarily be the same as those of the corresponding design sea states.

#### An alternative approach based directly on the structural response variable(s)

A potentially better approach is possible based on long-term simulation of a wide range of sea states, from which the distribution and extremes of the structural response variable(s) can be determined directly. Once the long-term sea state data has been simulated, several structural response variables and/or defences could be assessed quite quickly, without needing to know the corresponding sea states: the probability of simultaneous failure mechanisms occurring could also be evaluated.

#### An alternative risk-based approach

Design and assessment could thus be done directly in terms of any structural response variable(s) of interest. Using this approach, it would not be necessary to determine a design sea state, but instead the design would be based more directly on the overall risk of structural damage and/or unacceptable overtopping etc. A further point is that if a number of alternative designs and a number of different failure modes are to be analysed, then the risk-based approach may be quickest. This would imply a major change in design practice, but it is consistent with a gradual move towards more risk-based design.

#### 4.4 Recommended options for joint probability analysis

There are a range of techniques available: from an intelligent choice of a single water level to use with established wave conditions to a rigorous joint probability assessment using long time series data; from a general offshore study which might be valid over a wide area to a site-specific prediction of overtopping volumes.

##### Quality of the input data

As well as being consistent with the overall project value, the effort put into any joint probability assessment is dependent on the quantity and quality of relevant field data. For example, there is little point in carefully assessing the 'actual' dependence between high waves and high water levels, if the input data is of fairly low quality, perhaps being drawn from intermittent anecdotal evidence. Around most of the UK coast, there is sufficient good quality wind/wave/tide data for a proper joint probability assessment to be carried out. To justify a rigorous approach (as opposed to an intuitive assessment), involving analysis of long time series data, about three or more years of good quality wave and tide data should be available. This amount of recorded wave data is very rarely available, but all around the UK there are several years of good quality sequential wind data, which can be used in wave hindcasting. However, some parts of the UK coast are so far from the nearest long-term tide recorder that it may be impractical to derive reliable local long-term water level data. Similarly, there are some parts of the UK where wave hindcasting may be rather uncertain, perhaps due to the mix of wind-sea and swell, or due to the complicated coastline. In these circumstances the effort involved in a full joint probability study may not be justified.

##### Simpler joint probability methods

In most coastal engineering projects it is worth giving some thought to joint probability, even if it does not justify a formal study. At the simplest level, an engineer might decide to test the design wave conditions at Mean High Water Springs (if waves and water levels are almost uncorrelated) or at Highest Astronomical Tide (if they are well correlated). Alternatively (or additionally) the independent and dependent cases for waves and water levels might be considered to determine the maximum range of uncertainty in water level for use with any given extreme wave condition. A better, but still empirical, approach would be to determine the degree of dependence between waves and water levels and then to apply the intuitive method described in the third paragraph of Section 1.4. The necessary 'correlation factor' can be estimated from general experience or with reference to earlier studies in the same area. (In view of the uncertainty, a conservative value should be taken, as the method itself is not inherently conservative). Armed with this 'factor', extreme combinations of waves and water levels (expressed in terms of their marginal return periods) can easily be determined. These approaches carry a wide margin of uncertainty in terms of joint return period, but they are better than not taking any account of joint probability and cheaper than a more rigorous study.

##### Rigorous joint probability methods

The main distinguishing feature of a 'rigorous' joint probability analysis is that the dependence function, and its variability with threshold, is determined analytically from simultaneous data on the variables concerned. For waves and water levels, about three years of simultaneous data are necessary to justify the additional effort of a rigorous analysis. (Regrettably, the cost of purchasing this data, even where it already exists in accessible format, can be prohibitive, so this should be checked at an early stage.) The present JOIN-SEA approach described in Chapter 2 analyses the marginal distributions of the separate variables, and the dependence function(s) linking them. It then simulates a much larger quantity of data with the estimated marginal and joint distributions, effectively extrapolating the joint probability *density*. From this data, extreme joint exceedance probability combinations, and extreme values of structural response variables, can be determined. The format also provides appropriate input to risk analysis methods. Extension of the JOIN-SEA approach to three variables has been demonstrated during ongoing research on extreme water levels in estuaries. HR's earlier JOINPROB analysis method was less flexible and a little less objective in deriving joint exceedance extremes, and is no longer in frequent use.

### Better knowledge of marginal extremes

The three basic inputs to joint probability analysis are the distribution of the first variable, the distribution of the second variable, and knowledge of the dependence between the two. There may be additional information on one or more of these three aspects, beyond that which is used directly in the *joint* probability analysis. The most common example is a better knowledge of extreme water levels, based on previous analysis of a longer period of data, than is available from analysis of the period for which there is both wave and water level data. The most convenient way of incorporating this additional information is by re-scaling of the results. For example if the shorter period of data is thought to under-predict extremes by 10cm, then all extreme values are simply increased by 10cm. JOIN-SEA allows this to be done smoothly, interpolating between different amounts of adjustment specified by the user, during simulation of the very large sample of sea state data.

### Offshore and inshore joint probabilities

When specifying a joint probability study, the coastal engineer should, of course, have regard to the intended range of use of the results. If all of the existing coastal defences within a large bay are to be assessed, then a general offshore wave and water level study is appropriate, resulting in combinations of water levels and offshore wave conditions with given return periods. The offshore conditions will then be transformed to the various inshore locations as and when needed. However, if only one inshore location is of interest, it is probably better to transform the time series wave data to the inshore location and to carry out the joint probability study directly at the inshore position. This has the advantages of assessing the dependence between high waves and high water levels directly where they are needed, and of providing wave condition results which are directly useful without further work. In some situations it may also be necessary to make local allowance for the effects of wind set-up, wave set-up, river flow and seiching, where this is not already represented in the water level data used for the analysis. It may also be necessary to consider the dependence of wave transformation on water level. A common example of this is where waves are strongly depth-limited at a sea defence and where more extreme water levels will permit higher waves to reach the structure.

### Inclusion of wave period and direction

For design sea states, expressed in terms of the joint exceedance probability of waves and water levels, wave conditions are usually represented solely by wave height, with wave period and direction being treated as secondary variables. Wave periods can be assigned based on a standard wave steepness, although it may be worth checking the sensitivity of the end calculations to wave period. The new JOIN-SEA approach analyses the distribution of wave steepness in the original data and allows wave period to vary as a function of wave height. This variation is then automatically included in JOIN-SEA's long-term simulation of sea conditions. If relevant, wave direction can be incorporated by means of separate analyses for each wave direction sector of interest.

### Direct calculation of structural response variable

If only one particular structural response is of interest, for example overtopping or force on a wall at one particular location, then that variable can be hindcast and extrapolated directly. This has the advantages of including wave period and direction as separate *independent variables*, and of providing results in 'single variable' format exactly where they are needed. Similarly, the long-term simulation part of JOIN-SEA will incorporate the variability of wave period, which can then be used in the calculation of structural responses such as overtopping. However, the engineer should be aware that it is not possible to infer the more general results from the more specific results.

### Note on the use of multi-valued results

It should be emphasised again that where joint exceedance analysis yields multiple combinations of wave conditions and water levels, each with the same return period, then the worst of these potential 'design sea states' should be adopted for design purposes. The particular combination may vary from one location to another and from one response parameter to another.

### Note on climate change

The most convenient and most common way to make allowance for expected future climate changes is to perform the joint probability calculations at today's values and then to modify the results as and when required for design calculations. For example, to allow for 0.25m of future sea level rise, simply add 0.25m to all water level results derived from the joint probability analysis. Trends are harder to identify and model. A possibility is to eliminate trend by converting all records to today's values before joint probability analysis, and then to incorporate trend by modifications to the results as suggested for future climate change.

### Summary

To summarise, consideration of the dependence between high waves and high water levels should never be neglected, where both variables are important. However, the scope of each joint probability assessment should be decided on its own merits, in terms of input data available, the intended end use, and the potential benefits to be derived. HR's present practice in consultancy studies involving joint probability analysis follows the recommendations above. Just over half of the studies are carried using the one of the methods outlined in the paragraph headed 'Simpler joint probability methods', with most of the remainder being undertaken using JOIN-SEA. Onshore or offshore wave data, wave period and/or direction, better knowledge of marginal extremes, joint exceedance extremes and/or structural response variables, and allowance for climate change, are included as and when appropriate.

## **4.5 Performance of the various techniques**

### Overall conclusions

Several example calculations and case studies are presented in both parts of this report, demonstrating the relative merits of the different approaches to joint probability assessment. All of the methods seemed to work satisfactorily, subject to their own limitations, mainly relating to the manner in which dependence and wave period were assessed (if at all). Overall, JOIN-SEA performed best, perhaps because of its rigorous analysis of dependence and its incorporation of variability in wave period, but still some care is required in operation and interpretation of results. Conclusions from individual comparative tests are given in Chapter 3 of this part of the report (field data) and in Chapter 10 of the Lancaster University part of this report (simulated data). Some of the main points are repeated here.

### Relative importance of different uncertainties

General experience suggests that uncertainties in wave conditions, uncertainties in water levels and uncertainties in dependence are of roughly equal importance in determining the overall uncertainty in sea defence design. However, recent advances in extreme water level prediction, together with the large amount of high quality data available around the UK, mean that uncertainties in water levels are probably lower than in wave conditions or dependence. A conclusion in the Lancaster University part of this report, based on analysis of simulated data sets, is that refinement of extreme wave conditions is more important than refinement of dependence modelling. However, this is partly due to the direct use of offshore wave conditions in structural response variable analysis, when in reality shallow water effects would usually have moderated them before arrival at sea defences. Where wave heights are depth-limited by breaking at sea defences, refinement of extreme water levels is probably the most important of the three aspects of joint probability analysis, followed by dependence assessment. Where shallow water effects are important but waves are not depth-limited by breaking, refinement of extreme waves and dependence are probably of about equal importance.

### Dependence modelling

JOIN-SEA's statistical models have sufficient flexibility and robustness to capture the features of the joint distribution of sea conditions producing extreme sea states for a range of observational and simulated data sets. As with all methods, experience is required in handling data sets which do not conform to expectations: examples are an unusually wide distribution of wave steepness or more commonly a very small number of severe sea states exhibiting high dependence within an otherwise uncorrelated data set. With care, it is possible to treat such data sets less subjectively using JOIN-SEA than with other methods tested during this project.

### Wave period modelling

The importance of wave period was demonstrated in both parts of this report. Where a standard wave steepness was applied to obtain the wave period to use with extreme combinations of wave height and water level, significantly different overtopping rates were predicted for a site-specific value of wave steepness compared to a 'global' value. The use of a global value tended to under-predict the overtopping rate, due to its sensitivity to wave period. The facility to allow a distribution of wave steepness within JOIN-SEA worked well, but some care is needed to prevent over-prediction of low steepness waves and consequent over-prediction of overtopping rate.

### The discrepancy between the joint exceedance and joint density approaches

In the joint distribution of wave height and water level there is a discrepancy between the probability associated with the joint exceedance extremes expressed in terms of combinations of wave height and water level, and the failure region associated with structural response variables. The probability of the combinations (the green and yellow square areas in Figure 1) is smaller than the probabilities of the corresponding responses (the red and blue rounded areas in Figure 1). This means that a worst case combination with a given joint exceedance return period will under-predict the response with the same return period. This effect is well known and, without being quantified, is usually assumed to be the equivalent of a factor of 2-3 in return period and to be offset by conservative assumptions elsewhere in the analysis procedure. Tests with the simulated data in the Lancaster University part of this report suggest a factor of 1½-2 in return period, whereas tests with field data in this part of the report suggest a higher value of 2-4. Direct use of structural response functions, where known, avoids this difficulty but introduces others.

### Direct comparison between JOINPROB and JOIN-SEA

The comparison of JOINPROB with JOIN-SEA in Section 3.2, using the combinations method of determining the worst case overtopping event and assuming the same value of wave steepness, shows good agreement at all sites. This suggests that the method of marginal extrapolation at varying thresholds, for both variables, to construct contours of equal joint exceedance return period, gives similar results to the extrapolation of the joint density, as used in JOIN-SEA.

### Comparison between joint probability and structure variable methods

In general, the newly developed joint probability methods are better than structure variable methods. This was not necessarily the case for existing joint probability methods as, unlike structure variable methods, they ignored variation in wave period. Analysis presented in Chapter 9 of the Lancaster University part of this report shows that it is possible to produce very erroneous extreme values by direct extrapolation of the structural response variable. However, similar analysis in Section 3.1 of this part of the report suggests that HR's existing approach to direct hindcasting and extrapolation of the structural response variable is reasonably robust and reliable in this example, although not as good as the new JOIN-SEA method.

### The importance of site-specific nearshore data

The Somerset case study in Section 3.3 illustrated the importance of local variations in wave conditions and dependence which might not be represented in a joint probability analysis using offshore conditions. Different overtopping rate predictions (in this case higher, due to the increased wave period) were obtained using nearshore wave data. Reduced overtopping predictions were obtained when waves were assumed to be depth-limited by breaking before arrival at the sea wall. A similar pattern was seen in the armour size calculations, but differences between nearshore and offshore wave data were less, due to its lower sensitivity to wave period.

### A practical illustration of the conclusions

Some of the conclusions can be summarised in more practical terms in the form of the following example. For locations with a small positive correlation between waves and water levels, the assumption of complete dependence between wave heights and water levels could lead to sea defence crest levels being designed up to about two metres too high. Conversely, the assumption of independence could lead to sea defence crest levels being set too low. More realistically a poor but deliberately conservative estimate of dependence

might result in a sea wall being designed about half a metre higher than if a more reliable analysis of joint probability had been undertaken.

#### **4.6 Availability of methods and staff time involved**

##### Usage of joint probability analysis within coastal engineering studies

Joint probability has changed over the last ten years from being a major element of a coastal desk study to being a fairly routine tool for use in most coastal studies. A coastal engineer who is capable of deriving extreme wave conditions and extreme water levels should also be capable of making an intelligent estimate as to how likely they are to occur together, once the principles have been understood. A more detailed assessment of dependence and joint probability requires more experience, specialist knowledge, and good data on waves and water levels. However, coastal engineers who are familiar with wave predictions and numerical techniques should be capable of carrying out their own assessments. A rigorous joint probability analysis using long time series data requires a large volume of data, experience, specialist software, and expertise in interpretation of the results.

##### Relative costs of different analysis methods

The cost of a joint probability assessment obviously varies depending upon how much input data has to be purchased and upon the particular circumstances of the study. However, to give an idea of the effort involved, the following numbers of days of experienced staff time are typical, including time for assimilation of data, checking of marginal extremes, and for interpretation and reporting:

- Intelligent estimate of dependence, leading to sensible water levels at which to test derived extreme wave conditions: ½ day
- Intuitive assessment of joint probability extremes, leading to a range of combinations of waves and water levels with given joint exceedance return periods: 2 days
- Rigorous assessment of joint probability extremes based on long time series data, leading to a range of combinations of waves and water levels, from different direction sectors, with given joint exceedance return periods: 5 days
- Rigorous site-specific derivation and extrapolation of force or overtopping, based on long time series data on waves and water levels: 5 days

The times given above refer to analysis at the first point within a study area. Each subsequent analysis point within the same area and same report would add only about one third to the staff time for the first point.

*Acquisition of data, and wave generation and transformation modelling are not included in the times given.*

##### Approaches now used at HR Wallingford

Joint probability analysis is a fairly standard requirement in UK coastal defence studies where overtopping may be an issue. It is a less common requirement in overseas studies. Around two thirds of HR's joint probability studies are undertaken using desk study methods (even in cases where wave or tidal flow models may be needed elsewhere in the project). For larger studies and for final design, a rigorous analysis is desirable, but the data purchase costs will often be prohibitive. A full analysis will not consistently either increase or decrease the best estimate of the required height for a sea wall, but it should reduce the uncertainty by 10-20cm. If the potential saving in construction cost is high compared to the cost of buying or generating the reliable time series data needed for a full analysis, then this would seem to be a cost-effective option.

Since about 1998, HR Wallingford has stopped using the earlier JOINPROB programs, and has switched entirely to the new JOIN-SEA methods. Results continue to be usually quoted in terms of joint exceedance extremes, but direct simulation of responses such as overtopping is sometimes used.

## 4.7 Future developments

### Ongoing research

The methods are continuing to be developed and applied within other MAFF-funded research at HR Wallingford. For example, the same statistical methods have been adopted for use within a project on extreme water levels, flows and waves in estuaries. As part of another ongoing project, the programs have been released for specialist beta-testing within the industry, which hopefully will lead to new developments and applications.

### Application to other variables

Most of this report deals with joint probability as it affects large waves and high water levels. However, it is worth mentioning that, in principle, the methods have wider application, for example to waves and winds, swell waves and storm waves, waves and currents, and water levels and river flows. However, it remains necessary to have good data on the marginal extremes, and sufficient data to estimate the dependence between the two variables. Also, the new programs are specific to wave heights and water levels, with wave periods as a related third variable, so some re-programming would be needed before use with other variables.

### Move from 'design sea state' to risk-based design

In the longer-term, the methods offer the chance to make a significant change to the way in which sea defences are designed and assessed. An accurate joint distribution of wave height, wave period and water level can now be constructed, applied and analysed with relative ease. It would be feasible to work directly in terms of the return period for different structural response functions (eg overtopping or force) on a range of sea defence options, without the need for the less direct 'design sea state' approach used at present. The risk-based approach may even be quicker to apply than the more traditional methods where a number of alternative designs and failure modes are to be considered.

## 5. REFERENCES

CIRIA (1996). *Beach management manual*. CIRIA Report 153.

CIRIA/CUR (1991). *Manual on the use of rock in coastal and shoreline engineering*. CIRIA Special Publication 83.

S G Coles and J A Tawn (1994). *Statistical methods for multivariate extremes: an application to structural design*. Applied Statistics.

HR Wallingford (1980). *Design of seawalls allowing for wave overtopping*. HR Report EX 924.

HR Wallingford (1994). *Validation of joint probability methods for large waves and high water levels*. HR Report SR 347.

HR Wallingford (2000). *JOIN-SEA user manual*. HR Report TR 71.

Ministry of Agriculture, Fisheries and Food (1995). *Joint probabilities - a workshop to further research*. MAFF Flood and Coastal Defence Newsletter, July 1995.

M W Owen, P J Hawkes, J A Tawn and P Bortot (1997). *The joint probability of waves and water levels: A rigorous but practical new approach*. MAFF Conference of River and Coastal Engineers, Keele.

Proudman Oceanographic Laboratory (1997). *Estimates of extreme sea conditions: Spatial analyses for the UK coast*. POL Internal Document No 112.



# ***Appendices***



# Appendix 1

Comparisons between joint exceedance extremes for different analysis methods

Figure A1: Christchurch

Figure A2: Dover

Figure A3: Dowsing

Figure A4: Cardiff (0-190°N)

Figure A5: Cardiff (190-360°N)

Figure A6: North Wales

Notes: 1) Dots show original data

2) Prediction points show joint exceedance extremes with given return periods



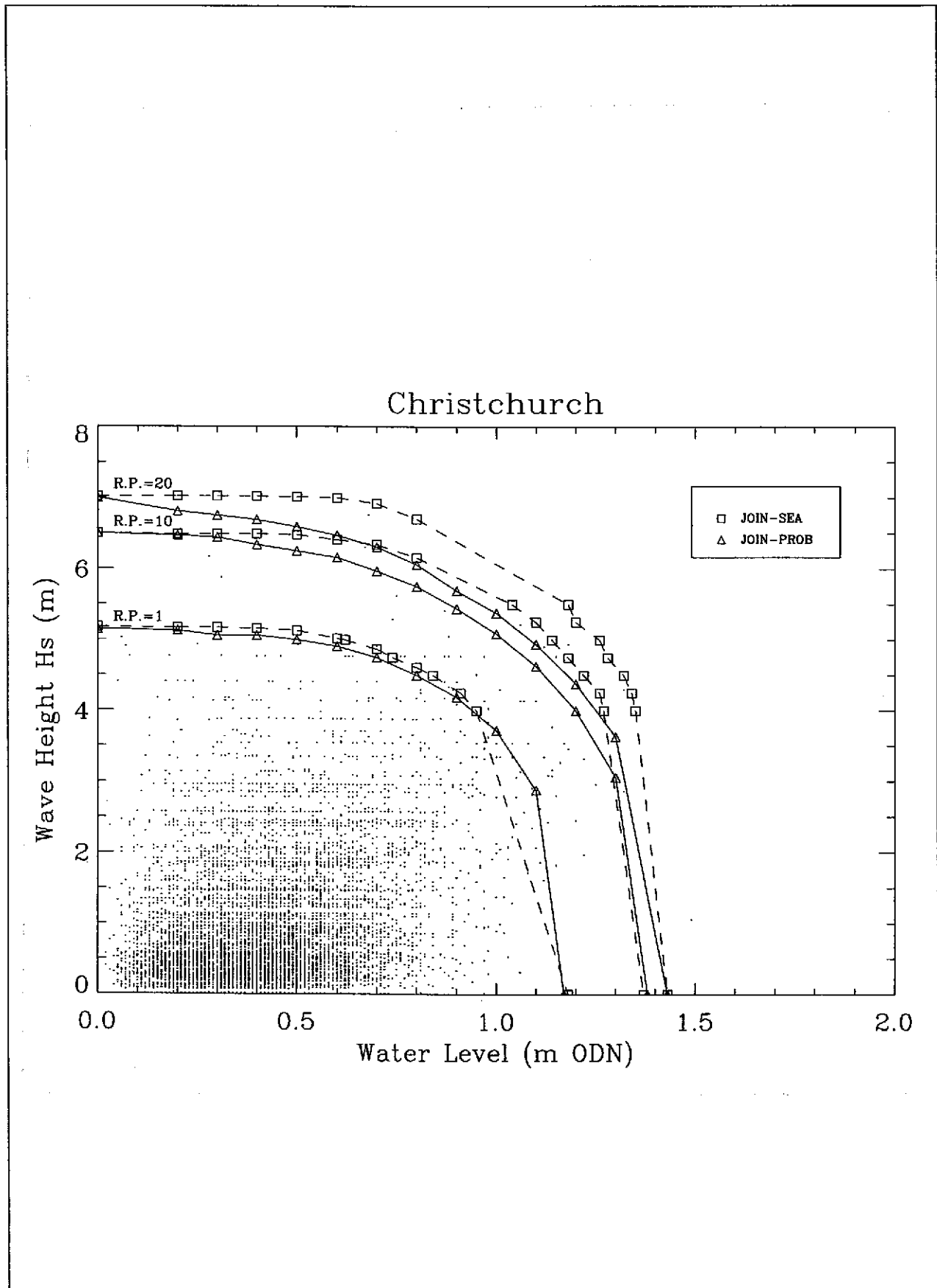


Figure A1 Christchurch

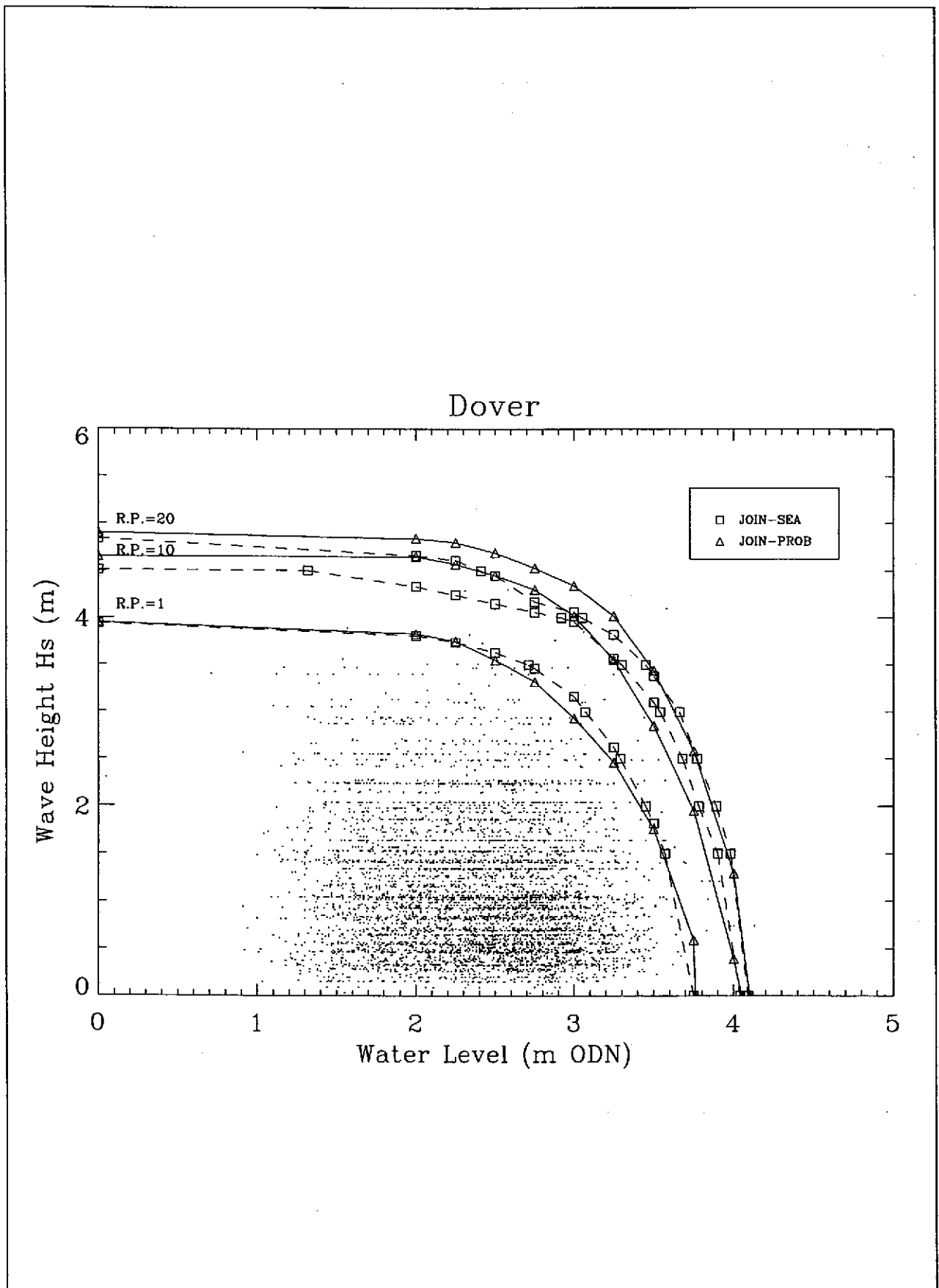


Figure A2 Dover

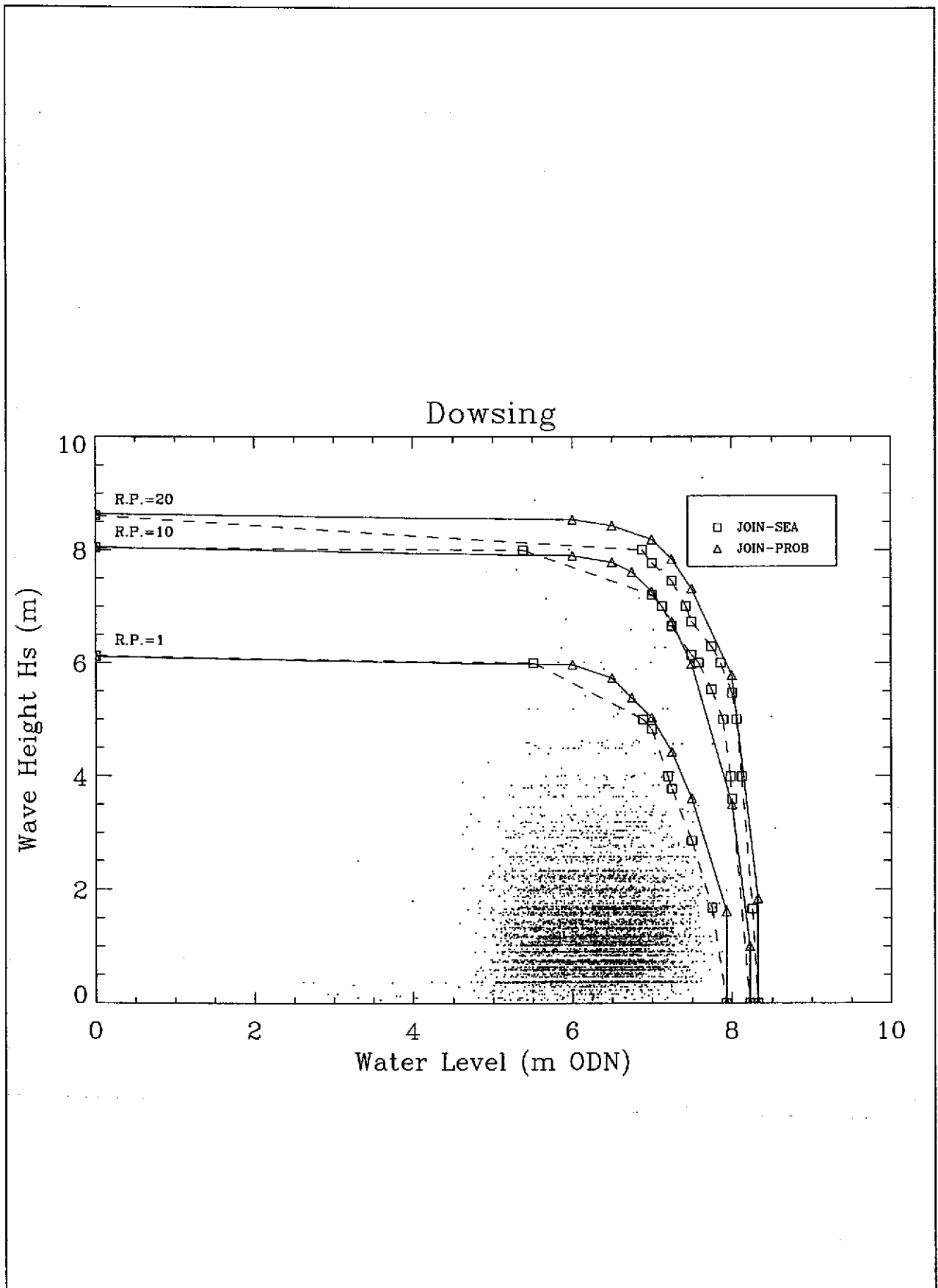


Figure A3 Dowsing

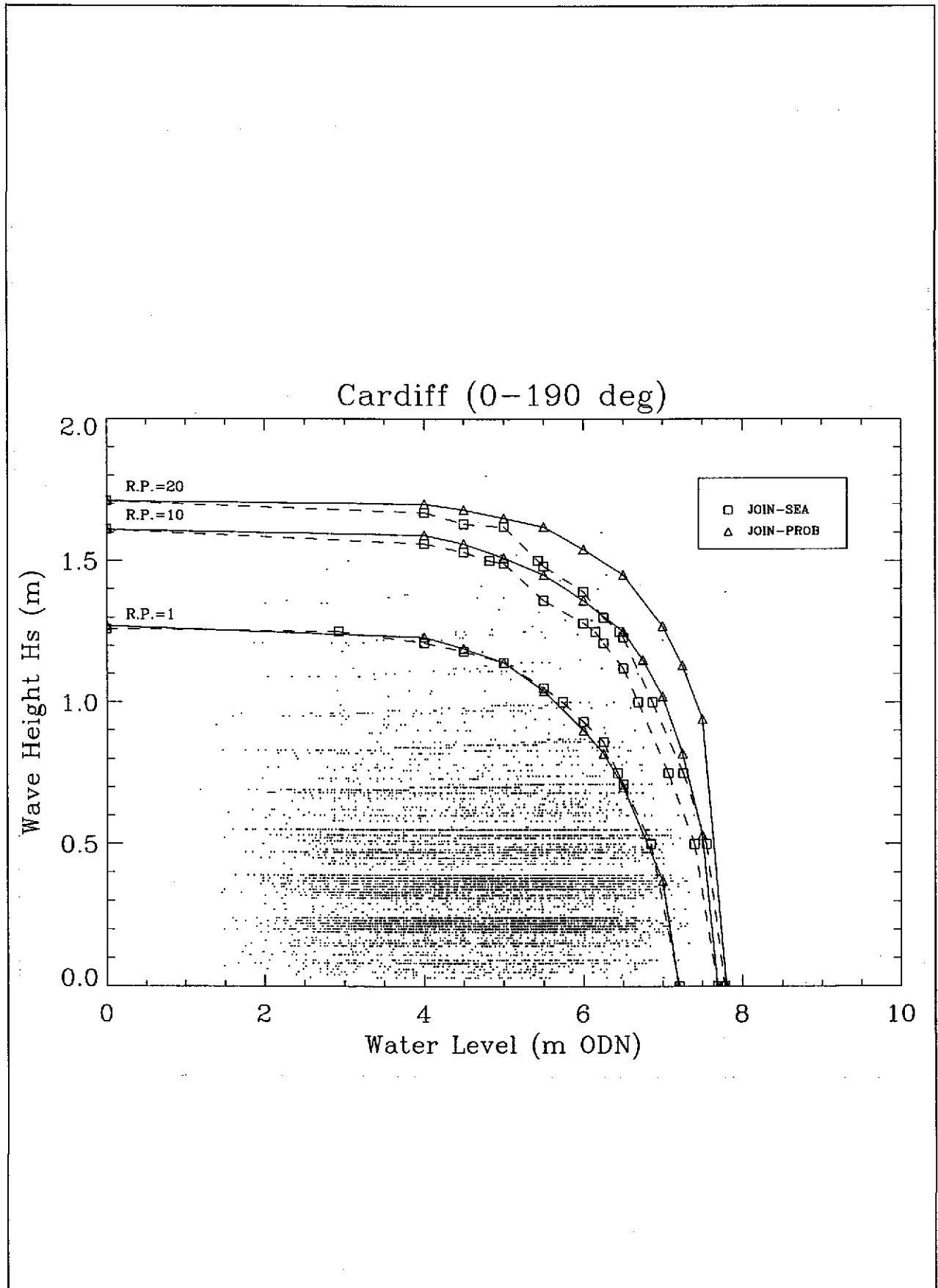


Figure A4 Cardiff (0-190°N)

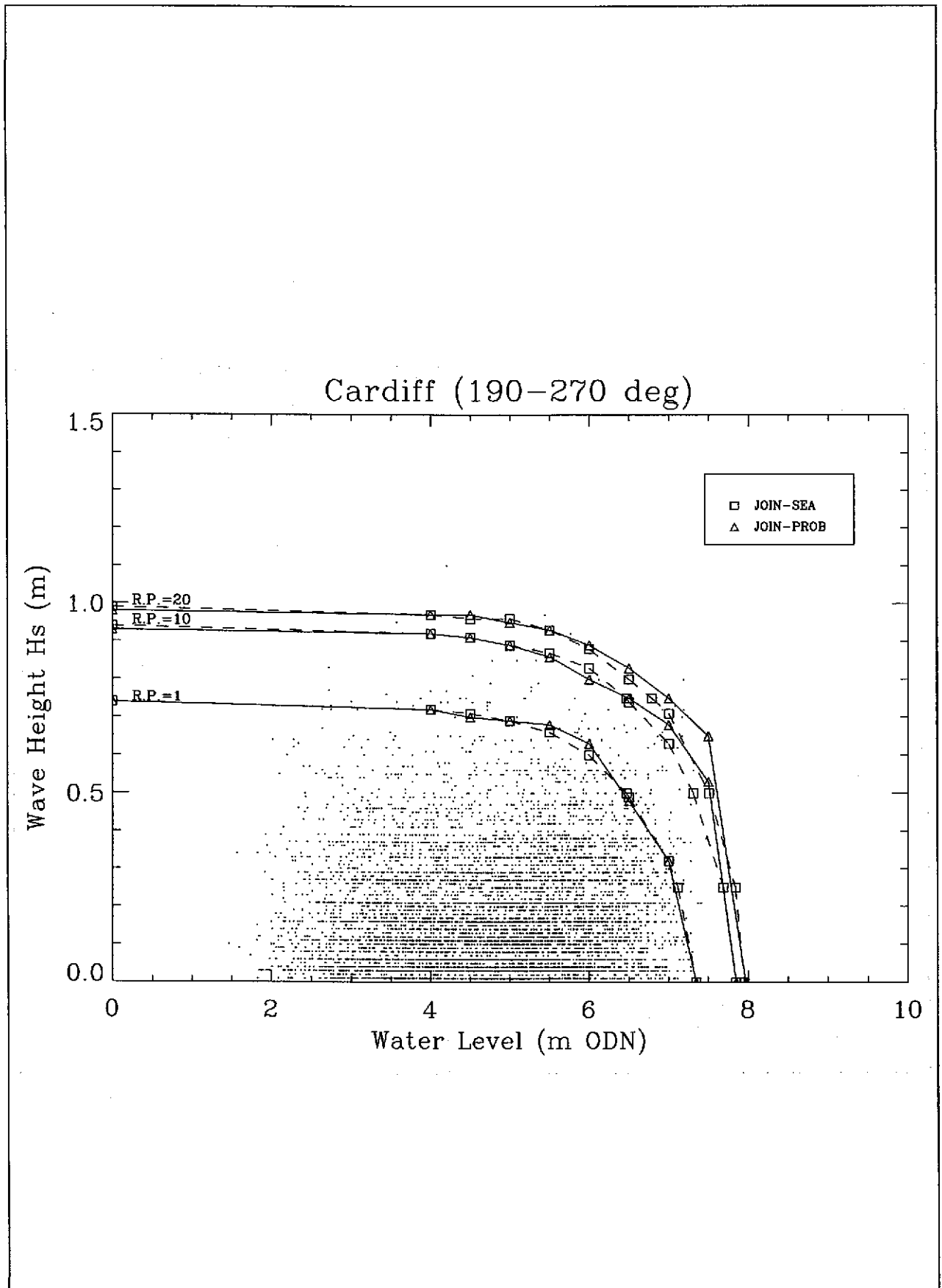


Figure A5 Cardiff (190-360°N)

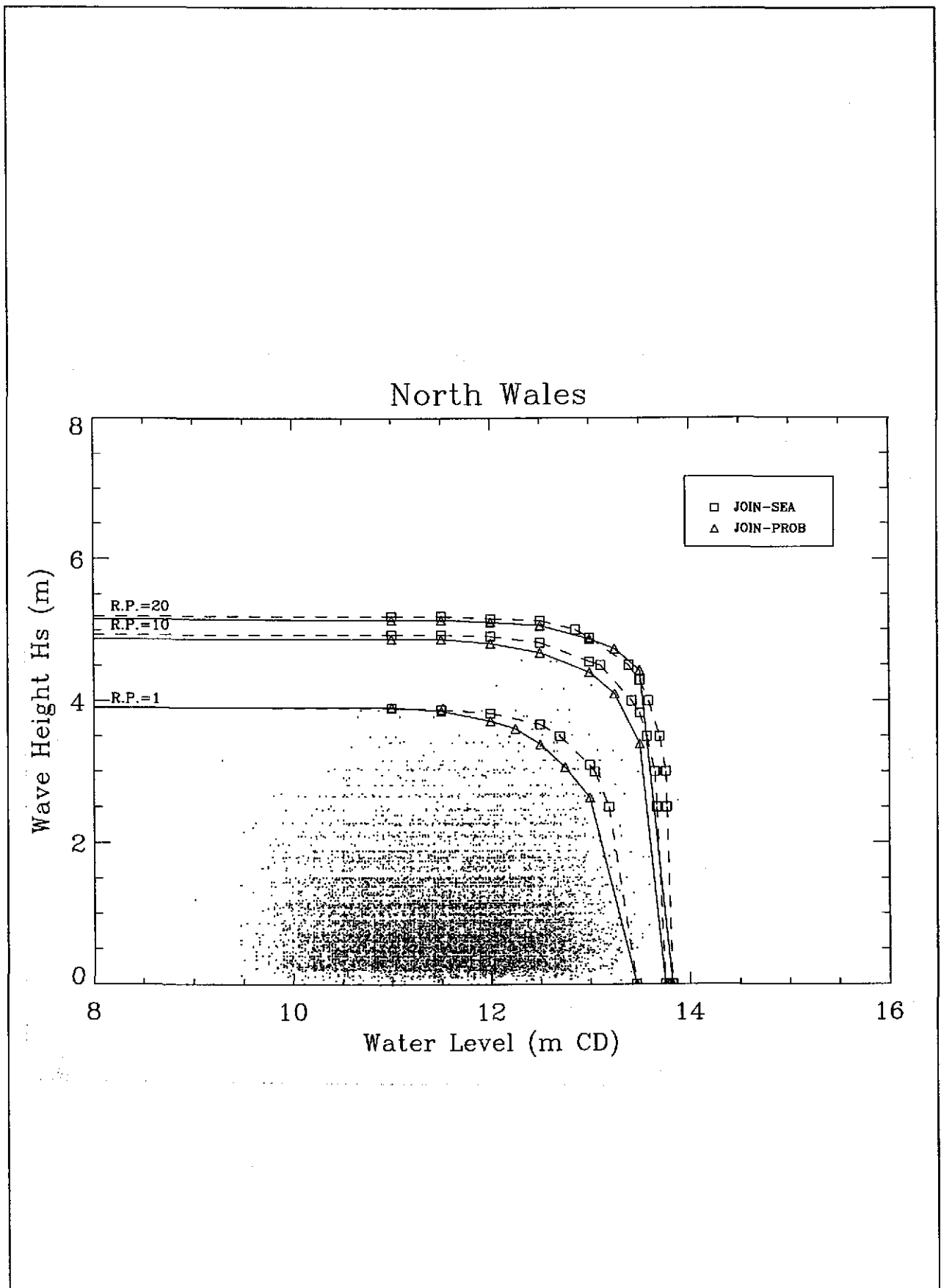


Figure A6 North Wales

## ***Part II Lancaster University Report***



**JOINT PROBABILITY METHODS FOR  
EXTREME STILL WATER LEVELS AND WAVES**

**Paola Bortot and Jonathan A. Tawn**  
*Department of Mathematics and Statistics,*  
*Lancaster University,*  
*Lancaster LA1 4YF.*

In collaboration with

**HR Wallingford.**

September 1997.



## CONTRACT

This report describes work funded by the Ministry of Agriculture, Fisheries and Food (Flood and Coastal Defence Division) under Commission FD0202 with HR Wallingford. HR's Nominated Officer was Dr S. W. Huntington. The Ministry's Project Officer was Mr A C Polson. Publication does not imply endorsement by the Ministry of the report's conclusions or recommendations.



# Contents

<b>1</b>	<b>Introduction</b>	<b>9</b>
1.1	Framework of the Study . . . . .	10
1.2	Current Implementation . . . . .	13
1.3	Comment on the Current Implementation . . . . .	14
1.4	Objectives . . . . .	15
1.5	Outline of the Report . . . . .	16
1.6	Good Statistical Practice . . . . .	17
<b>I</b>	<b>Theoretical Basis of the Joint Probability Method</b>	<b>19</b>
<b>2</b>	<b>Outline Statistical Methods</b>	<b>21</b>
2.1	Structure Variable Method (SVM) . . . . .	22
2.2	Joint Probabilities Method (JPM) . . . . .	23
2.3	Comparison of Methods . . . . .	24
<b>3</b>	<b>Extreme Value Methods</b>	<b>27</b>
3.1	Univariate Methods . . . . .	27
3.1.1	Annual maximum . . . . .	27
3.1.2	Threshold methods . . . . .	29
3.1.3	Properties of the GPD . . . . .	30
3.1.4	Threshold selection for GPD . . . . .	31
3.1.5	Goodness-of-fit for GPD . . . . .	31
3.1.6	Temporal dependence and non-stationarity . . . . .	32
3.2	Illustrative Dependence Examples . . . . .	33
3.2.1	The structure function of the minimum . . . . .	33
3.2.2	The structure function of the maximum . . . . .	34
3.3	Multivariate Methods . . . . .	35
3.3.1	Models . . . . .	35
3.3.2	Diagnostics . . . . .	40

3.3.3	Illustrative examples . . . . .	41
3.4	Technical Calculations . . . . .	42
3.4.1	Independence . . . . .	43
3.4.2	Bivariate extreme value dependence . . . . .	43
<b>4</b>	<b>Statistical Models used for JPM</b>	<b>45</b>
4.1	Marginal Statistical Models . . . . .	45
4.1.1	Still Water Level . . . . .	46
4.1.2	Significant Wave Height . . . . .	46
4.1.3	Steepness . . . . .	51
4.1.4	Wave Direction . . . . .	52
4.1.5	Wave Period . . . . .	52
4.2	Dependence Models . . . . .	56
4.2.1	Models for dependence between $SWL$ and $H_S$ . . . . .	59
4.2.2	Models for dependence between $H_S$ and $S$ . . . . .	62
4.3	Evaluation of the Probability of Failure using the JPM . . . . .	63
 <b>II Examples of Data Analysis using the Joint Probability Method</b>		 <b>67</b>
<b>5</b>	<b>Study Data</b>	<b>69</b>
5.1	Observational data . . . . .	69
5.2	Simulated data . . . . .	70
5.3	Principal differences between the simulated data sets . . . . .	75
5.4	Comparison of observed and simulated data . . . . .	76
<b>6</b>	<b>Marginal Estimation</b>	<b>89</b>
6.1	Still Water Level . . . . .	89
6.1.1	Observational Data . . . . .	89
6.1.2	Simulated Data . . . . .	95
6.2	Surge . . . . .	96
6.2.1	Observational Data . . . . .	96
6.2.2	Simulated Data . . . . .	101
6.3	Significant Wave Height . . . . .	101
6.3.1	Observational Data . . . . .	101
6.3.2	Simulated Data . . . . .	120
6.4	Steepness . . . . .	120
6.5	Wave Direction . . . . .	124

<b>7</b>	<b>Dependence Estimation</b>	<b>127</b>
7.1	$(SWL, H_S)$ Dependence . . . . .	127
7.1.1	Observational data . . . . .	127
7.1.2	Simulated data . . . . .	136
7.2	$(S, H_S)$ Dependence for Simulated Data . . . . .	148
<b>8</b>	<b>Simultaneous Extremes of <math>(SWL, H_S)</math></b>	<b>161</b>
8.1	Marginal distributions known . . . . .	163
8.1.1	Comparison with current implementation . . . . .	170
8.2	Marginal distributions unknown . . . . .	175
8.2.1	Comparison with current implementation . . . . .	182
<b>III Applications to the Estimation of the Probability of Failure for an Existing Design</b>		<b>185</b>
<b>9</b>	<b>Analysis of Overtopping Discharge Rates</b>	<b>187</b>
9.1	Background Methods . . . . .	188
9.2	Application to Sim1 . . . . .	190
9.3	Application to Sim2 . . . . .	193
9.4	Application to Sim3 . . . . .	196
9.5	Application to Sim4 . . . . .	199
9.6	Application to Sim5 . . . . .	203
9.7	Comment on Current Implementation Results . . . . .	207
9.8	Other Figures . . . . .	207
<b>10</b>	<b>Comparisons and Conclusions</b>	<b>217</b>
<b>11</b>	<b>References</b>	<b>219</b>
<b>A</b>	<b>Background information</b>	<b>221</b>
A.1	Joint Distributions . . . . .	221
A.2	The Normal Distribution . . . . .	223
A.2.1	Univariate Normal Distribution . . . . .	223
A.2.2	Multivariate Normal Distribution . . . . .	223
A.3	The Probability Integral Transform . . . . .	226
A.4	Likelihoods for Dependence Models . . . . .	226
A.4.1	Bivariate Normal Model . . . . .	227
A.4.2	Bivariate Normal Threshold Model . . . . .	227

A.4.3 Mixture of Bivariate Normals . . . . .	229
--	-----

## Notation

### Structure parameters

$\Delta$ : the structure function, which links the sea condition variables to the variable of interest (the structure variable).

$Y_t$ : the structure variable at time  $t$ .

$Q_C$ : the overtopping discharge rate (an example structure variable).

$\mathbf{X}_t$ : the (multivariate) sea conditions, at time  $t$ , for generality taken to be  $d$ -dimensional, but usually consisting of  $(SWL, H_S, T_Z, \theta, S)$  listed below.

$A_u$ : failure region for  $\mathbf{X}$ , corresponding to the set  $\{\mathbf{x} : \Delta(\mathbf{x}) \geq u\}$ .

### Input variables

$SWL$ : still water level.

$Surge$ : non-tidal component of still water level.

$H_S$ : significant wave height.

$T_Z$ : (zero mean crossing) wave period.

$\theta$ : (predominant) wave direction.

$S$ : wave steepness.

### Distributions, densities and probabilities

$f_X(x)$ : the (marginal) density function of  $X$  evaluated at  $x$ .

$F_X(x)$ : the distribution function of  $X$  evaluated at  $x$ , i.e.  $\Pr\{X \leq x\}$ .

$\Phi(x)$ : the distribution function of a standard Normal (Gaussian) random variable.

$f_{\mathbf{X}}$ : the joint density function of  $\mathbf{X}$ .

$\hat{f}_{\mathbf{X}}$ : the estimated joint density function of  $\mathbf{X}$ .

$F_{\mathbf{X}}(\mathbf{x})$ : the joint distribution function function of  $\mathbf{X} = (X_1, \dots, X_d)$ , i.e.  $\Pr\{X_1 \leq x_1, \dots, X_d \leq x_d\}$ .

$\bar{F}_{\mathbf{X}}(\mathbf{x})$ : the joint survivor function of  $\mathbf{X}$ , i.e.  $\Pr\{X_1 > x_1, \dots, X_d > x_d\}$ .

$\Pr(A)$ : the probability of event  $A$  occurring.

$\hat{\Pr}(A)$ : the estimated probability of event  $A$  occurring.

### Statistical Models and parameters

$\text{GPD}(\sigma, \xi)$ : the generalized Pareto distribution with scale parameter  $\sigma$  and shape parameter  $\xi$ , used as a model for excesses over a threshold.

$\text{GEV}(\mu, \sigma, \xi)$ : the generalized extreme value distribution with location parameter  $\mu$ , scale parameter  $\sigma$  and shape parameter  $\xi$ , used as a model for maxima.

$y_p$ : the return level with return period of  $1/p$ .

$\hat{y}_p$ : the estimated return level.

*BVN*: a bivariate normal distribution which has correlation parameter  $\rho$ .

$u$ : a threshold used in both marginal and dependence modelling.

Threshold *BVN* model: a model for the joint extremes which is of bivariate normal form with correlation,  $\rho_u$ , which depends on the threshold used to define a joint extreme.

Mixture of *BVN* model: a model for the dependence structure which is a mixture of two separate *BVN* models with potentially different correlations. The probabilities of the two *BVN* models in the mixture are  $p_M$  and  $1 - p_M$ .

### Transformed variables

$S^*$ : wave steepness variable transformed to follow a standard normal distribution.

$H_g^*$ : significant wave height variable transformed to follow a standard normal distribution.

### Diagnostics

$T(z)$ : a sample based diagnostic statistic, which is used to assess when a conservative dependence estimate, of complete dependence between the variables, can be used without substantial over-estimation.

# Chapter 1

## Introduction

Since 1991, MAFF have funded a study of joint probability methods at HR Wallingford. HR have developed practical methods of estimating the degree of correlation between waves and water levels for practising engineers to apply to the design of coastal flood defences. Under a separate MAFF-funded project, the Proudman Oceanographic Laboratory and Lancaster University have developed statistically rigorous methods for estimating the joint probability of tides and surges, and more generally, techniques for handling joint probabilities of extremes of any environmental variables. However, these rigorous methods can only be applied by specialist statisticians.

In previous work by Michael Owen, whilst at HR, joint probability methods were identified as being important in estimating the probability that coastal flooding occurs, as this is determined by overtopping discharge rates (given by sea-levels and waves) rather than by sea-levels alone.

In August 1994 MAFF hosted a Workshop on joint probability chaired by Michael Owen. As a result of the Workshop HR and Lancaster University submitted a joint research proposal to MAFF entitled *The use of joint probability data on waves and water levels in coastal engineering applications*. This proposed a 2 year study starting April 1995.

- During the first year Lancaster University would concentrate on developing generally applicable statistical techniques and software, suitable for eventual use by non-specialists for extrapolation in joint probability problems. These methods were to be tested on synthesised data and the results compared with those obtained using HR's existing methods.
- The second year would see further refinement of these techniques and extensive application in practical studies at HR.

MAFF funded this project with the aim of bringing together the best aspects of existing approaches, combining statistical rigour with engineering practicality, to provide more powerful tools for routine use by practising engineers and consultants. This report describes the work in the first year of the study focusing on the progress at Lancaster University into producing rigorous yet applicable methods.

## 1.1 Framework of the Study

When considering the design of a new sea-wall, or other sea defence, or when assessing the safety offered by an existing design, a key step is the estimation of the probability that the design fails to protect against extreme sea conditions. This probability assessment is a four stage process:

1. the selection of a design (either the existing design or one based on some preliminary analysis),
2. the identification of all possible types of failure for that design – the modes of failure,
3. for each mode of failure, the identification of the combinations of sea condition variables which cause failure,
4. the estimation of the probability of these combinations which give failure.

There are a number of modes of failure, such as

- overflow – when the water level exceeds the level of the crest of the defence,
- overtopping – when the combined effect of waves and water levels results in waves running up and breaking over the defence,
- structural failure such as severe damage to rock armour revetment or erosion of an embankment leading to the formation of a breach

For any particular mode of failure we term the associated variable of interest the **structure variable**. Generally the structure variable is related to the **sea conditions**

- tide,
- surge,
- significant wave height,
- wave period (here taken to be zero mean crossing period),

- wave direction (here taken to be predominant wave direction),

via the function  $\Delta$ , which we term the **structure function**. Thus

$$\text{structure variable} = \Delta(\text{tide, surge, significant wave height,} \\ \text{wave period, wave direction})$$

A more useful notation is that, at time  $t$ , we have sea conditions,  $\mathbf{X}_t$ , and the structure variable  $Y_t$ , with

$$Y_t = \Delta(\mathbf{X}_t) \text{ for all } t.$$

Here  $\mathbf{X}_t$  is multivariate (5-dimensional),  $(X_{1,t}, \dots, X_{5,t})$ , with  $X_{1,t}$  denoting the tide,  $X_{2,t}$  denoting the surge,  $X_{3,t}$  denoting significant wave height,  $X_{4,t}$  denoting wave period, and  $X_{5,t}$  denoting wave direction.

Throughout the study the methods that are developed apply to any mode of failure/structure function. However, to illustrate the methods in application we consider only overtopping as the mode of failure and take the structure variable to be the overtopping discharge rate. For this example the structure function is

$$\Delta(\mathbf{X}) = a_1 g X_3 X_4 \exp\{-a_2(v - X_2 - X_1)/[X_4(gX_3)^{1/2}]\}, \quad (1.1.1)$$

for a sea-wall of height  $v$  and where  $g$  is the acceleration due to gravity. This form was suggested by Hydraulics Research Station (1980) based on wave tank studies for a simple type of sea-wall. Here the sea-wall is a sloping design and the constants  $a_1$  and  $a_2$  in equation (1.1.1) depend on the characteristics of the sea-wall design. From equation (1.1.1) it is clear that overtopping will occur only if at least one of the variables

- still water level,  $X_1 + X_2$ ,
- significant wave height, or
- wave period

is sufficiently large.

*Aside: note that for this study the structure function ignores the directionality of the waves but wave direction is retained in the sea condition vector  $\mathbf{X}_t$  to aid the latter statistical modelling of the joint distribution of the other sea condition variables. Similarly, the decomposition of the still water level into tide and surge components is not essential other than to aid the statistical modelling.*

Now, the probability of some critical discharge rate,  $u$  say, being exceeded at time  $t$  is given by

$$\Pr\{Y_t \geq u\}.$$

In terms of the sea conditions  $\mathbf{X}_t$  we can re-write this probability as

$$\begin{aligned}\Pr\{Y_t \geq u\} &= \Pr\{\Delta(\mathbf{X}_t) \geq u\} \\ &= \Pr\{\mathbf{X}_t \in A_u\},\end{aligned}$$

where the set  $A_u$  corresponds to all combinations of the  $\mathbf{X}_t$  variables which lead to values of the structure variable which exceed  $u$ , i.e.

$$A_u = \{\mathbf{x} : \Delta(\mathbf{x}) \geq u\}.$$

We term the set  $A_u$  the **failure region**. Note that every combination in the failure region is not equally likely, for example moderately large still water levels and waves may give the same discharge rate as an extreme still water level with small waves, but one of these combinations will be more likely than another depending on the joint distribution of  $\mathbf{X}$ .

Motivated by the two forms for expressing the probability of the structure variable exceeding a critical level, i.e. a design failure occurring, two statistical methods have been proposed for estimating this probability, or the design parameters, in practice. These methods are:

### 1. Structure Variable Method

The sea condition data are used to construct a series of structure variable data. These structure variable data are extrapolated to more extreme levels, via a statistical model for the distribution of the structure variable.

### 2. Joint Probabilities Method

The sea condition data are themselves extrapolated to more extreme combinations. This is achieved via a statistical model for the joint distribution of the sea conditions. The probabilities of interest for the structure variable are then inferred by integrating the joint distribution over the failure region.

There are three key distinctions between the methods:

1. The variable extrapolated: the structure variable in the structure variable method, and the sea conditions for the joint probabilities method.
2. The use of the structure function beyond the data: this knowledge is ignored by the structure variable method but, if known, can be fully exploited by the joint probabilities method.
3. The generality of the analysis: the statistical extrapolations for the structure variable are specific to the site, design, and mode of failure under consideration, whereas for the joint probabilities method the design and site-specific features are excluded from the extrapolation as they are features of the structure function. Thus the statistical analysis for the joint probabilities method applies to any design analysis.

A consequence of these features is that the joint probabilities method is generally the preferred approach by both statisticians and design engineers but has the drawback of additional complexity, specifically the dimensionality of the extrapolation of the sea condition variables, which requires both

- extrapolation of the separate sea condition variables
- extrapolation of the dependence between the sea condition variables.

In this study we will develop both these methods for problems involving the estimation of the probability that overtopping discharge rates exceed critical levels.

## 1.2 Current Implementation

HR and consultant coastal engineers currently implement versions of both the structure variable and joint probability methods for clients and for internal research in a routine fashion (Hawkes and Hague, 1994).

### Structure Variable Method

Application of this method involves the use of the structure function, e.g. equation (1.1.1), which is viewed to be the most appropriate for the design under consideration. Data on the structure variable are used to extrapolate to more extreme events using statistical methods similar to those used in this report.

### Joint Probabilities Method

There are a number of levels of sophistication at which this method is currently applied. Here we review only the two most rigorous.

The approach currently used involves a number of stages.

1. The joint distribution of still water level,  $SWL$ , and significant wave height,  $H_S$ , is evaluated by estimation of the probabilities

$$\Pr\{SWL > x, H_S > y\}$$

for all  $x$  and  $y$  in which either  $x$  or  $y$  are large levels of the respective variables.

2. The wave steepness (a function of wave period and significant wave height) is taken to be a constant value. This constant is estimated as the average wave steepness value of the largest 1% of significant wave heights (or some standard value is taken).
3. The structure variable value associated with each  $(x, y)$  pair above is now evaluated. This evaluation requires the use of a wave period which can be inferred from  $y$  and the estimated constant wave steepness value.

4. The probability of the structure variable exceeding the level  $u$  is taken to be estimated by

$$\max \Pr\{SWL > x, H_S > y\}$$

where the maximum is taken over all combinations of  $(x, y)$  such that the resulting structure variable value is  $u$ .

A more refined version of this method follows the format above with certain steps modified as below:

- 1'. The probability  $\bar{F}(x, y) = \Pr\{SWL > x, H_S > y\}$  is estimated as above and from this the probability of  $(SWL, H_S)$  falling in a rectangular cell  $[x_0, x_1] \times [y_0, y_1]$  is obtained by

$$\Pr\{x_0 \leq SWL \leq x_1, y_0 \leq H_S \leq y_1\} = \bar{F}(x_0, y_0) + \bar{F}(x_1, y_1) - \bar{F}(x_0, y_1) - \bar{F}(x_1, y_0).$$

- 2'. Sometimes variation of the steepness of the waves is accounted for. Usually by trying different values of  $S$ .
- 3'. Step 3 is unchanged.
- 4'. The probability of the structure variable exceeding the level  $u$  is given by the sum of the cell probabilities over those cells for which the corresponding  $(SWL, H_S)$  pair, when combined with the constant wave steepness value, give a structure variable exceeding  $u$ .

### 1.3 Comment on the Current Implementation

There are three features which may potentially limit the accuracy of results obtained using the joint probabilities method as currently implemented. These features are not a restriction for the structure variable method.

1. The estimation of the joint probability  $\Pr\{SWL > x, H_S > y\}$  is essentially based on statistical estimates for the separate variables combined by an empirical estimate of the dependence between the variables. When both  $x$  and  $y$  are large it is well-known in statistical theory that such empirical estimates can be poor.
2. Wave period is taken to be given exactly by the significant wave height and the estimated constant wave steepness value. Waves with longer periods for a given wave height can occur and these will typically produce larger values of the structure variable. Sometimes in applications of the refined method this restriction is overcome by incorporation of variations in  $S$ .
3. A feature of the more basic current approach is that the failure region used to estimate the probability of failure,  $\Pr\{\mathbf{X} \in A_u\}$ , is a subset of the true failure region  $A_u$ . Thus, even if the joint distribution of the sea condition variables was

accurate, the probability of failure would be under-estimated by current methods. To illustrate this feature, ignoring wave period, the current method takes the failure region to be approximated by  $\{SWL > x, H_S > y\}$  for some suitably chosen  $(x, y)$ . All the elements of this set give a structure variable value which exceeds some level  $u$  say. However, this set does not contain all  $(SWL, H_S)$  values which give a structure variable greater than  $u$ . For some  $SWL > x$  with  $H_S \leq y$ , and for some  $SWL \leq x$  with  $H_S > y$ , the structure variable will exceed  $u$ . These potential failure values are excluded from the failure region leading to a biased estimate.

From work prior to the commencement of this project it was unclear how important any of these deficiencies/approximations in the existing methods were. They may cancel each other out, or they may cause additive errors. However, even if the errors are additive, the approximation may be sufficiently good to obtain the optimal design.

The only evidence prior to the project comes from inconsistent outputs from current implementations of the structure variable method and the joint probability method. Different approaches have been used from time to time, dependent on budget, availability of input data and intended end use of the results. However, when differences have arisen it has not been clear whether the discrepancy lies in the estimates provided by the structure variable method, due to its poor extrapolation features, or is due to the weaknesses in the implementation of the joint probability method. This feature has resulted in some doubts about the given estimates.

## 1.4 Objectives

This study proposes to examine each of the two statistical methods as aids to design assessment. The methods will be developed generally and applied, as an example application, to the estimation of the probability of overtopping discharge rates exceeding critical levels. In so doing, the study objectives are:

- To develop more fundamentally rigorous methods for analysing the dependence between still water level and wave extremes and improve the handling of the wave steepness component of the statistical model. These modifications should remove the statistical inadequacies in the current 'practical' approach and also lend themselves to application by practitioners;
- To remove any inconsistencies between the approaches in terms of the derived probability of failure, i.e. through using the same structure function/failure region for each method;

- To identify and comment on situations where the two most often used current versions of the joint probability method work well and those where they are poor;
- To incorporate the most up-to-date information on the separate distributions of extreme still water level and significant wave height;
- To provide statistical output directly usable by coastal engineers to assess probability of failure for the mode of failure under consideration;
- To validate the methods on simulated and observational/hindcast data sets.

The way that we shall approach a simple solution to the problem is to adopt the rigorous framework of Coles and Tawn (1994) but instead of using their complex statistical models for dependence in the extreme joint tail of the distribution we shall explore a much simpler but more flexible approach based on use of the multivariate normal distribution for the sea condition variables after suitable transformation. This differs from the Coles and Tawn approach where multivariate extreme value distributional models are used after a different marginal transform.

## 1.5 Outline of the Report

The report comprises three distinct parts. In Part I the theoretical basis for the joint probability method is given. In Part II the estimation of the joint distribution of the sea condition variables is considered for observational and simulated data. Finally in Part III we illustrate the use of the joint probability method to give the distribution of extreme values of the structure variable by application to the problem of estimating the probability of the overtopping discharge rate exceeding a critical level.

More explicitly, Part I contains the following: Chapter 2 gives a general review of the two statistical methods (structure variable and joint probability) and compares their properties. In Chapter 3 background information is given into the statistical methods used for extreme value modelling in univariate and multivariate problems. For multivariate problems we examine the importance of the degree of dependence and the form of the failure region in determining the probability of failure. Chapter 4 contains the details of the marginal and dependence statistical model components of the joint probability method. Also in Chapter 4 the evaluation of the probability of interest from the joint probability method is discussed.

Part II starts by introducing the study data sets in Chapter 5. Observational data from 6 sites and 5 data sets simulated from known statistical models are described. These data are studied throughout Chapters 6–8, where the methods developed in Chapters

2–4 are applied to these data. Specifically, for both types of data set, in Chapter 6 each of the separate sea condition variables is analysed with different statistical models being considered; in Chapter 7 the dependence between extremes of the sea condition variables is analysed; and in Chapter 8 the joint extremes of still water level and significant waves are estimated.

Part III comprises Chapter 9 where the distribution of the overtopping discharge variable is derived from both joint probability and structure variable methods. A key feature in this context is the assessment of the impact of extra knowledge on the separate sea condition variables on the estimation of the distribution of the structure variable. This chapter compares the structure variable and joint probability methods relative to each other and against the methods used by coastal engineers. For the simulated data the joint distribution of the sea condition variables is known (given in Chapter 5) so the true distribution of the structure variable (e.g. the overtopping discharge rate) can be inferred. Thus the true performance of the methods can be assessed for the simulated data. In Chapter 10 some conclusions are presented. Throughout, all technical statistical details have been kept to a minimum, with details when necessary given in a technical appendix.

## 1.6 Good Statistical Practice

There is a recognised standard framework for good statistical practice when modelling data using statistical techniques. This framework is

- Use of valid data
- Use of all available information
- Incorporation of scientific knowledge
- Rationally chosen statistical models
- Efficient method of inference
- Assessment of sensitivity
- Quantification of uncertainty
- Variety of ways of communicating results

In many applications the quality of the data, or the purpose of the investigation, sometimes lead to deviations from this framework. In this study when we have deviated

from the framework we have tried to follow the rationale behind the framework. The particular area where this study is weak, is on the quantification of uncertainty. There are three sources of uncertainty:

1. the data (as waves are typically hindcast)
2. the choice of statistical model
3. the estimation of the parameters in the statistical model.

The latter is given by standard errors of parameter estimates. The second is partially assessed by comparison of different models, but we make no attempt to address the former. Since the study was aimed at assessing whether there were gross errors in the existing methods, rather than whether they are close to optimal in terms of mean square error criteria, we have not given standard errors for most parameter estimates.

## **Part I**

# **Theoretical Basis of the Joint Probability Method**



# Chapter 2

## Outline Statistical Methods

When assessing the probability of failure for a single sea condition variable, the events which give failures are easily characterised as failures of the structure caused by extreme values of the variable, i.e. failures occur whenever the variable exceeds some level. When the sea condition variable is inherently multivariate evaluation/estimation of the probability of failure is more problematic as there is no general ordering which determines which are extreme values. However, given the context of the problem, a natural approach is to base the ordering on the associated structure variable, since a failure is deemed to have occurred, in a multivariate problem, if the structure variable,  $\Delta(\mathbf{X})$ , exceeds some critical level.

An added complication to the problem is that a design may have to satisfy several different design criteria, i.e. withstand the extremes of several structure variables. For simplicity we will focus on there being a single design criterion. The work in the second year of the project will extend this framework to more general cases.

Therefore for a structure function  $\Delta$ , where failures occur when  $\Delta(\mathbf{X}) > u$ , the extreme values of  $\mathbf{X}$  are the set  $A_u$ , given by

$$A_u = \{\mathbf{x} : \Delta(\mathbf{x}) \geq u\}.$$

In this project  $\Delta$  will be taken to be a general structure function until Part III of the report where it is taken to be given by equation (1.1.1) for overtopping discharge rates.

Now, in general, the probability of failure at some time  $t$  say, is given by

$$\begin{aligned} \Pr\{\mathbf{X}_t \in A_u\} &= \Pr\{\Delta(\mathbf{X}_t) \geq u\} \\ &= \Pr\{Y_t \geq u\}, \end{aligned}$$

where  $Y_t = \Delta(\mathbf{X}_t)$  is the structure variable. The left and right hand sides of the above equation provide alternative formulations for the probability of failure. Starting from each of these expressions in turn provides the basis for the derivation of the two statistical

approaches to the estimation of the probability of failure in multivariate problems where a design exists or has been specified. Working from the right hand side determines the **structure variable method**; whereas working from the left hand side determines the **joint probabilities method**.

In describing these methods below we will suppose that

- the observations of each of the processes under study are identically distributed through time, that is the distribution of observations remains the same whatever the time of the year.
- complete observations are available on the vector of sea conditions at each time.

These are reasonable assumptions, as

1. Observations are approximately independent as we focus on only high water levels, so observations are separated by 12 hours;
2. Observations are approximately identically distributed, at least over the winter storm season. This is a better assumption for the surge variable than the still water level as the long term non-stationarity induced by the astronomical tide is still present (e.g. the nodal cycle of 18.61 years);
3. Complete observations are available as the wave data are hindcast over the same time periods as the tide and surge data are available.

## 2.1 Structure Variable Method (SVM)

The structure variable method is an approach to the estimation of the probability that a given design fails. It is based on the statistical analysis of derived observations on the structure variable of interest for the given design, i.e. suppose there is a variable of interest  $Y$  which is a function  $\Delta$ , the structure function, of the vector of sea condition variables  $\mathbf{X}$ ,

$$Y_t = \Delta(\mathbf{X}_t) \quad (2.1.1)$$

for  $t = 1, \dots, n$ , where  $n$  is the number of observations. In practice we have observations of  $\mathbf{X}_t$  but not  $Y_t$ . Given  $\Delta$ , the approach involves two steps:

1. Create the structure variable,  $Y$ , of interest using equation (2.1.1) for the entire time series of sea condition observations.
2. For the time series  $\{Y_t, t = 1, \dots, n\}$  of the structure variable, use a suitable statistical model to extrapolate the series to the appropriate return level. This can involve either of two possibilities:

- Fitting a probability distribution to the entire sample of the structure variable.
- Fitting a statistical tail model to the extreme values of the structure variable, using techniques of the form outlined in Chapter 3.

The choice of which of these approaches to use depends on how simple the true distribution of the structure variable is. Clearly what is needed in practice is a good fitting statistical model which can be accurately estimated and extrapolates well. The method to choose is the approach which most adequately meets these criteria in practice.

Of the two approaches discussed above, generally the second is preferable, as the former is most influenced by observations in the bulk of the distribution which have no influence on the form of the tail of the distribution, and so is liable to give poor fits to the tail. An alternative viewpoint is that fitting a statistical model to the extremes of the sample only is wasteful of data. This is certainly true if a good statistical model for the whole distribution can be found.

For the example structure variable we consider in this study, we use the tail modelling approach for the structure variable of overtopping discharge rate. A key reason for this choice is that for most  $t$  we have  $Y_t = 0$ , i.e. no discharge, so it is only valuable to model the statistical distribution of discharge conditional on there being a discharge.

Once a distributional model has been fitted to the structure variable data then extrapolations can be obtained from the fitted statistical model in the standard method by solving the equation

$$\Pr\{Y \geq y_p\} = 1 - p$$

for the *return level*  $y_p$ , given a suitably chosen exceedance probability  $p$ .

## 2.2 Joint Probabilities Method (JPM)

The joint probabilities method is an approach for estimating the probability of a structure variable exceeding a critical level, based on the joint analysis of the sea condition variables,  $\mathbf{X}$ , from which the distribution of the structure variable can be inferred. The estimated joint distribution of the sea condition variables,  $\mathbf{X}$ , is of much wider use at the design stage of a sea-wall/structure as this can be used to aid the selection of a provisional form for the design which once selected is subjected to a more detailed probability of failure analysis using the full JPM. Here the focus is on the use of the estimated joint distribution of sea conditions for evaluating the probability of failure for a selected design.

If  $f_{\mathbf{X}}$  is the joint density of the sea conditions and  $A_u$  the failure region of  $\mathbf{X}$  (e.g. when the structure variable is overtopping discharge rates this corresponds to sea condition

combinations which give overtopping discharge rates exceeding  $u$ ), then the approach involves three steps:

1. Estimation of the joint density  $f_{\mathbf{X}}$  of the sea condition variables. This requires a selection of a statistical model for
  - the distribution of each of the  $d$  ( $d = 5$ ) separate variables,  $X_i, i = 1, \dots, d$ ,
  - the dependence between the components of  $\mathbf{X}$ .

We denote this estimate of  $f_{\mathbf{X}}$  by  $\hat{f}_{\mathbf{X}}$ .

2. Evaluation of the estimated probability of failure,  $\hat{\Pr}\{\mathbf{X}_t \in A_u\}$ , from the estimated joint density,  $\hat{f}_{\mathbf{X}}$ , using the relationship

$$\hat{\Pr}\{\mathbf{X}_t \in A_u\} = \int_{A_u} \hat{f}_{\mathbf{X}}(\mathbf{x}) d\mathbf{x},$$

i.e. integration of the estimated joint density over the set  $A_u$ .

3. Conversion of this estimate of the probability of failure from an observational scale to the annual scale. Since there are  $n_{yr}$  ( $n_{yr} = 705$ ) independent observations of  $\mathbf{X}$  over a year, we have that

$$\begin{aligned} \hat{\Pr}\{\text{no structure variable exceeds } u \text{ in a year}\} &= \hat{\Pr}\{\mathbf{X}_t \notin A_u \text{ for } t = 1, \dots, n_{yr}\} \\ &= \left(1 - \int_{A_u} \hat{f}_{\mathbf{X}}(\mathbf{x}) d\mathbf{x}\right)^{n_{yr}}. \end{aligned}$$

## 2.3 Comparison of Methods

The structure variable (SVM) and joint probability methods (JPM) outlined above can be used to address exactly the same design questions, however they are based on quite different assumptions. The validity of these assumptions compared with the simplicity of use determine which of these approaches should be used in practice. Specifically, features of the methods which influence selection of the approach are:

- Simplicity,
- Extrapolation properties,
- Flexibility to cover different designs,
- Requirements and exploitation of data,
- Useful input and output information.

In more detail these features are:

## Simplicity

The SVM is much the simpler to use as the statistical component of the method is routine relative to the JPM. For the SVM the analysis and extrapolation is for one variable only, the structure variable, whereas for the JPM analysis extrapolation is required for each of the separate sea condition variables and for the dependence between the separate variables.

## Extrapolation properties

When extrapolating the distribution of the structure variable the SVM makes no assumption about the form of the structure function beyond the observed data. Therefore information about more extreme structure variable values can only be inferred from the observed distribution of the largest structure variable values, i.e. a purely statistical extrapolation. By comparison the JPM extrapolates the sea condition variables and then builds in knowledge of the structure function beyond the data when integrating the joint density. This omission of the knowledge of the structure function from the extrapolation of the SVM can influence to the extrapolation as shown by the following example.

If  $\Delta_1$  and  $\Delta_2$  are two structure functions, which are such that  $\Delta_1(\mathbf{x}_t) = \Delta_2(\mathbf{x}_t)$  for all  $t = 1, \dots, n$  then the associated observations on the two structure variables are identical. Applying the SVM to the two data sets gives identical extrapolations even though  $\Delta_1$  and  $\Delta_2$  may be quite different outside the observed range of the data. These differences in  $\Delta_1$  and  $\Delta_2$ , if known, are incorporated into the JPM through the use of different failure regions over which the common joint density of sea conditions is integrated.

## Flexibility to cover different designs

If a number of structure functions are to be considered covering a range of designs for one site or neighbouring sites, or different modes of failure for a given design, then the whole statistical analysis (i.e. including the extrapolation of the structure variable) has to be repeated for each structure function for the SVM, whereas a single statistical analysis is required by the JPM with different integrations of the fitted joint distribution ( $\int_{A_u} \hat{f}_{\mathbf{X}}(\mathbf{x}) d\mathbf{x}$ ) as the failure region  $A_u$  will be different for each design (but  $f_{\mathbf{X}}$  is independent of the design). As the JPM separates statistical extrapolation from the specification of the structure function/failure region it is much more economical on effort when many designs are considered. Additionally, at the stage of the selection of a provisional form of

a design a detailed statistical analysis is too computationally intensive for each possible design. Typically, infeasible designs are eliminated from consideration by applying methods such as those described in Section 1.2. Here the estimated joint distribution of the sea condition variables is required, hence the JPM estimate of this joint distribution can be used, so aspects of this method can be used in design selection.

## Requirements and exploitation of data

To be able to create data on the *structure variable*, simultaneous observations are required on each of the sea condition variables. If, for any time period, we have observations on a subset of the sea condition variables then these cannot be utilised by the SVM, however these incomplete data may provide valuable information about the separate sea condition variables which the JPM is able to exploit. An extreme example is when there are no simultaneous observations of the sea condition variables, so no structure variable data, yet the distribution of separate sea condition variables can be estimated, and the dependence inferred from other neighbouring sites, so the JPM can still be used to assess the probability of failure.

## Useful input and output information

For both waves and still water levels much independent research has provided accurate information on the distribution of these separate sea condition variables. This information cannot be exploited by the SVM but is a valuable input to the JPM. A by-product of the JPM is that considerable additional information about the processes under study is obtained in the form of return levels for each of the separate sea condition variables, and knowledge of the *dependence structure* between the sea condition variables.

In conclusion, the SVM is much the simpler of the two methods to apply but has drawbacks concerning the requirement to have simultaneous data on the sea condition variables, and the necessity to assume that the form of the structure function does not change beyond the data. The JPM is difficult to implement which has often led to independence or complete dependence being assumed. However if it is properly applied the JPM is preferable since it separates the statistical analysis from the oceanographic and engineering component of the assessment of the probability that the structure variable is extreme and hence has wider applicability.

# Chapter 3

## Extreme Value Methods

In this chapter we briefly overview the extreme value methods and ideas that provide a basis for the joint probability and structure variable methods of Chapter 2. Specifically:

**univariate methods** for analysis of

- structure variable data in the SVM,
- the separate marginal variables in the JPM;

**multivariate methods** for the dependence analysis in the JPM.

There is much literature on the subject but the most suitable reviews are Davison and Smith (1990), Smith (1989) and Tawn (1992) *on univariate extremes*, and Coles and Tawn (1994) and Ledford and Tawn (1996) for multivariate extremes.

### 3.1 Univariate Methods

Consider a sequence of random variables which have the same distribution at each time point, i.e. they are identically distributed. Here we will consider the distribution of the annual maximum of these variables and the distribution of exceedances of a high threshold.

#### 3.1.1 Annual maximum

The distribution of the maximum, after normalisation, of such a sequence of size  $n$ , as  $n \rightarrow \infty$ , is the generalised extreme value distribution, GEV. This characterisation of the limit distribution is subject to the minimal requirement that observations of the process which are well separated in time are approximately independent (see Leadbetter, Lindgren and Rootzen, 1983). These conditions will typically be satisfied by all the sea condition

variables (and hence also the structure variable). If  $Y$  follows the  $GEV(\mu, \sigma, \xi)$  distribution it has distribution function

$$\Pr\{Y \leq y\} = \exp\{-[1 + \xi(y - \mu)/\sigma]_+^{-1/\xi}\},$$

where the notation  $s_+$  denotes  $\max(s, 0)$ . The three parameters of this distribution are:

- $\mu$  a location parameter,
- $\sigma$  a scale parameter ( $\sigma > 0$ ),
- $\xi$  a shape parameter.

The level,  $y_p$ , exceeded with probability  $p$ , i.e. which satisfies  $\Pr\{Y > y_p\} = p$ , is given by

$$y_p = \mu + \sigma\{-\log(1 - p)\}^{-\xi} - 1/\xi,$$

so  $y_p$  is the return level for return period  $1/p$  time units.

The key property of the GEV for applications is that it is the asymptotic distribution of the maximum of a sample whatever the distribution of the original observations. Thus if interest is only in the extreme values then this whole family can be fitted instead of trying many candidate distributions to fit the original observations. Furthermore the theoretical justification for the GEV provides a basis for extrapolation beyond the data to long return period events.

The application of the GEV distribution typically involves taking the annual maximum values in a sequence of relevant variables as following a GEV distribution. Using annual maximum data, the three parameters of the distribution are fitted using maximum likelihood, or some equivalent statistical method of fit, to give estimates  $\hat{\mu}$ ,  $\hat{\sigma}$  and  $\hat{\xi}$ . The justification for using annual maximum data is that there are a large number of observations within a year which justifies the use of the limiting distribution, the distribution has been found to work well in practice principally due to its flexibility, and because it removes the potential for seasonal bias. The estimated return level, with return period  $1/p$  years, is then

$$\hat{y}_p = \hat{\mu} + \hat{\sigma}\{-\log(1 - p)\}^{-\hat{\xi}} - 1/\hat{\xi}.$$

The biggest drawback in using the GEV applied to annual maximum data is that it is wasteful of data: the number of data points to base the estimation on corresponds to the number of years of data (often less than 10). An alternative approach is to use all the large values in the sequence, not just the annual maximum observations. In the following section we review such approaches.

### 3.1.2 Threshold methods

In this section a brief description of one of the most commonly used methods for the statistical analysis of extreme values is given. This method is referred to in the literature as the *Threshold Method* (Davison and Smith, 1990, for example) and is found to be both flexible and widely applicable. In essence, the Threshold Method consists of fixing a threshold,  $u$  say, and fitting a suitable distribution to the values which exceed  $u$ , while ignoring observations below  $u$ . The main components of this procedure are the threshold  $u$  and the distribution of the exceedances of  $u$ .

Let  $\{X_i, i = 1, \dots, n\}$  denote the sequence of observations, which are assumed to be independent and identically distributed,  $\phi$  denote the vector of unknown parameters, and  $g_\phi$  denote the density function of the distribution  $G_\phi$  adopted to describe the exceedances over  $u$ . Under these assumptions, the marginal distribution of  $X$  (a typical observation from the sequence) is

$$P(X \leq x) = G_\phi(x)P(X > u) + \{1 - P(X > u)\}, \quad \text{for } x > u.$$

Letting  $\lambda = P(X > u)$ , it follows that the likelihood function associated with the Threshold Method is given by

$$L(\lambda, \phi) = (1 - \lambda)^{n-N} \lambda^N \prod_{i \in I} g_\phi(X_i), \quad (3.1.1)$$

where  $I = \{1 \leq i \leq n : X_i > u\}$ ,  $N$  is the number of elements of  $I$ , i.e. the number of exceedances of the threshold  $u$ . The parameters  $\phi$  and  $\lambda$  are estimated by maximum likelihood, which involves maximizing the likelihood,  $L(\lambda, \phi)$ , with respect to the unknown parameters. Sometimes,  $\lambda$  is unconstrained and treated as a parameter of the statistical model (see below); in this case, the maximum likelihood estimate of  $\lambda$  is  $N/n$ , i.e. the proportion of exceedances of the threshold. In other situations,  $\lambda$  is explicitly linked to the parameters of the exceedance distribution (cf. Section 4.1.2).

So far no mention has been made of how to choose  $G_\phi$ , and, in fact, no unique specification for  $G_\phi$  can be given, unless the true distribution is known.

However, based on essentially the same asymptotic arguments that justified the use of the GEV for the annual maximum above, it can be argued that the natural family of distributions to use in order to describe the excess levels of observations above a high threshold is the generalised Pareto distribution (Pickands, 1975). That is, if the threshold  $u$  is sufficiently high, the conditional distribution of a random variable  $X$  given  $X > u$ ,

$$P(X \leq x | X > u) = \frac{F(x) - F(u)}{1 - F(u)}, \quad x > u, \quad (3.1.2)$$

with  $F$  being the true distribution of  $X$ , can be well approximated by the generalised Pareto distribution,  $\text{GPD}(\sigma, \xi)$ , with distribution function

$$1 - \{1 + \xi(x - u)/\sigma\}_+^{-1/\xi}, \quad \text{for } x > u, \quad (3.1.3)$$

where  $s_+ = \max(s, 0)$ . The two parameters of this distribution are:

- $\sigma$  ( $\sigma > 0$ ) is a scale parameter
- $\xi$  is a shape parameter.

A special case of this distribution is the  $\text{GPD}(\sigma, 0)$ , i.e. when  $\xi = 0$ : this is the exponential distribution with distribution function

$$1 - \exp\{-(x - u)/\sigma\}, \quad \text{for } x > u.$$

To fit this statistical model we let  $G_\phi(x)$  be the distribution function given by equation (3.1.3) with  $\phi = (\sigma, \xi)$  and we leave  $\lambda$  unconstrained. Maximum likelihood estimates of  $\sigma$  and  $\xi$  are obtained by maximising equation (3.1.1).

Despite the GPD having a theoretical justification as a distribution for the exceedances of a high threshold, this does not exclude the possibility of employing a different parametric statistical model, as will be done in Section 4.1.2, where the threshold approach is applied to wave heights, with  $G_\phi$  given by the *Truncated Weibull Distribution*.

### 3.1.3 Properties of the GPD

A key property of the GPD is that it is invariant to the threshold level.

Let  $X$  denote the values which exceed  $u$ , and suppose that  $X - u$  follows a  $\text{GPD}(\sigma, \xi)$ . Then, for  $x > 0$ ,

$$\begin{aligned} \Pr\{X - \tilde{u} \leq x | X > \tilde{u}\} &= 1 - \frac{[1 + \xi(\tilde{u} + x - u)/\sigma]_+^{-1/\xi}}{[1 + \xi(\tilde{u} - u)/\sigma]_+^{-1/\xi}} \\ &= 1 - [1 + \xi x/\sigma^*]_+^{-1/\xi} \end{aligned} \quad (3.1.4)$$

which corresponds to a  $\text{GPD}(\sigma^*, \xi)$ , where  $\sigma^* = \sigma + \xi(\tilde{u} - u)$ . Thus excesses of the higher threshold,  $\tilde{u}$ , are also GPD.

There is a direct relationship between the GPD and the GEV distributions. Davison and Smith (1990) show that if there are  $n$  observations in a year, each with the probability  $\lambda$  of exceeding the threshold  $u$ , and where excess values of the threshold are  $\text{GPD}(\sigma, \xi)$  then

$$\Pr\{\text{annual maximum} \leq x\} = \exp\{-\lambda n[1 + \xi(x - u)/\sigma]_+^{-1/\xi}\} \text{ for } x > u.$$

This is a GEV distribution with location, scale and shape parameters

$$u + \sigma\{(n\lambda)^\xi - 1\}/\xi, \sigma(n\lambda)^\xi \text{ and } \xi$$

respectively. Comparing parameters, we see that the GEV and GPD shape parameters are identical. This property helps to explain the potential benefits of the Threshold Method as the parameters of the GPD give the GEV parameters yet can be estimated from all large values rather than just annual maximum values. Consequently the GPD approach should provide improved precision of estimates over the GEV as all relevant data are used in the estimation.

### 3.1.4 Threshold selection for GPD

The drawback with the threshold approach is that the parameter estimates are dependent on the subjective selection of a threshold. The choice of the threshold has to be made with considerable care, as Davison and Smith (1990) show: too high a threshold and there are insufficient exceedances to estimate the GPD parameters with required accuracy, too low a threshold and the asymptotic justification for the GPD will no longer hold, so it is likely the GPD will not provide a good statistical model for the threshold excesses.

For the GPD, a tool which helps in the selection of a suitable threshold  $u$  is the so-called *mean residual life plot* (Davison and Smith, 1990). Following the property of threshold invariance in equation (3.1.4), i.e. if  $X$  is such that  $X - u|X > u$  is  $\text{GPD}(\sigma, \xi)$ , then for all thresholds  $\tilde{u} > u$ ,  $X - \tilde{u}|X > \tilde{u}$  is  $\text{GPD}(\sigma + \xi(\tilde{u} - u), \xi)$ , it follows that provided  $\xi < 1$ , for  $\tilde{u}$  such that  $\sigma + \xi(\tilde{u} - u) > 0$ ,

$$E(X - \tilde{u}|X > \tilde{u}) = \frac{\sigma + (\tilde{u} - u)\xi}{1 - \xi}. \quad (3.1.5)$$

Equation (3.1.5) shows that the mean excess of  $X$  over  $\tilde{u}$  is a linear function of  $\tilde{u}$ . This result suggests the construction of a graph in which the empirical mean excesses of  $\tilde{u}$  are plotted against  $\tilde{u}$ , with  $u$  taken to be the smallest value of  $\tilde{u}$  over which the mean residual life plot exhibits approximately a linear behaviour.

### 3.1.5 Goodness-of-fit for GPD

Once a threshold  $u$  has been selected and a suitable parametric distribution fitted to the exceedances of  $u$  via maximum likelihood, the goodness-of-fit of the statistical model to the observed data needs to be verified. Some easy checks may be carried out graphically using probability plots (P-P plots) and quantile plots (Q-Q plots). Both are based on the same logic, that is, to compare the fitted and the empirical distributions of the exceedances

either on a probability or a quantile scale, respectively. Explicitly, for the fitted statistical model with distribution function  $G(x)$ , and ordered sample values  $x_{(1)} \leq x_{(2)} \leq \dots \leq x_{(n)}$ : in the P–P plot we plot

$$G(x_{(i)}) \text{ against } i/(n+1) \text{ for } i = 1, \dots, n;$$

and in the Q–Q plot we plot

$$x_{(i)} \text{ against } G^{-1}(i/(n+1)) \text{ for } i = 1, \dots, n.$$

For each plot departures from the  $x = y$  line suggests model inadequacy. For assessing extreme value models the Q–Q plot is more informative since it highlights discrepancies in the upper tail.

### 3.1.6 Temporal dependence and non-stationarity

In the previous sections it was assumed that the observed time series are independent and identically distributed. However, sea condition data depart from these assumptions, demonstrating:

- a short-range dependence, leading to clusters of extreme values;
- non-stationarity, generally due to seasonality, trends and tides.

As far as temporal dependence is concerned, a declustering procedure is required to produce sequences of independent observations. In multivariate studies, the identification of a suitable declustering procedure is generally a difficult step (Coles and Tawn, 1994). However, for sea condition data a natural way of declustering is to use only concurrent measurements at times of high water. At U.K. sites variation in the sea-level process is dominated by semi-diurnal tidal variation. Consequently, events which threaten to cause coastal flooding occur only at times of high tide, approximately every 12 hours and 26 minutes. This form of declustering

- is consistent with current practice in oceanographic analyses (Hawkes and Hague, 1994),
- does not differ substantially from studies on still water level (Dixon and Tawn, 1994, 1995).

There are additional benefits of this declustering scheme as it also largely removes the still water level (or surge) variable non-stationarity due to tide, and it enables data sites which only possess high water level data to be analysed.

## 3.2 Illustrative Dependence Examples

In this section we motivate the need for dependence models for extreme events. In particular we show the impact of the degree of dependence and the form of the failure region on the probability of a structure failing.

For a bivariate problem with two identically distributed variables  $(X_1, X_2)$  we consider two structure variables

- $Y = \min(X_1, X_2)$ ,
- $Y = \max(X_1, X_2)$ ,

these are idealised cases to illustrate extreme design conditions. They are given to aid the illustration of the methods in a problem where we can explicitly evaluate the probability of failure, and do not necessarily represent realistic structure variables. For example, the second structure function corresponds to failure from two unrelated failure types, in which an extreme of one variable and/or the other leads to failure irrespective of the associated value of the other variable.

We also consider three forms of dependence between  $(X_1, X_2)$

- complete positive dependence,
- independence,
- complete negative dependence.

Again these are idealised and are presented with illustration, rather than practice, in mind.

Throughout we take the structure to fail when  $Y > u$ , for large  $u$ , and to simplify notation let  $\Pr\{X_1 > u\} = \Pr\{X_2 > u\} = p$ .

### 3.2.1 The structure function of the minimum

Here we will evaluate the level of protection of the design for the structure variable,  $\min(X_1, X_2)$ , for the three different dependence structures. Writing the probability of failure in terms of an event for  $(X_1, X_2)$  we have

$$\begin{aligned}
 \Pr\{Y > u\} &= \Pr\{\min(X_1, X_2) > u\} \\
 &= \Pr\{X_1 > u, X_2 > u\} \\
 &= \Pr\{X_1 > u\} \Pr\{X_2 > u | X_1 > u\}
 \end{aligned} \tag{3.2.1}$$

where the second term in equation (3.2.1) is the conditional probability of  $X_2 > u$  given  $X_1 > u$ , see Appendix A.1. The dependence between  $(X_1, X_2)$  influences the value of the conditional probability with

$$\Pr\{X_2 > u | X_1 > u\} = \begin{cases} 1 & \text{under complete positive dependence} \\ \Pr\{X_2 > u\} & \text{under independence} \\ 0 & \text{under complete negative dependence.} \end{cases} \quad (3.2.2)$$

Combining the expressions in equations (3.2.1) and (3.2.2) gives the probability of design failure to be

$$\Pr\{Y > u\} = \begin{cases} p & \text{under complete positive dependence} \\ p^2 & \text{under independence} \\ 0 & \text{under complete negative dependence.} \end{cases} \quad (3.2.3)$$

To illustrate what this means consider the situation when  $u$  is taken to be the 10 year return level for each marginal variable, and there are 705 independent events per year, the return period (in years) of design failure is

$$\begin{array}{lll} 10 & \text{under} & \text{complete positive dependence} \\ 70500 & \text{under} & \text{independence} \\ \infty & \text{under} & \text{complete negative dependence,} \end{array}$$

see Section 3.4 for working. Similarly, for the design to have a 100 year return period,  $u$  must be chosen to give marginal return periods (in years) for  $X_1$  and  $X_2$  of

$$\begin{array}{lll} 100 & \text{under} & \text{complete positive dependence} \\ 0.38 & \text{under} & \text{independence} \end{array}$$

*Aside: note that for complete negative dependence any level is adequate for the marginal return level as design failure is impossible.*

### 3.2.2 The structure function of the maximum

Now consider the  $\max(X_1, X_2)$  structure variable for the three different dependence structures. Writing the probability of failure in terms of an event for  $(X_1, X_2)$  we have

$$\begin{aligned} \Pr\{Y > u\} &= \Pr\{\max(X_1, X_2) > u\} \\ &= \Pr\{X_1 > u \text{ and/or } X_2 > u\} \\ &= \Pr\{X_1 > u\} + \Pr\{X_2 > u\} - \Pr\{X_1 > u, X_2 > u\}. \end{aligned} \quad (3.2.4)$$

The joint probability in the final term in equation (3.2.4) was calculated in Section 3.2.1. It follows that the probability of design failure is

$$\Pr\{Y > u\} = \begin{cases} p & \text{under complete positive dependence} \\ p(2-p) & \text{under independence} \\ 2p & \text{under complete negative dependence.} \end{cases} \quad (3.2.5)$$

To illustrate this, consider  $u$  to be taken as the 10 year return level for each marginal variable the return period (in years) of design failure is

$$\begin{array}{lll} 10 & \text{under} & \text{complete positive dependence} \\ 5 & \text{under} & \text{independence} \\ 5 & \text{under} & \text{complete negative dependence,} \end{array}$$

see Section 3.4 for working. Similarly, for the design to have a 100 year return period  $u$  must be chosen to give marginal return periods (in years) for  $X_1$  and  $X_2$  of

$$\begin{array}{lll} 100 & \text{under} & \text{complete positive dependence} \\ 200 & \text{under} & \text{independence} \\ 200 & \text{under} & \text{complete negative dependence.} \end{array}$$

### 3.3 Multivariate Methods

#### 3.3.1 Models

This section gives a simple introduction to dependence modelling in multivariate extremes. We focus on bivariate extremal dependence only and restrict attention to  $\Pr\{X_2 > u | X_1 > u\}$  where  $(X_1, X_2)$  are identically distributed random variables. In Section 3.2 we considered three special cases of dependence between two variables  $(X_1, X_2)$ , and found that for large  $u$

$$\Pr\{X_2 > u | X_1 > u\} = \begin{cases} 1 & \text{under complete positive dependence} \\ \Pr\{X_2 > u\} & \text{under independence} \\ 0 & \text{under complete negative dependence.} \end{cases}$$

Clearly many different statistical models for intermediate degrees of dependence between  $(X_1, X_2)$  exist, however for joint probability methods it is the dependence between the extreme values of  $X_1$  and  $X_2$  that are of interest, and the form of this dependence is well identified by considering how  $\Pr\{X_2 > u | X_1 > u\}$  behaves for large  $u$ , i.e. how does the knowledge that  $X_1$  is big influence the probability that  $X_2$  is big?

Here we will give this conditional probability for two statistical dependence models that are often used in joint probability studies.

### Bivariate Extreme Value Distribution

Coles and Tawn (1994) propose the use of this statistical model for dependence between extreme values. After transformation of each marginal variable to a unit Fréchet distribution (i.e. with distribution function  $\Pr\{X_1 \leq x\} = \Pr\{X_2 \leq x\} = \exp(-1/x)$  for  $x > 0$ ) the form of the dependence between the two variables  $(X_1, X_2)$  is taken to follow a bivariate extreme value distribution (with logistic dependence structure) given by

$$\Pr\{X_1 \leq x_1, X_2 \leq x_2\} = \exp\{-(x_1^{-1/\alpha} + x_2^{-1/\alpha})^\alpha\}, \quad (3.3.1)$$

where  $0 < \alpha \leq 1$  determines the degree of dependence. For general (identically distributed) marginal variables with this form of dependence structure

$$\Pr\{X_1 \leq u, X_2 \leq u\} = (\Pr\{X_1 \leq u\})^{2^\alpha},$$

where  $0 < \alpha \leq 1$  determines the degree of dependence with

- $\alpha = 1$  corresponding to independence,
- $\alpha \rightarrow 0$  corresponding to complete dependence,
- decreasing  $\alpha$  leading to increased dependence,
- negative dependence being impossible.

For this joint distribution it follows that

$$\begin{aligned} \Pr\{X_1 > u, X_2 > u\} &= 1 - \Pr\{X_1 \leq u\} - \Pr\{X_2 \leq u\} + \Pr\{X_1 \leq u, X_2 \leq u\} \\ &= 2 \Pr\{X_1 > u\} - 1 + \Pr\{X_1 \leq u\}^{2^\alpha} \\ &\approx (2 - 2^\alpha) \Pr\{X_1 > u\} + 2^{\alpha-1}(2^\alpha - 1) \Pr\{X_1 > u\}^2, \end{aligned} \quad (3.3.2)$$

for large  $u$  since :

$$\Pr\{X_1 \leq u\}^{2^\alpha} = (1 - \Pr\{X_1 > u\})^{2^\alpha} \approx 1 - 2^\alpha \Pr\{X_1 > u\} + 2^{\alpha-1}(2^\alpha - 1) \Pr\{X_1 > u\}^2.$$

Hence the conditional probability is

$$\Pr\{X_2 > u | X_1 > u\} \approx (2 - 2^\alpha) + 2^{\alpha-1}(2^\alpha - 1) \Pr\{X_2 > u\} \text{ for large } u.$$

This statistical model gives a very specific class of dependence models between the variables which leads to dependence between the extreme values. To clarify this, note that given the variable  $X_1$  is extreme (i.e  $u \rightarrow \infty$  so that  $\Pr\{X_1 > u\} \rightarrow 0$ ) there is a reasonable probability,  $(2 - 2^\alpha)$ , that  $X_2$  will be equally extreme. The degree of dependence in the extreme values is determined by the value of  $\alpha$ , so that when  $\alpha = 1$  the first term

of this conditional probability is zero and the second term reduces to  $\Pr\{X_2 > u\}$ . For complete dependence (i.e. when  $\alpha \rightarrow 0$ ) the conditional probability is 1.

Finally, in Figure 3.1 we give the joint density contours for the bivariate logistic dependence structure when the marginal distributions follow standard normal distributions. The figure shows how dependence, particularly in the joint tail region, grows as  $\alpha$  is decreased. When  $\alpha = 1$  the variables are independent and here the contours are circles. For  $\alpha < 1$  the contours are elliptical in form but with a distinct pointedness on the diagonal in the joint upper tail.

### Bivariate Normal Distribution

The joint distribution and dependence structure for the bivariate normal distribution are given in detail in Appendix A.2.2. For general (identically distributed) marginal variables with this form of dependence structure, Ledford and Tawn (1996) show that to a reasonable approximation

$$\Pr\{X_1 > u, X_2 > u\} \approx C_\rho (\Pr\{X_1 > u\})^{2/(1+\rho)}$$

for large  $u$ , where  $C_\rho$  is a constant and  $-1 < \rho < 1$  determines the degree of dependence with

- $0 < \rho < 1$  corresponding to positive dependence,
- $\rho = 0$  corresponding to independence,
- $-1 < \rho < 0$  corresponding to negative dependence.

It follows that

$$\Pr\{X_2 > u | X_1 > u\} \approx C_\rho (\Pr\{X_1 > u\})^{(1-\rho)/(1+\rho)} \text{ for large } u. \quad (3.3.3)$$

From equation (3.3.3) the conditional probability decreases to 0 as  $u$  increases (whatever  $\rho$ ), with the conditional probability increasing as  $\rho$  increases (for fixed  $u$ ). This distribution has dependence in the extremes, but unlike the bivariate extreme value distribution, the probability of  $(X_1, X_2)$  being simultaneously extreme tends to zero as more extreme values are considered.

Finally, in Figure 3.2 we give the joint density contours for the bivariate normal dependence structure when the marginal distributions follow standard normal distributions. The figure shows that the contours are exact ellipses whatever the correlation coefficient,  $\rho$ . When  $\rho$  is negative the contours are identical to contours for  $-\rho$  after reflection around the  $y = x$  line. When  $\rho = 0$  the variables are independent and the contours circular, as for  $\alpha = 1$  for the bivariate logistic dependence structure above.

Figure 3.1: Joint density contours for the bivariate logistic dependence structure when the marginal distributions are standard normal, i.e.  $Z_i = \Phi^{-1}(\exp(-1/X_i))$  for  $X_i$  a unit Fréchet variable and  $i = 1, 2$ . The dependence parameter  $\alpha = 1, 0.9, 0.8, 0.7, 0.5, 0.3$ .

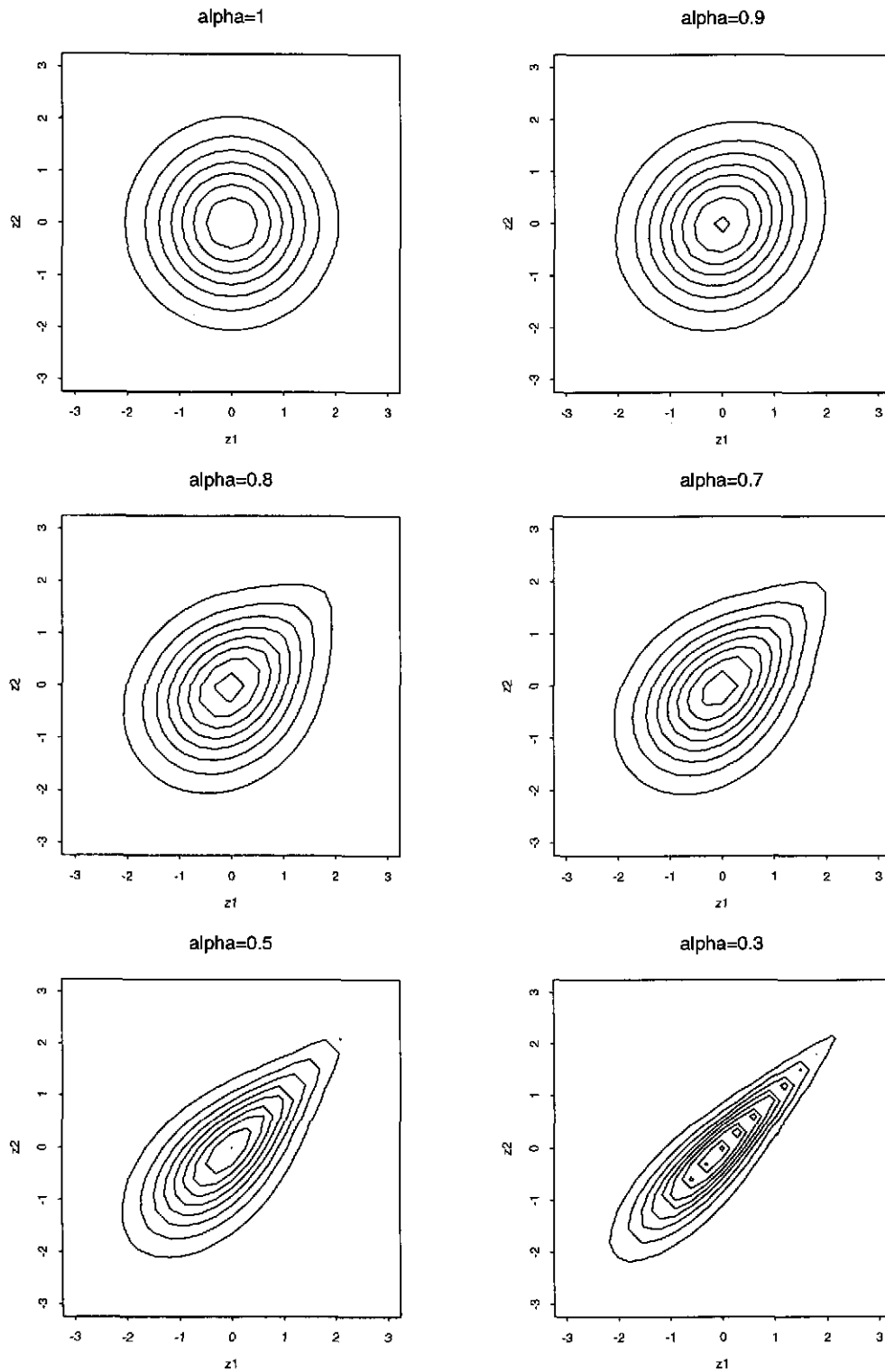
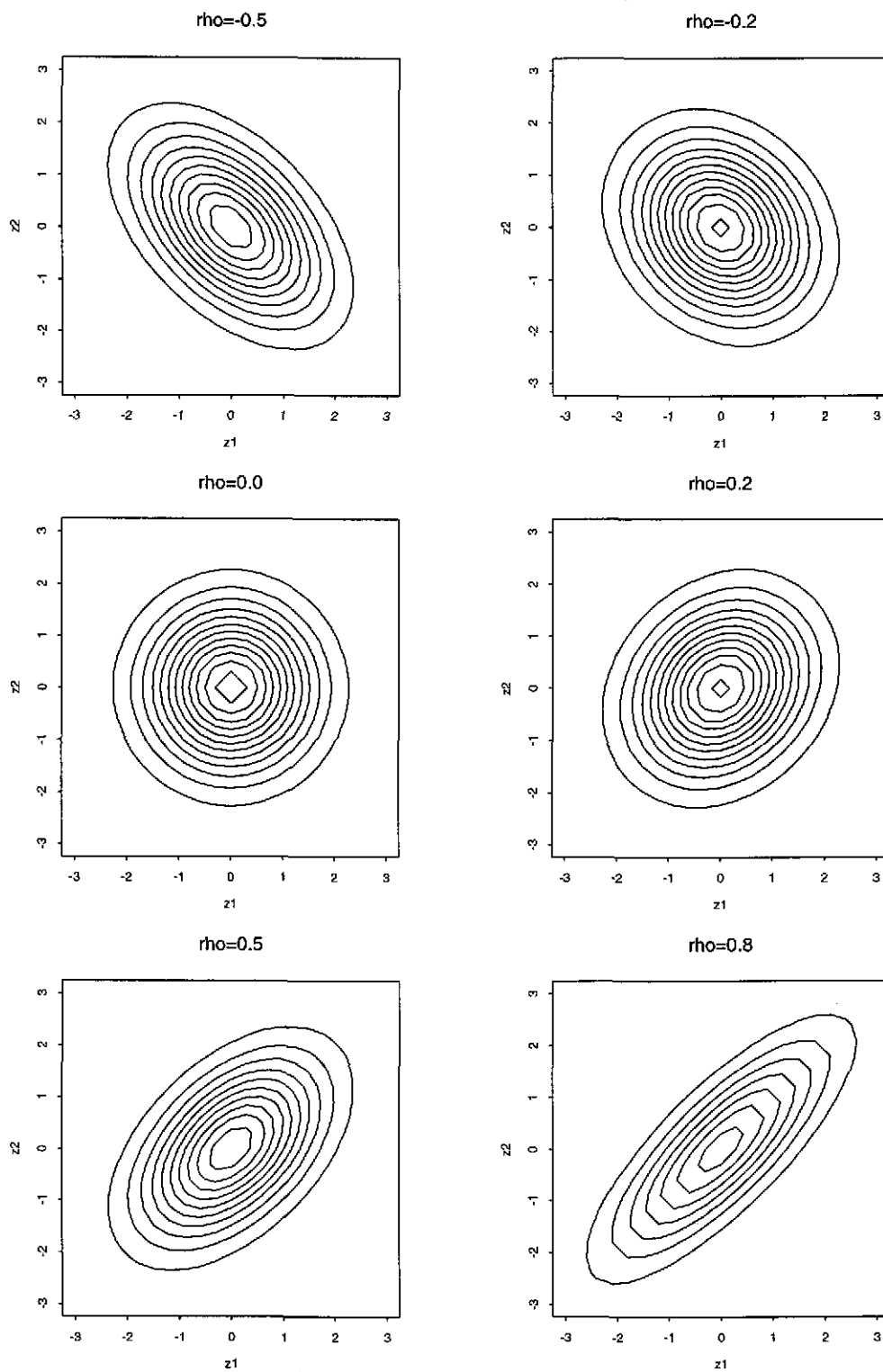


Figure 3.2: Joint density contours for the bivariate normal dependence structure when the marginal distributions are standard normal, i.e.  $Z_i = \Phi^{-1}(\exp(-1/X_i))$  for  $X_i$  a unit Fréchet variable and  $i = 1, 2$ . The dependence parameter  $\rho = -0.5, -0.2, 0.0, 0.2, 0.5, 0.8$ .



### 3.3.2 Diagnostics

In applications it turns out to be important to distinguish between three forms of dependence structure illustrated by

1. the bivariate extreme value distribution
2. the bivariate normal distribution
3. independence.

The underlying reason is that these dependence models have different behaviour of  $\Pr\{X_2 > u|X_1 > u\}$  for large  $u$ .

If, as  $u \rightarrow \infty$ ,  $\Pr\{X_2 > u|X_1 > u\} \rightarrow c > 0$ , where  $c$  is a constant, as is the case for the bivariate extreme value distribution, then precise dependence modelling is often not important, as subsequent inference is relatively insensitive to the value of the constant  $c$ . This suggests adopting a conservative approach of taking  $c = 1$ , i.e. taking the variables  $(X_1, X_2)$  to be completely dependent. To clarify this, for the logistic model in the bivariate extreme value family,  $c = 2 - 2^\alpha$ , so  $c = 1$  when  $\alpha = 0$ .

In contrast, for other dependence structures, such as the bivariate normal distribution,  $\Pr\{X_2 > u|X_1 > u\} \rightarrow 0$  as  $u \rightarrow \infty$ , with the rate of convergence to zero determined by the degree of dependence. For this class of dependence structures it is important to model the dependence structure. However, a special case of the bivariate normal distribution, for which no explicit dependence modelling is required, is when the variables are independent (i.e.  $\rho = 0$ ).

Distinguishing between these classes of dependence structure is important as it enables us to identify when we can approximate the dependence by complete dependence, independence, or need to carefully model dependence. The following diagnostic,  $T(z)$ , enables us to identify from the data to hand which approach to take.

Specifically consider identically distributed random variables  $X_1$  and  $X_2$  with each following a unit Fréchet distribution, i.e.  $\Pr\{X_1 > u\} = \Pr\{X_2 > u\} \approx u^{-1}$  for large  $u$ . Define the diagnostic statistic

$$T(z) = -\log \left\{ \frac{\Pr\{X_1 > uz, X_2 > uz\}z}{\Pr\{X_1 > u, X_2 > u\}} \right\} \quad (3.3.4)$$

for large  $u$  and all  $z > 1$ . The diagnostic test is to plot  $T(z)$ , estimated by replacing the probabilities by the associated empirical proportions, against  $\log z$  for a range of  $z$ . If  $\Pr\{X_2 > u|X_1 > u\} \rightarrow c > 0$  then  $T(z)$  is approximately zero for all  $z$ , whereas for  $\Pr\{X_2 > u|X_1 > u\} \rightarrow 0$ , we have that  $T(z)$  is linearly increasing with  $\log z$ , with the gradient related to the rate at which  $\Pr\{X_2 > u|X_1 > u\} \rightarrow 0$ . Specifically, the

faster the convergence of the conditional probability to zero the steeper the gradient, with independence corresponding to a gradient of one.

To illustrate this theoretically first consider the bivariate extreme value distribution with logistic dependence structure. For large  $u$  this distribution gives

$$\Pr\{X_1 > u, X_2 > u\} \approx \frac{2 - 2^\alpha}{u}.$$

Then for large  $u$

$$T(z) \approx -\log \left\{ \frac{(uz)^{-1}(2 - 2^\alpha)z}{u^{-1}(2 - 2^\alpha)} \right\} = -\log\{1\} = 0.$$

Similarly, for the bivariate normal distribution, with Fréchet marginal distributions,

$$\Pr\{X_1 > u, X_2 > u\} \approx C_\rho u^{-2/(1+\rho)}.$$

Then for large  $u$

$$T(z) \approx -\log \left\{ \frac{C_\rho (uz)^{-2/(1+\rho)} z}{C_\rho u^{-2/(1+\rho)}} \right\} = -\log\{z^{(\rho-1)/(1+\rho)}\} = \frac{1-\rho}{1+\rho} \log z, \quad (3.3.5)$$

so is linearly increasing in  $\log z$ , with gradient  $(1-\rho)/(1+\rho)$  for all  $\rho < 1$ . When  $\rho = 0$ , i.e. independence, then expression (3.3.5) gives the gradient to be one.

In Section 7.1.2 we use this form of diagnostic statistic plot prior to dependence analysis to identify the line of attack that can be taken.

### 3.3.3 Illustrative examples

We now return to the illustrative examples of Section 3.2 and examine the impact of the dependence models discussed in Section 3.3.1 which provide intermediate degrees of dependence to the extreme cases (complete positive dependence, independence and complete negative dependence) considered there.

#### Structure function of the minimum

For the structure function  $Y = \min(X_1, X_2)$  the probability  $\Pr\{Y > u\}$  is given by equation (3.2.1). Using equation (3.3.2), for a bivariate extreme value dependence structure, with logistic form,

$$\Pr\{Y > u\} = (2 - 2^\alpha)p + 2^{\alpha-1}(2^\alpha - 1)p^2,$$

where  $\Pr\{X_1 > u\} = \Pr\{X_2 > u\} = p$ . Similarly, using equation (3.3.3), we have, for the bivariate normal dependence structure, that

$$\Pr\{Y > u\} = C_\rho p^{2/(1+\rho)}.$$

To illustrate these results we focus on the bivariate extreme value logistic model case with  $\alpha = 0.8$  (the value used for one of the case study data sets in Chapter 5). When  $u$  is taken to be the 10 year return level for each marginal variable, then the return period of the design is 38.6 years. Similarly, for the design to have a 100 year return period  $u$  must be chosen to give marginal return periods of 26 years (working is given in Section 3.4).

### Structure function of the maximum

For the structure function  $Y = \max(X_1, X_2)$  the probability  $\Pr\{Y > u\}$  is given by equation (3.2.4). Using equation (3.3.2), for a bivariate extreme value dependence structure, with logistic form,

$$\begin{aligned}\Pr\{Y > u\} &= 2^\alpha p - 2^{\alpha-1}(2^\alpha - 1)p^2 \\ &\approx 2^\alpha p \text{ for large } u.\end{aligned}$$

Similarly, using equation (3.3.3), for the bivariate normal dependence structure

$$\begin{aligned}\Pr\{Y > u\} &= 2p - C_\rho p^{2/(1+\rho)} \\ &\approx 2p \text{ for large } u.\end{aligned}$$

Interestingly, for this structure function, whatever the degree of correlation for the bivariate normal dependence structure, the probability of failure tends to zero (with decreasing  $p$ ) in the same way as if there were no dependence between the variables (i.e. as if  $\rho = 0$ ).

To illustrate these results we focus on the bivariate extreme value logistic model case with  $\alpha = 0.8$ . When  $u$  is taken to be the 10 year return level for each marginal variable, then the return period of the design is 5.7 years. Similarly, for the design to have a 100 year return period,  $u$  must be chosen to give marginal return periods of 174 years (working is given in Section 3.4).

## 3.4 Technical Calculations

In this section we derive the mathematical equations through which the probabilities of joint events in Sections 3.2 and 3.3.3 are converted into annual return periods. We consider the cases of independent and bivariate extreme value (logistic dependence model) separately. Throughout we assume there are  $n_{yr} = 705$  independent events per year, and  $u$  is such that

$$\Pr\{\text{annual maximum } X_1 \leq u\} = \Pr\{X_1 \leq u\}^{n_{yr}} = 1 - p_A,$$

i.e.  $u$  is the  $p_A^{-1}$  year return level for variable  $X_1$ . As  $X_1$  and  $X_2$  are identically distributed,  $u$  is the return level for  $X_2$  as well. It follows that

$$\Pr\{X_1 \leq u\} = \Pr\{X_2 \leq u\} = (1 - p_A)^{1/n_{yr}}.$$

### 3.4.1 Independence

First consider  $Y = \min(X_1, X_2)$ . Then

$$\Pr\{Y \leq u\} = \Pr\{X_1 \leq u\} + \Pr\{X_2 \leq u\} - \Pr\{X_1 \leq u, X_2 \leq u\},$$

and from this

$$\Pr\{\text{annual maximum } Y \leq u\} = \left[2(1 - p_A)^{1/n_{yr}} - (1 - p_A)^{2/n_{yr}}\right]^{n_{yr}}.$$

Now consider the Binomial approximation

$$(1 - p_A)^a \approx 1 - ap + p^2 a(a - 1)/2 \text{ for small } p.$$

Applying this approximation to the above

$$\Pr\{\text{annual maximum } Y \leq u\} \approx \left[1 - p_A^2/n_{yr}^2\right]^{n_{yr}} \approx 1 - p_A^2/n_{yr},$$

which implies that the return period (in years) of the structure variable exceeding  $u$  is  $n_{yr}/p_A^2$ . For the example of  $p_A = 0.1$  the return period is  $705 \times 10^2$  years.

Now consider the structure variable  $Y = \max(X_1, X_2)$ . Then

$$\Pr\{Y \leq u\} = \Pr\{X_1 \leq u, X_2 \leq u\}.$$

and

$$\Pr\{\text{annual maximum } Y \leq u\} = \left[(1 - p_A)^{2/n_{yr}}\right]^{n_{yr}} = (1 - p_A)^2 \approx 1 - 2p_A,$$

which implies that the return period (in years) of the structure variable exceeding  $u$  is  $(2p_A)^{-1}$ . For the example of  $p_A = 0.1$  the return period is 5 years.

### 3.4.2 Bivariate extreme value dependence

First consider  $Y = \min(X_1, X_2)$ . Then

$$\Pr\{Y \leq u\} = \Pr\{X_1 \leq u\} + \Pr\{X_2 \leq u\} - \Pr\{X_1 \leq u, X_2 \leq u\},$$

and

$$\Pr\{\text{annual maximum } Y \leq u\} = \left[2(1 - p_A)^{1/n_{yr}} - (1 - p_A)^{2/n_{yr}}\right]^{n_{yr}}.$$

Applying the Binomial approximation

$$\Pr\{\text{annual maximum } Y \leq u\} \approx [1 - (2 - 2^\alpha)p_A/n_{yr}]^{n_{yr}} \approx 1 - (2 - 2^\alpha)p_A,$$

which implies that the return period of the structure variable exceeding  $u$  is  $[(2 - 2^\alpha)p_A]^{-1}$ .

For the example of  $p_A = 0.1$ , with  $\alpha = 0.8$ , the return period is 38.6 years.

Now consider the structure variable  $Y = \max(X_1, X_2)$ . Then

$$\Pr\{Y \leq u\} = \Pr\{X_1 \leq u, X_2 \leq u\},$$

and

$$\Pr\{\text{annual maximum } Y \leq u\} = [(1 - p_A)^{2^\alpha/n_{yr}}]^{n_{yr}} = (1 - p_A)^{2^\alpha} \approx 1 - 2^\alpha p_A,$$

which implies that the return period (in years) of the structure variable exceeding  $u$  is  $(2^\alpha p_A)^{-1}$ . The example of  $p_A = 0.1$  gives a return period of 5.7 years for the design.

# Chapter 4

## Statistical Models used for JPM

The three components of the JPM are

- marginal statistical models
- statistical models for dependence
- evaluation of the probability of failure.

In Sections 4.1 and 4.2 we develop statistical models for both marginal and dependence features whilst in Section 4.3 we examine methods for evaluating the integral of the estimated joint density over the failure region required for the calculation of the estimated probability of failure.

### 4.1 Marginal Statistical Models

In this section we develop statistical models for each of the separate sea condition variables listed below:

- Still Water Level (tide and surge)
- Significant Wave Height
- Steepness
- Wave Direction
- Wave Period (via statistical models for significant wave height and steepness).

The suitability of these statistical models is assessed in Chapter 6 where they are applied to all the observational and simulated data sets.

### 4.1.1 Still Water Level

The still water level (SWL) is the sea-level after waves have been averaged out. It is the composition of the mean sea-level, the astronomical tidal level (tide) and the meteorological surge level (Surge). The mean sea-level component is treated as a fixed constant in this work; therefore, variations in still water levels are considered a consequence of the tide and surge components.

There are two approaches to the analysis of extreme still water levels: direct and indirect (Tawn, 1992; Dixon and Tawn, 1994). The direct methods analyse explicitly the observed extremes of the SWL process, whereas the indirect methods decompose the SWL into the two constituent components, analyse each of these separately, and then re-combine results to produce the distribution of extreme still water levels. There are reasons why the indirect methods should be preferred. For example, they keep separate the deterministic tidal component, for which no extrapolation is required as it can be predicted exactly, from the stochastic surge component, which needs to be statistically modelled. However, indirect methods require the dependence between tide and surge to be statistically modelled.

As we are primarily interested in the relationship between extreme water levels and waves in this study we essentially adopt a direct approach but consider one example where a simple version of the indirect style of approach is adopted for comparison purposes. The statistical model we use for the still water level (in the direct approach) and the surge (in the indirect approach) is based on the Threshold Method, as described in Section 3.1.2, with the distribution of exceedances modelled parametrically through the GPD. Additionally, in the indirect approach we take

- the tide to be given by the empirical distribution of high tide values,
- the high tides and surges (at high tides) to be independent.

### 4.1.2 Significant Wave Height

The significant wave height ( $H_S$ ) is defined as the mean height of the highest 1/3 of the waves in a period of a given duration (generally 20 minutes). The standard distribution adopted for statistically modelling significant wave height,  $H_S$ , is the three parameter Weibull distribution, which has distribution function

$$W(x) = \Pr\{H_S \leq x\} = 1 - \exp\{-[(x - a)/b]^c\} \text{ for } x \geq a. \quad (4.1.1)$$

Here the parameters  $a$ ,  $b$  and  $c$  are respectively location, scale and shape parameters. Both  $b$  and  $c$  are positive parameters, and since significant wave height is a positive random

variable, we should expect  $a$  to be positive also. This distribution is widely used for wave data and has generally been found to fit reasonably well throughout the entire range of observed data (Carter and Challenor, 1981).

A procedure often adopted by HR for fitting this statistical model is the Threshold Method discussed in Section 3.1.2. After fixing a suitable threshold  $u$ , they fit to the exceedances a Truncated Weibull distribution, defined by

$$\begin{aligned} P(H_S \leq x | H_S > u) &= \frac{W(x) - W(u)}{1 - W(u)} \\ &= 1 - \exp \left[ - \left( \frac{x - a}{b} \right)^c + \left( \frac{u - a}{b} \right)^c \right], \text{ for } x > u, \end{aligned} \quad (4.1.2)$$

where the parameters  $(a, b, c)$  satisfy the conditions required for the Weibull distribution, i.e. equation (4.1.1), together with the additional constraint that  $u > a$ . This statistical model is fitted here using the threshold likelihood (3.1.1) to the observations of  $H_S$  which exceed  $u$ . Here the density of the values which exceed the threshold is

$$\exp \left\{ - \left( \frac{x - a}{b} \right)^c + \left( \frac{u - a}{b} \right)^c \right\} \frac{c}{b} \left( \frac{x - a}{b} \right)^{c-1} \text{ for } x > u$$

and  $\lambda$ , the probability that the threshold is exceeded, is linked to the parametric distribution for exceedances by

$$\lambda = 1 - W(u) = \exp \left\{ - \left( \frac{u - a}{b} \right)^c \right\}.$$

Three motivations for this approach/fitting method are:

- If extreme waves are of primary interest then fitting the wave distribution with most attention on the quality of the fit paid to the largest observations is natural. The choice of the Weibull distribution is more questionable, but is an obvious starting point when moving away from the standard approach.
- Suppose waves come from a number of different populations, e.g. different classes of waves determined by their generation – which is apparent through different directions or steepness characteristics of the observed waves. Then if the wave heights from each population follow a standard Weibull form, the mixing of the different populations produces a complex distribution for all wave heights. However, if one population produces wave heights which dominate the extremes in the sample, then the Truncated Weibull distribution will fit well even when the Weibull distribution does not.
- Hindcast significant wave height data are sometimes generated only for extreme storms over the period of interest, for example for all storms which have significant

wave heights over some threshold level  $u$ . Consequently, if all significant wave heights follow a Weibull distribution, then the distribution of these observed values is a truncated Weibull distribution.

Relative to the standard Weibull distribution the Truncated Weibull is more flexible owing to the introduction of the threshold,  $u$ , which is essentially a fourth parameter of the distribution. However, there is no theoretical argument to suggest that the Truncated Weibull should be preferred to other distributions (Carter and Challenor, 1981). By contrast, in Chapter 3 statistical models for threshold exceedances which have some theoretical justification were discussed. For this reason, we also consider the Threshold Method with the GPD used as the distribution for exceedances for  $H_S$ .

To compare the Weibull and GPD threshold approaches more generally we assess them on the basis of their stability with respect to different thresholds. As remarked in Section 3.1.4, a property required from tail models is the non-sensitivity of the results to threshold selection. To assess the impact of making this choice when in fact the Weibull distribution is the true distribution of the population, 10000 samples of size 6000 (a typical sample size of the observational data) were simulated from a three-parameter Weibull distribution with parameters  $a$ ,  $b$  and  $c$ . A range of values of  $c$  were selected to represent typical estimates derived from applications to data. Without loss of generality, we set  $a = 0$  and  $b = 1$ , since the corresponding behaviour for all other location and scale parameters can be derived from this case. For each sample, the GPD and the Truncated Weibull distributions were fitted to exceedances of the 95% empirical quantile. Bias and mean squared error of the estimates of various extreme quantiles for the two fitted distributions are given in Tables 4.1–4.4. As expected, the bias of the estimates provided by the Weibull distribution is practically zero. For the fitted GPD the bias is low, but the mean squared error, especially for the most extreme quantiles, is consistently bigger than for the Truncated Weibull. This implies that even if the underlying true distribution were the Weibull, the GPD should provide acceptable results in terms of bias, but at the cost of greater sampling variability.

Our proposed approach in practical studies is to fit both the Truncated Weibull and the GPD via the Threshold Method and to assess the two methods based on their ability to provide good estimates of return levels in the tail of the observed sample, the realism of the extrapolations to long return periods, and the quality of fit of the models. For this project, since the GPD tail model is robust to the underlying distribution and unbiased when the true population is Weibull, we adopt it in preference to the Truncated Weibull distribution. Hence only the GPD will be considered for the simulated data, even though both are assessed for the observational data.

Quantiles		$1 - 1/10^2$	$1 - 1/10^3$	$1 - 1/10^4$	$1 - 1/10^5$
GPD	Bias	-0.0005	-0.0286	-0.098	-0.1989
	Mean Squared Error	0.0053	0.0395	0.2549	0.9491
Weibull	Bias	-0.0045	-0.0085	-0.0177	-0.0144
	Mean Squared Error	0.0049	0.0263	0.0741	0.1535

Table 4.1: Results from simulating 10000 samples of size 6000 from a Weibull distribution with known parameters  $a = 0$ ,  $b = 1$  and  $c = 1.2$ .

Quantiles		$1 - 1/10^2$	$1 - 1/10^3$	$1 - 1/10^4$	$1 - 1/10^5$
GPD	Bias	0.0004	-0.0108	-0.0595	-0.1453
	Mean Squared Error	0.0019	0.0125	0.076	0.2672
Weibull	Bias	-0.0026	-0.0042	-0.0054	-0.0062
	Mean Squared Error	0.0017	0.0084	0.0216	0.0418

Table 4.2: Results from simulating 10000 samples of size 6000 from a Weibull distribution with known parameters  $a = 0$ ,  $b = 1$  and  $c = 1.5$ .

Quantiles		$1 - 1/10^2$	$1 - 1/10^3$	$1 - 1/10^4$	$1 - 1/10^5$
GPD	Bias	0.001	-0.0107	-0.06	-0.1451
	Mean Squared Error	0.0012	0.0074	0.0448	0.1535
Weibull	Bias	-0.0023	-0.0033	-0.0041	-0.0045
	Mean Squared Error	0.0011	0.0048	0.0118	0.0221

Table 4.3: Results from simulating 10000 samples of size 6000 from a Weibull distribution with known parameters  $a = 0$ ,  $b = 1$  and  $c = 1.7$ .

Quantiles		$1 - 1/10^2$	$1 - 1/10^3$	$1 - 1/10^4$	$1 - 1/10^5$
GPD	Bias	-0.0064	-0.0269	0.1476	0.7735
	Mean Squared Error	0.008	0.1077	1.099	6.838
Weibull	Bias	0.0079	0.0331	0.081	0.153
	Mean Squared Error	0.0009	0.0072	0.0358	0.1041

Table 4.4: Results from simulating 10000 samples of size 6000 from a Weibull distribution with known parameters  $a = 0$ ,  $b = 1$  and  $c = 0.7$ .

### 4.1.3 Steepness

We model the joint distribution of  $(H_S, S)$  instead of  $(H_S, T_Z)$  for the wave characteristics. Wave steepness,  $S$ , and  $T_Z$  are related by the following equation

$$S = \frac{2\pi H_S}{gT_Z^2}, \quad (4.1.3)$$

where  $g$  denotes the gravitational constant, so a statistical model for  $(H_S, S)$  determines also the distribution of  $T_Z$ .

There are a number of reasons which support an analysis based on the variable  $S$  instead of  $T_Z$ .

- It is common practice in oceanographic studies to estimate extremes of wave period by fixing a typical value of steepness and employing the distribution of  $H_S$  and equation (4.1.3) to derive  $T_Z$  (Alcock, 1984). The average,  $\hat{s}_e$ , of the observed steepness of the 1% largest wave heights is calculated and the value of  $T_Z$  associated to an estimated extreme level of  $H_S$  is obtained from

$$T_Z = \sqrt{\frac{2\pi H_S}{g\hat{s}_e}}. \quad (4.1.4)$$

- For most of the sites analysed in this work the relationship between  $H_S$  and  $T_Z$  tends to assume a *quadratic* form, whereas the relationship between  $H_S$  and  $S$  is more linear, and hence statistically modelled more easily.
- Steepness is a variable of interest in its own right, regardless of its relationship to  $T_Z$ .
- There are theoretical restrictions to the maximum value that  $S$  can assume: theory predicts that random waves with  $S$  bigger than approximately 1:10 must break.

No parametric statistical model is proposed for the marginal distribution of steepness. The statistical model we have adopted is based simply on the observed data; that is, the empirical distribution. A restriction in the use of empirical models is the inability to extrapolate beyond the observed range of data, but this is not an important issue when modelling  $S$ , as we are mainly interested in waves characterised by high values in both  $H_S$  and  $T_Z$ , which produce mid-range/typical values of steepness. One situation in which extrapolation with respect to  $S$  might be relevant is in the presence of swell waves, which have relatively low significant wave heights and long periods. Historically, however, swell waves have been omitted in studies of probability of extreme waves because:

- observations on swell waves are of limited extent, as values for this variable are not produced by standard hindcast studies using the local wind climate;

- swell waves are only important at some exposed sites;
- swell waves alone are rarely believed to pose a significant threat and, furthermore, they are deemed to be independent of the other sea condition variables.

#### 4.1.4 Wave Direction

As with steepness, there is no requirement to extrapolate the wave direction variable, so again we estimate this distribution empirically. The empirical estimate of the density for wave direction is given by the proportion of the observed/hindcast wave directions that fall in each direction sector.

In practice, if wave direction is not explicitly in the structure function for the design under consideration, we should take the direction sectors as large as possible, subject to simple statistical modelling of the joint distribution of the other sea condition variables over this sector. This is the case for overtopping discharge rates, see equation (1.1.1). Experience at HR suggests that sectors of widths less than  $30^\circ$  are impractical as there are insufficient data on the other variables within each sector for an adequate statistical analysis.

#### 4.1.5 Wave Period

Wave period is a key variable in the sea condition vector. Its behaviour in this study is described by the joint behaviour of  $(H_S, S)$ . So the discussion of the choice of statistical model here should be treated as expository rather than as a basis for subsequent fitting.

Two possible approaches for developing a statistical model for the marginal distribution of wave period are:

- the use of distributions based on theoretical wave processes;
- empirical forms based on observed data.

The reason that neither approach is adopted in practice is that the theoretical models do not capture important features of observational data and that the empirical models do not provide extrapolations to wave periods beyond those observed in the data.

Instead, current practice is to develop statistical models for wave period through statistical models for the conditional distribution of wave period given the associated significant wave height measurement. The current approach HR recommend is to take wave period,  $T_Z$ , as being completely determined by the significant wave height,  $H_S$ , i.e. the value of  $T_Z$  can be determined given the associated  $H_S$ . The statistical model recommended here

is to link these variables via wave steepness,  $S$ . Taking a typical value of steepness,  $\hat{s}_e$ , as the average steepness of the observed 1% largest significant wave heights, then

$$T_Z = \left( \frac{2\pi H_S}{g\hat{s}_e} \right)^{1/2}. \quad (4.1.5)$$

Consequently, the implied marginal distribution of wave period is

$$\begin{aligned} \Pr\{T_Z \leq x\} &= \Pr\{(2\pi H_S / (g\hat{s}_e))^{1/2} \leq x\} \\ &= \Pr\{H_S \leq x^2 g\hat{s}_e / (2\pi)\}. \end{aligned}$$

Thus the distribution of  $T_Z$  is determined by the distribution of  $H_S$ . To illustrate this, if  $H_S$  follows a Weibull distribution, see equation (4.1.1), then

$$\Pr\{T_Z \leq x\} = 1 - \exp \left\{ - \left( \frac{x^2 g\hat{s}_e / (2\pi) - a}{b} \right)^c \right\} \text{ for } x \geq (2\pi a / g\hat{s}_e)^{1/2}. \quad (4.1.6)$$

Similarly, if  $H_S$  is GPD( $\sigma, \xi$ ) above the threshold  $u$ , then

$$\Pr\{T_Z \leq x\} = 1 - \lambda \left( 1 + \xi \frac{x^2 g\hat{s}_e / (2\pi) - u}{\sigma} \right)_+^{-1/\xi} \text{ for } x \geq (2\pi u / g\hat{s}_e)^{1/2}. \quad (4.1.7)$$

These derivations assume that  $S$  is constant. In practice  $S$  is variable and is dependent on  $H_S$ . If a statistical model for the joint distribution of  $(H_S, S)$  were available then the distribution of  $T_Z$  could be obtained from relationship (4.1.5). To show this let  $F_{X,Y}(x, y) = \Pr\{X \leq x, Y \leq y\}$  denote the joint distribution function of general variables  $X$  and  $Y$ . It follows from joint distribution results that

$$\begin{aligned} P\{T_Z \leq x\} &= \int_0^\infty \frac{\partial F_{T_Z, S}(x, s)}{\partial s} ds \\ &= \int_0^\infty \frac{\partial F_{H_S, S}(gsx^2 / (2\pi), s)}{\partial s} ds. \end{aligned} \quad (4.1.8)$$

Dependence aspects of the joint distribution of  $(H_S, S)$  are considered in Section 4.2.2. Clearly the impact of variation in  $S$ , and the dependence of  $S$  on  $H_S$ , are different factors. Here we illustrate the impact of the former by producing a statistical model for the distribution of wave period using representation (4.1.8) under the false assumption of independence of  $H_S$  and  $S$ . We estimate the marginal distribution of  $S$  using the empirical distribution for  $S$ . For the marginal distribution of  $H_S$  we use the Threshold Method with the GPD for values greater than the threshold (taken as the 95% empirical quantile) and the empirical distribution function for values below this threshold. By comparison with equation (4.1.7), where  $S$  is taken to be constant, we have

$$P\{T_Z \leq x\} = \frac{1}{n} \sum_{i=1}^n F_{H_S} \left( \frac{gs_i x^2}{2\pi} \right), \quad (4.1.9)$$

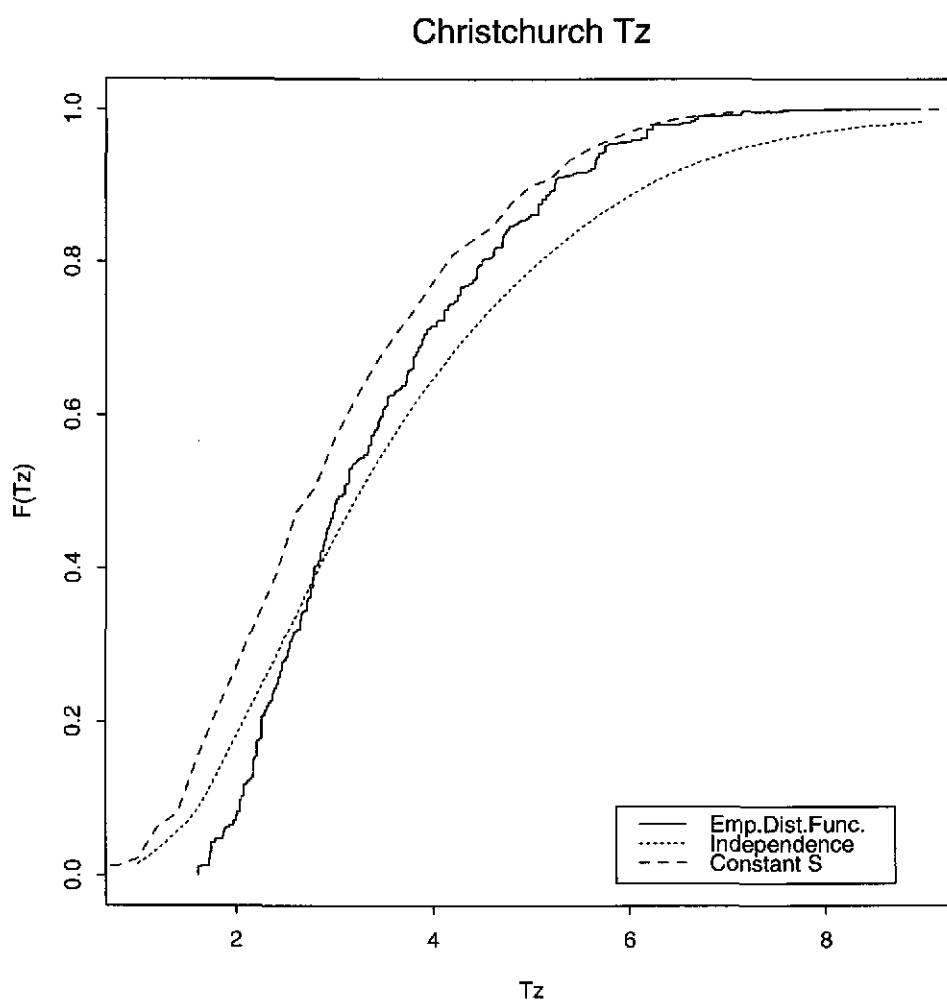
where  $n$  is the number of observations,  $s_i$ ,  $i = 1, \dots, n$  denote the observed values of  $S$ , and  $F_{H_S}$  is the distribution function of  $H_S$ , which is given by the GPD for values greater than the threshold and by the empirical distribution function for values below  $u$ . This is quite different from equation (4.1.7), where  $S$  was taken to be constant.

To illustrate these distributional models Figure 4.1 shows estimates of the distribution function of  $T_Z$  for observational data for Christchurch (described in Chapter 5). The estimates shown are based on different approaches. These are:

- the assumption of independence of  $H_S$  and  $S$ , i.e. equation (4.1.9);
- the empirical distribution function of  $T_Z$ ;
- the distribution function based on the constant  $S$  assumption, i.e. equation (4.1.7).

The distribution of  $T_Z$  obtained by fixing  $S$  to be  $\hat{s}_e$ , shows more substantial departures from the empirical distribution for typical values of wave period, but has good performance in the tail, reflecting the presence of dependence between high values of  $H_S$  and  $S$ . As this feature is not present in the statistical model based on independence of  $S$  and  $H_S$ , the tail is quite different in that case. However, the introduction of the variation of  $S$  gives a better fit in the bulk of the distribution. This suggests that once we have developed a suitable statistical model for the dependence between  $(H_S, S)$  we should have a good description of the whole distribution of  $T_Z$ .

Figure 4.1: Estimation of the distribution function of  $T_Z$  at Christchurch: estimates from the empirical distribution of  $T_Z$ , constant  $S$  and independence of  $(H_S, S)$ .



## 4.2 Dependence Models

In this section we describe statistical models for the inter-relationships between the separate sea condition variables. Typically the analysis of the joint distribution of the sea condition variables will be for an offshore location (a 20m depth is the usual depth limit to which waves can be hindcast without the use of a site-specific wave transformation model). At such a location the sea condition variables generally exhibit, or are taken to have, the following relationships:

- Surges and Waves are dependent.
- Significant wave height, wave period and direction are dependent.
- Tides and Surges are dependent processes.
- Tides and Waves are independent.

There are essentially two physical mechanisms which generate the sea condition variables

1. astronomical
2. meteorological.

Variables generated by the different physical mechanisms are independent unless they interact with each other. Offshore, the water depth is sufficient for the waves to be effectively independent of tides (not exactly independent because of the effect of currents), but the surges typically depend on the tide. In shallower water, waves become dependent on the tide, as the water depth influences the speed of the waves and through depth-dependent frictional effects, causes them to break.

That the tides and surges are dependent processes in shallow water areas is well known. Prandle and Wolf (1978) discuss the nature of observed interaction, which subsequent numerical model results show to be remarkably well captured by the known dynamical processes of depth based friction effects (Flather, 1987). However, if only high water levels are considered then, to a reasonable approximation, the associated tide and surge levels are independent.

Since surge and waves (significant wave height, wave period and wave direction) are both influenced by the wind climate, it should be expected that there is a relationship between these variables. The form of dependence at a site depends on the coastal location of the site, its associated fetch length and direction. For some sites positive dependence between surge and significant wave height is expected. At other sites negative dependence (or independence) between these variables is expected.

Often the dependence between still water level and wave characteristics is required since the still water level is not decomposed into its constituent components of tide and surge. Dependence is anticipated between waves and still water levels, but is almost certain to be closer to independence than the dependence between surges and waves, since the addition of the ‘independent’ tidal level masks the relationship.

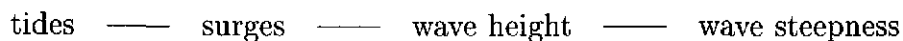
We need to describe the full joint distribution of the sea condition variables,  $\mathbf{X}$ . Each separate variable has been widely studied, see Section 4.1, and, as discussed above, physical understanding exists for the presence of dependence between  $SWL/Surge$  and  $H_S$ . However, little appears to be known about the pairwise relationships between

- $H_S$  and  $S$ ,
- $SWL/Surge$  and  $S$ ,
- $Surge$  and wave direction ( $\theta$ ),

or of the higher dimensional relationships. Through some limited studies we have identified:

1. stronger dependence between the pairs  $(SWL, H_S)$  and  $(H_S, S)$  than between the pair  $(SWL, S)$ ;
2. stronger dependence between the pairs  $(SWL, H_S)$  and  $(H_S, \theta)$  than between the pair  $(SWL, \theta)$ .

These features substantiate the argument that surges can only be linked to wave steepness and direction through the occurrence of waves, i.e. both pairs  $(Surge, S)$  and  $(Surge, \theta)$  are related through  $H_S$ . This corresponds to conditional independence between  $SWL/Surge$  and  $S$  given  $H_S$ , and between  $SWL/Surge$  and  $\theta$  given  $H_S$ . A graphical representation of the claimed dependence structure is as follows:



Here lines joining the variables show a direct relationship between that pair of variables; and a variable linked to a second only through a third variable is conditionally independent of the second variable given the third variable.

Wave direction is omitted from this graphical representation. For purposes of statistical modelling we examine the above structure for separate wave direction sectors, so separate analyses are performed for each direction sector which appears to have a different impact on the distribution of the other variables.

A key advantage of decomposing the joint distribution of  $\mathbf{X}$  into the conditional independence structure shown above is that to examine the joint distribution we only need

to examine the joint distribution of linked pairs, i.e. conditionally on the wave direction we estimate the joint distributions of

- $(SWL, H_S)$
- $(H_S, S)$ .

In this case we may write the joint density of  $(SWL, H_S, S)$  as

$$\frac{f_{SWL, H_S}(x, y) f_{H_S, S}(y, z)}{f_{H_S}(y)},$$

where the subscripts indicate the marginal and joint distribution variables. Equivalently, the joint density can be rewritten as

$$f_{SWL, H_S}(x, y) f_{S|H_S}(z|y),$$

where  $f_{S|H_S}$  is the conditional density of  $S|H_S$ . In Sections 4.2.1 and 4.2.2 we examine statistical models for estimating the joint distribution of  $(SWL, H_S)$  and  $(H_S, S)$  respectively. More specifically in the latter case we describe the conditional distribution  $S|H_S$ . Together, these distributions provide the full joint distribution of the sea condition variables.

In the following sections it is easiest to describe the dependence between the variables if the marginal variables take a standard form, such as a standard normal distribution (see Appendix A.4.1). It is possible to transform any continuous random variable to any other by repeated use of the probability integral transform (see Appendix A.3). Specifically, the random variable  $X$  with distribution function  $F_X$  can be transformed to a standard normal random variable  $X^*$  by

$$X^* = \Phi^{-1}(F_X(X)),$$

where  $\Phi^{-1}$  is the inverse of the distribution function of a standard normal random variable. Thus we have that

$$SWL^* = \Phi^{-1}(F_{SWL}(SWL)), \quad (4.2.1)$$

$$H_S^* = \Phi^{-1}(F_{H_S}(H_S)), \quad (4.2.2)$$

$$S^* = \Phi^{-1}(F_S(S)), \quad (4.2.3)$$

are standard normal versions of the random variables  $SWL, H_S$  and  $S$  respectively.

### 4.2.1 Models for dependence between $SWL$ and $H_S$

In this section three statistical models for the dependence structure of the variables  $(SWL, H_S)$  are proposed. These dependence models are for the marginal variables after transformation to standard normal form  $(SWL^*, H_S^*)$ :

- the bivariate normal model;
- the bivariate normal threshold model;
- the mixture of bivariate normals model.

The second and third models are both extensions of the bivariate normal model.

#### Bivariate Normal Model

Here we assume  $(SWL^*, H_S^*) \sim \text{BVN}(\mathbf{0}, \Sigma)$  (for notation see Appendix A.4.1) where

$$\Sigma = \begin{pmatrix} 1 & \rho \\ \rho & 1 \end{pmatrix}.$$

This statistical model is fitted using the likelihood given in Appendix A.4.1. The maximum likelihood estimator of  $\rho$ , the single parameter in this statistical dependence model, is approximately the sample correlation between  $(SWL^*, H_S^*)$  pairs.

#### Bivariate Normal Threshold Model

The bivariate normal model above assumes that there is the same degree of dependence between  $SWL^*$  and  $H_S^*$  whatever values these variables take. However, the dependence between still water levels and waves is expected to change as more extreme events are observed since the larger the surge event the less the masking effect of the tide and hence for large still water levels the true relationship between the surge and waves is identified. This is because tides are independent of the other variables and so weakens any form of dependence between the surge and waves.

Thus, to capture this potential for changing correlation, we adopt a statistically model consisting of a bivariate normal dependence structure in a region where both  $SWL^*$  and  $H_S^*$  are sufficiently large. Explicitly, for  $SWL^* > u$  and  $H_S^* > u$  for some threshold level  $u$ , we take the joint density for  $(SWL^*, H_S^*)$  to be identical in form to that of bivariate normal random variables, i.e.  $\text{BVN}(\mathbf{0}, \Sigma)$  where

$$\Sigma = \begin{pmatrix} 1 & \rho_u \\ \rho_u & 1 \end{pmatrix}.$$

This model is only completely explicit in this joint extreme region. The known marginal distributions and information derived from this joint extreme region impose structure on the positions of observations in regions where one or other variable is large, and also the region where neither is large.

For a given threshold this statistical model is fitted using the threshold likelihood given in Appendix A.4.2. The maximum likelihood estimator of  $\rho_u$ , the single parameter in this statistical dependence model, is essentially the correlation between  $(SWL^*, H_S^*)$  pairs which are simultaneously above the threshold  $u$  in each variable. However, the estimation of this parameter takes into account the number of observations in each of the four regions determined by the thresholds, and for the regions  $(SWL^* > u, H_S^* > u)$ ,  $(SWL^* > u, H_S^* < u)$  and  $(SWL^* < u, H_S^* > u)$  the sizes of the threshold exceedance values are accounted for.

We can treat  $\rho_u$  as a function of the common marginal threshold,  $u$ . For  $u$  less than the minimum data value this estimate is approximately the estimate of  $\rho$  for the bivariate normal model, i.e. the correlation coefficient, whereas for large  $u$  this measures the dependence between the extreme pairs. If in fact the data were from a bivariate normal distribution then  $\rho_u$  would be independent of  $u$ .

A threshold has to be chosen for this statistical model. What is required is that  $u$  is high enough so that the degree of correlation does not change above that threshold. A suitable threshold can be identified from the estimated  $\rho_u$  function, by taking the smallest  $u$  above which the function is constant.

## Mixture of Bivariate Normals Model

A disadvantage of the bivariate normal threshold model is that the dependence is taken to be constant above a threshold level. If the correlation function  $\rho_u$  shows no evidence of constancy then fixing dependence to be constant above a threshold can lead to bias in extrapolations of the dependence structure. Thus there is a need to model the change in the correlation function with threshold, to increase confidence in extrapolations.

One idealised example in which the correlation function varies with threshold level is as follows. Suppose

- there are two distinct ‘meteorological mechanisms’ which produce still water level and wave events.
- each different mechanism produces different levels of dependence between still water level and waves.
- from the  $(SWL, H_S)$  data only, we cannot identify which of the different mechanisms produced a particular data pair.

A crude example of this is given in situations where

1. regionally generated waves and still water levels are dependent, but
2. locally generated waves and still water levels are independent.

A consequence of such a structure is that the dependence between still water level and significant wave height is a mixture of two different dependence forms. If one component of the mixture describes the dependence between low values and the other between high values then the correlation function  $\rho_u$  will change with  $u$  to give the correlation of the second form for the largest events.

The statistical model here is more complex than for the above cases, being given by Appendix A.4.3. For each form of dependence a bivariate normal distribution is used to describe the variations. The overall statistical dependence model has seven parameters, which can be fitted by maximum likelihood:

- one parameter  $p_M$ : determining the proportion of the data of each dependence type ( $p_M = 0$  or  $p_M = 1$  suggests that there is only one type of dependence and a bivariate normal model would fit well);
- two parameters  $\rho_1$  and  $\rho_2$ : which measure the correlation associated with each type of dependence form; and
- four parameters  $\mu_2 = (\mu_{21}, \mu_{22}), \sigma_{21}, \sigma_{22}$ : which explain the differences in mean level and variation between events generated by the two mechanisms after transformation to the standard normal marginal scale.

This statistical model has two major benefits over the bivariate normal threshold model:

1. the model is fitted with all the data having equal weight contrasting with the threshold model where the most extreme values are given most weight;
2. the model fits and extrapolates cases where the dependence continues to change throughout the data and beyond, so the arbitrary specification of a threshold is avoided.

On the negative side the main disadvantage is that the statistical dependence model is more complex to fit and parameter estimates more difficult to interpret. Critical to its application is testing whether two, or one, bivariate normal dependence forms exist. Unless there is significant evidence for two forms, only one (i.e. the standard bivariate normal model) should be used.

### 4.2.2 Models for dependence between $H_S$ and $S$

In this section we develop statistical models for the distribution of  $S$  conditional on the variable  $H_S$ . The current approach used by practising engineers is to take this distribution as degenerate, i.e. the steepness is given a fixed estimate,  $\hat{s}_e$ , irrespective of the value of  $H_S$ . The estimate  $\hat{s}_e$  is given by the average steepness of the 1% largest significant wave height values.

We propose a model for the distribution of  $S$  given  $H_S$  which

- depends on the value of  $H_S$ ,
- has variation in  $S$  values for a given  $H_S$  value,
- contains the existing model as a special case.

In the transformed standard normal (Gaussian) random variable space  $(H_S^*, S^*)$ , see equations (4.2.2) and (4.2.3), we statistically model the conditional distribution of  $S^*|H_S^*$  subject to  $H_S^*$  being sufficiently large. Our reason for focusing on large  $H_S^*$ , say  $H_S^* > u$ , is that we are only interested in  $S$  conditional on  $H_S$  being large. Specifically, we take

$$S^*|(H_S^* = h) \sim N(a + b(h - u), \sigma^2), \text{ for } h > u \quad (4.2.4)$$

i.e. a linear statistical regression model for  $S^*$  with explanatory variable  $h - u$ , having intercept, gradient and variance parameters  $(a, b, \sigma^2)$  respectively, and a Normal distribution for the error variable.

This method of describing the dependence is strongly related to the assumption of a bivariate normal dependence model (see Appendix A.4.1) between  $S^*$  and  $H_S^*$ . For example, if  $(S^*, H_S^*)$  follow a bivariate normal distribution with correlation  $\rho$ , then the parameters of equation (4.2.4) would take the form

$$\begin{aligned} a &= 0 \\ b &= \rho \\ \sigma^2 &= 1 - \rho^2. \end{aligned}$$

Thus the statistical model we propose is slightly more general than a bivariate normal dependence structure as our model does not require a zero intercept to the linear model or a link between the residual variation and the gradient of the linear model.

Finally we have the problem of threshold selection again. The choice of threshold is less important than for other aspects of the modelling of the joint distribution as results are reasonably insensitive to threshold choice here. To aid threshold choice we produce plots of

$$E(S^*|H_S^* > u) \text{ and } \text{Var}(S^*|H_S^* > u)$$

using equivalent sample based moments, for a range of potential threshold values. We look for approximate linearity in the expectation and constancy in the variance as indicators that a sufficiently high level has been used. These plots are best used for identifying whether the dependence is positive, negative, or independence. Positive/negative dependence is indicated by rising/falling values for  $E(S^*|H_S^* > u)$ , whereas for independence both the above plots show constancy.

Strictly these are not the most useful plots for threshold selection, since for the linear regression model to be appropriate, we need  $E(S^*|H_S^* = u)$  to be linear and  $\text{Var}(S^*|H_S^* = u)$  to be constant. Plots based on these features require common  $H_S^*$  values to be pooled, so here we have the problem of the choice of the degree of pooling. In Chapter 7 we adopt the simpler, though less informative approach where conditioning is based on  $H_S^* > u$ .

### 4.3 Evaluation of the Probability of Failure using the JPM

As described in Section 2.2 the final step in the implementation of the JPM is the evaluation of the integral expression

$$\hat{\text{Pr}}\{\mathbf{X} \in A_u\} = \int_{A_u} \hat{f}_{\mathbf{X}}(\mathbf{x}) d\mathbf{x},$$

where  $\hat{f}$  is the estimated joint density of  $\mathbf{X}$  and  $A_u$  is the failure region. This may seem simple, but the joint density of the sea condition variables is (4/5)-dimensional and the set over which the integration is required (the failure region) is a complex set, so this integration requires some care.

No analytical expression is obtainable in these problems so numerical methods of some form need to be used. There are two approaches:

- numerical integration;
- simulation.

There are many numerical methods for integration, but in practice these are not ideal when the dimension of the integral is relatively high and the form of the failure region is non-linear. Therefore the simulation approach is proposed, which involves a three stage procedure:

1. simulation of a large number,  $n_s$  say, of pseudo observations from the fitted joint distribution of  $\mathbf{X}$ ;
2. evaluation of the structure variable,  $\Delta(\mathbf{X})$ , for each pseudo observation;

3. evaluation of the integral as the proportion of the pseudo observations on the structure variable that exceed the critical level  $u$ . Letting  $\mathbf{X}_s$  denote the  $s$ th simulation from the joint density  $\hat{f}$ , then the Monte Carlo estimate of the integral is

$$\frac{\text{number of the points } \mathbf{X}_s, s = 1, \dots, n_s \text{ in the set } A_u}{n_s}.$$

Step 1 above is general and independent of the form of the structure function. Thus if a wide range of designs are to be considered this step only needs to be undertaken once. The output in the form of a series of events so is of interest for a range of design studies. By itself this is a valuable output from the analysis for coastal engineers.

Increasing  $n_s$  improves the precision of the evaluation of the estimated probability of failure. In practice  $n_s$  should correspond to 10-100 times the length of the return period of interest, so the largest simulation sample sizes are required for the most extreme extrapolations. This can be computationally intensive although straight forward to implement. More generally, methods exist for improving the precision without increasing  $n_s$ . These methods use importance sampling in the simulation stage, which involves simulating a disproportionate number of extreme sea condition observations at the simulation stage and appropriately down-weighting the proportion of failures in the estimation stage. More specifically, pseudo observations are generated from a suitably chosen joint distribution with density,  $g(\mathbf{x})$ , giving a disproportionate number of extreme  $\mathbf{X}$  values. The importance sampling factor for a simulated value  $\mathbf{X}$  is

$$\frac{f_{\mathbf{X}}(\mathbf{X})}{g(\mathbf{X})},$$

i.e. the fitted joint density relative to the joint density used for the simulation of the pseudo observations. So Step 1 involves generating  $n_s$  values  $\mathbf{X}_i$ , from  $g$ , with importance sampling factors  $f_{\mathbf{X}}(\mathbf{X}_i)/g(\mathbf{X}_i)$  for  $i = 1, \dots, n_s$ . The estimated probability of failure, i.e.  $\Pr\{\mathbf{X} \in A_u\}$ , is then given by

$$\frac{1}{n_s} \sum_{i=1}^{n_s} I(\mathbf{X}_i \in A_u) f_{\mathbf{X}}(\mathbf{X}_i)/g(\mathbf{X}_i),$$

where

$$I(\mathbf{X}_i \in A_u) = \begin{cases} 1 & \text{if } \mathbf{X}_i \in A_u \\ 0 & \text{if } \mathbf{X}_i \notin A_u. \end{cases}$$

This method is less computationally intensive than the direct simulation method but requires some experience in the selection of an appropriate joint density function  $g$ .

In this report we have used the importance sampling techniques in Chapters 7 and 8, but for applications of the JPM to the estimation of the probability of failure in Chapter

9 we found the direct approach was suitable. In other applications, where the structure function is too computationally intensive to evaluate many thousands of times, importance sampling may be necessary.



## **Part II**

# **Examples of Data Analysis using the Joint Probability Method**



# Chapter 5

## Study Data

Within the project two formats of data were considered:

1. Observational data – consisting of measured data and hindcast data;
2. Simulated data – consisting of synthetically generated data from a known statistical model.

In this chapter we describe the two different types of data sets used in the study, and for the simulated data give the statistical model used to generate these.

### 5.1 Observational data

A number of sites were identified as having interesting characteristics relevant to the study. Primary interest was in obtaining sites which had a wide range of dependence structures, so sites with negative dependence, independence and positive dependence between still water levels and waves were selected. Sites with the still water level separated into tides and surges, and where the directionality of the wave processes is influential to the joint distribution of the other sea condition variables, were also selected to enable these features to be examined. An additional criterion was that each site should have a number of years of data available.

Six sites which possessed the relevant properties were Cardiff, Christchurch, Dover, Dowsing, North Wales and Shoreham. Table 5.1 gives details of the data for these sites. In each case, the wave data are hindcast values. Other sites where measured wave data are also available were studied to a lesser extent.

Site	Variables	Sampling	Years
Cardiff	SWL, Surge, Waves	High Waters	60–87
Christchurch	SWL, Surge, Waves	Hourly	78–90
Dover	SWL, Surge, Waves	Hourly	71–79
Dowsing	SWL, Surge, Waves	Hourly	78–87
North Wales	SWL, Surge, Waves	High Waters	70–83
Shoreham	SWL, Surge, Waves	High Waters	81–91

Table 5.1: Information about the observational data sites: SWL – still water level, Waves – significant wave height, wave period, wave direction.

## 5.2 Simulated data

Five data sets have been simulated to reproduce the main features of five of the six main data sets (excluding Shoreham). The true statistical model for the joint distribution of the five simulated data sets (Sim1 – Sim5) is described below for each data set.

In each case we have simulated 7000 independent points, approximately equivalent to 10 years of separate high water levels. Marginal aspects of the joint distribution are taken as either

- the empirical distribution of the variable from one of the observational data sets, or
- based on parametric models fitted to the observational data.

Dependence aspects are not as representative of the characteristics of the observational data sets as the marginal features. A number of dependence models were selected to have different, but simple, dependence forms and a range of dependence levels.

For each simulated data set we generated complete data on the vector

- still water level (*SWL*). (In addition for Sim3, the tide and surge constituents were separately generated);
- significant wave height ( $H_S$ );
- wave direction ( $\theta$ );
- wave period ( $T_Z$ ).

In the simulations wave period was obtained by generating  $H_S$  and the *wave steepness*,  $S$ , and using the relationship

$$T_Z = \left( \frac{2\pi H_S}{gS} \right)^{1/2},$$

where  $g$  is the acceleration due to gravity.

## Siml data

### Marginal distributions

The marginal distribution of  $\theta$  is taken to be the same as the equivalent empirical distribution of the Cardiff data. For both  $SWL$  and  $H_S$  a mixture of the empirical distribution and parametric models are used. For  $SWL$  below the 95% empirical quantile of the Cardiff  $SWL$  data, the empirical distribution is used; above this threshold, the distribution follows a generalised Pareto distribution (see Chapter 3, equation (3.1.3)) with parameters  $\sigma = 0.362$  and  $\xi = -0.264$ .

Both  $S$  and  $H_S$  have distributions which depend on  $\theta$ :

- When  $0^\circ < \theta < 110^\circ$ :

For  $H_S$ : below the 95% empirical quantile of the Cardiff  $H_S$  data from this direction sector, the empirical distribution is used whereas above this threshold, the distribution follows a generalised Pareto distribution with parameters  $\sigma = 0.1958$  and  $\xi = -0.102$ .

For  $S$  the empirical distribution of the Cardiff data in this sector is used.

- When  $110^\circ < \theta < 360^\circ$ :

For  $H_S$ : below the 95% empirical quantile of the Cardiff  $H_S$  data from this direction sector, the empirical distribution is used, whereas above this threshold, the distribution follows a generalised Pareto distribution with parameters  $\sigma = 0.1417$  and  $\xi = -0.0604$ .

For  $S$ , the empirical distribution of the Cardiff data in this sector is used.

### Dependence Structure

After transformation of each marginal variable ( $H_S, SWL, S$ ) to a standard normal distribution, the form of the dependence between the three variables is a trivariate normal distribution with zero-mean vector (see Appendix A.2.2). However the variance-covariance matrix,  $\Sigma$ , depends on wave direction, with  $\Sigma$  given by

$$\Sigma = \begin{pmatrix} 1 & 0.3 & 0.62 \\ 0.3 & 1 & 0.3 \times 0.62 \\ 0.62 & 0.3 \times 0.62 & 1 \end{pmatrix},$$

when  $\theta < 110^\circ$ , and

$$\Sigma = \begin{pmatrix} 1 & 0.3 & 0.742 \\ 0.3 & 1 & 0.3 \times 0.742 \\ 0.742 & 0.3 \times 0.742 & 1 \end{pmatrix},$$

when  $\theta \geq 110^\circ$ .

This dependence structure corresponds to positive dependence between  $(H_S, SWL)$  and between  $(H_S, S)$ , but with  $(SWL, S)$  only related via their relationship with  $H_S$ . The directionality of the waves influences the dependence structure by increasing the dependence between  $H_S$  and  $S$  when  $\theta \geq 110^\circ$ .

## Sim2 data

### Marginal distributions

The marginal distributions of  $\theta$  and  $S$  are taken to be the same as the equivalent empirical distributions of the Dover data. For both  $SWL$  and  $H_S$  a mixture of the empirical distribution and the parametric model is used. Specifically, for  $SWL$  below the 95% empirical quantile of the Dover  $SWL$  data, the empirical distribution is used, whereas above this threshold, the distribution follows a generalised Pareto distribution with parameters  $\sigma = 0.1866$  and  $\xi = -0.0764$ .

Significant wave height has a distribution which depends on the wave direction:

- For  $0^\circ < \theta < 110^\circ$ :

below the 95% empirical quantile of the Dover  $H_S$  data from this direction sector, the empirical distribution is used, whereas above this threshold, the distribution follows a generalised Pareto distribution with parameters  $\sigma = 0.731$  and  $\xi = -0.4215$ .

- For  $110^\circ < \theta < 360^\circ$ :

below the 95% empirical quantile of the Dover  $H_S$  data from this direction sector, the empirical distribution is used whereas above this threshold, the distribution follows a generalised Pareto distribution with parameters  $\sigma = 0.46$  and  $\xi = -0.112$ .

### Dependence Structure

The direction,  $\theta$ , only influences the marginal distributions of the variables, but not their dependence structure which is assumed to be constant across sectors. The  $(H_S, SWL, S)$  variables are taken to be dependent. After transformation of each marginal variable to a standard normal distribution, the form of the dependence between the  $(H_S, SWL, S)$  variables is a trivariate normal distribution with zero-mean vector and variance-covariance matrix,  $\Sigma$ , given by

$$\Sigma = \begin{pmatrix} 1 & -0.2 & -0.1 \\ -0.2 & 1 & -0.2 \times -0.1 \\ -0.1 & -0.2 \times -0.1 & 1 \end{pmatrix}.$$

This dependence structure corresponds to negative dependence between  $(H_S, SWL)$  and

between  $(H_S, S)$ , but with  $(SWL, S)$  positively dependent through their relationship with  $H_S$ .

Finally to ensure that no artificially large values of  $T_Z$  are produced as a result of a high  $H_S$  value occurring with a small  $S$  value, we modify the simulated data set by setting  $H_S$  to be the minimum observed  $H_S$  value when  $S \leq 0.02$ .

## Sim3 data

### Marginal distributions

The marginal distributions of  $\theta$ ,  $S$  and tides are taken to be the same as the equivalent empirical distributions of the North Wales data. For both *Surge* and  $H_S$  variables a mixture of the empirical distribution and the parametric model is used. Specifically, for both *Surge* and  $H_S$  below the 95% empirical quantile of the associated North Wales data, the empirical distribution is used, whereas above these thresholds the distribution follows a generalised Pareto distribution, with parameters  $\sigma = 0.1446$  and  $\xi = 0.0803$  for *Surge* and  $\sigma = 0.6119$  and  $\xi = -0.1583$  for  $H_S$ .

### Dependence Structure

The wave direction and tide are taken to be independent of the  $(H_S, \textit{Surge}, S)$  variables, which are taken to be dependent. After transformation of each marginal variable to a standard normal distribution, the form of the dependence between the three variables is a trivariate normal distribution with zero-mean vector and variance-covariance matrix,  $\Sigma$ , given by

$$\Sigma = \begin{pmatrix} 1 & 0.16 & 0.0497 \\ 0.16 & 1 & 0.16 \times 0.0497 \\ 0.0497 & 0.16 \times 0.0497 & 1 \end{pmatrix}.$$

This dependence structure corresponds to positive dependence between  $(H_S, \textit{Surge})$  and very weak positive dependence between  $(H_S, S)$ , and with  $(\textit{Surge}, S)$  almost independent.

## Sim4 data

### Marginal distributions

The marginal distributions of  $\theta$  and  $S$  are taken to be the same as the equivalent empirical distributions of the Christchurch data. For both *SWL* and  $H_S$  values a mixture of the empirical distribution and parametric models is used. Specifically, for both *SWL* and  $H_S$  below the 95% empirical quantile of the associated Christchurch data, the empirical distribution is used, whereas above these thresholds the distribution follows a generalised Pareto distribution, with parameters  $\sigma = 0.126$  and  $\xi = -0.15$  for *SWL* and  $\sigma = 0.6685$  and  $\xi = 0.15$  for  $H_S$ .

### Dependence Structure

The wave direction and  $S$  variables are taken to be independent of the  $(H_S, SWL)$  variables, which are taken to be dependent. After transformation of each marginal variable to a unit Fréchet distribution, (i.e. with distribution function  $\Pr\{X \leq x\} = \exp(-1/x)$  for  $x > 0$ ) the form of the dependence between the two variables  $(X, Y)$ , is taken to be a bivariate extreme value distribution (with logistic dependence structure) given by

$$\Pr\{X \leq x, Y \leq y\} = \exp\{-(x^{-1/\alpha} + y^{-1/\alpha})^\alpha\}, \quad (5.2.1)$$

where  $0 < \alpha \leq 1$  determines the degree of dependence. We took  $\alpha = 0.8$ . This dependence structure corresponds to a strong form of positive dependence between  $(H_S, SWL)$  with particularly high levels of dependence between the most extreme values of each variable, see Section 3.3.1.

Finally, to ensure that no artificially large values of  $T_Z$  are produced as a result of a high  $H_S$  value occurring with a small  $S$  value, we modify the simulated data set by setting  $H_S$  to be the minimum observed  $H_S$  value when  $S \leq 0.014$ .

## Sim5 data

### Marginal distributions

The marginal distributions of  $\theta$  and  $S$  are taken to be the same as the equivalent empirical distributions of the Dowsing data. For both  $SWL$  and  $H_S$  values a mixture of the empirical distribution and parametric models is used. Specifically, for both  $SWL$  and  $H_S$  below the 95% empirical quantile of the associated Dowsing data, the empirical distribution is used, whereas above these thresholds the distribution follows a generalised Pareto distribution, with parameters  $\sigma = 0.2091$  and  $\xi = -0.0711$  for  $SWL$  and  $\sigma = 0.8091$  and  $\xi = 0.1121$  for  $H_S$ .

### Dependence Structure

The wave direction and  $S$  variables are taken to be independent of the  $(H_S, SWL)$  variables, which are taken to be dependent. After transformation of each marginal variable to a standard normal variable, the joint distribution of these variables is given by by the mixture of bivariate normal distributions described in Appendix A.4.3. The parameters of this dependence model are

$$\mu_2 = (0.3, 0.3), \sigma_{21} = \sigma_{22} = 1, p = 0.9, \rho_1 = 0, \text{ and } \rho_2 = 0.8.$$

### 5.3 Principal differences between the simulated data sets

The key differences between the simulated data sets are summarised in Table 5.2. These differences are largely self explanatory, with

- the  $SWL$  and  $H_S$  tails determined by the value of the shape parameter,  $\xi$ , used to simulate values from the GPD distribution for the tail of the variable,
- the distorted tails for Sim4 are a consequence of the way that the tails of  $H_S$  and  $SWL$  have been deliberately lengthened and shortened respectively from values estimated at Christchurch to illustrate how the SVM and JPM compare when the two variables have quite different tail forms. The simulated data do not reproduce the hindcast data well at this site.

data	key feature	$SWL$ tail	$H_S$ tail	Dependence
Sim1	directionality important	short	medium	+ medium
Sim2	directionality of $H_S$	medium	short/medium	- medium
Sim3	tide and surge data	long	short	+ medium
Sim4	distorted tails	short	long	+ high
Sim5	complex dependence	medium	long	+ medium/high

Table 5.2: Differences in the statistical models for the simulated data sets Sim1-Sim5.

## 5.4 Comparison of observed and simulated data

Figures 5.1-5.22 show various aspects of the joint distribution of the sea condition variables for both the observational and the simulated data sets in the report. Specifically, joint scatter plots of the data are shown for

- still water level (SWL) and significant wave height ( $H_S$ )
- surge and  $H_S$
- $H_S$  and wave period ( $T_Z$ )
- SWL and  $T_Z$ .

In addition, for both Cardiff and Sim1 data sets, wave direction is plotted against  $H_S$  and  $T_Z$ .

Features of interest are:

**For Cardiff and Sim1** Larger  $T_Z$  values occur in Sim1 than the observational data. The reason for this is that the simulation model for dependence between  $H_S$  and  $S$  has not sufficiently restricted small  $S$  values to occur only with small  $H_S$  values. Other than this the simulated data reproduces the key characteristics of the Cardiff data well, possibly with the exception of not giving large enough  $T_Z$  values for directions less than  $100^\circ$ . The probable explanation of this is our use of  $110^\circ$  rather than  $190^\circ$  as a basis to separate direction types when setting up the Sim1 data. Later analysis of the Cardiff observational data takes the split at  $190^\circ$ .

**For Dover and Sim2** The agreement here is very good. Figure 5.8 shows some apparent difference in the relationship of  $(H_S, T_Z)$  but this is primarily due to ties in the observational data which appear as a single point on the plot.

**North Wales and Sim3** There is a good agreement with the observational data. Note the outlier in the observational surge data.

**Christchurch and Sim4** Here the key difference is in the scale of the  $T_Z$  upper tail, which is much longer (almost twice as long) for Sim4 than the observational data. This is due to the  $(H_S, S)$  values being taken to be independent, thus allowing small  $S$  values to occur with large  $H_S$  values (to produce very large  $T_Z$ ) in the simulation model. The  $T_Z$  values are unrealistically large for Sim4. Sim4 was the simulated data set where the  $H_S$  tail was deliberately lengthened. However, this does not seem to have made a notable change from the observational data set (as seen from Figure 5.15). As a result of these features, Sim4 cannot be considered to be a realistic representation of sea conditions at Christchurch.

**For Dowsing and Sim5** The main difference between these sets is that the simulated data have a few much larger values of  $H_S$  (almost twice as large) than appear in the observational data. Correspondingly, these observations produce a few larger  $T_Z$  values for Sim5 than the Dowsing observational data.

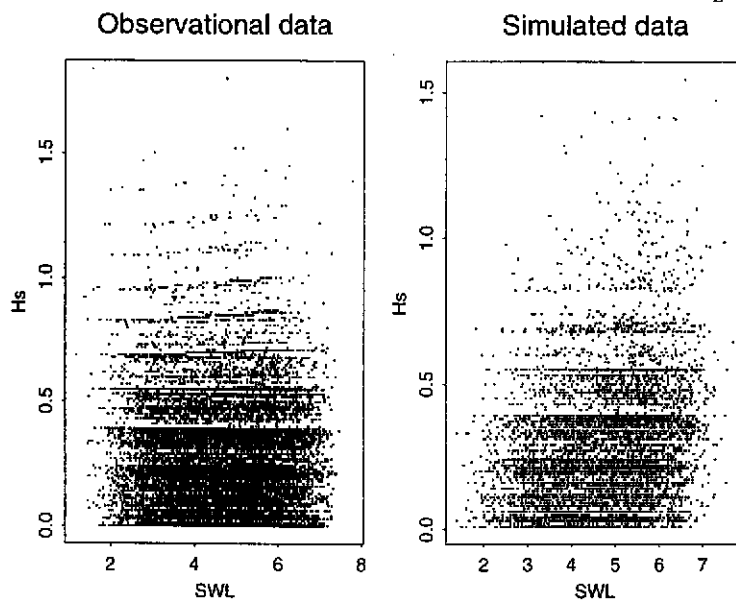
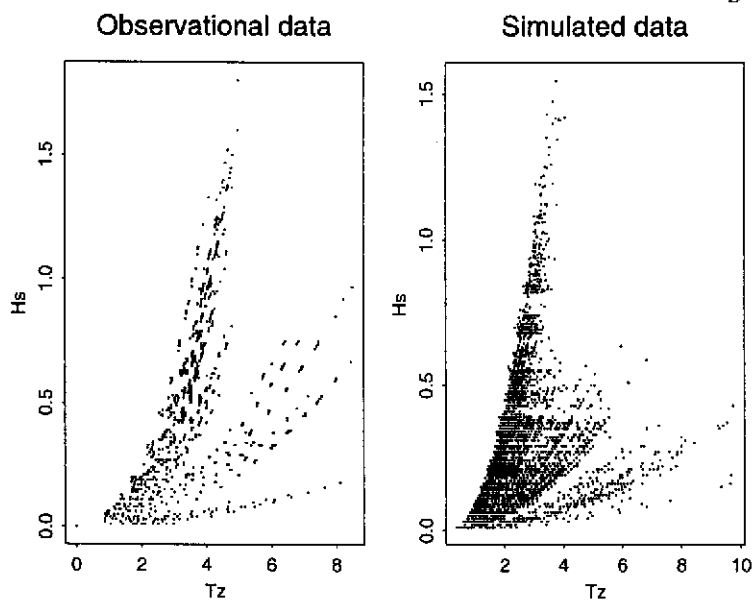
Figure 5.1: Cardiff observational data and Sim1 data:  $H_S$  vs SWLFigure 5.2: Cardiff observational data and Sim1 data:  $H_S$  vs  $T_Z$ 

Figure 5.3: Cardiff observational data and Sim1 data: SWL vs  $T_Z$

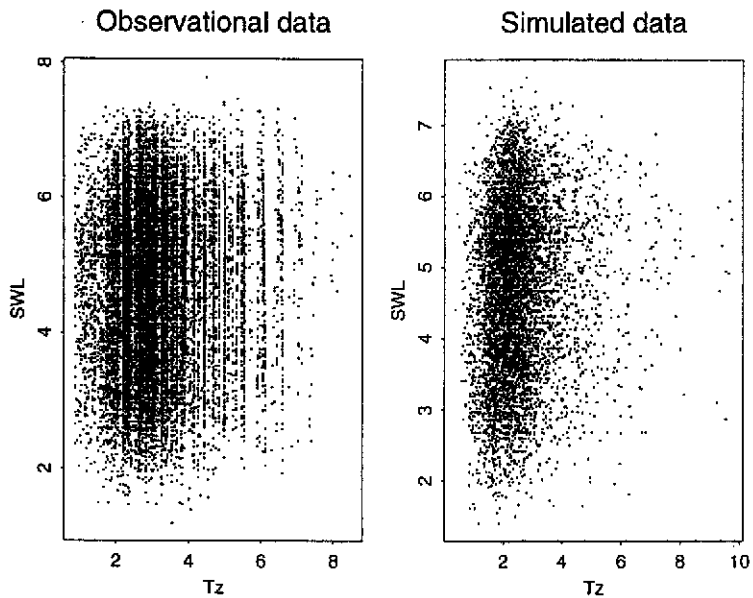


Figure 5.4: Cardiff observational data and Sim1 data:  $H_S$  vs  $\theta$

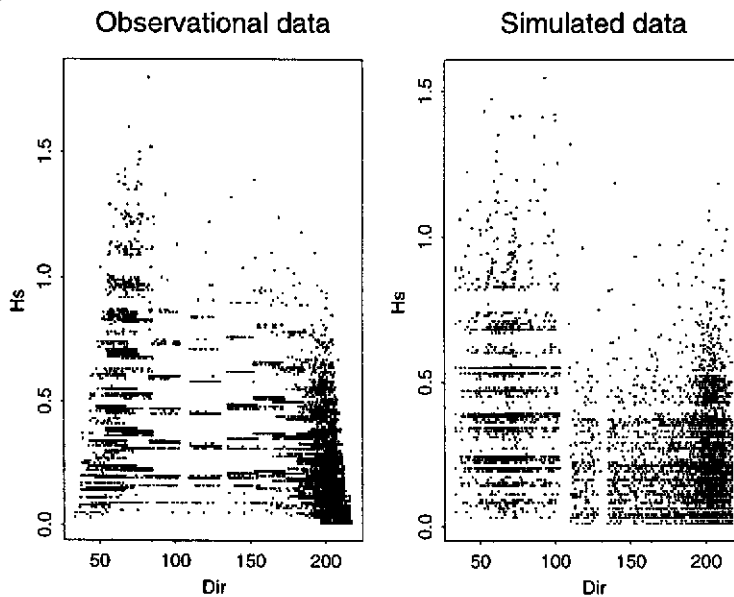


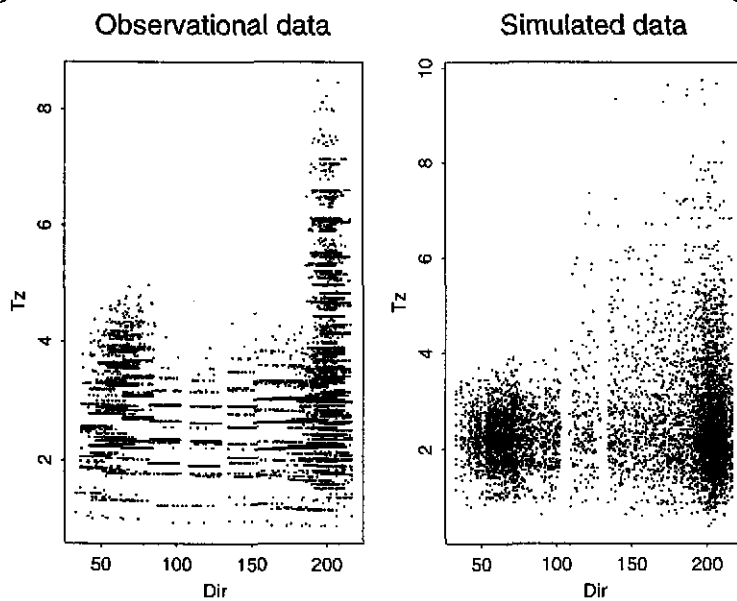
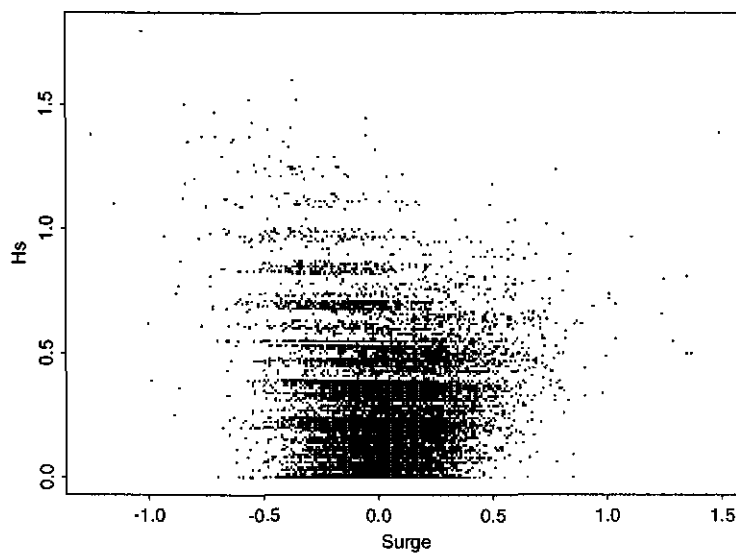
Figure 5.5: Cardiff observational data and Sim1 data:  $T_Z$  vs  $\theta$ Figure 5.6: Cardiff observational data:  $H_S$  vs Surge  
Cardiff

Figure 5.7: Dover observational data and Sim2 data:  $H_S$  vs SWL

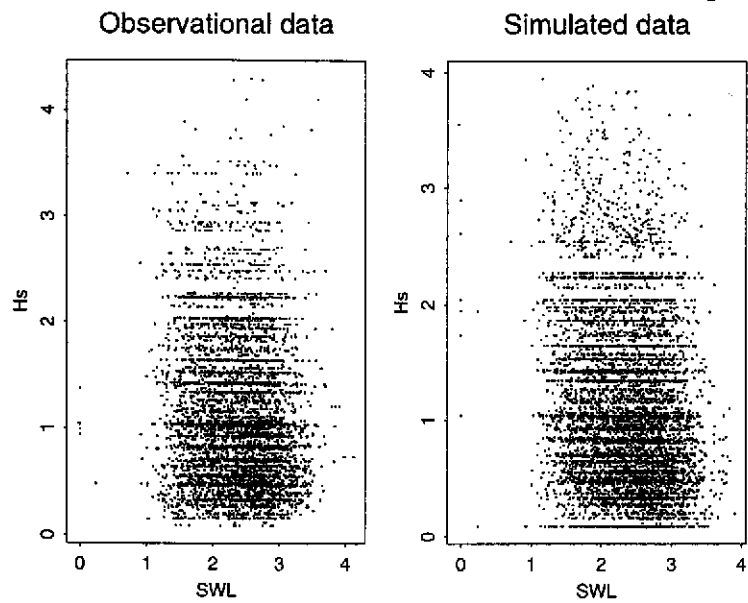


Figure 5.8: Dover observational data and Sim2 data:  $H_S$  vs  $T_z$

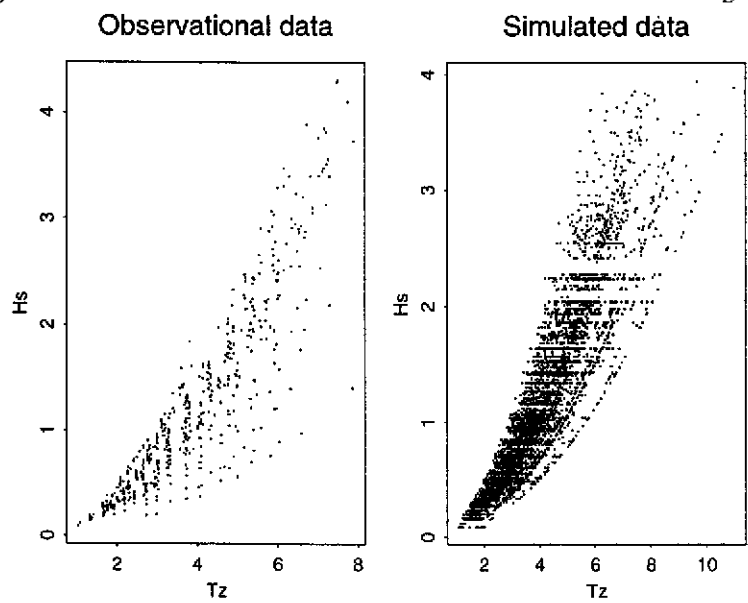


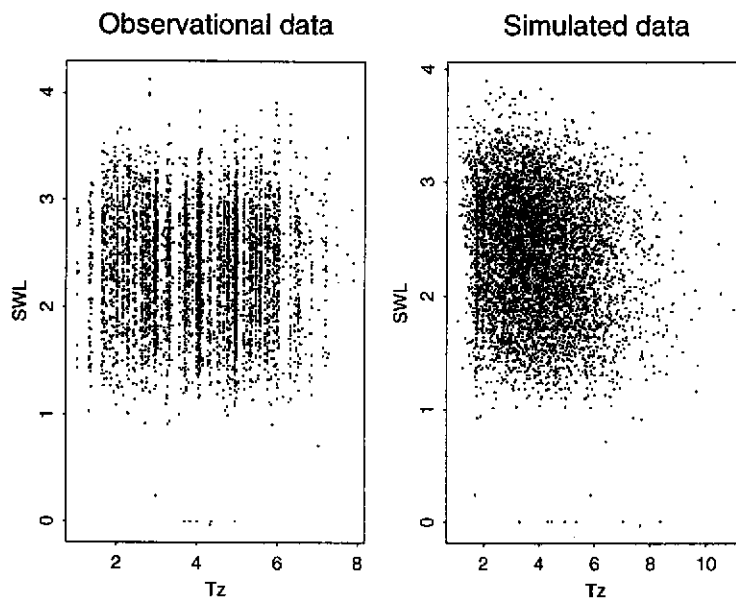
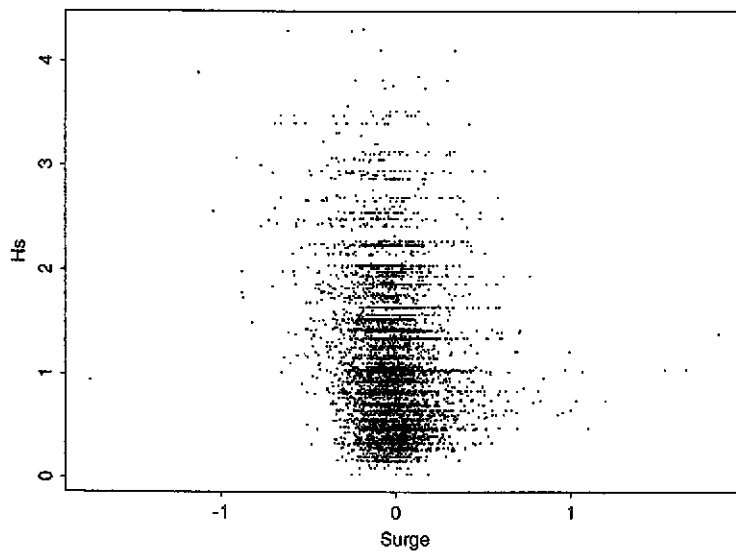
Figure 5.9: Dover observational data and Sim3 data: SWL vs  $T_z$ Figure 5.10: Dover observational data:  $H_S$  vs Surge  
Dover

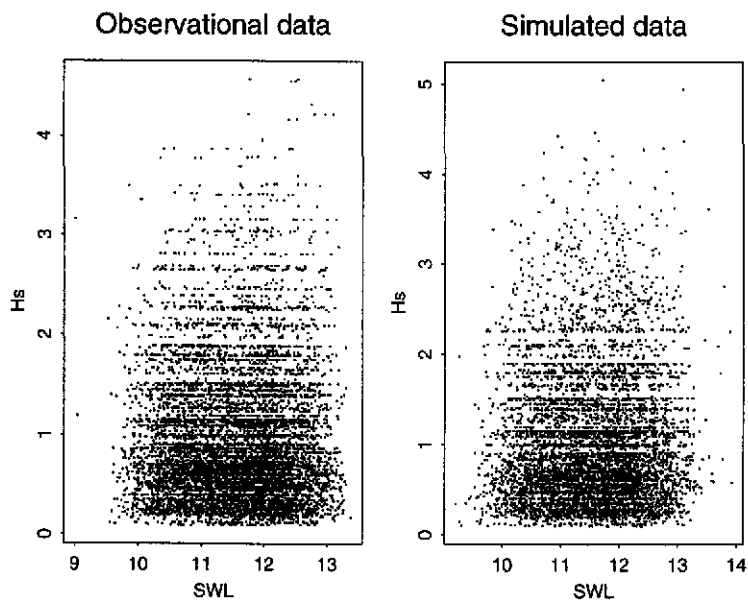
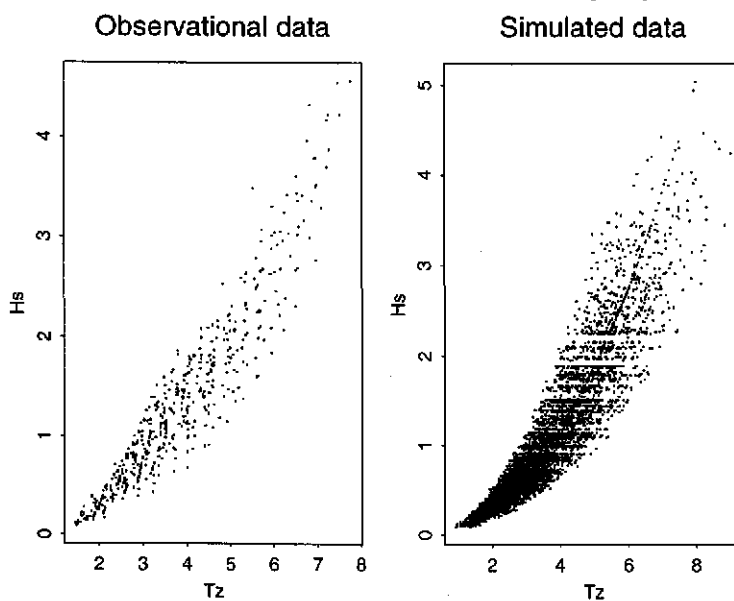
Figure 5.11: North Wales observational data and Sim3 data:  $H_S$  vs SWLFigure 5.12: North Wales observational data and Sim3 data:  $H_S$  vs  $T_Z$ 

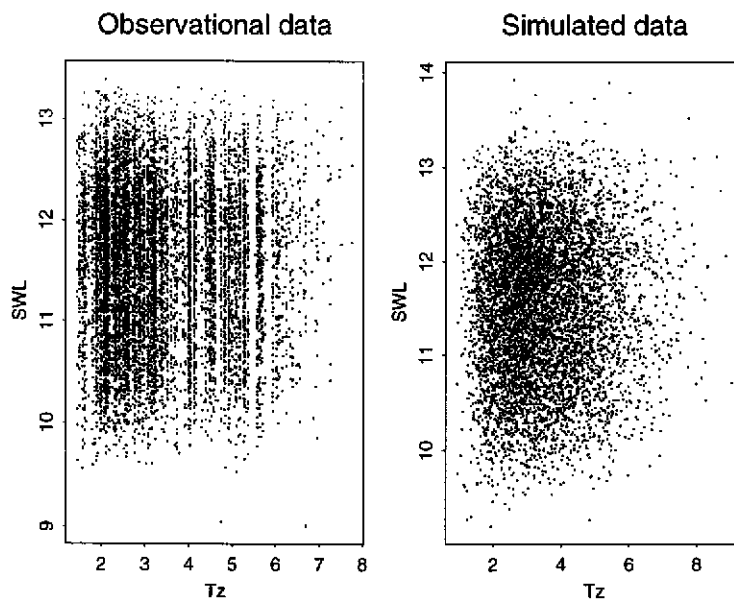
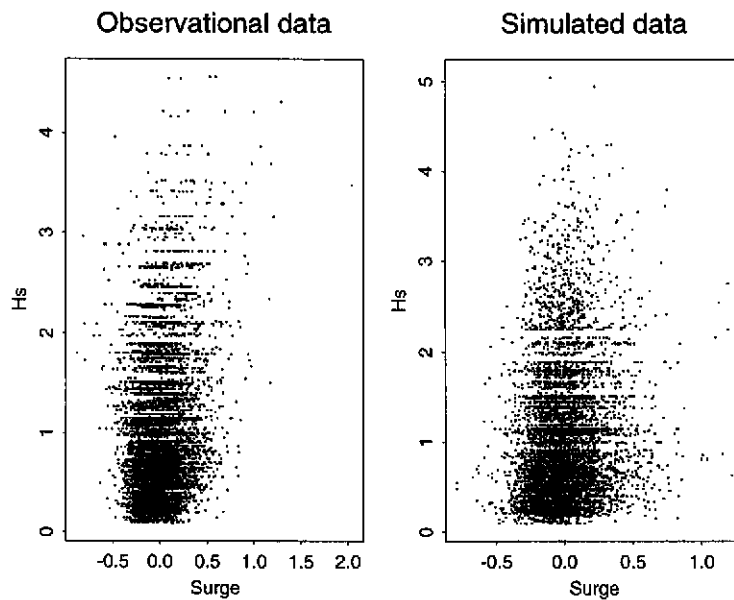
Figure 5.13: North Wales observational data and Sim3 data: SWL vs  $T_Z$ Figure 5.14: North Wales observational data and Sim3 data:  $H_S$  vs Surge

Figure 5.15: Christchurch observational data and Sim4 data:  $H_S$  vs SWL

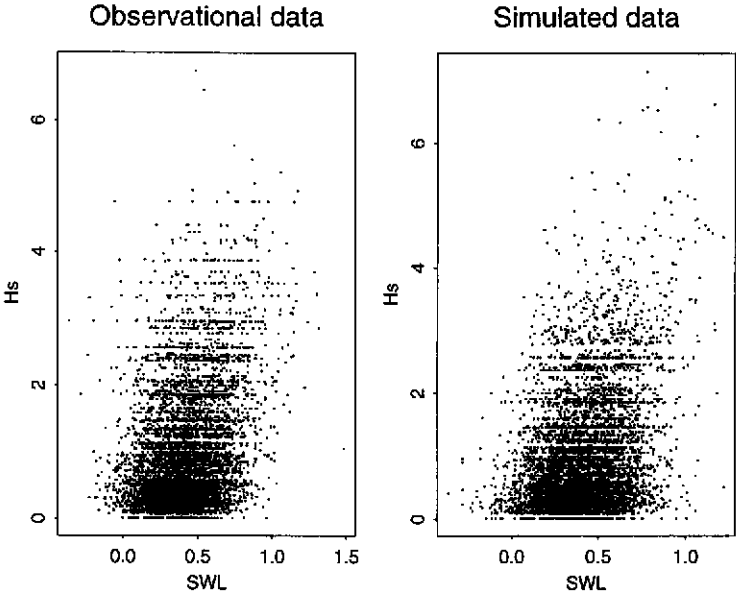


Figure 5.16: Christchurch observational data and Sim4 data:  $H_S$  vs  $T_Z$

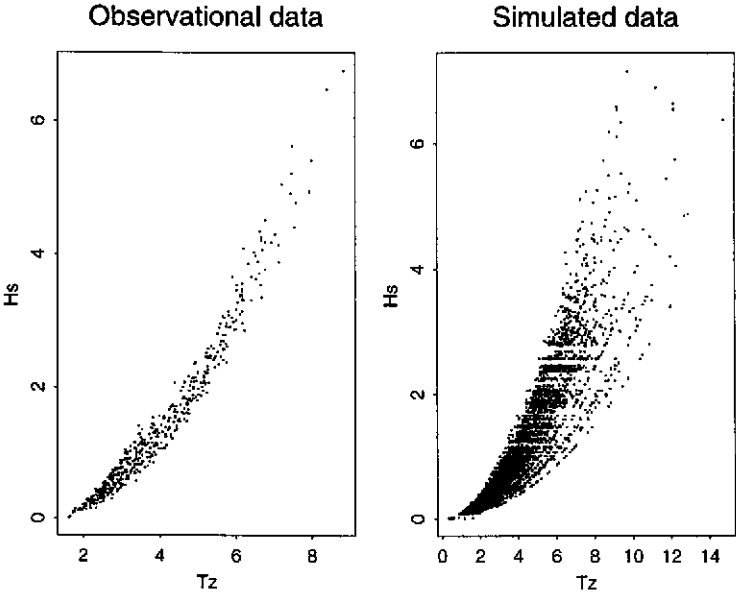


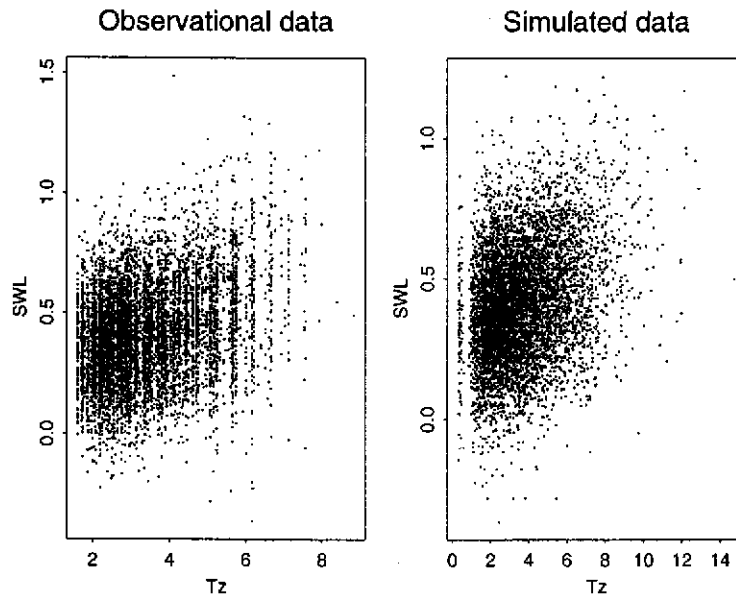
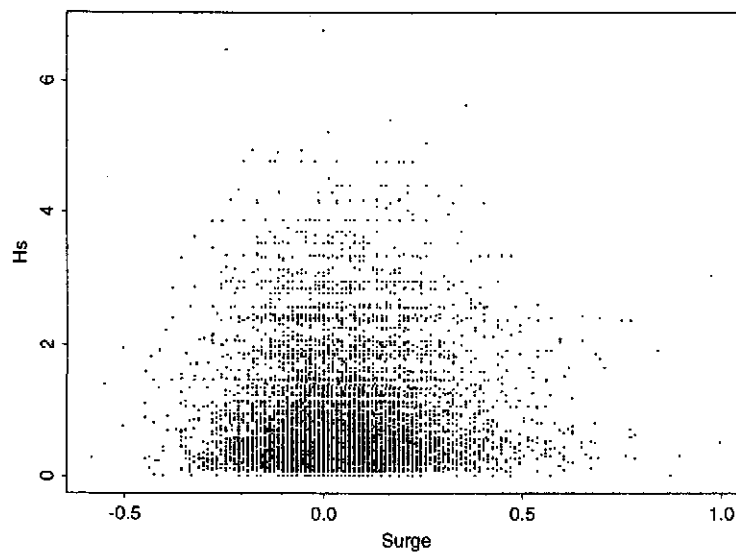
Figure 5.17: Christchurch observational data and Sim4 data: SWL vs  $T_Z$ Figure 5.18: Christchurch observational data:  $H_S$  vs Surge  
Christchurch

Figure 5.19: Dowsing observational data and Sim5 data:  $H_S$  vs SWL

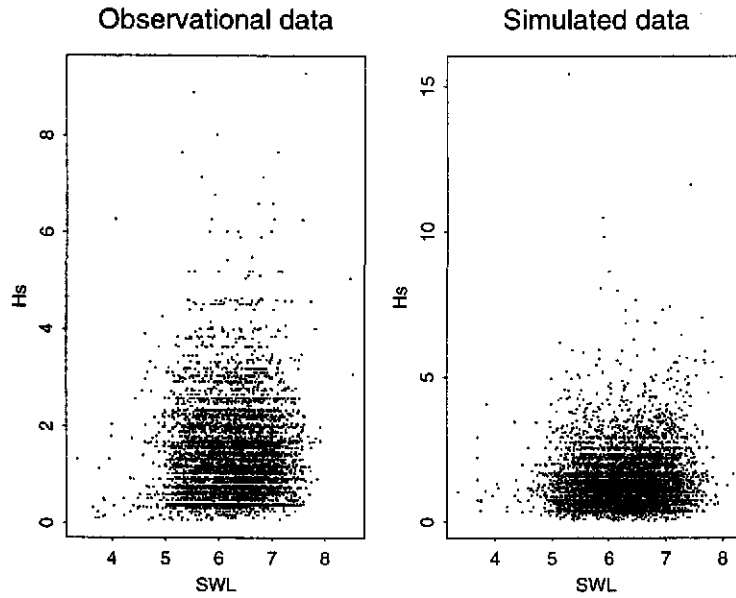


Figure 5.20: Dowsing observational data and Sim5 data:  $H_S$  vs  $T_Z$

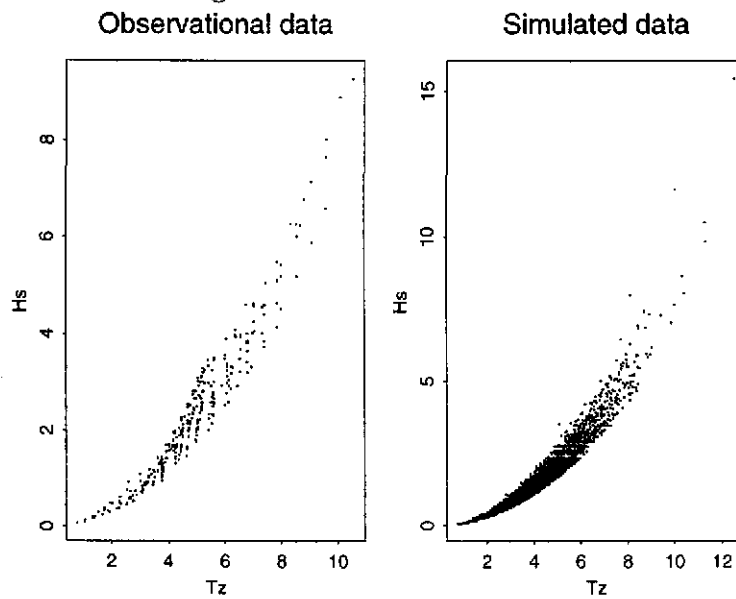
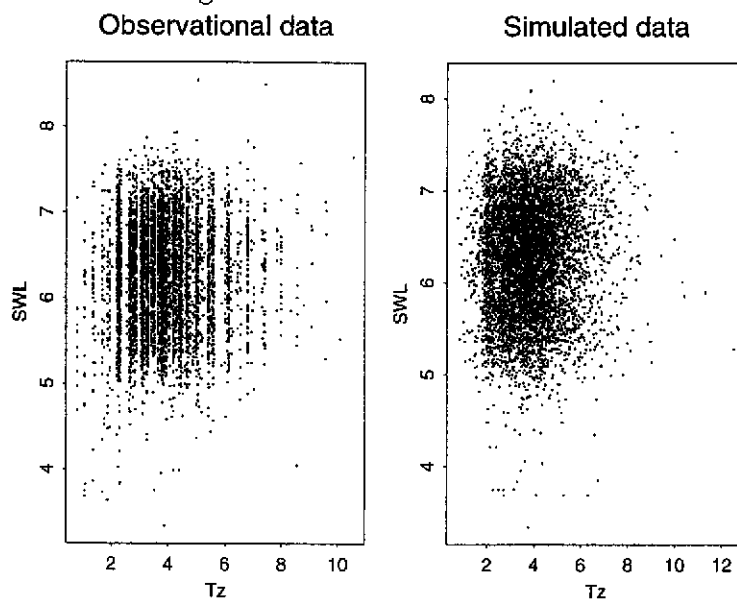
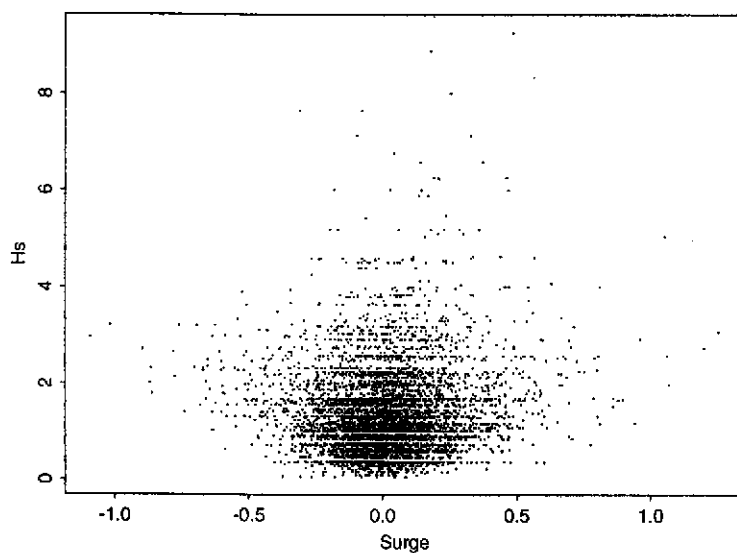


Figure 5.21: Dowsing observational data and Sim5 data: SWL vs  $T_Z$ Figure 5.22: Dowsing observational data:  $H_S$  vs Surge  
Dowsing

# Chapter 6

## Marginal Estimation

In this chapter we apply the models proposed in Chapter 4 to each of the marginal variables of the sea condition vector.

### 6.1 Still Water Level

#### 6.1.1 Observational Data

The threshold method of Section 3.1.2 is now applied to the still water level data from the observational sites (Cardiff, Christchurch, Dowsing, Shoreham, North Wales and Dover). To eliminate time dependence, observations at Dowsing, Christchurch and Dover were declustered by means of the procedure described in Section 3.1.6. This step was unnecessary for time series at Cardiff, Shoreham and North Wales, as they consist only of high water data.

#### Threshold Choice and Estimation

For threshold selection, a mean residual life plot was constructed for each of the 6 sites. Except at Cardiff, for which no linearity could be detected, a threshold fixed at the 95% quantile of the empirical distribution seemed a reasonable choice for all sites. Figures 6.1–6.3 contain plots of maximum likelihood estimates of the shape parameter  $\xi$  of the GPD plotted against the threshold  $u$  (expressed as the non-exceedance probability,  $F(u)$ , of  $u$ ) for each site. For all sites the estimate of  $\xi$  is a negative value, which indicates short-tailed distributions with finite upper end point. Again, with the exception of Cardiff, a stability of the estimates can be seen to hold above the 95% empirical quantile. Thus, this value of  $u$  is used at all sites with the associated maximum likelihood estimates of the GPD parameters  $\xi$  and  $\sigma$  given in Table 6.1.

#### Goodness-of-fit

To assess the goodness-of-fit of the fitted GPD tail model to still water level, probability

(P-P) and quantile (Q-Q) plots were constructed. Figure 6.4 contains results obtained for Cardiff and North Wales. As expected from the preliminary analyses on the threshold, Cardiff presents a poor fit, as indicated in the quantile plot by the observed upper tail being shorter than the fitted GPD model. For North Wales the goodness-of-fit of the GPD is satisfactory, as the probability and quantile plots exhibit no systematic departure from linearity. The other sites exhibit a quality of fit which is similar to that of North Wales. Overall, we can conclude that the GPD model gives an acceptable description of the observed tail of SWL at most sites, though for extrapolation beyond the range of the data, estimates based on an indirect method may be preferable, as discussed in Section 4.1.1.

Site	Shape Parameter $\xi$	Scale Parameter $\sigma$
Cardiff	-0.264 (0.0124)	0.362 (0.0121)
Christchurch	-0.0593 (0.0474)	0.126 (0.00863)
Dowsing	-0.0711 (0.0371)	0.2091 (0.0141)
Shoreham	-0.1324 (0.0486)	0.1796 (0.01325)
North Wales	-0.0457 (0.0482)	0.2246 (0.015)
Dover	-0.0764 (0.0537)	0.1866 (0.0151)

Table 6.1: Maximum likelihood estimates of the parameters of the GPD fitted to *SWL* data at observation sites (standard errors in parentheses).

Figure 6.1: GPD shape parameter estimates versus the empirical distribution function calculated in  $u$  for *SWL* data at Cardiff and Christchurch. Dots denote maximum likelihood estimates. Lines denote lower and upper bounds of the 95% confidence intervals.

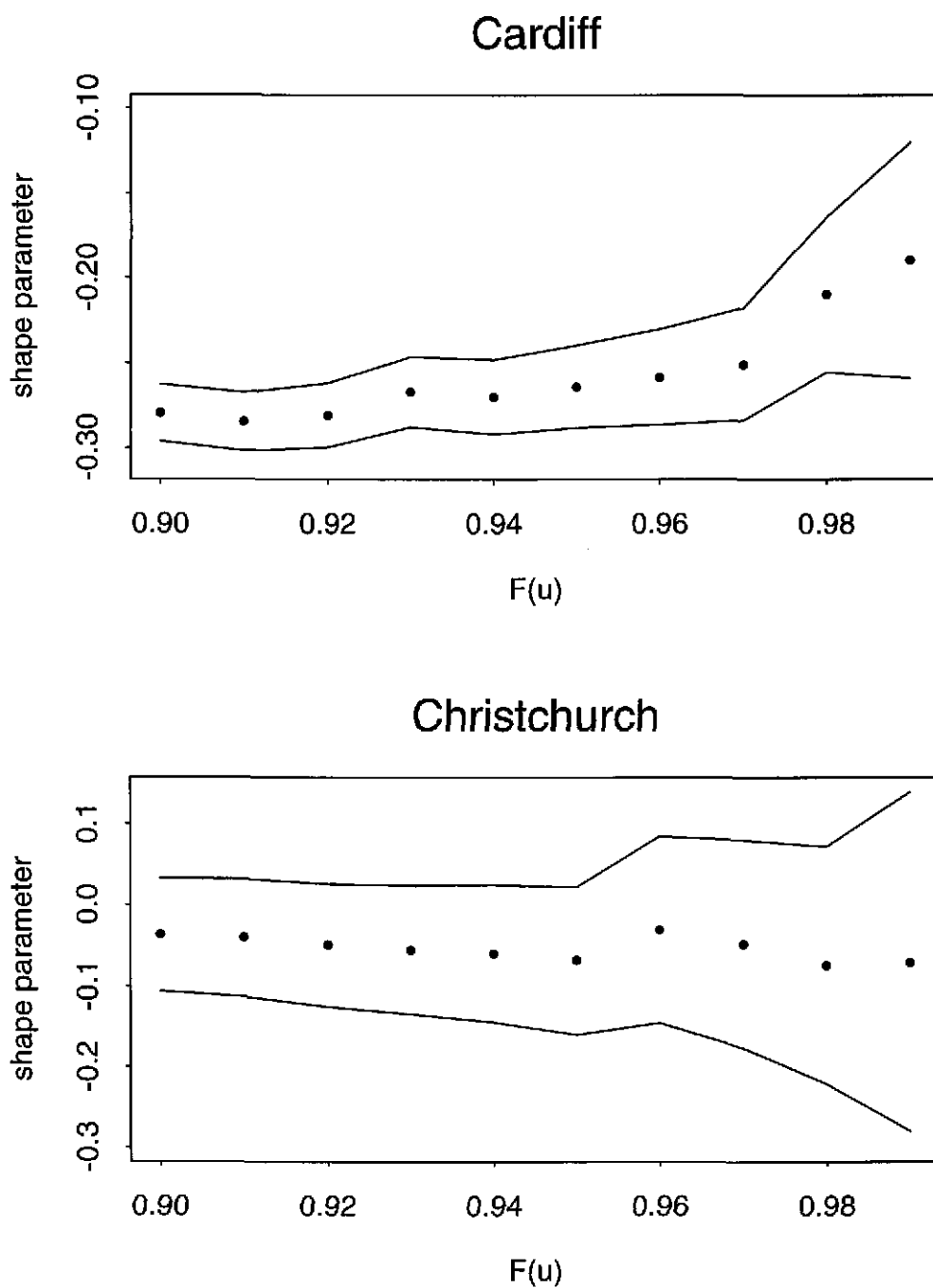


Figure 6.2: GPD shape parameter estimates versus the empirical distribution function calculated in  $u$  for *SWL* data at Dowsing and Shoreham. Dots denote maximum likelihood estimates. Lines denote lower and upper bounds of the 95% confidence intervals.

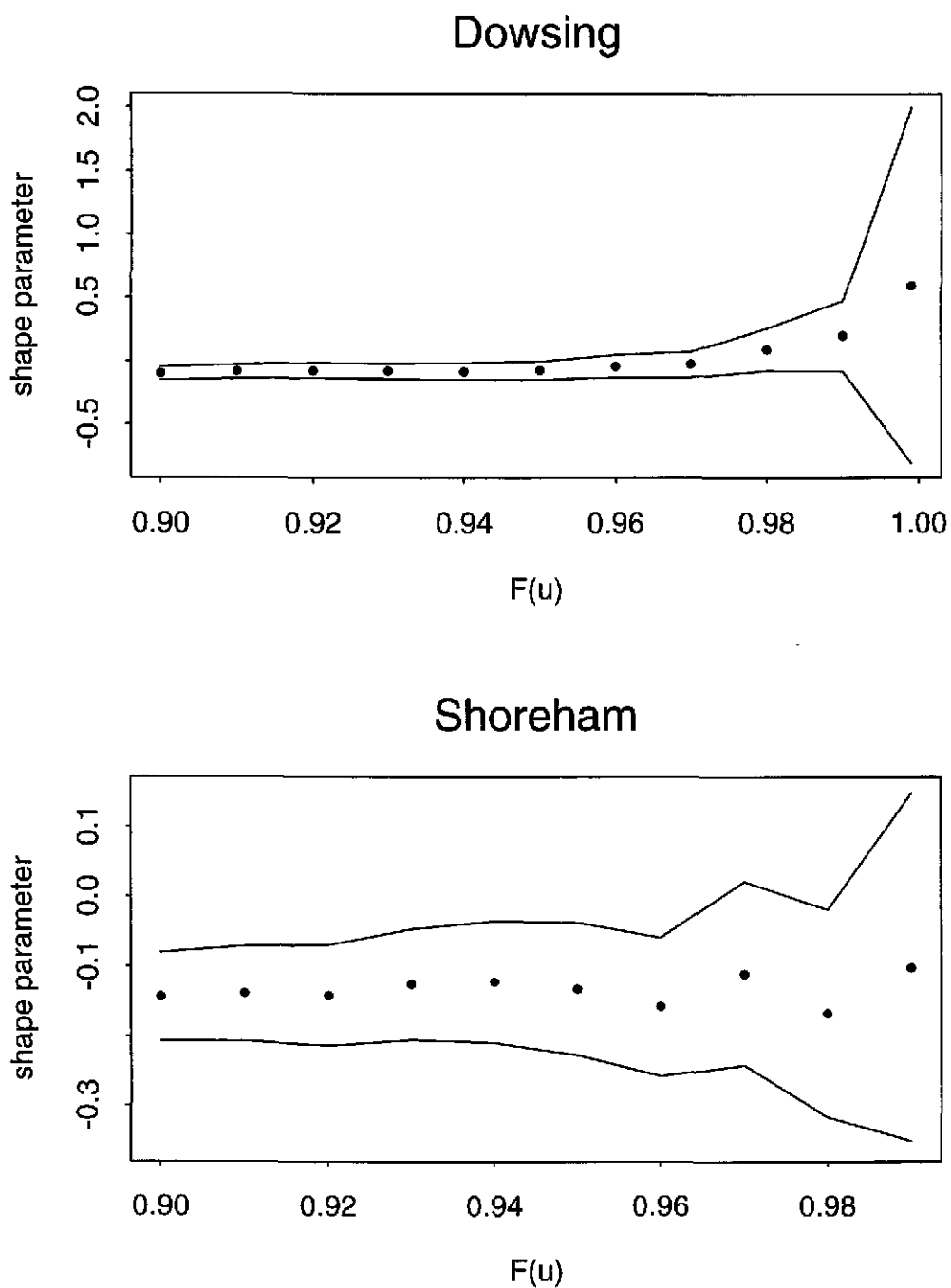


Figure 6.3: GPD shape parameter estimates versus the empirical distribution function calculated in  $u$  for SWL data at North Wales and Dover. Dots denote maximum likelihood estimates. Lines denote lower and upper bounds of the 95% confidence intervals.

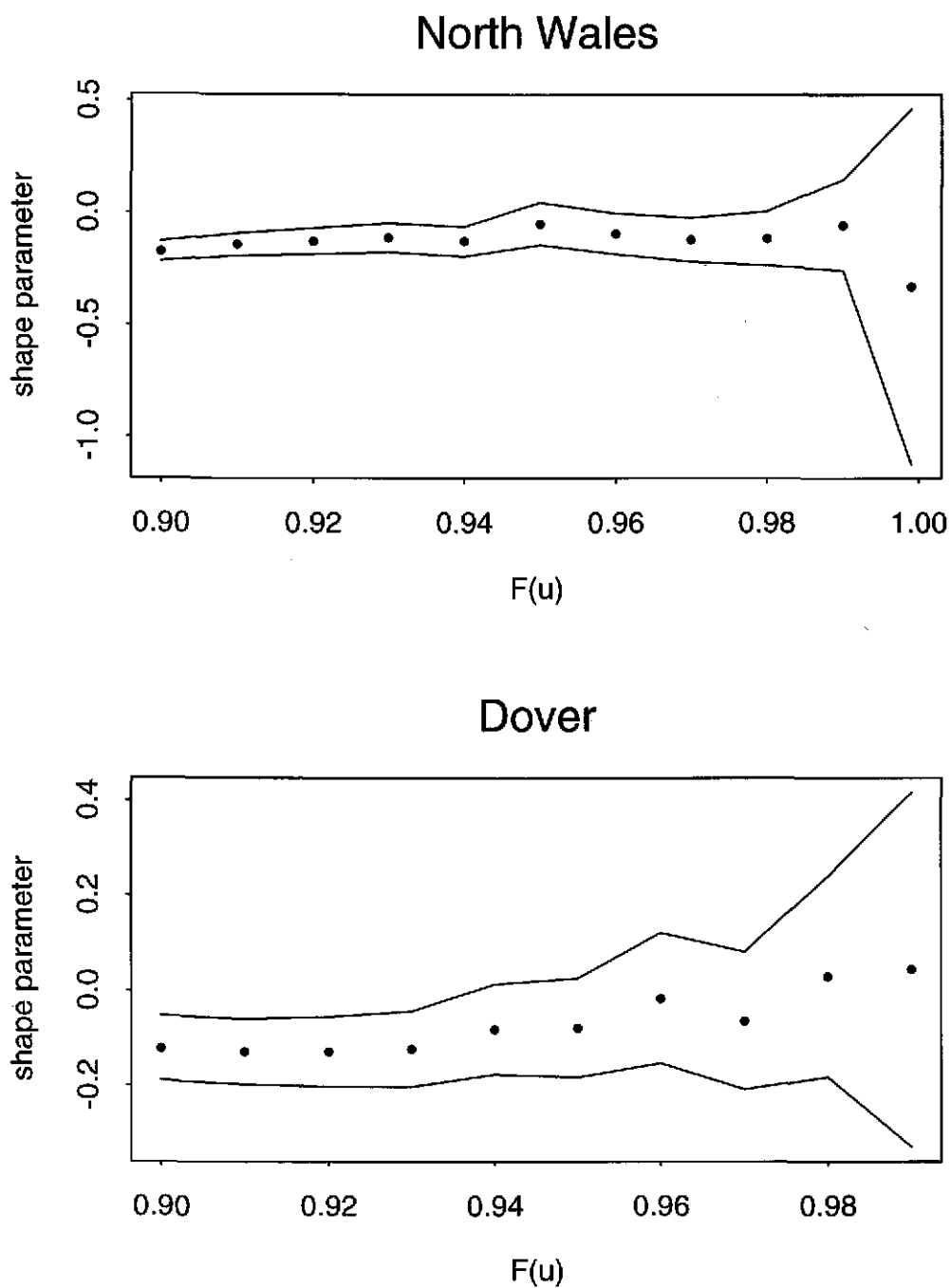
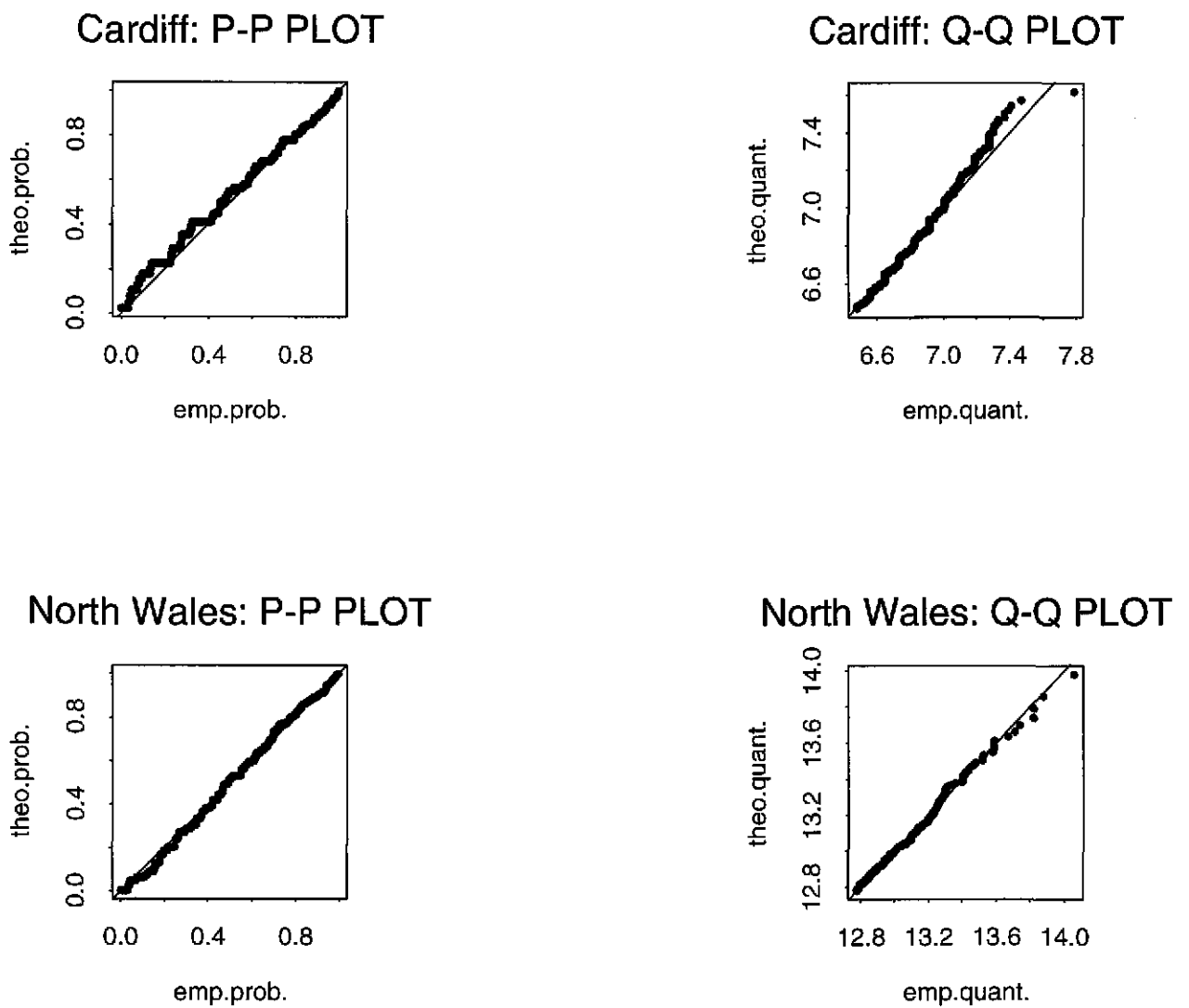


Figure 6.4: Probability and quantile plots for the GPD fitted to *SWL* data at Cardiff and North Wales. Also shown in each plot is the  $x = y$  line.



### 6.1.2 Simulated Data

For the simulated still water level data the 95% empirical quantile is used as a threshold to fit the GPD model to the exceedances. It follows that for all data sets the exceedance probability estimate is 0.05. Table 6.2 gives estimates of the GPD parameter estimates for the five simulated data sets. For Sim1, Sim2, Sim4 and Sim5 the statistical model that is fitted is of the same structure as the model used to simulate the data. For Sim3 however the data were generated as independent tide and surge, so the still water level is not guaranteed to fit well above the selected threshold.

For Sim1 and Sim2 the parameter estimates are very close to the true values used to simulate the data (see Chapter 5). For Sim4 and Sim5 the two parameters differ from the true values, but the change in the tail form due to the two mis-estimations largely cancels out as one error lengthens the tail while the other shortens it. Little can be said about Sim3 at this stage except that the shape parameter estimates for the still water level/surge correspond to an upper endpoint existing/not existing respectively. This is consistent with the errors found by Dixon and Tawn (1994, 1995) for direct analysis of still water levels.

Data	Shape Parameter $\xi$	Scale Parameter $\sigma$
Sim1	-0.2246 (0.041)	0.3402 (0.023)
Sim2	-0.1284 (0.054)	0.1843 (0.014)
Sim3	-0.11 (0.045)	0.24 (0.0167)
Sim4	-0.1811 (0.05)	0.1344 (0.0098)
Sim5	-0.1166 (0.049)	0.2151 (0.016)

Table 6.2: Maximum likelihood estimates of the parameters of the GPD fitted to *SWL* simulated for the synthetic data sets (standard errors in parentheses).

## 6.2 Surge

### 6.2.1 Observational Data

The Threshold Method was applied also to declustered surge data. Figures 6.5–6.7 contain sensitivity plots on the basis of which a threshold equal to the empirical 95% surge quantile was chosen for all sites. Maximum likelihood estimates are shown in Table 6.3. With the exception of Christchurch, estimates of the shape parameter tend to be higher than the values obtained from still water level. This is consistent with the Sim3 data results above. Dixon and Tawn (1994, 1995) noticed that for sites at which still water level is dominated by the tidal variation, extreme value models applied to extreme surge data indicate longer tail distributions than the same models when fitted to extreme still water levels. In contrast, they observe an agreement in the results for sites in which the surge variation is dominant. Christchurch belongs to this latter class of sites, and as seen from Tables 6.1 and 6.3, the shape parameters are of the same sign in each case. Graphical assessments of goodness-of-fit for Cardiff and Christchurch are contained in Figure 6.8. For still water level, some departure from linearity is observable in the Cardiff Q–Q plot. At the other sites, the GPD seems to provide a reasonable fit to the surge exceedances of  $u$ .

Site	Shape Parameter $\xi$	Scale Parameter $\sigma$
Cardiff	0.0123 (0.0293)	0.137 (0.0061)
Christchurch	-0.0954 (0.049)	0.142 (0.01)
Dowsing	0.0158 (0.058)	0.1473 (0.012)
Shoreham	0.02691 (0.0468)	0.104 (0.0076)
North Wales	0.0803 (0.048)	0.1446 (0.0097)
Dover	0.2 (0.072)	0.131 (0.0122)

Table 6.3: Maximum likelihood estimates of the parameters of the GPD fitted to Surge level data at various sites (standard errors in parentheses).

Figure 6.5: GPD shape parameter estimates versus the empirical distribution function calculated in  $u$  for Surge level data at Cardiff and Christchurch. Dots denote maximum likelihood estimates. Lines denote lower and upper bounds of the 95% confidence intervals.

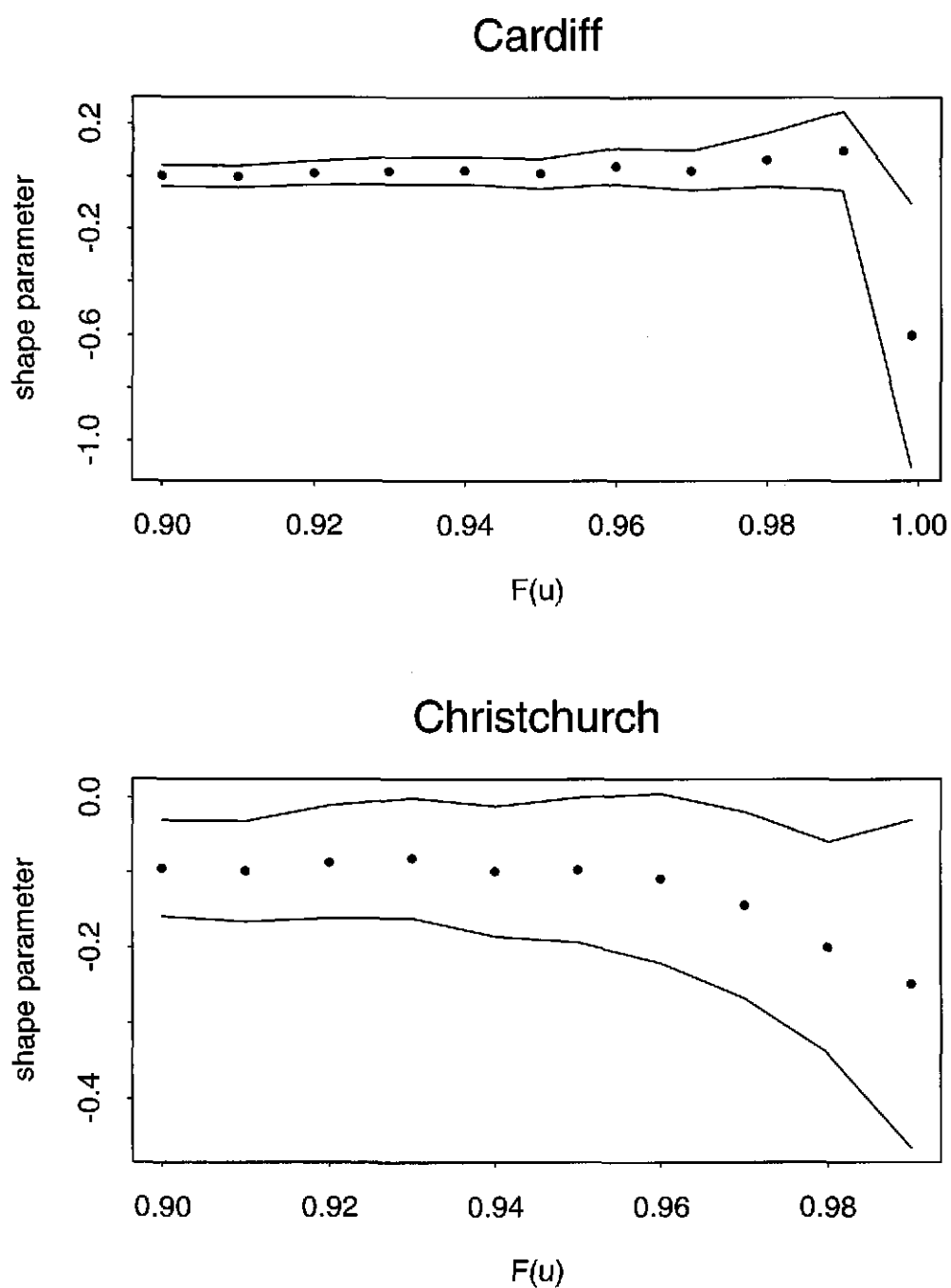


Figure 6.6: GPD shape parameter estimates versus the empirical distribution function calculated in  $u$  for Surge level data at Dowsing and Shoreham. Dots denote maximum likelihood estimates. Lines denote lower and upper bounds of the 95% confidence intervals.

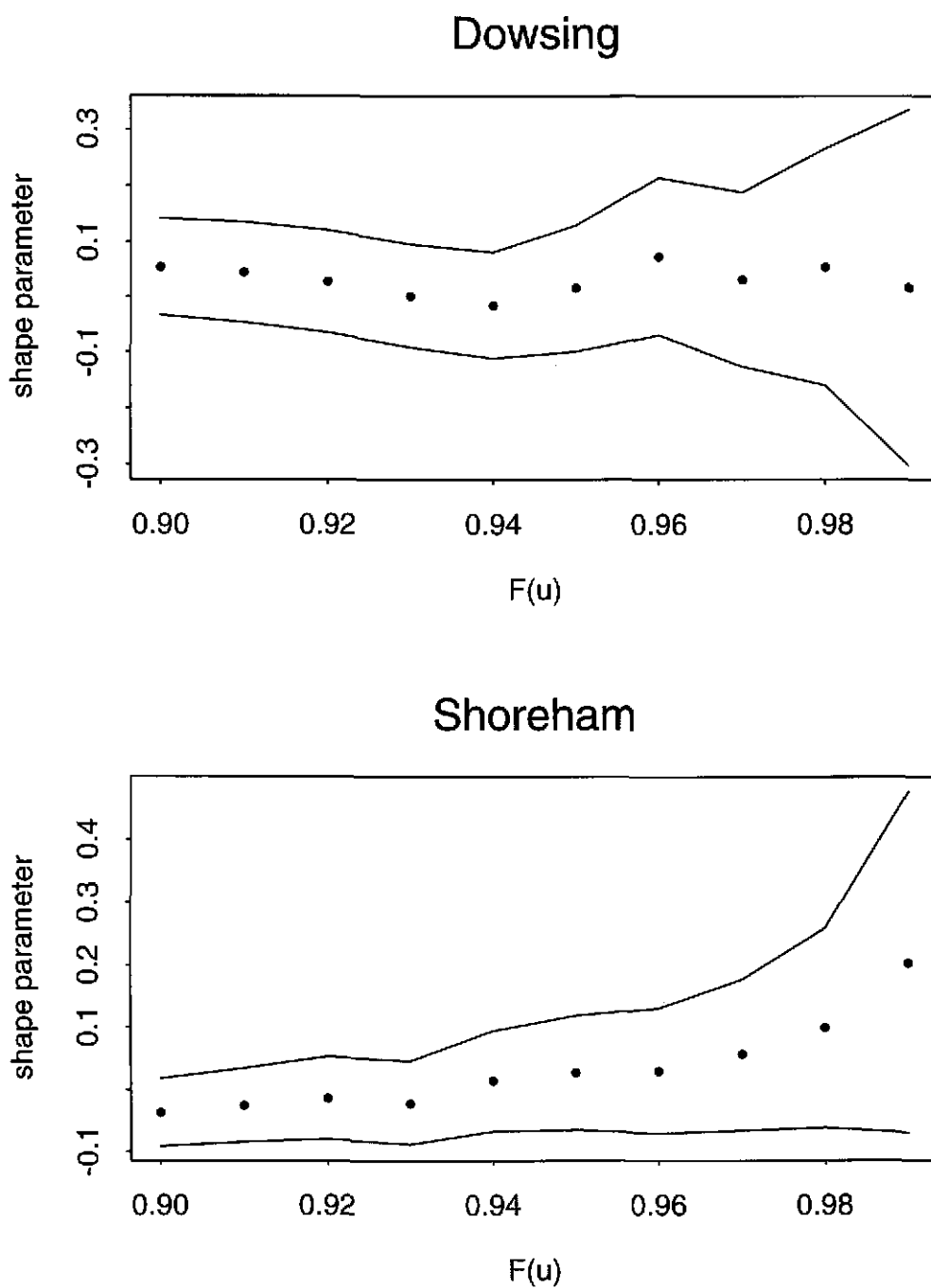


Figure 6.7: GPD shape parameter estimates versus the empirical distribution function calculated in  $u$  for Surge level data at North Wales and Dover. Dots denote maximum likelihood estimates. Lines denote lower and upper bounds of the 95% confidence intervals.

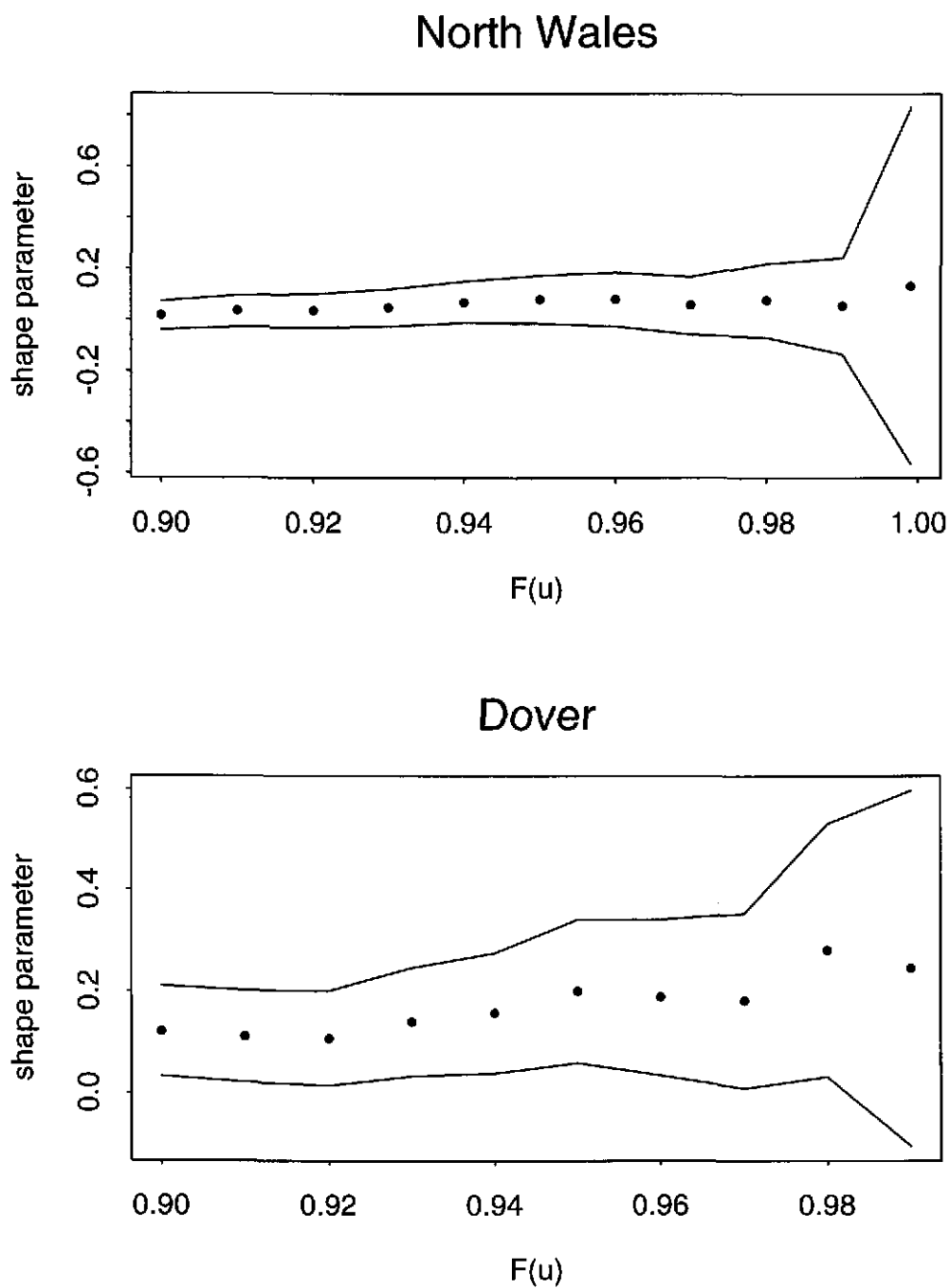
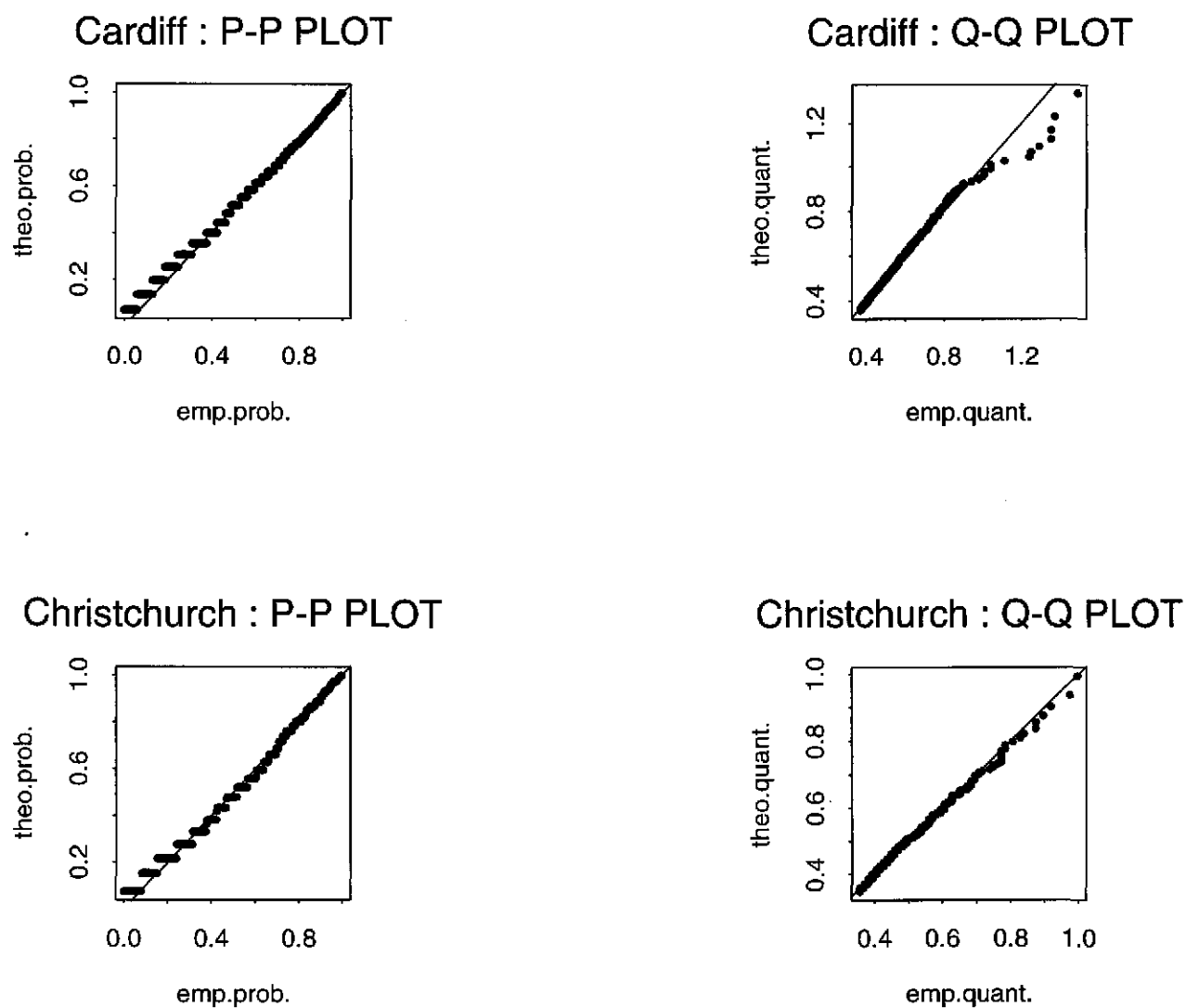


Figure 6.8: Probability and quantile plots for the GPD fitted to Surge level data at Cardiff and Christchurch. Also shown in each plot is the  $x = y$  line.



### 6.2.2 Simulated Data

The only simulated data set with surge data is Sim3. The parameter estimates obtained by applying the threshold method with threshold corresponding to the 95% empirical quantile, and GPD for exceedances, are given in Table 6.4. From this table we see that the parameter estimates are close to the true values (see Chapter 5).

Data	Shape Parameter $\xi$	Scale Parameter $\sigma$
Sim3	-0.026 (0.052)	0.167 (0.012)

Table 6.4: Maximum likelihood estimates of the parameters of the GPD fitted to simulated Surge level data (standard errors in parentheses).

## 6.3 Significant Wave Height

### 6.3.1 Observational Data

In this section we fit three distributional models to the hindcast  $H_S$  wave data from the sites Cardiff, Christchurch, Dowsing, Shoreham, North Wales and Dover. All six time series consist of hindcast data where the temporal dependence has been removed by applying the declustering procedure of Section 3.1.6. Since for these sites water level data are also available. The three statistical models considered are:

1. Weibull;
2. Truncated Weibull;
3. GPD,

the latter two being fitted through the threshold methods, but all fitted using maximum likelihood. The first two models can be compared by examining their parameter estimates, the latter two by comparing estimate stability to threshold level. In each case P–P and Q–Q plots are used to assess goodness of fit.

First consider the Weibull distribution fitted to all  $H_S$  values. Table 6.5 shows maximum likelihood estimates of the Weibull distribution parameters  $(a, b, c)$  for each site. The goodness of fit at each site is most easily assessed using the Q–Q plots shown in Figures 6.9–6.11. The model fits well for the Dover data; for Cardiff and Christchurch the fitted model has a slightly longer upper tail than the empirical upper tail, with the

reverse behaviour observed at North Wales. However, for both Dowsing and Shoreham the fit is extremely poor. In one case the Weibull model over-estimates the upper tail, in the other it under-estimates the upper tail. Clearly, for these two sites the basic Weibull model is inadequate.

Now consider the Truncated Weibull distribution. Table 6.6 contains maximum likelihood estimates of the parameters  $(a, b, c)$  for the same sites, obtained by applying the Threshold Method with the distribution of exceedances given by the Truncated Weibull distribution, c.f. equation (4.1.2), with the threshold taken at the 95% empirical  $H_S$  quantile. If the Weibull distribution were the true underlying distribution, then the estimates of  $(a, b, c)$  would be similar to those from the previous Weibull model fit to the whole data set. This only seems true for the Dover data. The worst agreement occurs with the Dowsing and Shoreham data. These findings confirm the observations made from the Weibull model fit above. Probability plots and quantile plots for the Truncated Weibull are shown in Figures 6.12–6.14.

We can conclude that the Weibull distribution, while providing an acceptable fit to the bulk of the data, is a poor description of the upper tail for  $H_S$  at these sites. In some cases, as for Dowsing and North Wales, it leads to shorter tailed distributions than is indicated by the observations, whereas for Cardiff, Christchurch and Shoreham, it overestimates the empirical extreme quantiles. Only Dover demonstrates a reasonable fit. As a consequence, for most of the sites considered, the Weibull distribution will produce unreliable estimates of values associated with long return periods.

Now consider the GPD threshold model using the same threshold as for the Truncated Weibull model. The GPD has the potential advantage over the Truncated Weibull model that it is asymptotically justified. However, this does not guarantee that it will fit better to data in practice, so we must assess how well it describes the data relative to the Truncated Weibull model.

Results obtained by maximum likelihood estimation of the shape and scale parameters of the GPD are given in Table 6.7. The parameter estimates show that with the exception of Dowsing we estimate an upper endpoint to the  $H_S$  distribution for each site. Probability plots and quantile plots are contained in Figures 6.15–6.17. The GPD model seems to perform well – in each case there is a strong similarity with the associated Truncated Weibull plots. Discrimination between the Truncated Weibull and the GPD, based only on this graphical tool, is difficult.

A further comparison between the two tail models may be made on the basis of their stability with respect to different thresholds. As remarked in Section 3.1.4, a property required from tail models is the non-sensitivity of the results to threshold selection. Figures 6.18–6.23 show estimates, for each of the six sites, of two fixed quantiles, one within and

one beyond the range of the data, as functions of threshold under each tail model. For both quantiles the GPD seems more stable, giving empirical support for the preference of this tail model. Furthermore, with the exception of Dowsing (which was the site for which we estimated no upper endpoint), the GPD leads to lower quantile estimates than the Truncated Weibull, suggesting that the latter is unduly conservative.

Site	Location Parameter $a$	Shape Parameter $c$	Scale Parameter $b$
Cardiff	0.00532 (0.0293)	1.276 (0.01)	0.3069 (0.00209)
Christchurch	0.00827 (0.00057)	1.1194 (0.0106)	0.972 (0.0107)
Dowsing	0.0565 (0.00158)	1.563 (0.0149)	1.443 (0.0126)
Shoreham	0.00598 (0.001)	1.144 (0.01286)	0.945 (0.01124)
North Wales	0.00873 (0.0006)	1.493 (0.0118)	1.032 (0.0077)
Dover	0.0271 (0.00141)	1.61 (0.016)	1.231 (0.0104)

Table 6.5: Maximum likelihood estimates of the parameters of the Weibull distribution fitted to  $H_S$  observations at various sites (standard errors in parentheses).

Site	Location Parameter $a$	Shape Parameter $c$	Scale Parameter $b$
Cardiff	0.0861 (0.133)	1.1166 (0.197)	0.2227 (0.088)
Christchurch	0.234 (0.5145)	1.251 (0.212)	1.0496 (0.3667)
Dowsing	1.417 (0.486)	0.658 (0.14)	0.2895 (0.192)
Shoreham	0.0006 (0.0182)	1.585 (0.0744)	1.267 (0.0479)
North Wales	0.0003 (0.0096)	1.363 (0.0527)	1.015 (0.0367)
Dover	0.0235 (0.0102)	1.683 (0.0821)	1.312 (0.0489)

Table 6.6: Maximum likelihood estimates of the parameters of the Truncated Weibull distribution fitted to  $H_S$  exceedances at various sites (standard errors in parentheses).

Site	Shape Parameter $\xi$	Scale Parameter $\sigma$
Cardiff	-0.0375 (0.0373)	0.1793 (0.0091)
Christchurch	-0.0474 (0.0511)	0.6685 (0.0489)
Dowsing	0.1121 (0.0693)	0.8091 (0.0739)
Shoreham	-0.1703 (0.044)	0.5788 (0.0411)
North Wales	-0.1583 (0.0433)	0.6119 (0.0386)
Dover	-0.237 (0.0513)	0.5689 (0.0435)

Table 6.7: Maximum likelihood estimates of the parameters of the GPD fitted to  $H_S$  exceedances at various sites (standard errors in parentheses).

Figure 6.9: Probability and quantile plots for the Weibull distribution fitted to  $H_S$  observations at Cardiff and Christchurch. Also shown in each plot is the  $x = y$  line.

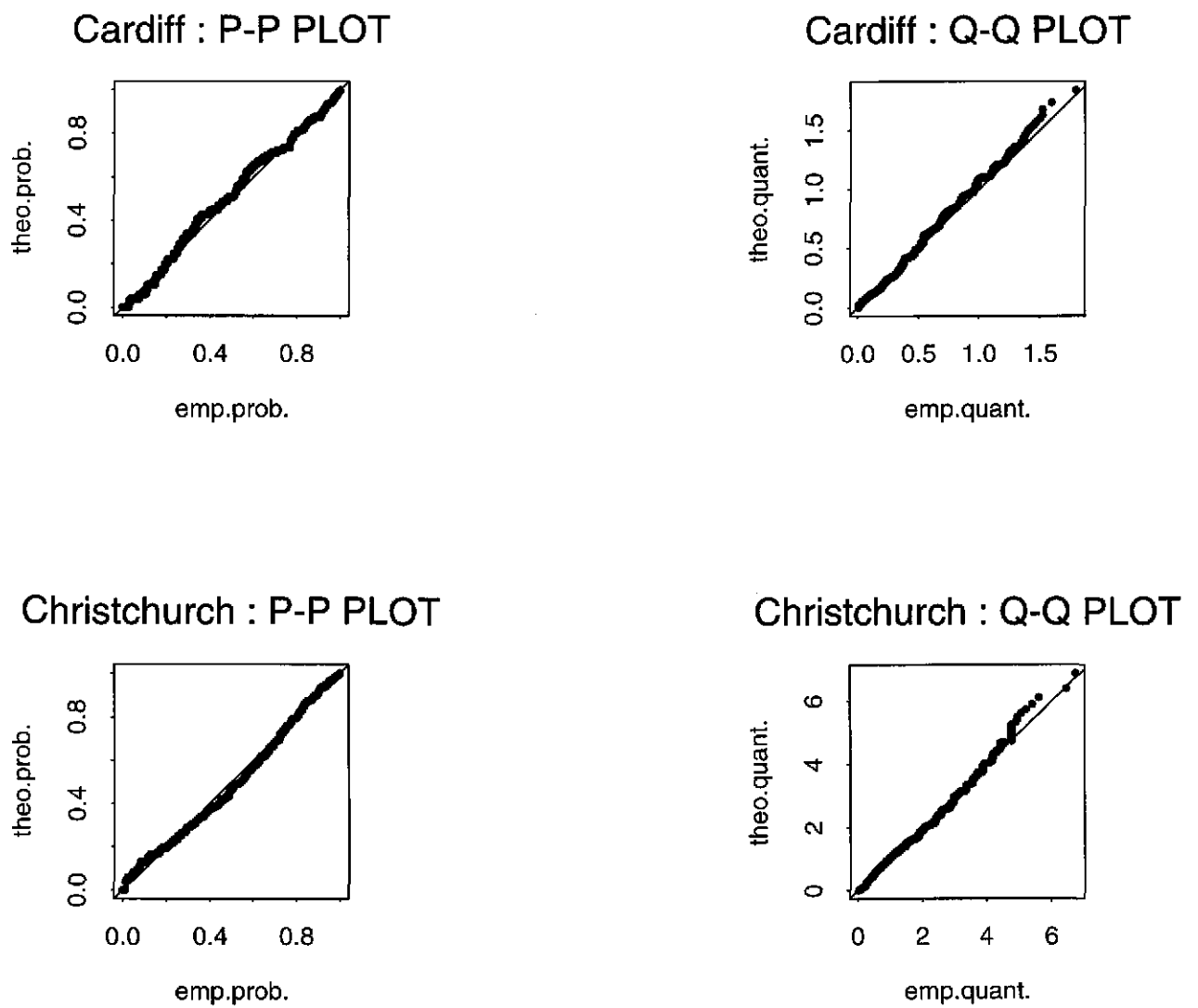


Figure 6.10: Probability and quantile plots for the Weibull distribution fitted to  $H_S$  observations at Dowsing and Shoreham. Also shown in each plot is the  $x = y$  line.

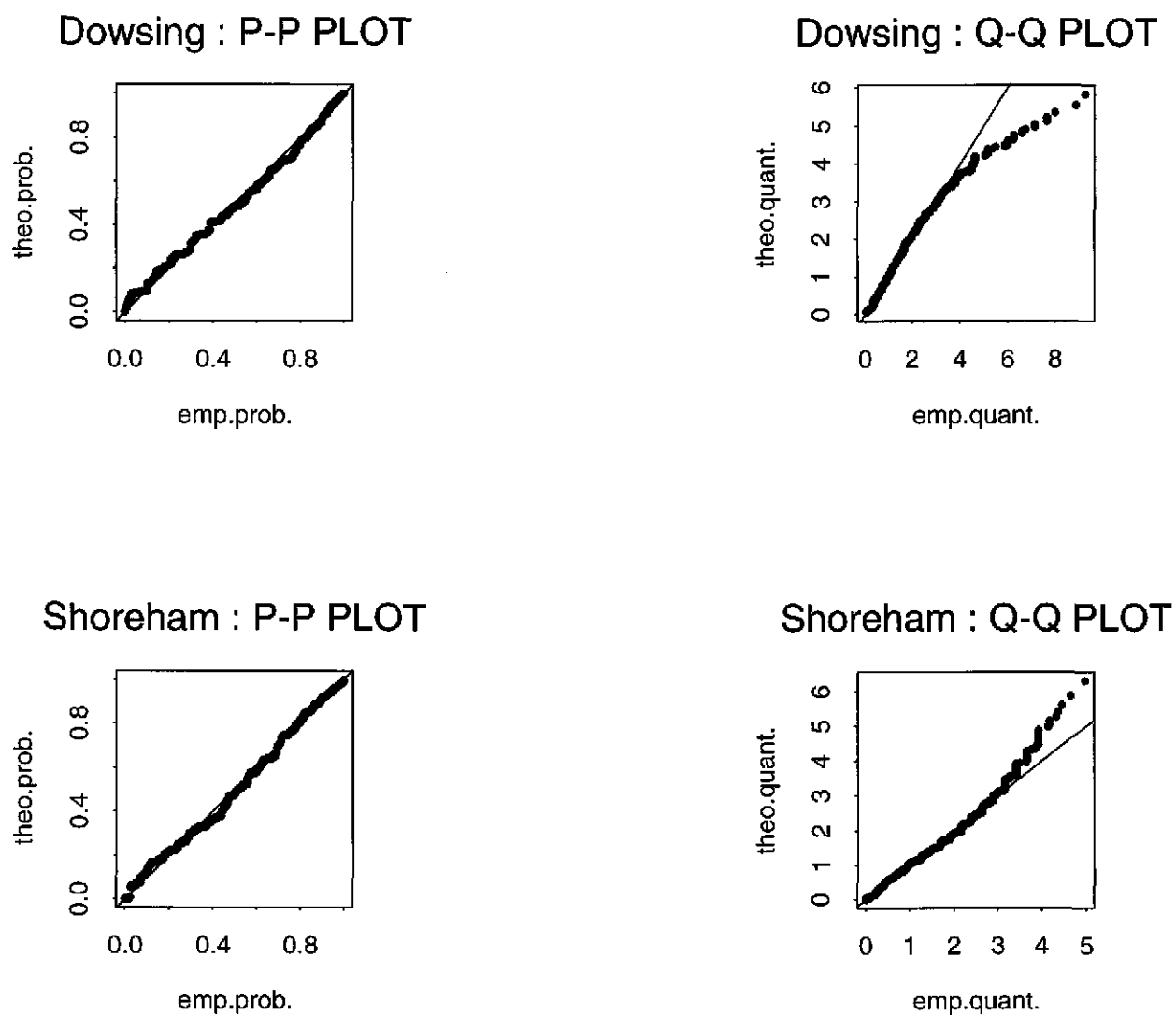
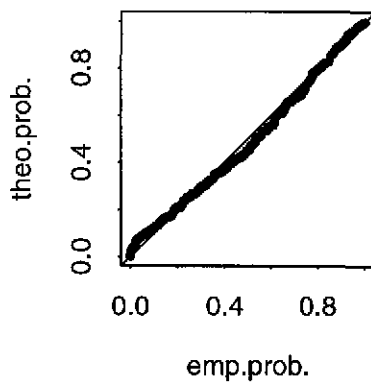
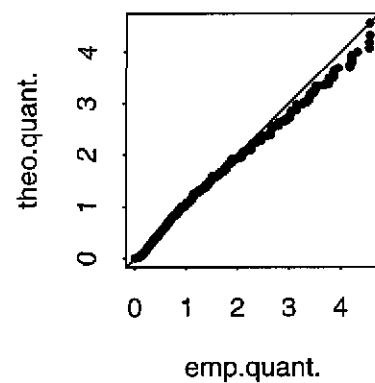


Figure 6.11: Probability and quantile plots for the Weibull distribution fitted to  $H_S$  observations at North Wales and Dover. Also shown in each plot is the  $x = y$  line.

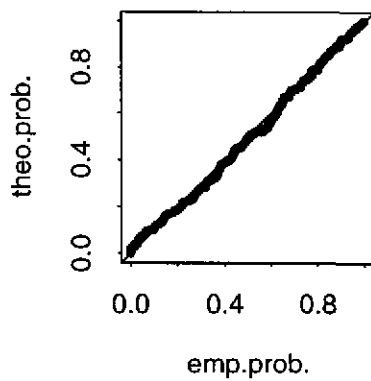
North Wales: P-P PLOT



North Wales : Q-Q PLOT



Dover : P-P PLOT



Dover : Q-Q PLOT

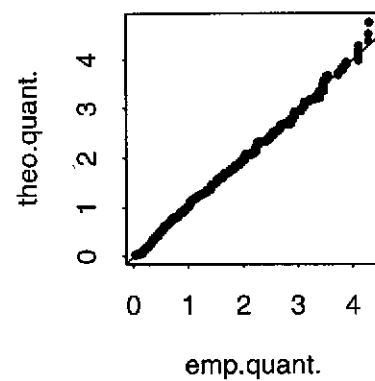


Figure 6.12: Probability and quantile plots for the Truncated Weibull distribution fitted to  $H_S$  exceedances at Cardiff and Christchurch. Also shown in each plot is the  $x = y$  line.

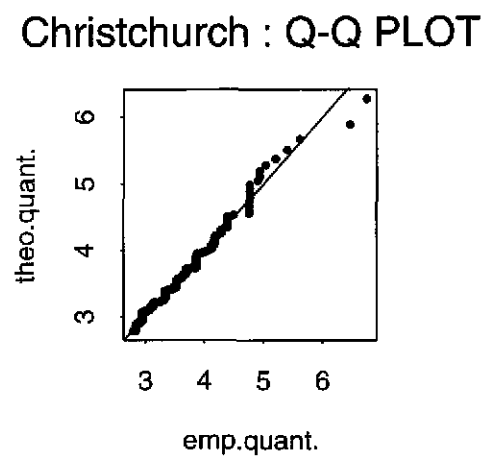
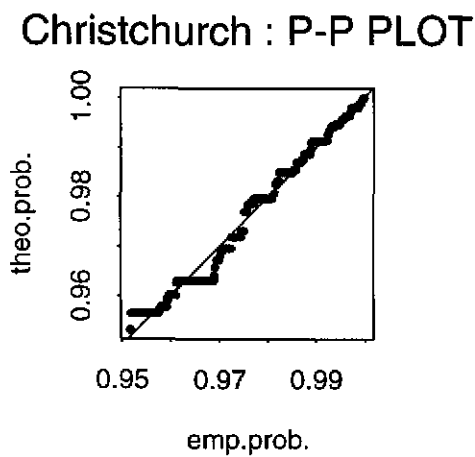
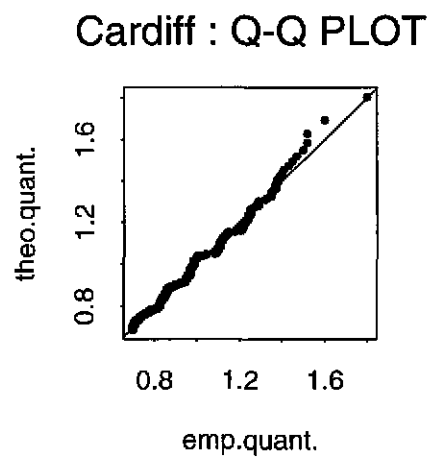
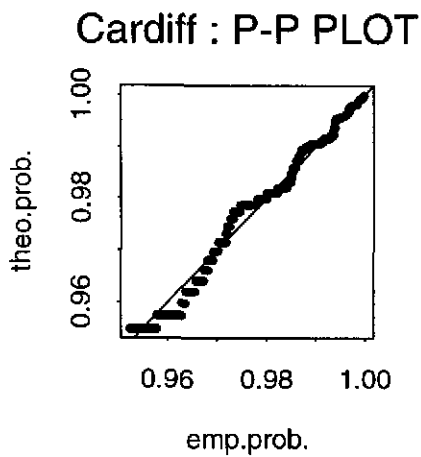


Figure 6.13: Probability and quantile plots for the Truncated Weibull distribution fitted to  $H_S$  exceedances at Dowsing and Shoreham. Also shown in each plot is the  $x = y$  line.

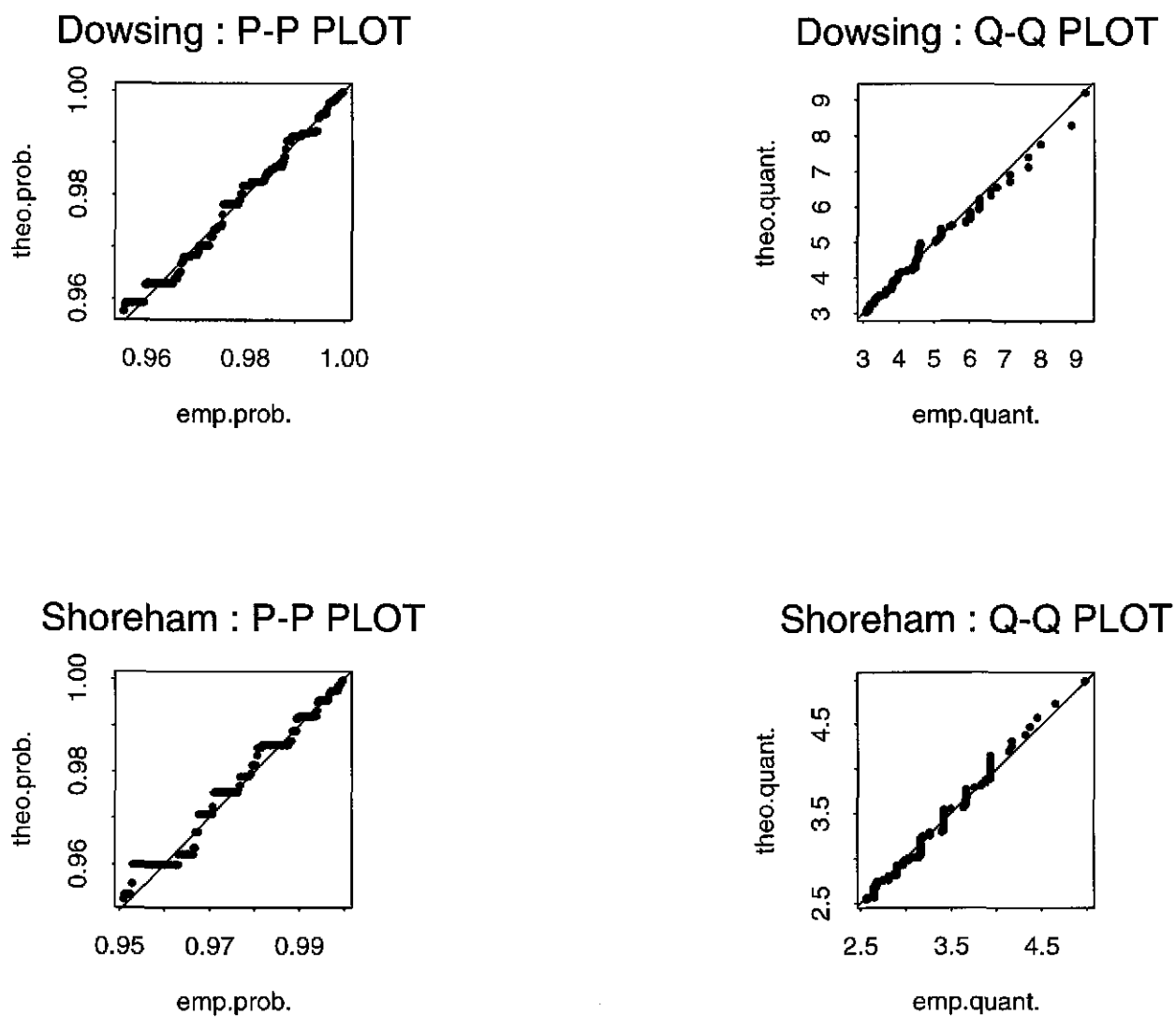
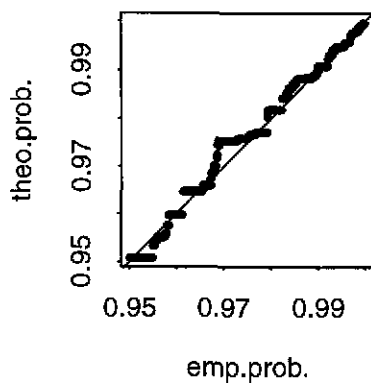
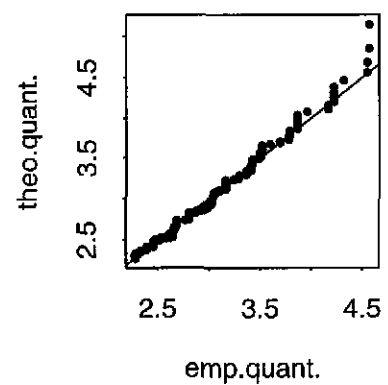


Figure 6.14: Probability and quantile plots for the Truncated Weibull distribution fitted to  $H_S$  exceedances at North Wales and Dover. Also shown in each plot is the  $x = y$  line.

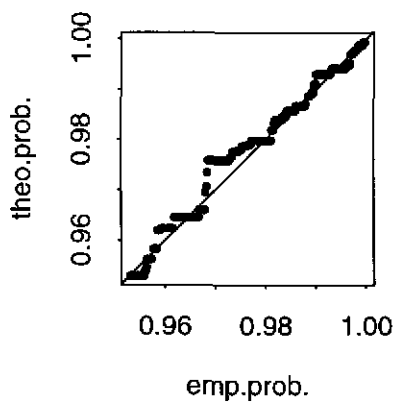
North Wales : P-P PLOT



North Wales : Q-Q PLOT



Dover : P-P PLOT



Dover : Q-Q PLOT

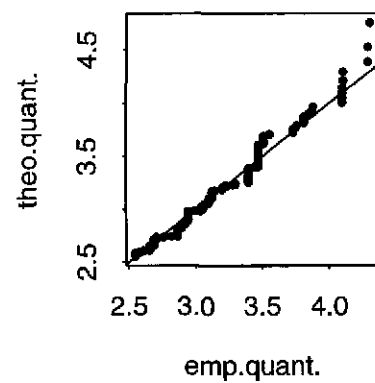


Figure 6.15: Probability and quantile plots for the GPD fitted to  $H_S$  exceedances at Cardiff and Christchurch. Also shown in each plot is the  $x = y$  line.

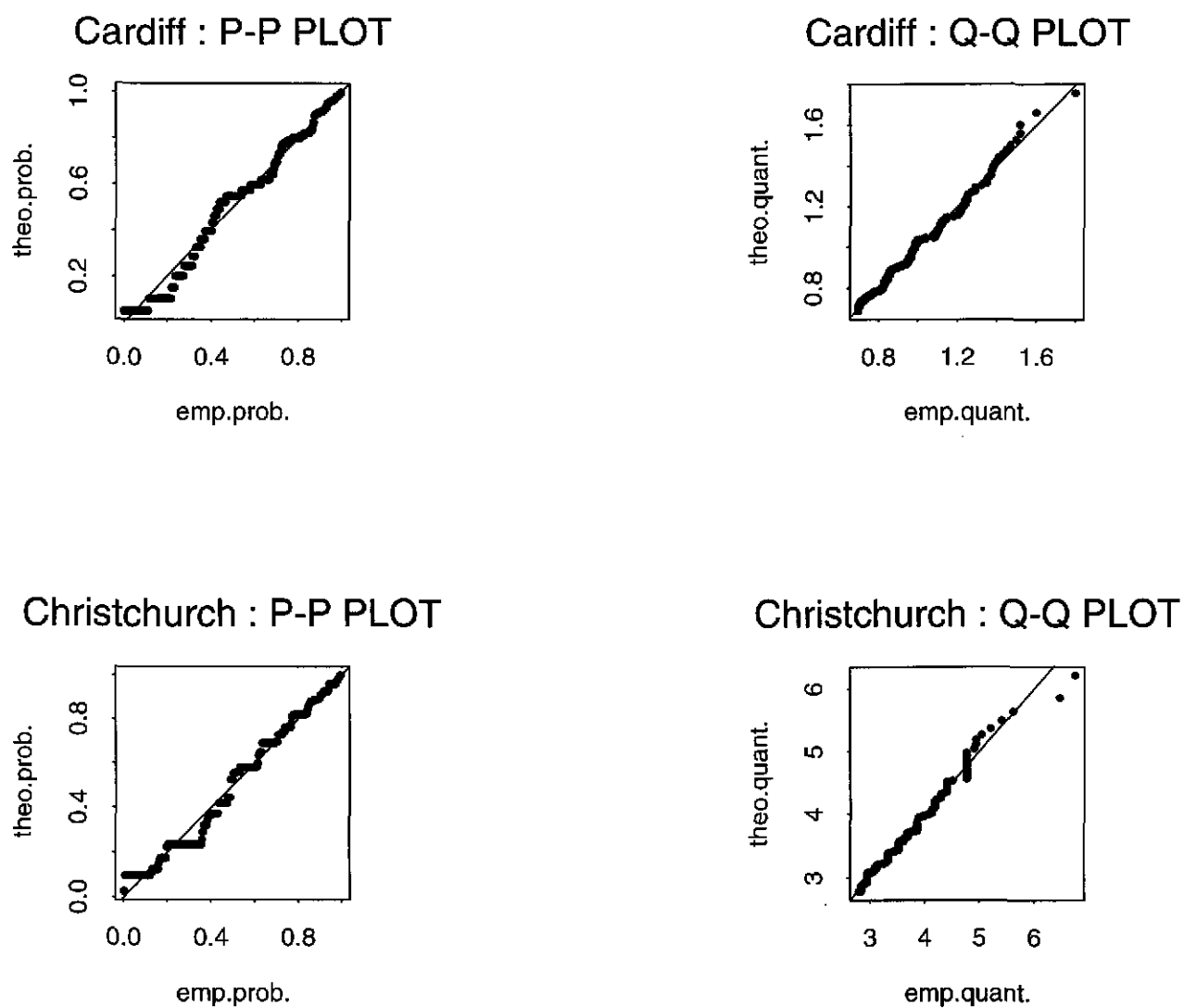


Figure 6.16: Probability and quantile plots for the GPD fitted to  $H_5$  exceedances at Dowsing and Shoreham. Also shown in each plot is the  $x = y$  line.

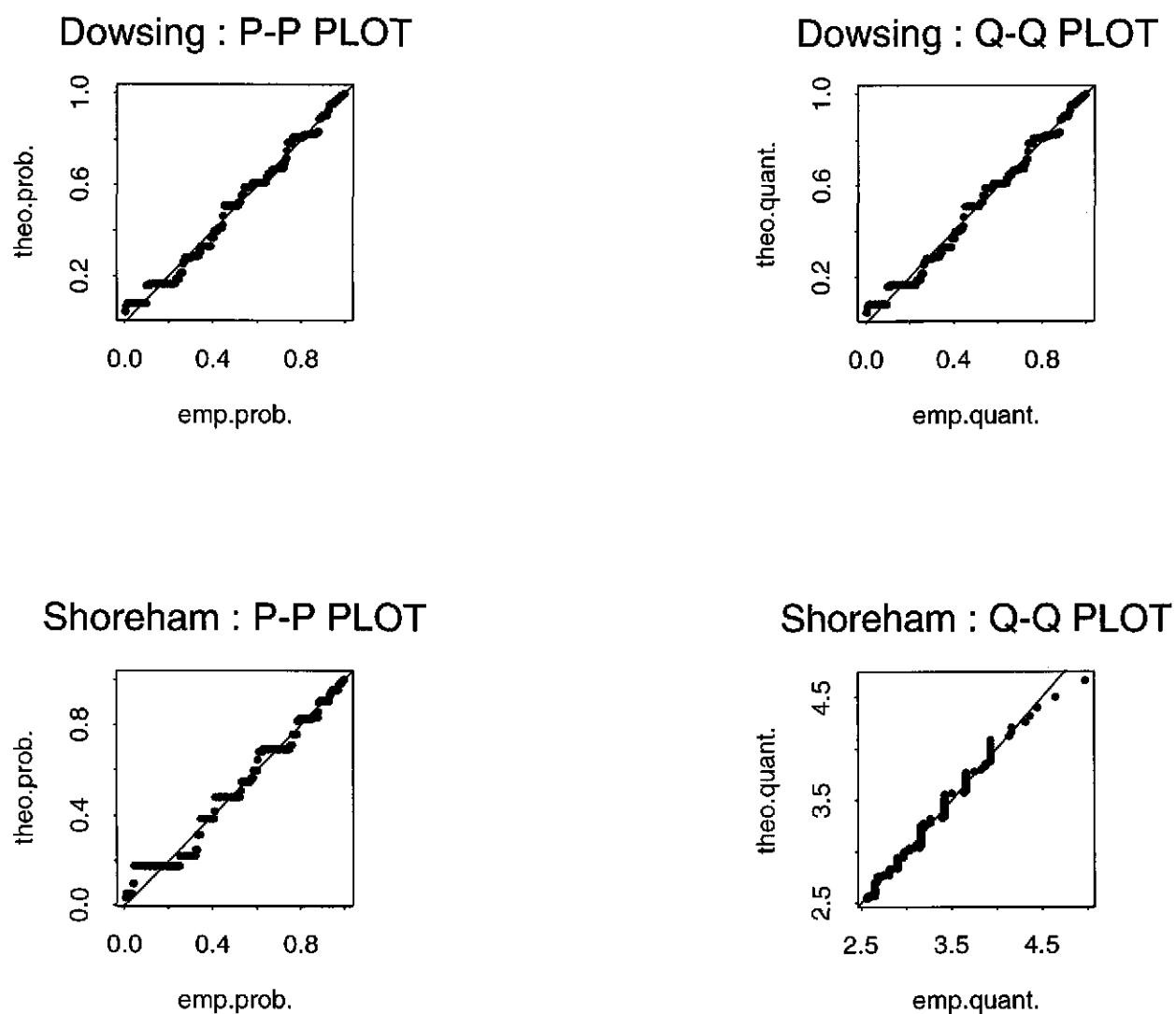
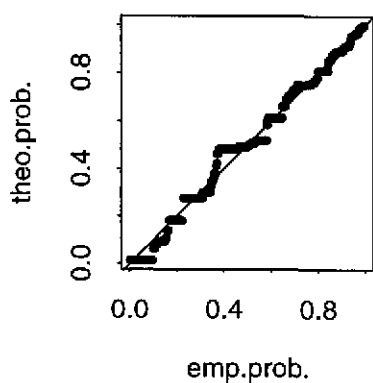
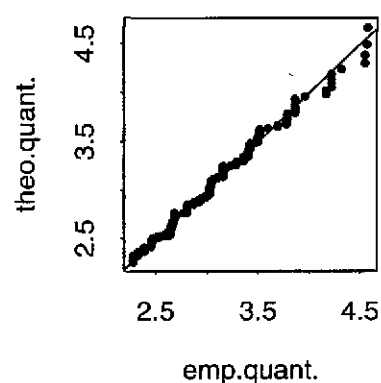


Figure 6.17: Probability and quantile plots for the GPD fitted to  $H_S$  exceedances at North Wales and Dover. Also shown in each plot is the  $x = y$  line.

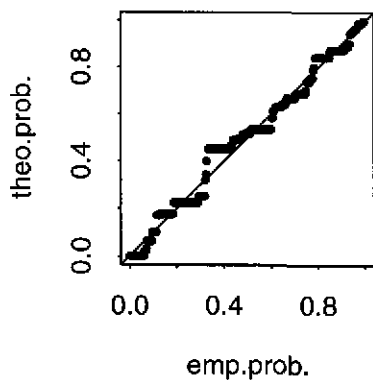
North Wales : P-P PLOT



North Wales : Q-Q PLOT



Dover : P-P PLOT



Dover : Q-Q PLOT

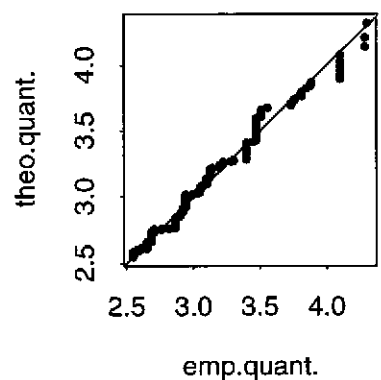


Figure 6.18: Cardiff: Estimates of two extreme quantiles under the Weibull and the GPD models versus the empirical distribution function calculated in  $u$ .

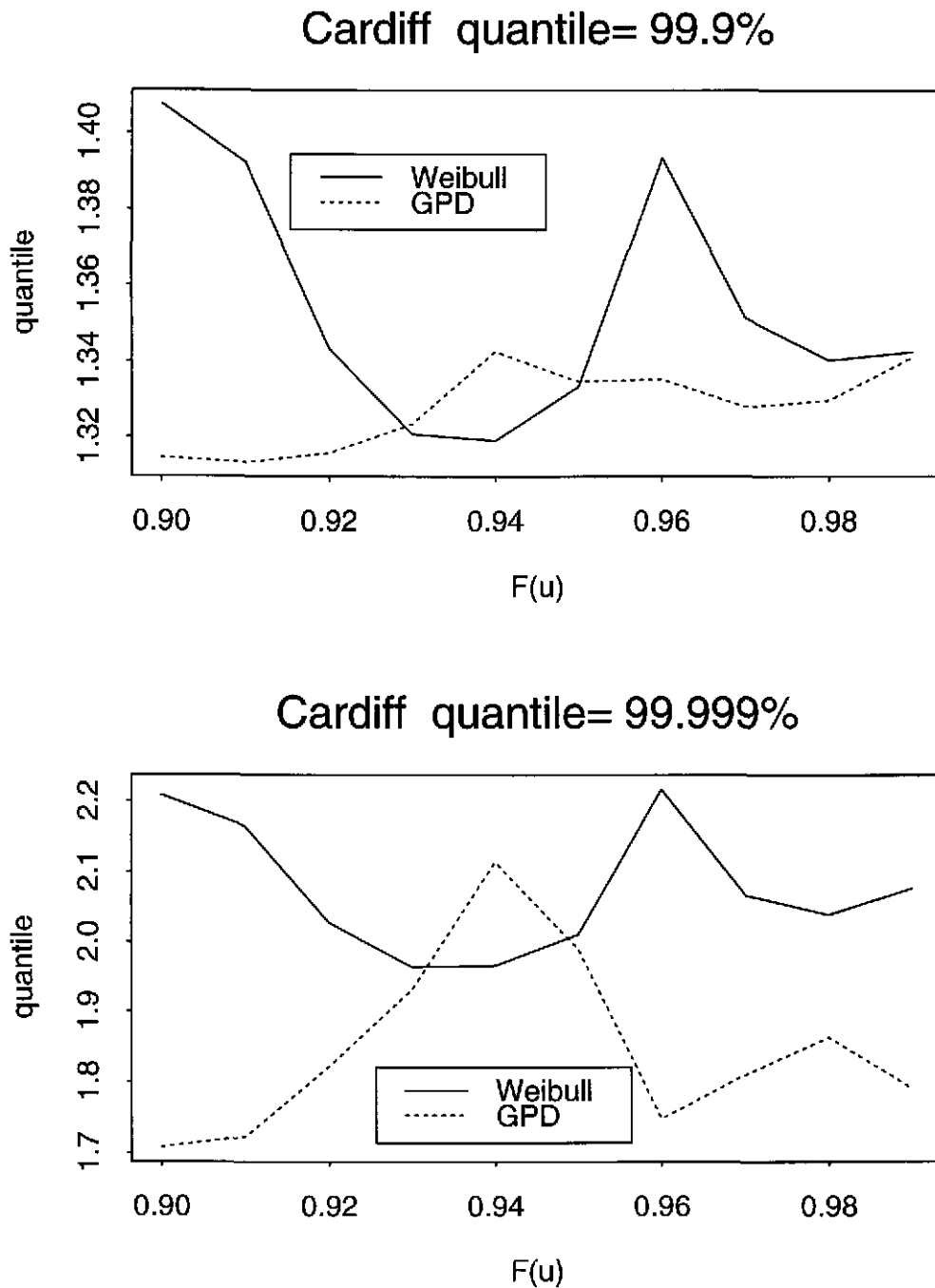


Figure 6.19: Christchurch: Estimates of two extreme quantiles under the Weibull and the GPD models versus the empirical distribution function calculated in  $u$ .

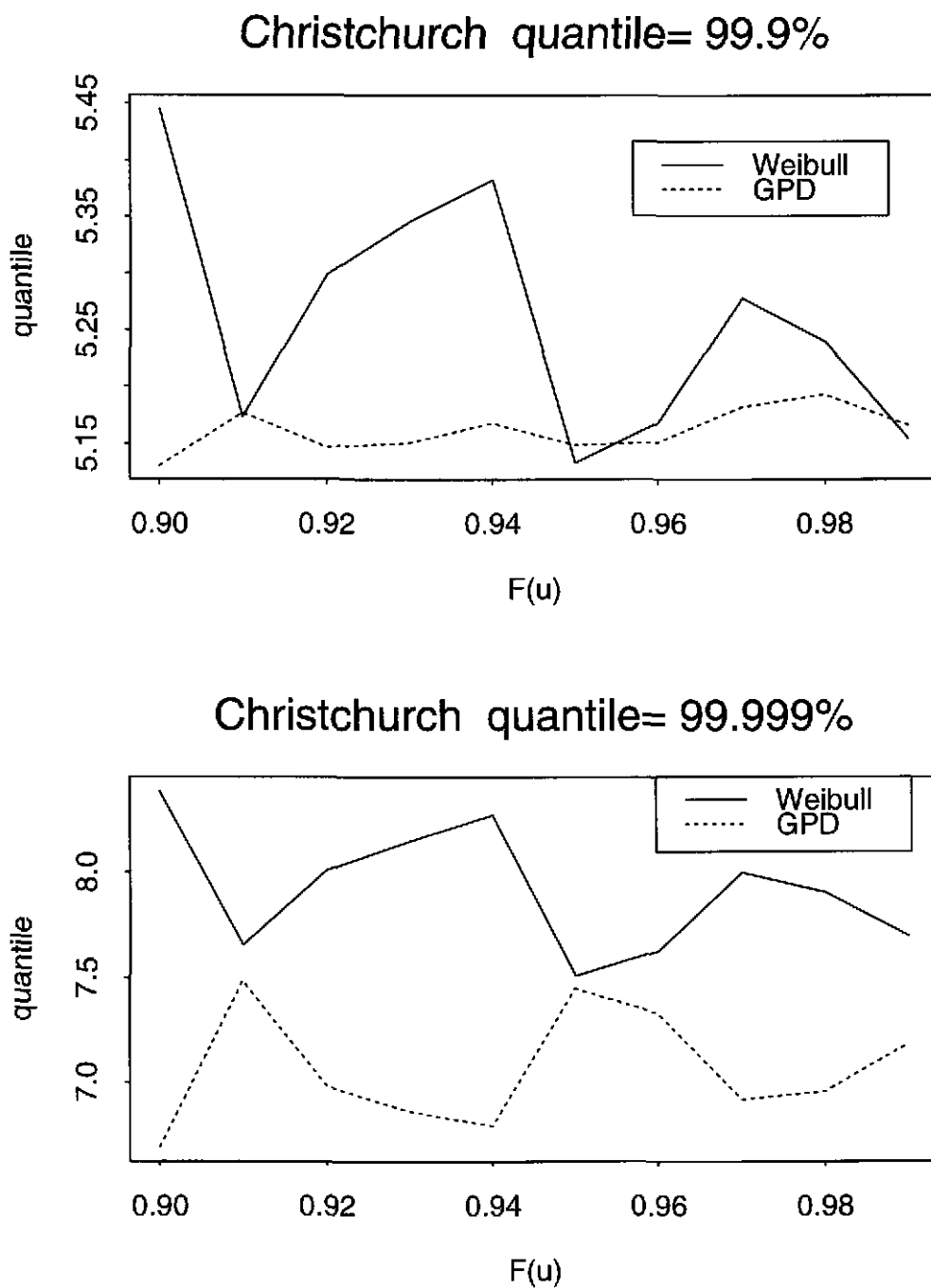


Figure 6.20: Dowsing: Estimates of two extreme quantiles under the Weibull and the GPD models versus the empirical distribution function calculated in  $u$ .

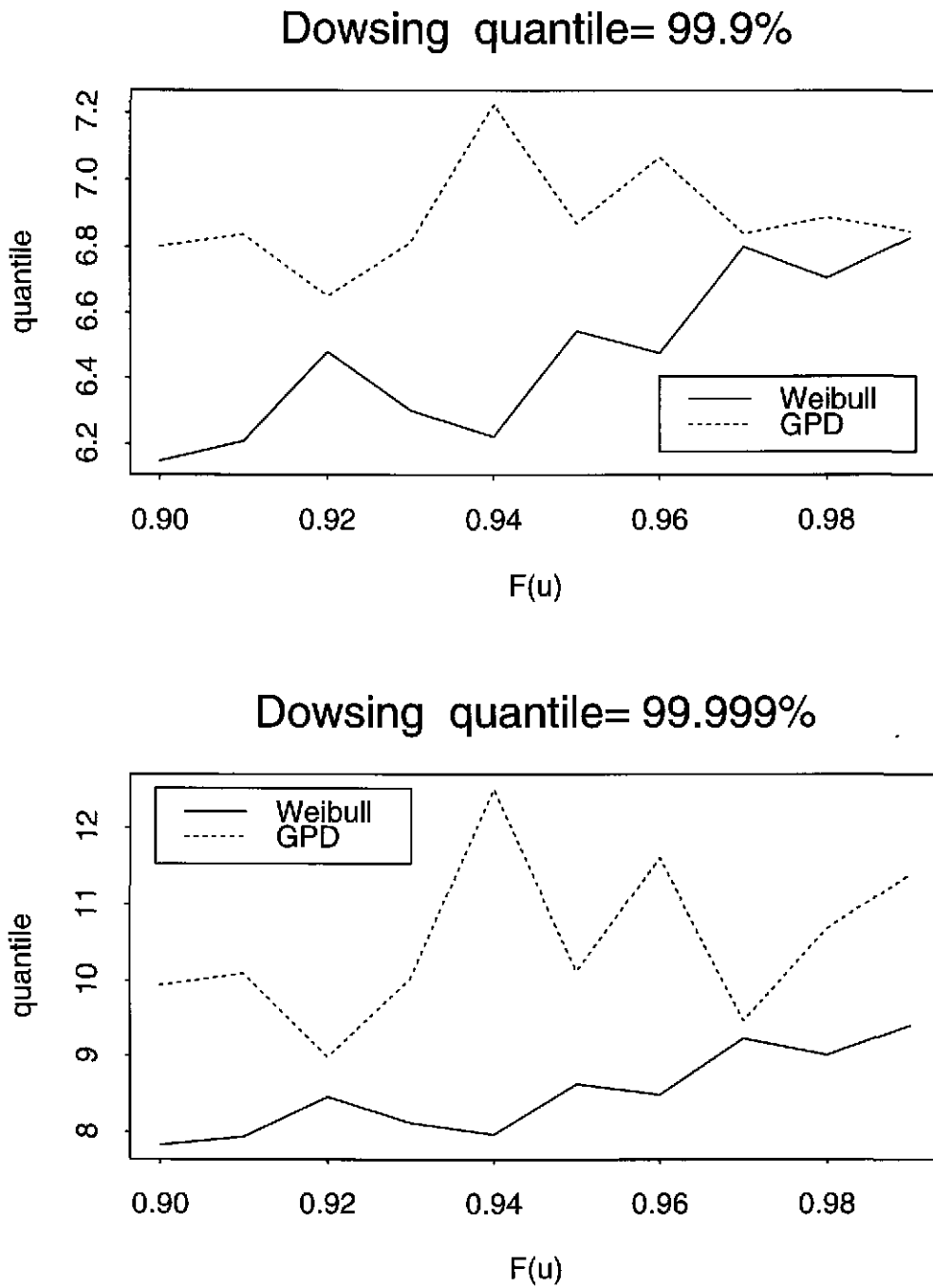


Figure 6.21: Shoreham: Estimates of two extreme quantiles under the Weibull and the GPD models versus the empirical distribution function calculated in  $u$ .

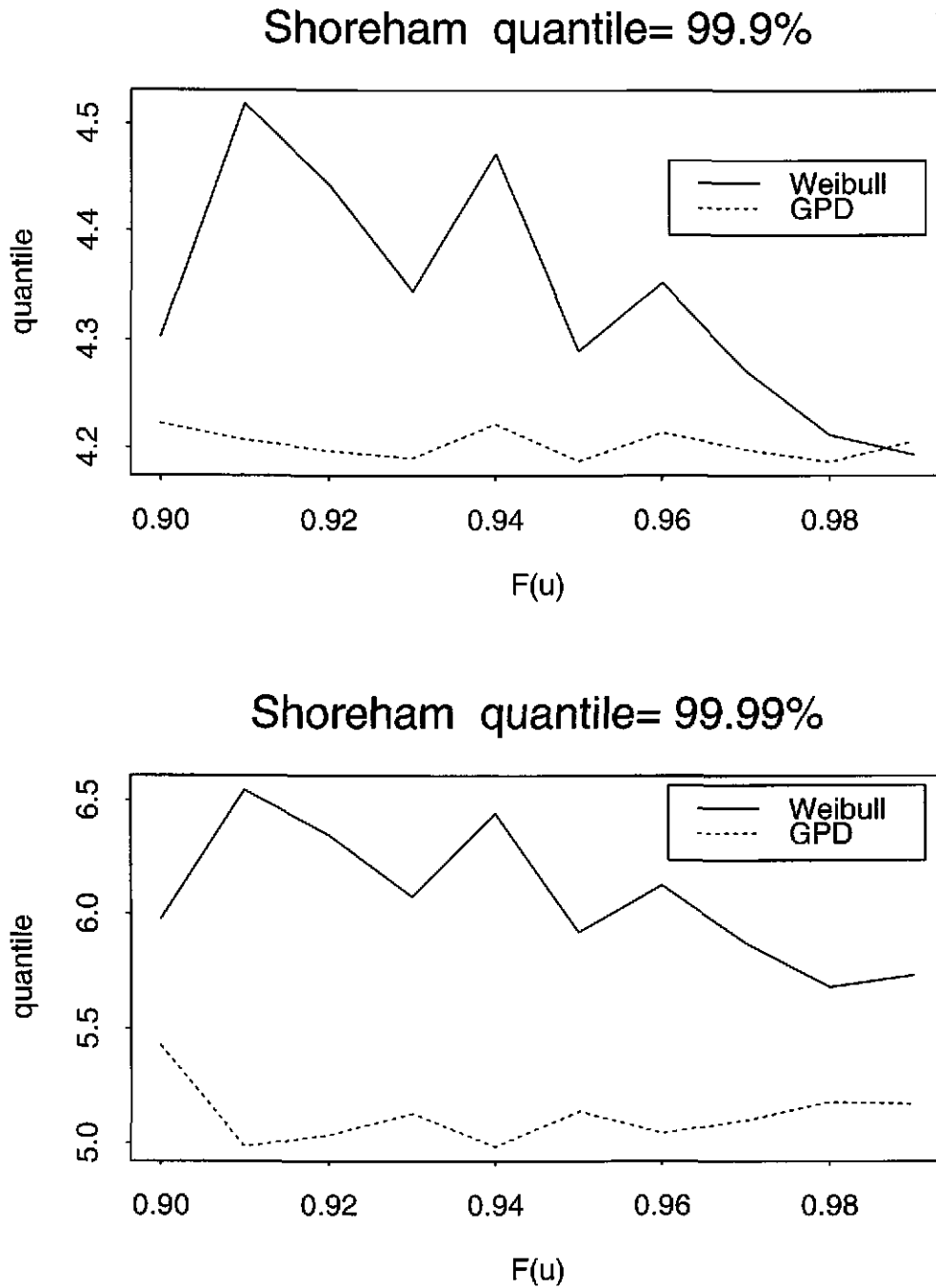


Figure 6.22: North Wales: Estimates of two extreme quantiles under the Weibull and the GPD models versus the empirical distribution function calculated in  $u$ .

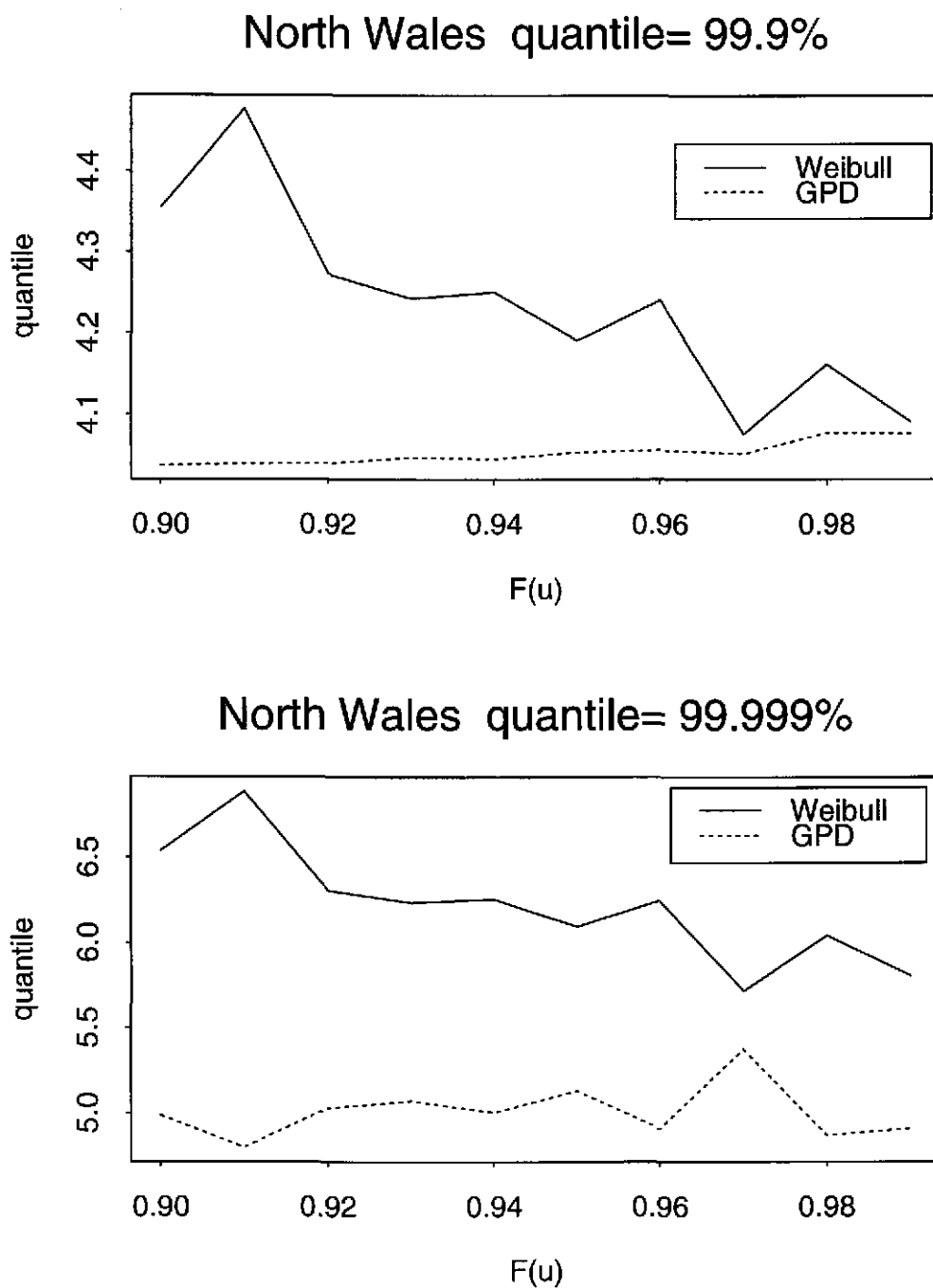
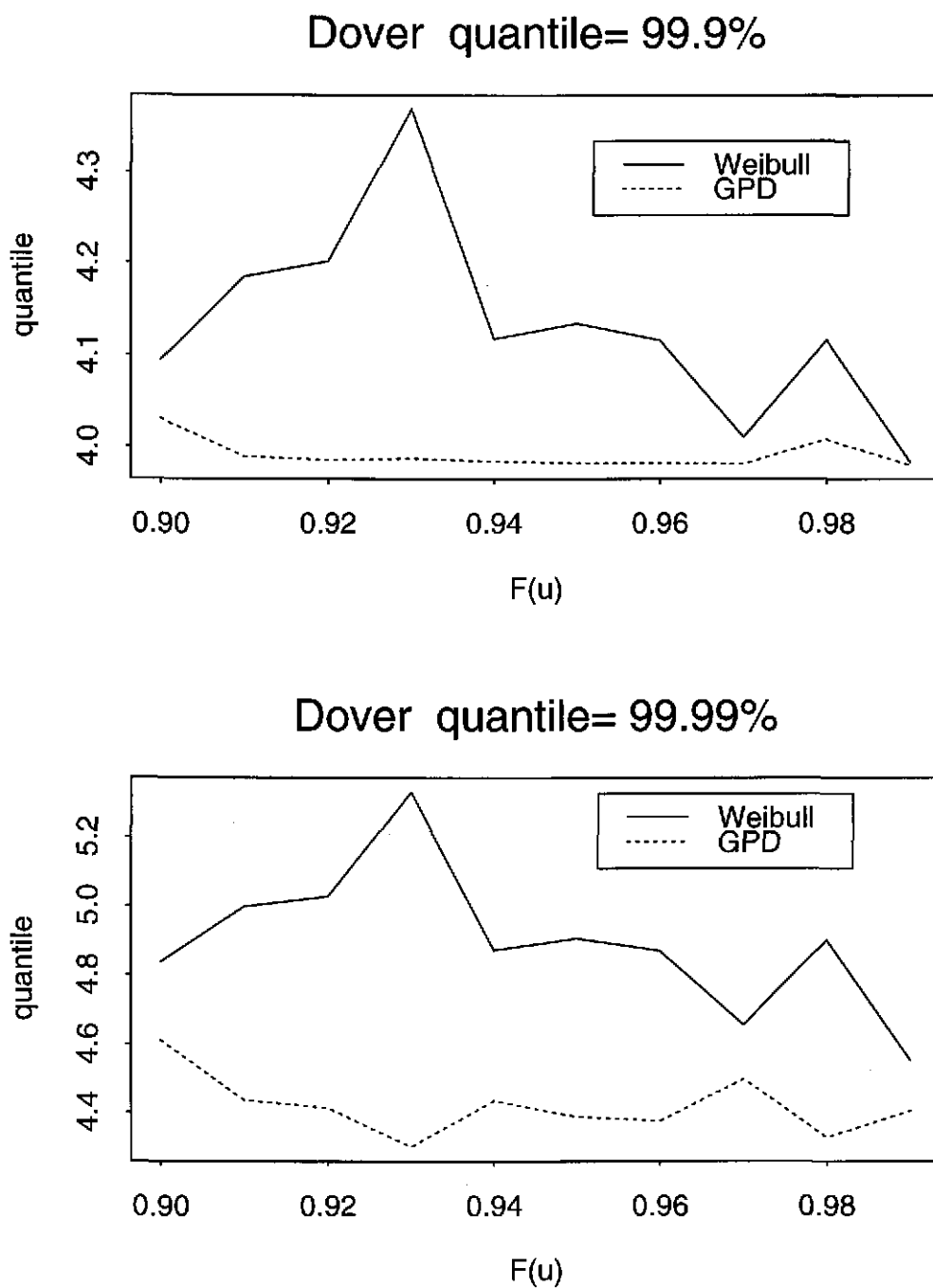


Figure 6.23: Dover: Estimates of two extreme quantiles under the Weibull and the GPD models versus the empirical distribution function calculated in  $u$ .



### 6.3.2 Simulated Data

For the simulated  $H_S$  data we only fitted the GPD threshold model. In each case we took the 95% empirical quantile of  $H_S$  as the threshold. From Section 5.2 we can see that for Sim3–Sim5 this is the correct specification of the distributional form, whereas for Sim1 and Sim2 the marginal distribution of  $H_S$  is more complex than this as, in each case, the distribution of  $H_S$  depends on the associated wave direction. Table 6.8 gives estimates of the fitted GPD parameters for each simulated data set. For Sim1–Sim3/Sim4–Sim5 the  $H_S$  distribution is estimated to have a finite/infinite upper endpoint respectively, which is consistent with the true simulation models. For Sim3 and Sim4 the estimates are close to the true values (see Chapter 5) whereas for Sim5 the shape parameter estimate is slightly too large, corresponding to an over-estimated upper tail. Comparisons for Sim1 and Sim2 are more difficult. For Sim2 the fitted model approximately is an average of the models for the two directional  $H_S$  distribution. This is reasonable, as each direction sector is approximately equally likely to produce extreme  $H_S$  values. For Sim1 the fitted model closely resembles the  $H_S$  distribution for  $\theta \geq 110^\circ$ . Again this is reasonable, as most waves, including the largest waves, come from this direction sector.

Data	Shape Parameter $\xi$	Scale Parameter $\sigma$
Sim1	-0.0727 (0.061)	0.1942 (0.016)
Sim2	-0.2712 (0.063)	0.5125 (0.042)
Sim3	-0.136 (0.05)	0.605 (0.044)
Sim4	0.1329 (0.071)	0.6506 (0.057)
Sim5	0.2108 (0.067)	0.802 (0.068)

Table 6.8: Maximum likelihood estimates of the parameters of the GPD fitted to simulated  $H_S$  threshold exceedances for the synthetic data sets (standard errors in parentheses).

## 6.4 Steepness

Figure 6.24 contains histograms of steepness for Cardiff, Christchurch, Dowsing, Shoreham, North Wales and Dover. Our approach for modelling the distribution of  $S$  is to

use the empirical distribution of  $S$ , i.e. the observed histogram with no extrapolation of  $S$  beyond the largest or smallest observations of  $S$ . For the simulated data we used the empirical distribution of  $S$  from the associated site (cf. Section 5.2).

For all sites, the most likely values of steepness lie between 0.04 and 0.06. With the exception of Cardiff, all histograms are uni-modal, exhibiting either positive or negative skewness. At Cardiff, the empirical distribution of  $S$  is bimodal, with peaks approximately corresponding to 0.01 and 0.05. The explanation of this feature is that for Cardiff the hindcast wave model predicts two types of wave:

1. locally generated (steeper waves), and
2. externally generated (shallower waves) which have only been able to reach Cardiff due to refraction.

As specified above, all six data sets consist of hindcast wave data. Despite the hindcasting model complexity, there remains the risk that some aspects of the actual observed  $S$  process may be missed. To illustrate that the distributions of measured and hindcast steepness are not substantially different, histograms of measured  $S$  at Morecambe, Lyme and Boygrift are shown in Figure 6.25. They seem consistent with the corresponding plots of hindcast steepness, possibly showing more variability and longer tails, but this difference was not considered important for this study.

Figure 6.24: Histogram of Steepness at various sites.

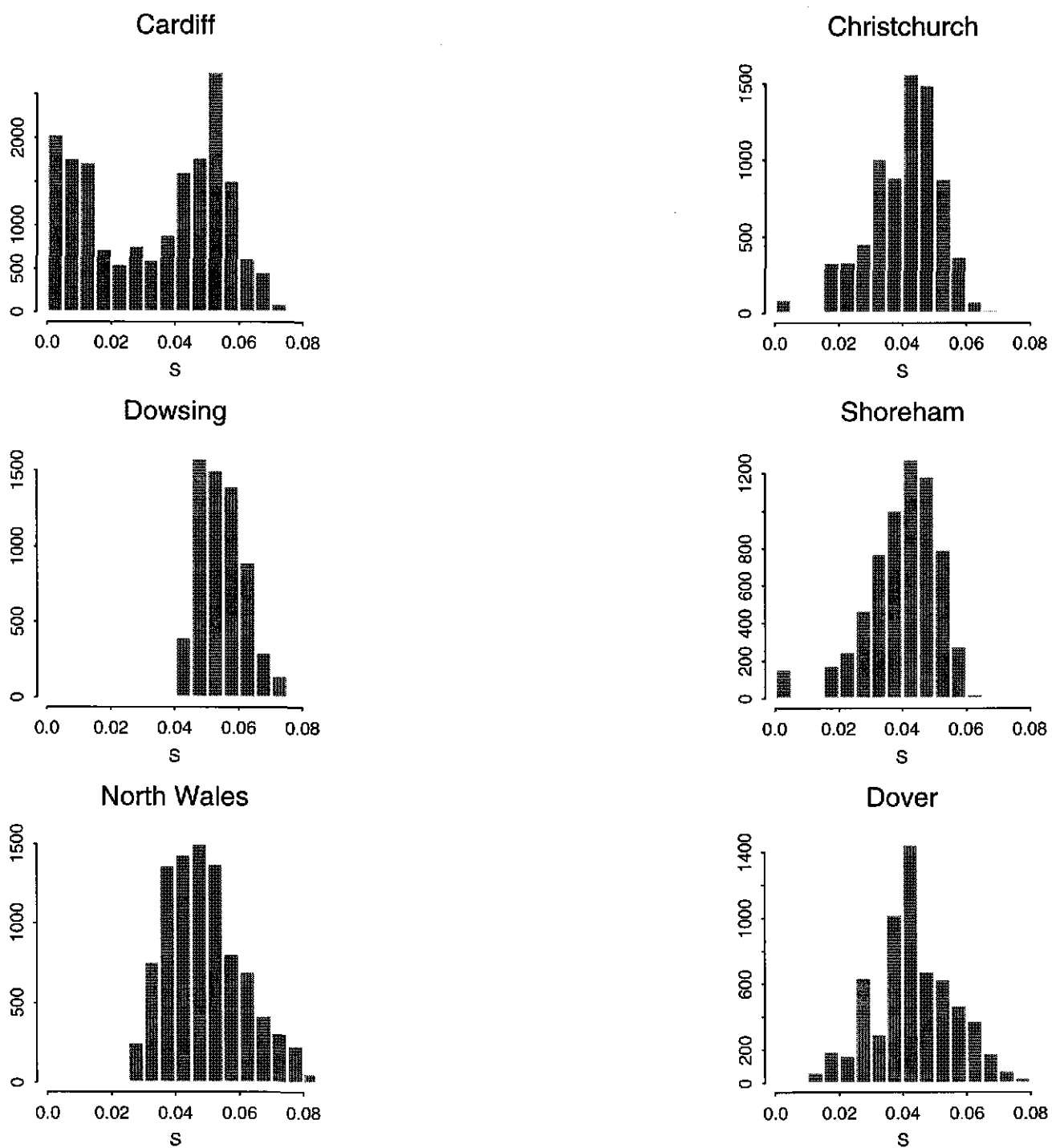
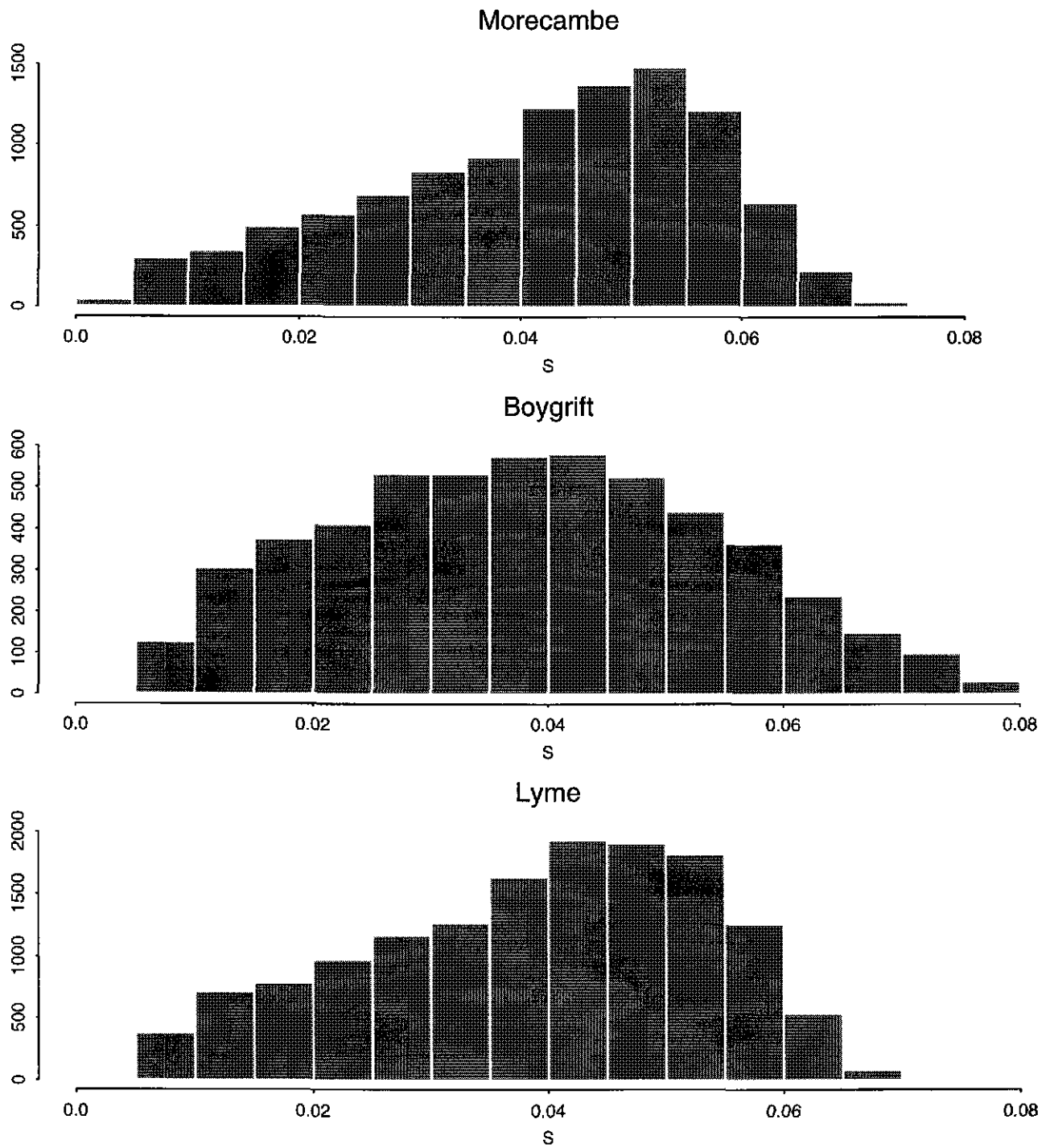


Figure 6.25: Histogram of measured steepness at Morecambe, Boygrift and Lyme.

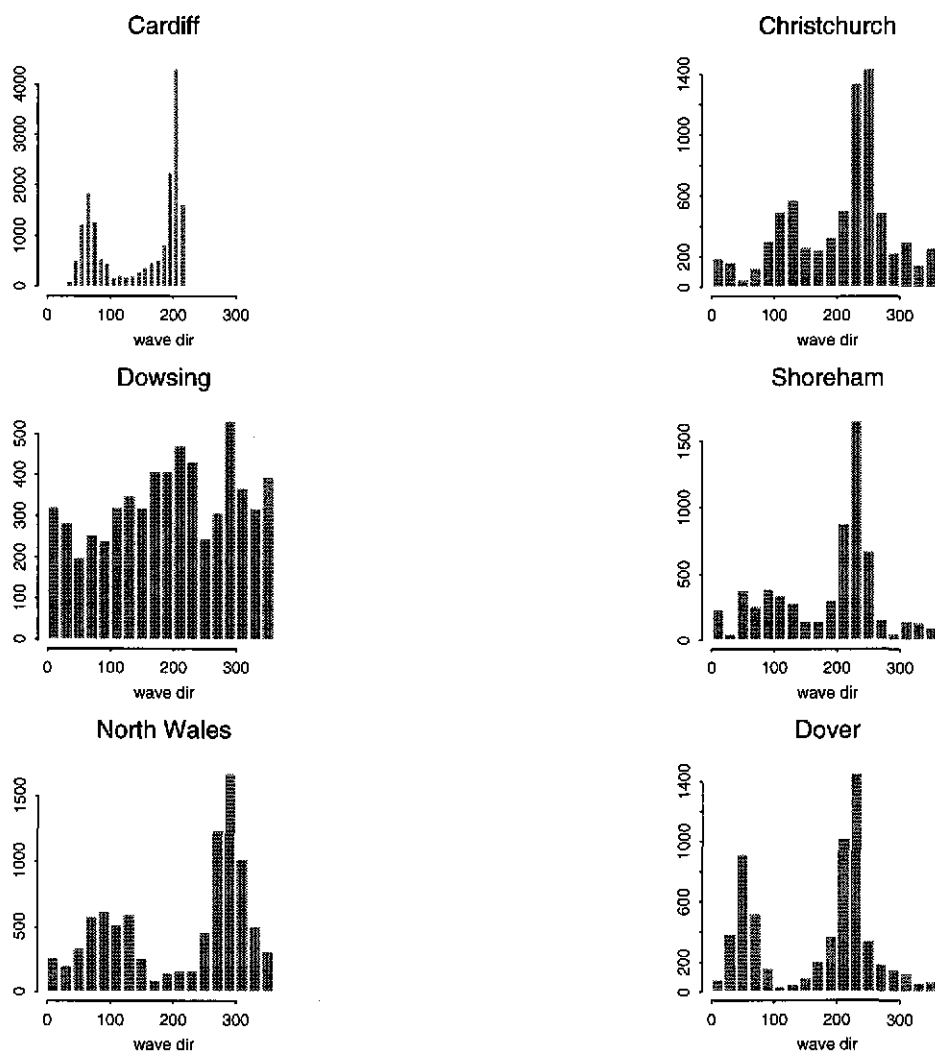


## 6.5 Wave Direction

Figure 6.26 shows histograms of wave direction for Cardiff, Christchurch, Dowsing, Shoreham, North Wales and Dover. Our approach for statistically modelling the distribution of  $\theta$  is similar to that of  $S$ , i.e. through the empirical distribution of  $\theta$ . For the simulated data we used the empirical distribution of  $\theta$  for the associated data site (cf. Section 5.2).

The distribution of  $\theta$  seems quite different at Dowsing compared with the other sites. At Dowsing all directions are approximately equally likely, whereas at other sites the distribution is bi-modal, with peaks at  $80^\circ - 100^\circ$  (the secondary peak) and  $200^\circ - 300^\circ$  (the dominant peak). A possible reason for this difference is that Dowsing is further offshore than the other sites. For Cardiff, the mode around  $200^\circ$  includes the externally generated waves with lower  $S$  values.

Figure 6.26: Histogram of Wave Direction at various sites.





# Chapter 7

## Dependence Estimation

In this chapter we examine the suitability of the statistical dependence models proposed in Chapter 4 when applied to observational/hindcast data and the five simulated data sets. Because of the structure of the statistical models proposed we can separately examine the dependence between  $(H_S, SWL)$  and  $(H_S, S)$ . In Section 7.1 we examine both types of data when applying statistical models for  $(H_S, SWL)$ , whereas we only give results for the simulated data sets when examining  $(H_S, S)$  in Section 7.2.

### 7.1 $(SWL, H_S)$ Dependence

#### 7.1.1 Observational data

First we estimate the correlation function,  $\rho_u$ , given by the bivariate normal threshold model of Section 4.2.1. Constancy of this function above a given level suggests that a bivariate normal model can be used above this level to describe the dependence structure. However, if the function is

- constant for all  $u$ : this suggests the bivariate normal dependence model is appropriate for all the values;
- not constant above any  $u$ : then a more complex statistical dependence model, such as the mixture of bivariate normals dependence model, is required.

Figures 7.1 and 7.2 show the correlation function,  $\rho_u$ , plotted against the threshold non-exceedance probability  $p = \Pr\{H_S < u\} = \Pr\{SWL < u\}$  for  $(H_S, SWL)$  and  $(H_S, Surge)$  respectively (note on the plots  $\rho_u$  is shown as  $\rho(p)$ ). The main features of these plots are:

1. the weaker correlation between  $(H_S, SWL)$  than between  $(H_S, Surge)$ ;

2. all sites show a limited increase in the  $(H_S, Surge)$  values of  $\rho_u$  as  $u$ , or equivalently  $p$ , is increased;
3. greater stability of  $\rho_u$ , with respect to  $u$ , is seen for  $(H_S, SWL)$ ;
4. Christchurch has a strong correlation of 0.6 in the extreme  $Surge$  and  $H_S$  levels, whereas for Dover  $(H_S, Surge)$  are generally negatively correlated, with extreme levels possibly being independent;
5. in all cases, as the threshold is increased, the confidence intervals (not shown on these plots) grow so any irregular changes in the function for large  $u$  can be ignored.

For Cardiff the direction of the waves is known to be important to the form of the joint distribution of the other sea condition variables, so in Figures 7.3 and 7.4 the corresponding correlation function plots are produced conditionally on the wave direction variable,  $\theta$ , being  $\theta < 190^\circ$  or  $\theta > 190^\circ$ . Here we see a distinct difference in the degree of dependence found, with strongest dependence for  $\theta > 190^\circ$ , and that the feature of rising correlation at more extreme levels observed in Figures 7.1 and 7.2 is retained.

These findings suggest that the mixture of bivariate normals model should be considered as a feasible candidate at all sites. Tables 7.1 and 7.2 give the parameter estimates of this statistical model for each site.

Although the parameters of the dependence model are of some interest, it is really how they combine to produce a changing degree of dependence when looking further into the joint tail of the distribution that is important. To examine this we evaluate the  $\rho_u$  function for this dependence model. This cannot be evaluated in closed form so we use simulation techniques. Figures 7.5–7.10 show the resulting  $\rho_u$  plots for the mixture of bivariate normals model together with the threshold model estimate of  $\rho_u$  for comparison. These plots are shown for each site and for both  $(H_S, SWL)$  and  $(H_S, Surge)$  data. In each case the mixture model gives a very good approximation to the  $\rho_u$  curve. This suggests the use of the mixture of bivariate normals model, as this has the added benefits of:

1. the inference uses all data, not just the values of threshold exceedances and down-weighted (censored) values of other observations;
2. the fit does not depend on an arbitrary/subjective selection of a threshold level;
3. the fit provides extrapolations for dependence which allow for an increased, or decreased, degree of dependence beyond the data.

The disadvantages of the mixture of bivariate normals model are:

1. that it is indicative of a dependence structure which is more complex than the bivariate normal, or the threshold bivariate normal;
2. it may be an approximation to a situation in which a mixture of different types of dependence apply, but a mixture of two types of dependence structure may be too simplistic;
3. it doesn't provide a relationship between the un-mixed dependence forms and the other wave variables (period and direction);
4. it is quite highly parametrised with the parameters (for the variables with Gaussian marginals) not easily interpretable from practical considerations.

Of the data sets, the parameter estimates for Dowsing, Dover, and Cardiff suggest that the simpler bivariate normal dependence structure is appropriate as a dependence model in these cases. We have subsequently used the simpler model for dependence, but if we had continued with the broader family, given by the mixture model, we would have obtained similar results.

Figure 7.1: Correlation function,  $\rho_u$ , between  $(H_S, SWL)$  versus the threshold (in probability of non-exceedance) for the different sites

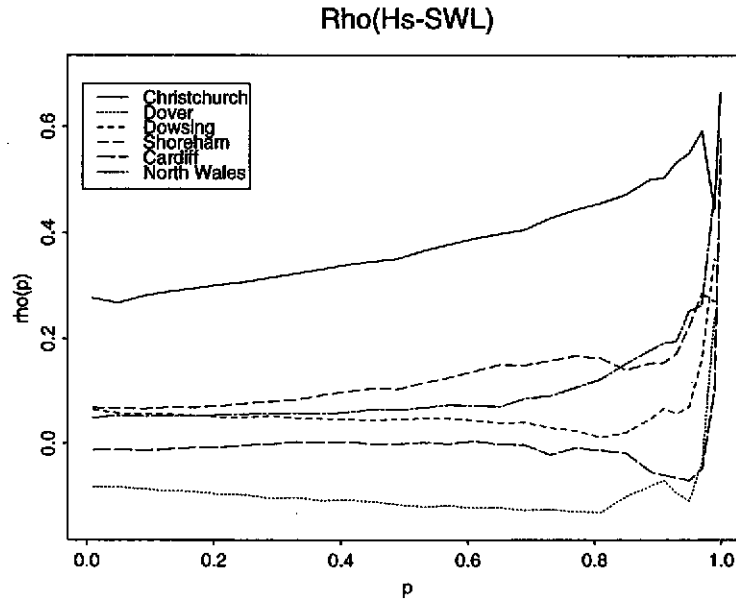


Figure 7.2: Correlation function,  $\rho_u$ , between  $(H_S, Surge)$  versus the threshold (in probability of non-exceedance) for the different sites

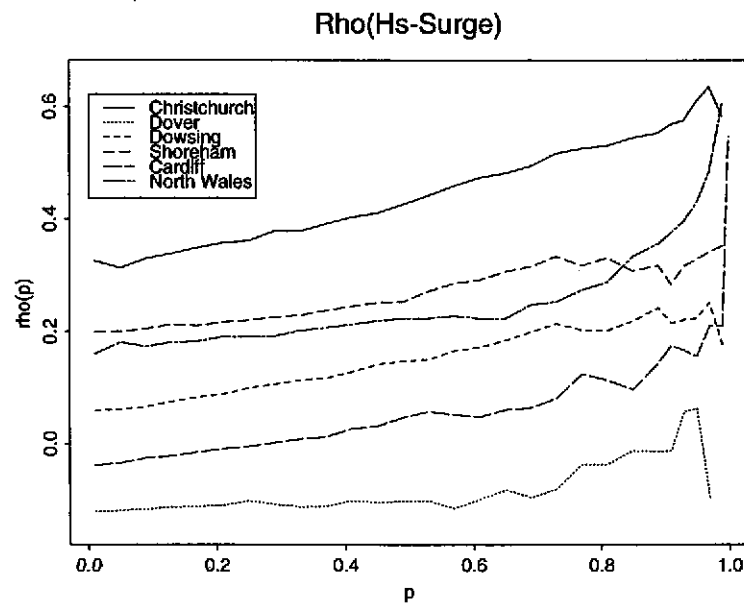


Figure 7.3: Cardiff: Correlation function,  $\rho_u$ , between ( $H_S, SWL$ ) versus the threshold (in probability of non-exceedance) separately for  $\theta < 190^\circ$  and  $\theta > 190^\circ$

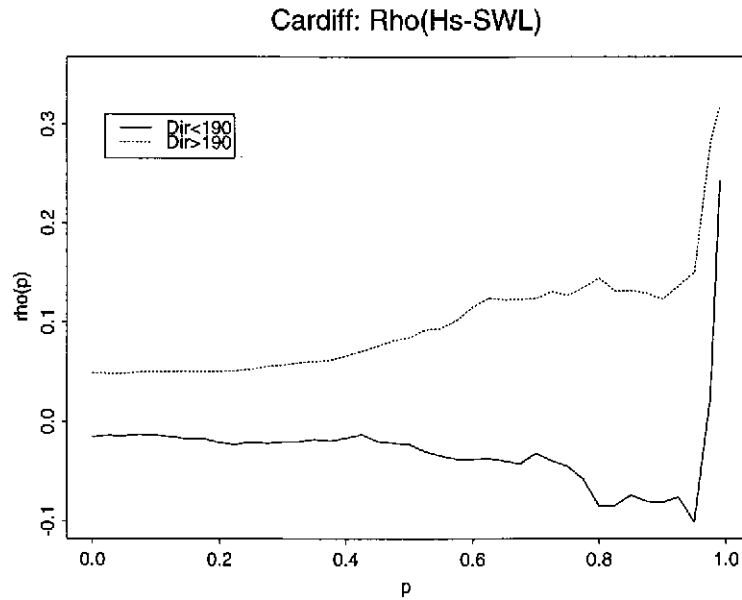
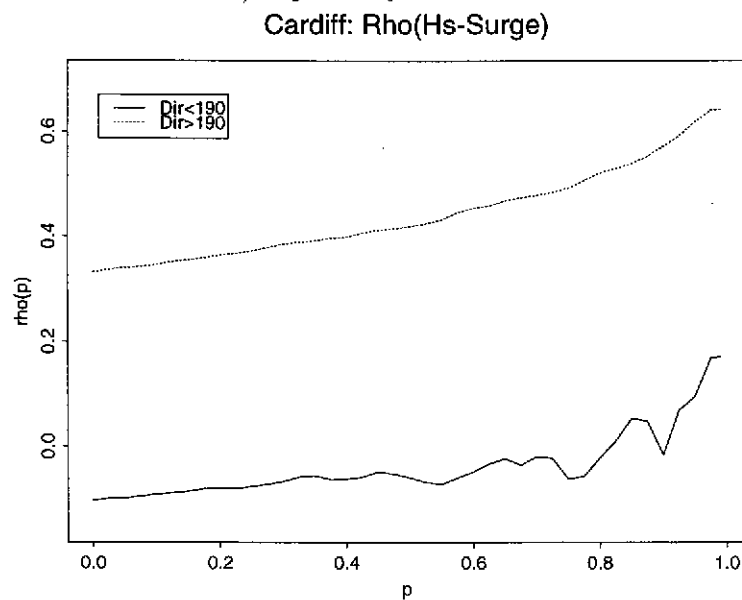


Figure 7.4: Cardiff: Correlation function,  $\rho_u$ , between ( $H_S, Surge$ ) versus the threshold (in probability of non-exceedance) separately for  $\theta < 190^\circ$  and  $\theta > 190^\circ$



Parameters	Christchurch	Dowsing	Dover	North Wales	Cardiff	Shoreham
$p_M$	0.51	0.05	0.50	0.968	0.52	0.88
$\rho_1$	-0.13	0.32	0.13	0.02	-0.05	-0.048
$\rho_2$	0.52	0.03	-0.12	0.48	-0.09	0.36
$\mu_{21}$	0.7	0.0	1.1	1.8	1.5	0.7
$\mu_{22}$	0.6	0.6	-0.4	0.3	0.1	1.2
$\sigma_{21}$	0.9	0.3	0.5	0.8	0.4	0.6
$\sigma_{22}$	1.2	0.3	0.7	2.1	1.2	1.0

Table 7.1: Parameter estimates for the mixture of bivariate normals applied to observational ( $H_S, SWL$ ) data.

Parameters	Christchurch	Dowsing	Dover	North Wales	Cardiff	Shoreham
$p_M$	0.47	0.33	0.21	0.25	0.45	0.76
$\rho_1$	-0.17	-0.40	-0.48	-0.28	-0.42	-0.04
$\rho_2$	0.56	0.28	-0.05	0.31	0.33	0.3
$\mu_{21}$	0.8	0.0	0.0	0.0	0.0	0.8
$\mu_{22}$	0.7	1.3	1.7	1.1	1.3	1.5
$\sigma_{21}$	0.9	1.2	0.7	1.3	0.5	0.6
$\sigma_{22}$	1.3	1.0	0.8	0.9	1.2	1.0

Table 7.2: Parameter estimates for the mixture of bivariate normals applied to observational ( $H_S, Surge$ ) data.

Figure 7.5: Christchurch: Estimated correlation function,  $\rho_u$ , between  $(H_S, SWL)$  and  $(H_S, Surge)$  versus the threshold (in probability of non-exceedance) for the fitted mixture of bivariate normals and the threshold bivariate normal

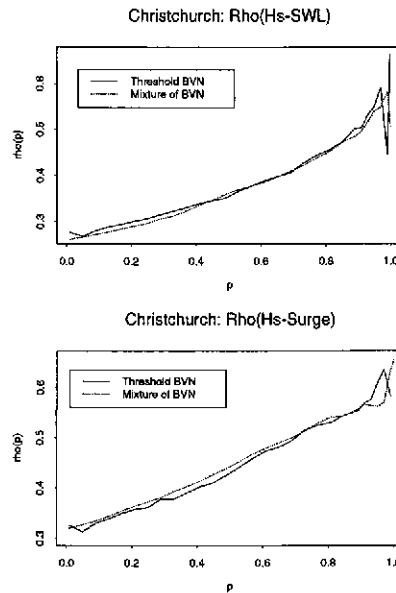


Figure 7.6: Dowsing: Estimated correlation function,  $\rho_u$ , between  $(H_S, SWL)$  and  $(H_S, Surge)$  versus the threshold (in probability of non-exceedance) for the fitted mixture of bivariate normals and the threshold bivariate normal

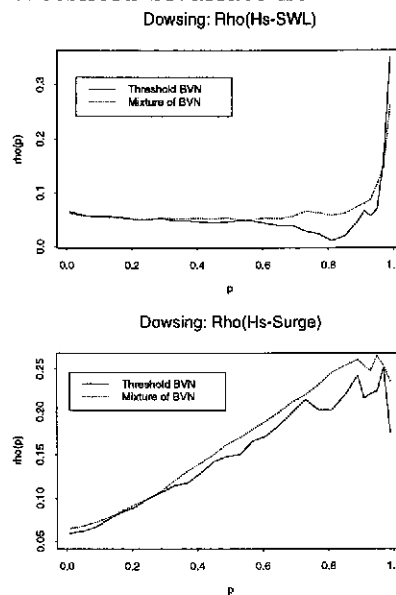


Figure 7.7: Dover: Correlation function,  $\rho_u$ , between  $(H_S, SWL)$  and  $(H_S, Surge)$  versus the threshold (in probability of non-exceedance) for the fitted mixture of bivariate normals and the threshold bivariate normal

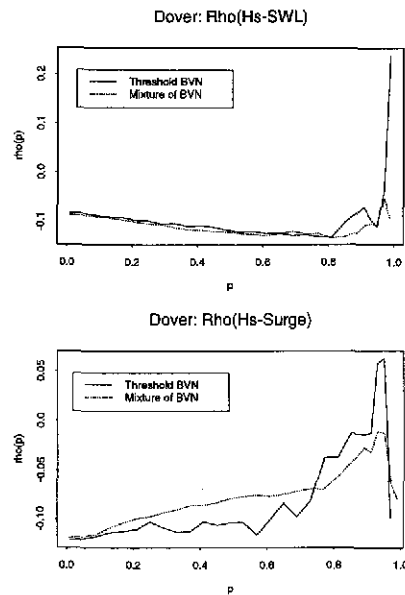


Figure 7.8: North Wales: Estimated correlation function,  $\rho_u$ , between  $(H_S, SWL)$  and  $(H_S, Surge)$  versus the threshold (in probability of non-exceedance) for the fitted mixture of bivariate normals and the threshold bivariate normal

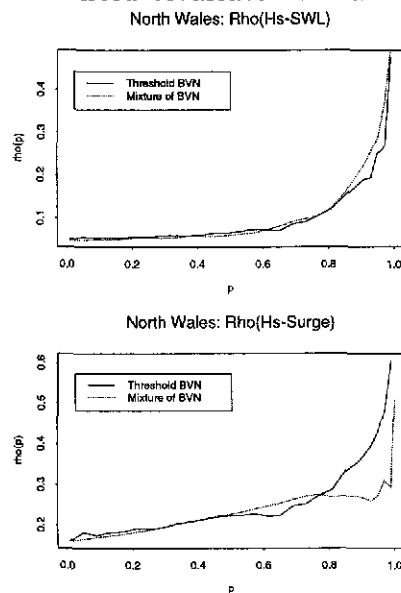


Figure 7.9: Cardiff: Correlation function,  $\rho_u$ , between  $(H_S, SWL)$  and  $(H_S, Surge)$  versus the threshold (in probability of non-exceedance) for the fitted mixture of bivariate normals and the threshold bivariate normal

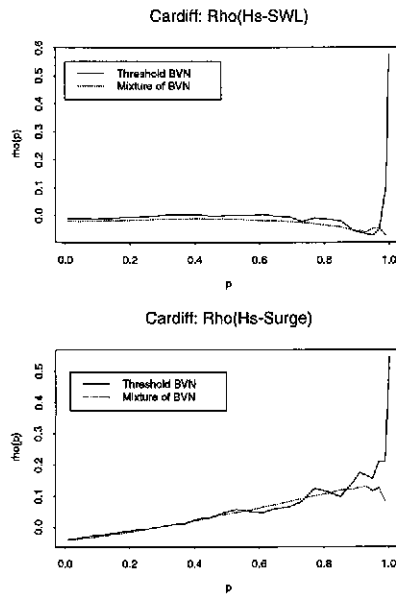
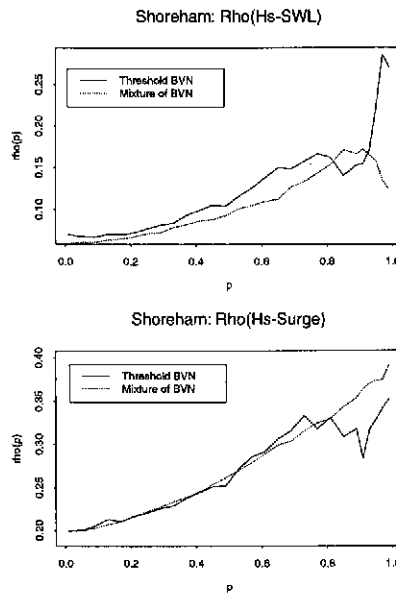


Figure 7.10: Shoreham: Estimated correlation function,  $\rho_u$ , between  $(H_S, SWL)$  and  $(H_S, Surge)$  versus the threshold (in probability of non-exceedance) for the fitted mixture of bivariate normals and the threshold bivariate normal



### 7.1.2 Simulated data

In this section we consider estimation of an appropriate dependence structure for the five Sim data sets. The section is split into two stages: diagnostic assessment and dependence modelling. In the diagnostic subsection we try to identify for which, if any, of the data sets we can adopt a conservative approach for by taking the variables ( $SWL, H_S$ ) to be completely dependent, without badly over-estimating the dependence. When complete dependence is a poor representation of the dependence, we are also interested in testing whether taking the variables to be independent is an over-simplification.

#### Diagnostics for dependence form

We use the diagnostic statistic,  $T(z)$ , given by equation (3.3.4), applied to Sim1-Sim5 in turn. The statistic, with associated pointwise confidence intervals, is shown for the respective data sets in Figures 7.11-7.15.

For Sim1, the gradient of the diagnostic plot is approximately  $\frac{1}{2}$  and, judging by the confidence intervals, the gradient of this plot is significantly greater than zero and less than one. This suggests that careful modelling of the dependence is required for these data. The gradient is in line with the simulation model, which is essentially a bivariate normal distribution with  $\rho = 0.3$ , so following equation (3.3.5) should have gradient  $(1 - 0.3)/(1 + 0.3) = 0.54$ .

The diagnostic plots for Sim2 and Sim3 are similar to that for Sim1. The respective gradients are approximately 1.5 and 0.75, and are significantly greater than zero. For each data set, the confidence interval includes a gradient of one, so independence is not inconsistent with the observed dependence. These findings suggest that careful modelling of the dependence is required for these data, but that the dependence is weak, so independence may be an adequate approximation. The gradient is in line with the simulation models, which are in essence a bivariate normal distribution with  $\rho = -0.2$  and 0.16, so following equation (3.3.5) should have respective gradients  $(1 + 0.2)/(1 - 0.2) = 1.5$  and  $(1 - 0.16)/(1 + 0.16) = 0.72$ .

Sim4 has a notably different diagnostic plot than the other simulated data sets as the confidence interval for the diagnostic statistic contains zero for all  $\log z$ , and the gradient of the plot is not significantly different from zero (this is consistent with the bivariate extreme value dependence model we have used to simulate the Sim4 data). For these data we can take the dependence to be complete dependence without being overly conservative. In the subsequent analyses we will try to model the dependence for these data and comment on differences between estimates based on these models and the complete dependence model. Independence is a very poor description of the observed dependence.

The dependence model used to generate the Sim5 data was more complex than the others, being a mixture of independence for low levels, and high correlation (0.8) for

high levels. The diagnostic plot identifies this transition in dependence with a gradient of approximately 1 up to  $\log z = 0.5$ , and a gradient of approximately 0.12 subsequently. The plot has a gradient significantly different from zero and one, so the positive dependence needs modelling.

### Dependence Models

We start by fitting the mixture of bivariate normals model to each simulated data set and examining the correlation function  $\rho_u$ . For selected dependence models we continue by evaluating the fitted joint density function, and compare it to the true joint density (used for the simulation) via comparison of contours of equal joint density function.

Table 7.3 gives parameter estimates of the mixture of bivariate normals model. For Sim1–Sim3 we find  $p_M \approx 1$ , i.e. there is only one bivariate normal dependence structure in the data, so that the bivariate normal model is sufficient. For Sim4,  $p_M$  is large, but  $\rho_1$  and  $\rho_2$  are quite different, suggesting that the extreme observations have a different degree of dependence from the bulk of the distribution. Note,  $\rho_2 = 0.7$  effectively measures the correlation in the extremes here. Finally, for Sim5 the fitted dependence model is in the same statistical family as was used to simulate the data, and from Section 5.2 we can see that the dependence model gives parameter estimates very close to the values used for the simulation.

To confirm these findings we now estimate the correlation function,  $\rho_u$ , for each simulated  $(H_S, SWL)$  data set. This function is shown in Figure 7.16, where we see stability for Sim1–Sim3, but rising correlation levels for the joint extreme values in Sim4 and Sim5. For Sim3 we additionally estimate the correlation function for  $(H_S, Surge)$ , shown in Figure 7.17. This has the property, noted earlier, of weaker dependence between  $(H_S, SWL)$  than between  $(H_S, Surge)$ . In each case, for Sim3, the correlation function appears to be independent of  $u$ .

To assess the fit of the mixture of bivariate normals model for Sim4 and Sim5, we also evaluate the  $\rho_u$  function for this dependence model by fitting the bivariate normal threshold model to simulated data from the fitted model. Figures 7.18 and 7.19 show that the corresponding functions capture the  $\rho_u$  curves extremely well. Of course, in Figure 7.19 this fitted model is of the same form as the simulation model.

Based on the findings above, for the remainder of the report we consider only the following dependence models estimated for Sim1–Sim5:

**Sim1** bivariate normal dependence with correlation coefficient 0.24;

**Sim2** bivariate normal dependence with correlation coefficient  $-0.21$ ;

**Sim3** for  $(H_S, Surge)$  a bivariate normal dependence with correlation coefficient 0.14, whereas for  $(H_S, SWL)$  a bivariate normal dependence with correlation coefficient

Figure 7.11: Sim1: Diagnostic test for the form of the dependence in the extremes of  $H_S$ - $SWL$ . The solid line is the test statistic and the dotted line its pointwise 95% confidence interval.

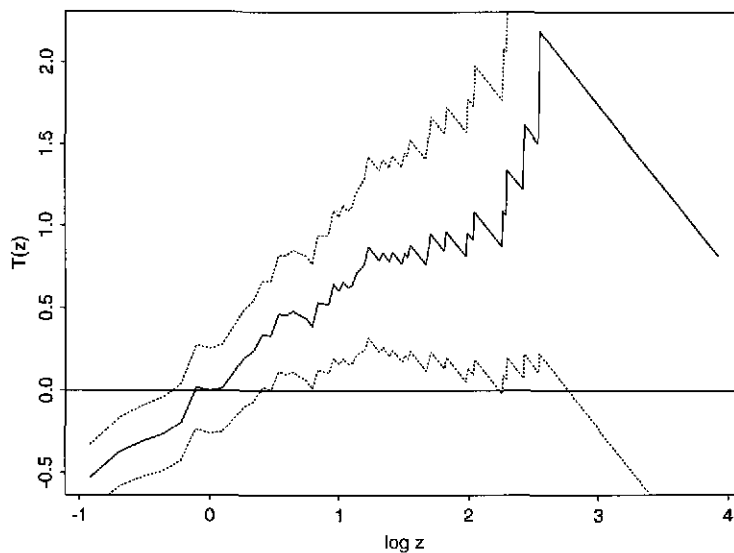


Figure 7.12: Sim2: Diagnostic test for the form of the dependence in the extremes of  $H_S$ - $SWL$ . The solid line is the test statistic and the dotted line its pointwise 95% confidence interval.

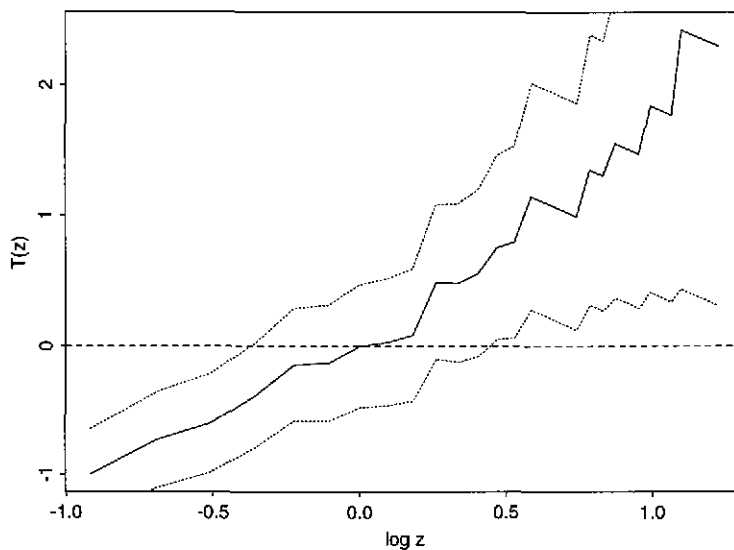


Figure 7.13: Sim3: Diagnostic test for the form of the dependence in the extremes of  $H_S$ - $SWL$ . The solid line is the test statistic and the dotted line its pointwise 95% confidence interval.

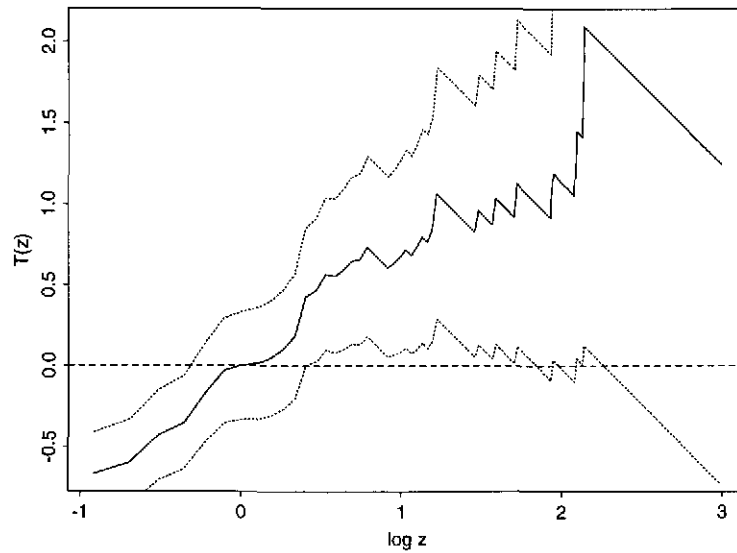
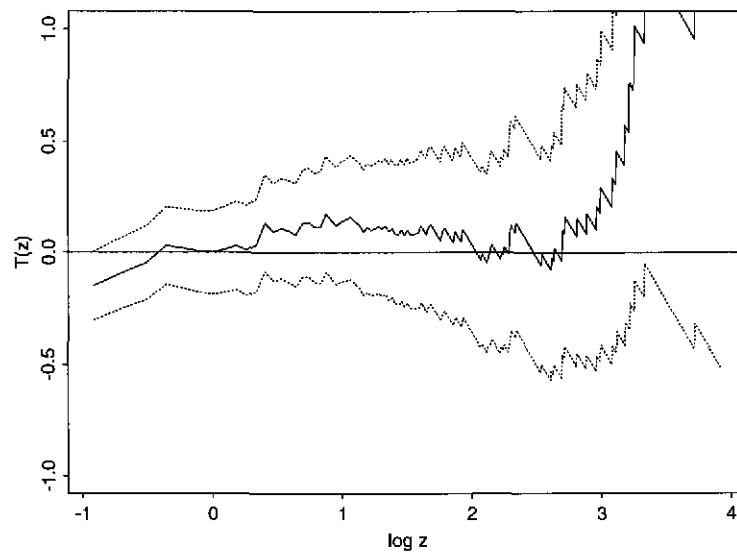


Figure 7.14: Sim4: Diagnostic test for the form of the dependence in the extremes of  $H_S$ - $SWL$ . The solid line is the test statistic and the dotted line its pointwise 95% confidence interval.



0.03;

**Sim4** bivariate normal threshold model with  $\rho_u = 0.588$  for  $u$  equal to the 95% threshold, and the fitted mixture of bivariate normals (parameter estimates in Table 7.3);

**Sim5** bivariate normal threshold model with  $\rho_u = 0.335$  for  $u$  equal to the 97.5% threshold, and the fitted mixture of bivariate normals (parameter estimates in Table 7.3).

Figures 7.20 and 7.21 show the fitted and true/simulation joint density contours for Sim1 and Sim2 respectively. In each case the bivariate normal model is of the correct form for the dependence modelling, so inconsistencies in the estimates are due to parameter estimation rather than mis-specification of the statistical model. The agreement is very good for Sim1, and reasonable for Sim2. In the latter the upper tail of the  $H_S$  variable is a bit short in the estimated joint density model.

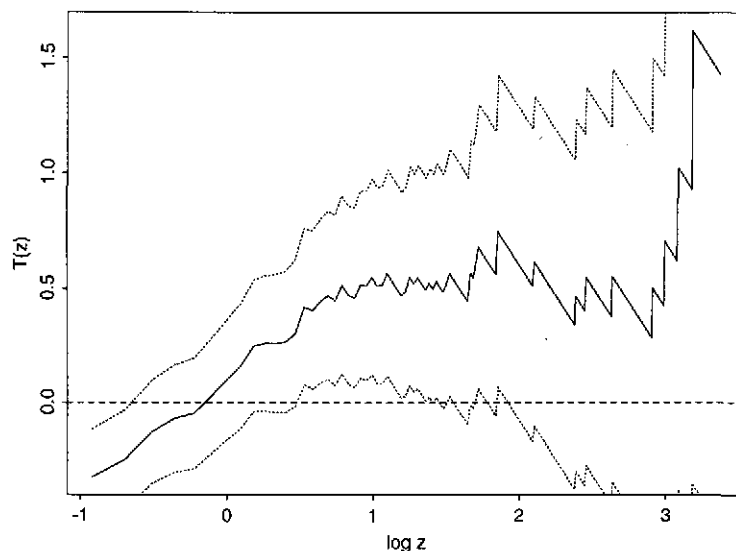
For Sim3 we have dependence models for both  $(H_S, SWL)$  and  $(H_S, Surge)$ . Joint density contours are shown in Figures 7.22 and 7.23. The agreement is good in both cases, with the only obvious disagreement arising from the estimated joint distribution having a shorter upper tail for *Surge* and *SWL* than the simulated values.

For Sim4 we have two fitted statistical models to compare. Figures 7.24 and 7.25 show joint density estimates for the threshold and mixture bivariate normal models respectively. For the former the estimation of the dependence structure is extremely poor, with the contours in poor agreement over most of the distribution. By comparison, the mixture model is in good agreement, with the exception of the *SWL* upper tail, which is underestimated.

Finally consider estimates for Sim5 shown in Figures 7.26 and 7.27. Again the threshold based dependence model fits poorly, and the mixture model is a marked improvement. However, whatever dependence model is fitted the joint density estimate is poor as the marginal models over-estimates/under-estimate the tails of  $H_S$  and *SWL* respectively.

In Chapters 8–9 we examine how important these discrepancies are when considered from the design perspective, and by taking the margins to be both known and estimated, we examine the importance of marginal and dependence modelling/estimation.

Figure 7.15: Sim5: Diagnostic test for the form of the dependence in the extremes of  $H_S$ - $SWL$ . The solid line is the test statistic and the dotted line its pointwise 95% confidence interval.



Parameters	Sim1	Sim2	Sim3	Sim3*	Sim4	Sim5
$p_M$	1.00	0.99	1.00	1.00	0.85	0.90
$\rho_1$	0.24	-0.21	0.034	0.14	0.15	0.00
$\rho_2$	-	-0.78	-	-	0.70	0.76
$\mu_{21}$	-	0.0	-	-	0.9	0.5
$\mu_{22}$	-	1.2	-	-	0.8	0.3
$\sigma_{21}$	-	0.5	-	-	1.0	0.9
$\sigma_{22}$	-	0.1	-	-	1.1	0.8

Table 7.3: Parameter estimates for the mixture of bivariate normals applied to the simulated  $(H_S, SWL)$  data and for Sim3\* to  $(H_S, Surge)$ .

Figure 7.16: Correlation function,  $\rho_u$ , between  $(H_S, SWL)$  versus the threshold (in probability of non-exceedance) for the different simulated data sets.

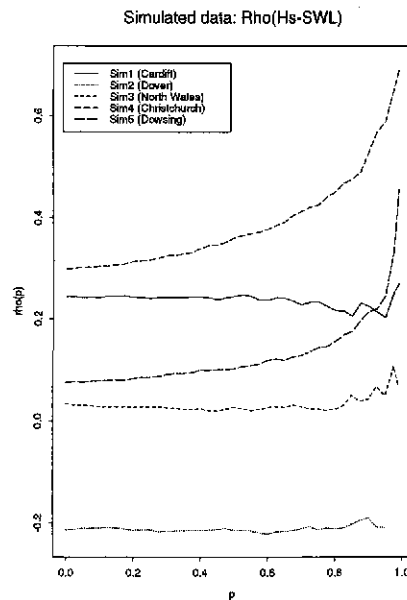


Figure 7.17: Sim3: Correlation function,  $\rho_u$ , between  $(H_S, SWL)$  and  $(H_S, Surge)$  versus the threshold (in probability of non-exceedance)

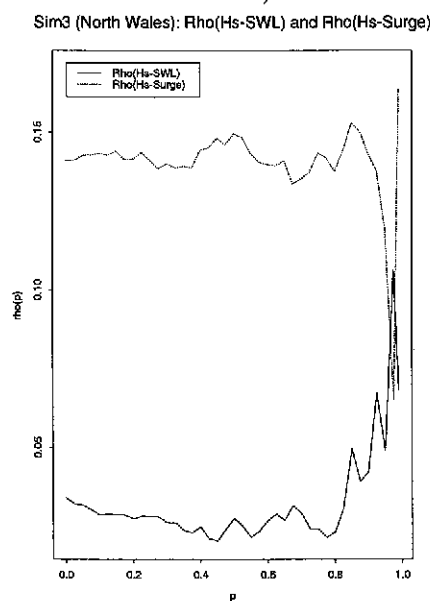


Figure 7.18: Sim4: Correlation function,  $\rho_u$ , between  $(H_S, SWL)$  versus the threshold (in probability of non-exceedance) for the fitted mixture of bivariate normals and the threshold bivariate normal

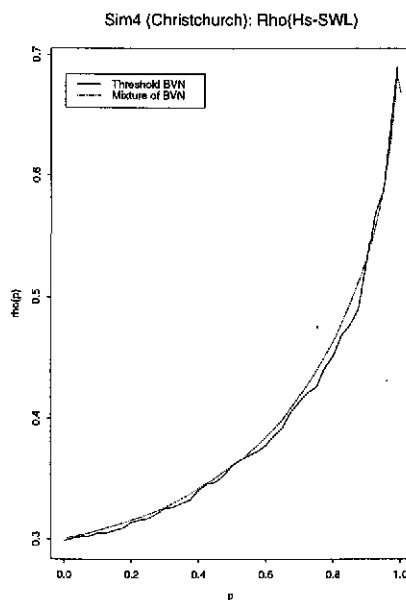


Figure 7.19: Sim5: Correlation function,  $\rho_u$ , between  $(H_S, SWL)$  versus the threshold (in probability of non-exceedance) for the fitted mixture of bivariate normals and the threshold bivariate normal

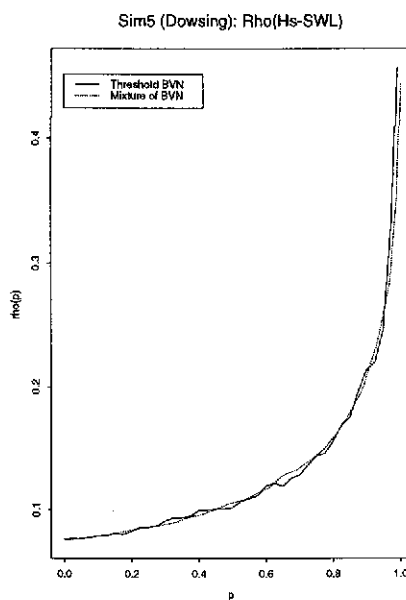


Figure 7.20: Sim1  $H_S$ - $SWL$  joint density contours: the contours of joint density value 0.01, 0.001, 0.0001, 0.00001 are shown. The estimated model is the bivariate normal model.

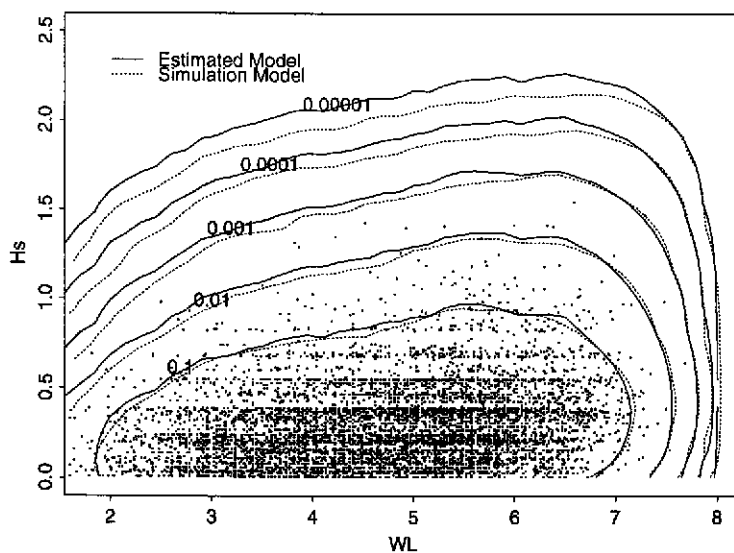


Figure 7.21: Sim2  $H_S$ - $SWL$  joint density contours: the contours of joint density value 0.01, 0.001, 0.0001, 0.00001 are shown. The estimated model is the bivariate normal model.

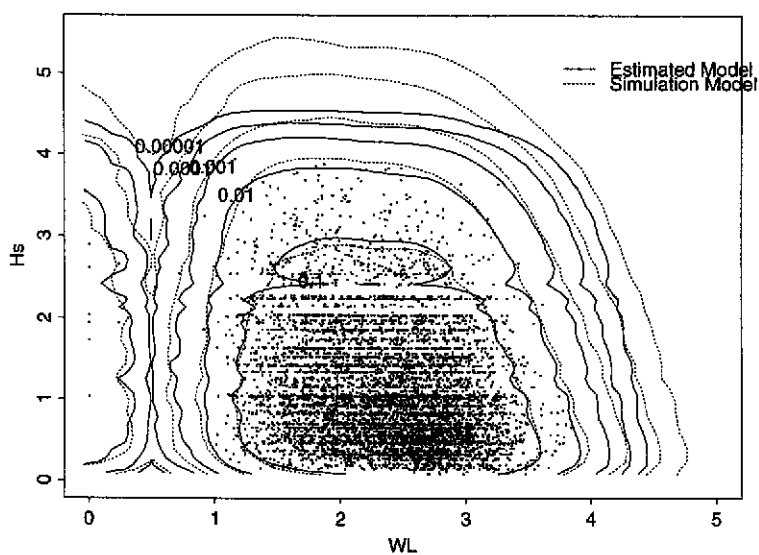


Figure 7.22: Sim3  $H_S$ -Surge joint density contours: the contours of joint density value 0.01, 0.001, 0.0001, 0.00001 are shown. The estimated model is the bivariate normal model.

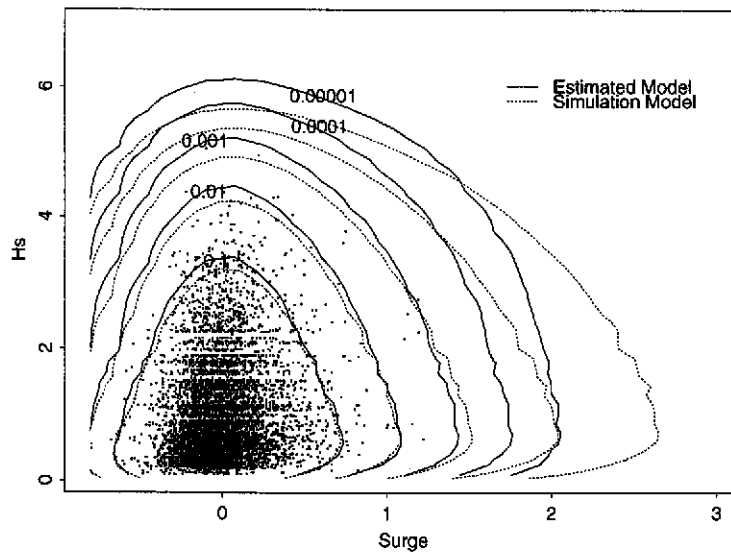


Figure 7.23: Sim3  $H_S$ - $SWL$  joint density contours: the contours of joint density value 0.01, 0.001, 0.0001, 0.00001 are shown. The estimated model is the bivariate normal model.

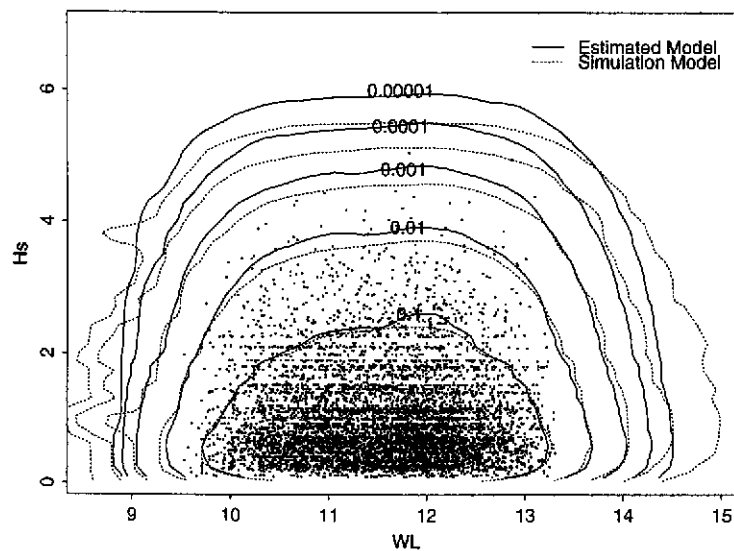


Figure 7.24: Sim4  $H_S$ - $SWL$  joint density contours: the contours of joint density value 0.01, 0.001, 0.0001, 0.00001 are shown. The estimated model is the threshold bivariate normal model.

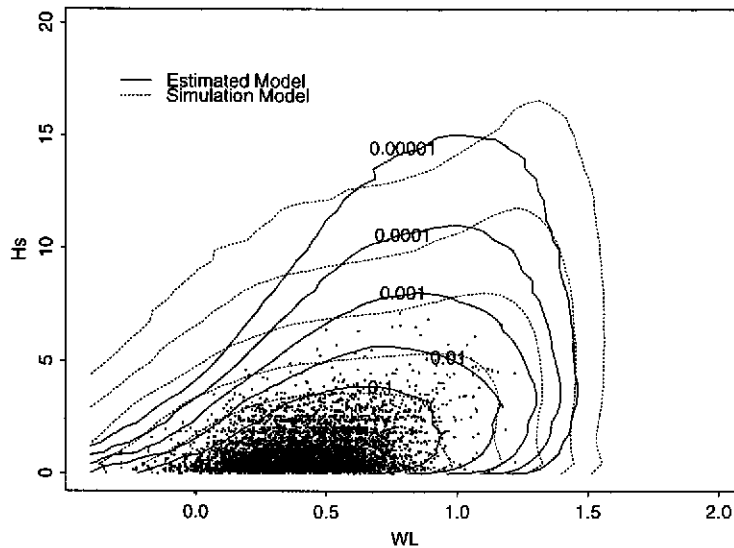


Figure 7.25: Sim4  $H_S$ - $SWL$  joint density contours: the contours of joint density value 0.01, 0.001, 0.0001, 0.00001 are shown. The estimated model is the mixture of bivariate normals model.

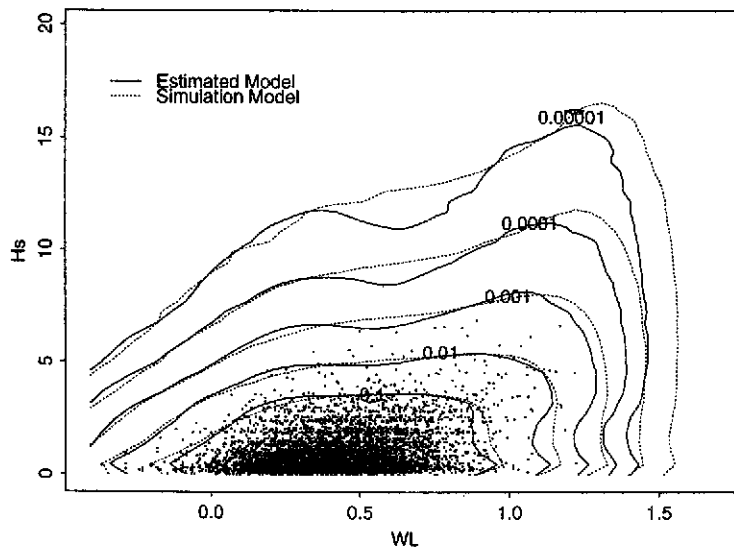


Figure 7.26: Sim5  $H_S$ - $SWL$  joint density contours: the contours of joint density value 0.01, 0.001, 0.0001, 0.00001 are shown. The estimated model is the threshold bivariate normal model.

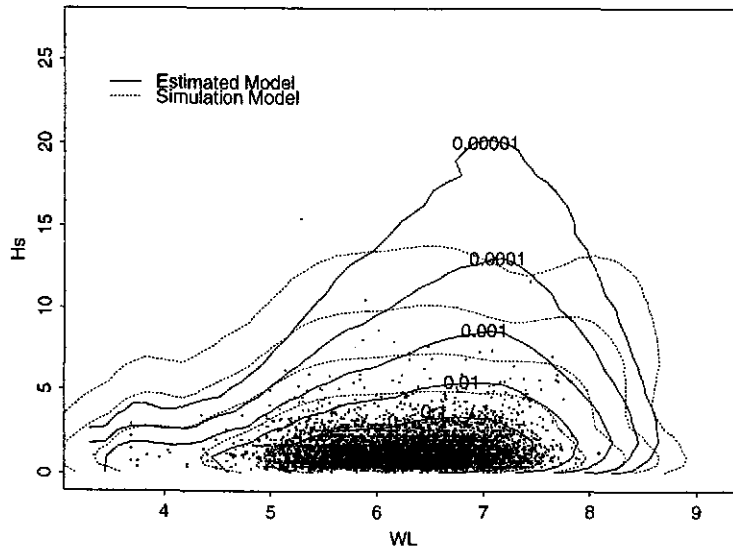
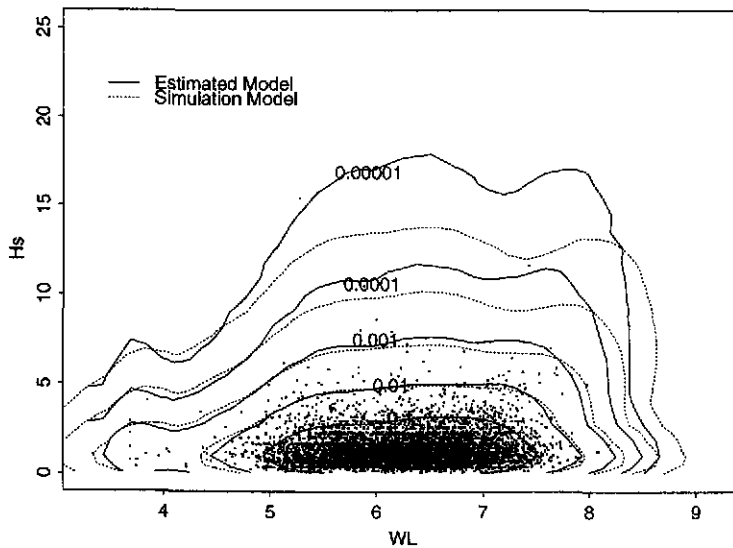


Figure 7.27: Sim5  $H_S$ - $SWL$  joint density contours: the contours of joint density value 0.01, 0.001, 0.0001, 0.00001 are shown. The estimated model is the mixture of bivariate normals model.



## 7.2 $(S, H_S)$ Dependence for Simulated Data

Scatter plots of the  $(S, H_S)$  data for the five simulated data sets are shown in Figures 7.28-7.32. From these plots we see that there is a strong positive dependence between the variables for Sim1 (Figure 7.28) and weak dependence/independence between the variables for Sim2-Sim5. This is consistent with the simulation models for these variables (see Chapter 5), for which Sim2 and Sim3 have small degrees of negative/positive dependence respectively, while Sim4 and Sim5 have independent variables.

To estimate the dependence between the variables we fit the linear regression model, given by equation (4.2.4), after transformation of each variable to a Gaussian scale, i.e.  $(S^*, H_S^*)$  with the variables defined by equations (4.2.2) and (4.2.3). First we plot the  $(S, H_S)$  data after transformation to the Gaussian scale in Figures 7.33-7.37. In the Gaussian scale (once ties in the data and modified  $H_S$  values for small  $S$  levels are accounted for) we see a clear linear relationship between the variables for Sim1 and little or no evidence of linear relationships in the other cases.

To assess what threshold level to use for  $H_S$  (or equivalently for  $H_S^*$ ) in the regression model we now consider plots of  $E(S^*|H_S^* > u)$  and  $\text{Var}(S^*|H_S^* > u)$  against the threshold  $u$  in Figures 7.38-7.42. These plots show that for

**Sim1** the rising mean shows a strong positive relationship between the variables. The variance stabilises above a threshold  $u = 0.5$ , so this level is taken for subsequent analysis.

**Sim2** the falling mean with threshold shows a weak negative relationship between the variables. The variance is stable above a threshold level of  $u = -0.5$ , so this level is used in the subsequent analysis.

**Sim3** the rising mean shows a weak positive relationship, with stability of the variance obtained above a threshold of  $u = 0.5$ .

**Sim4 and Sim5** There is no evidence of non-constant mean or variance here, indicating independence of the variables. It is therefore unnecessary to adopt a threshold.

Now we fit the linear regression threshold model to  $S^*$  given  $H_S^*$ . Estimates of the intercept,  $a$ , gradient,  $b$ , and residual variance,  $\sigma^2$ , for Sim1-Sim5 are given in Table 7.4. The estimates confirm the empirical evidence found above: highly significant dependence for Sim1, significant (but small) dependence for Sim2 – Sim4, and independence for Sim5. Sim4 is surprising as the data were generated using an independence statistical model, while the estimated dependence is non-zero but still very weak.

We now examine the quality of the fitted regression model by plotting the estimated regression function (transformed back to the original space shown in Figures 7.28-7.32), and by comparing a sample simulated from the fitted model with the original sample (shown in Figures 7.43-7.47).

- The fitted mean function is difficult to assess for Sim2-Sim5 due to the small variations in the mean relative to the high variability of the data. By contrast the mean function for Sim1 provides a very good model for the substantive variations of  $S$  on  $H_S$ .
- For Sim1 the data simulated from the fitted model reproduce the main features of the original data very well. The corresponding plots for Sim2-Sim5 are less easy to assess, but in each case the original data structure appears to be well replicated.

Data	Threshold $u$	$a$	$b$	$\sigma^2$
Sim1	0.5	0.43 (0.02)	0.67 (0.03)	0.43 (0.03)
Sim2	-0.5	0.16 (0.02)	-0.11 (0.02)	0.80 (0.06)
Sim3	0.5	-0.02 (0.03)	0.11 (0.04)	0.89 (0.12)
Sim4	$-\infty$	0.00 (0.01)	0.05 (0.01)	0.93 (0.10)
Sim5	$-\infty$	0.00 (0.01)	0.00 (0.01)	1.00 (0.10)

Table 7.4: Parameter estimates for the linear regression of  $S^*$  on  $H_S^*$  applied above a threshold  $u$  (on the Gaussian scale). Standard errors are given in parentheses. For Sim4 and Sim5 the value of  $u$  used in the regression model is  $u = 0$ .

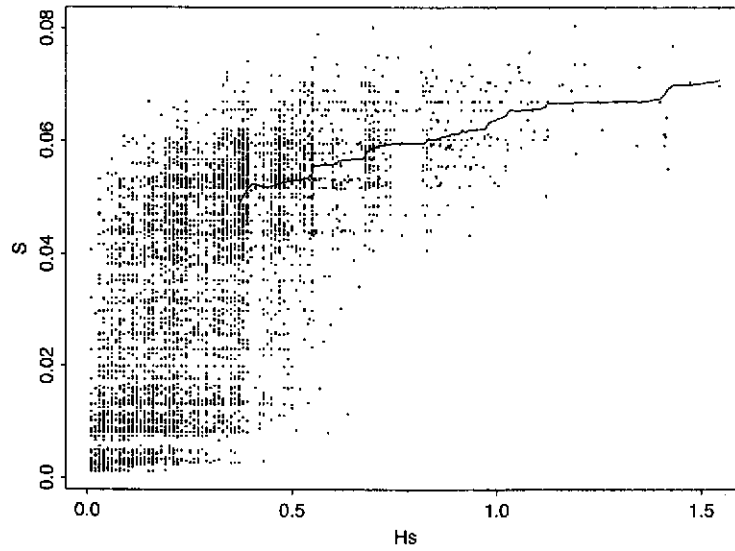
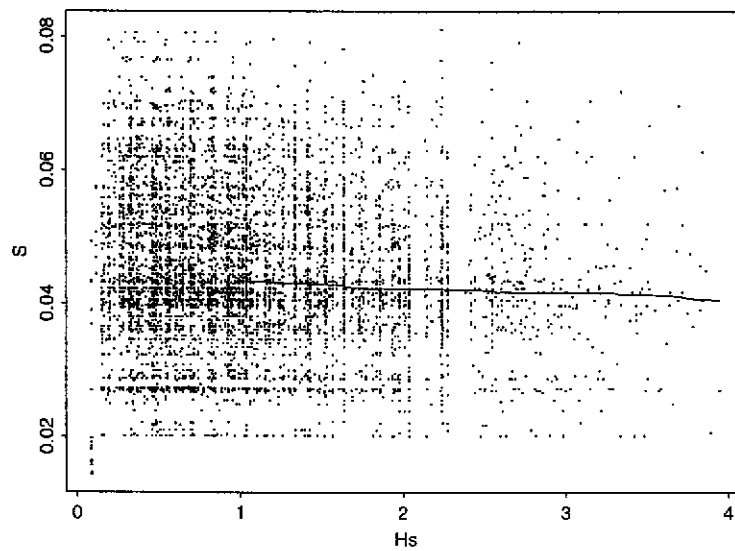
Figure 7.28: Sim1:  $S$  versus  $H_S$  and regression curve (plotted on the original scale).Figure 7.29: Sim2:  $S$  versus  $H_S$  and regression curve (plotted on the original scale).

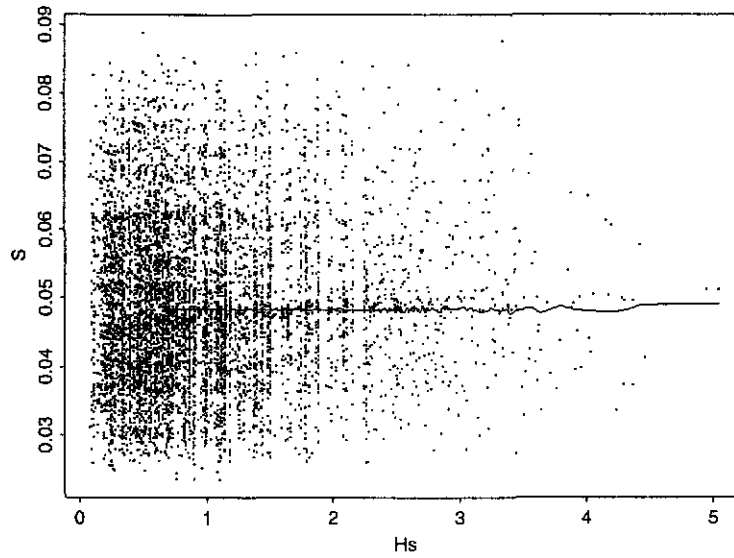
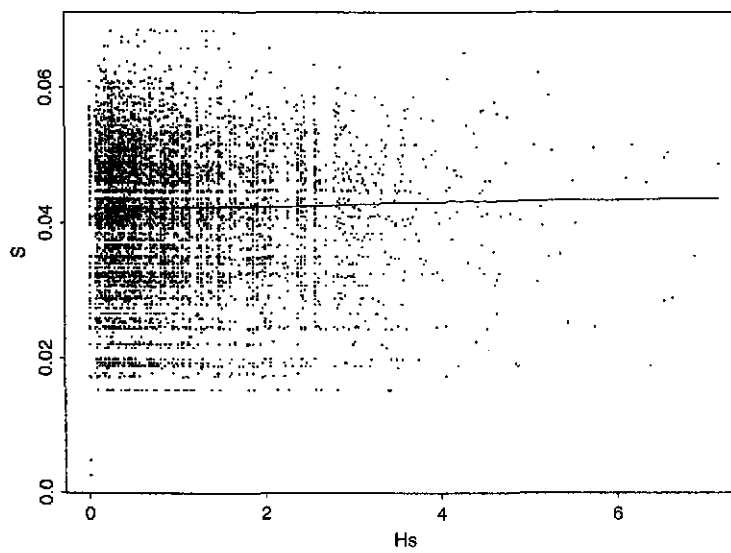
Figure 7.30: Sim3:  $S$  versus  $H_S$  and regression curve (plotted on the original scale).Figure 7.31: Sim4:  $S$  versus  $H_S$  and regression curve (plotted on the original scale).

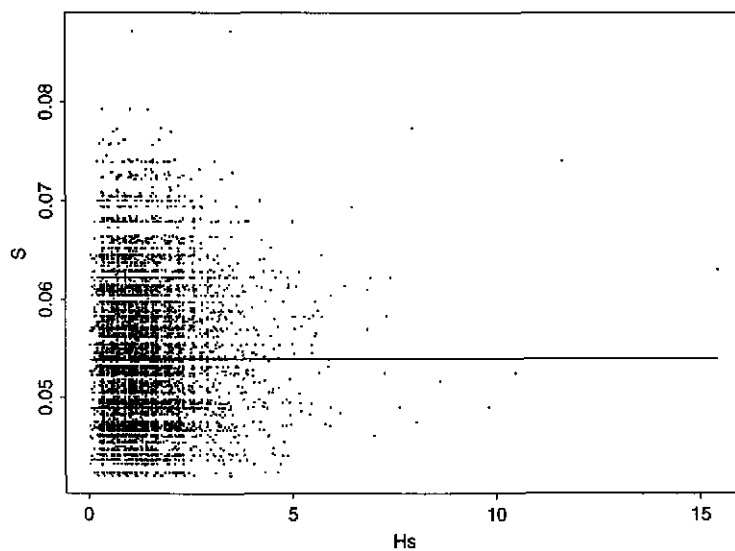
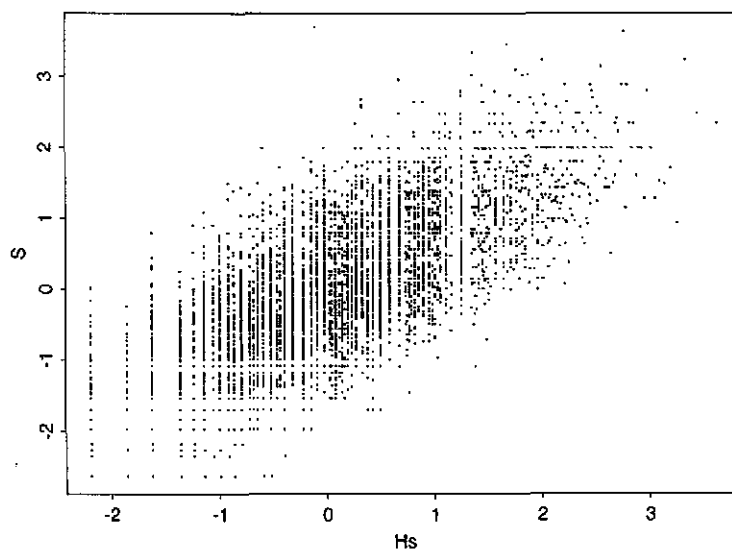
Figure 7.32: Sim5:  $S$  versus  $H_S$  and regression curve (plotted on the original scale).Figure 7.33: Sim1:  $S$  versus  $H_S$  (plotted on the Gaussian scale).

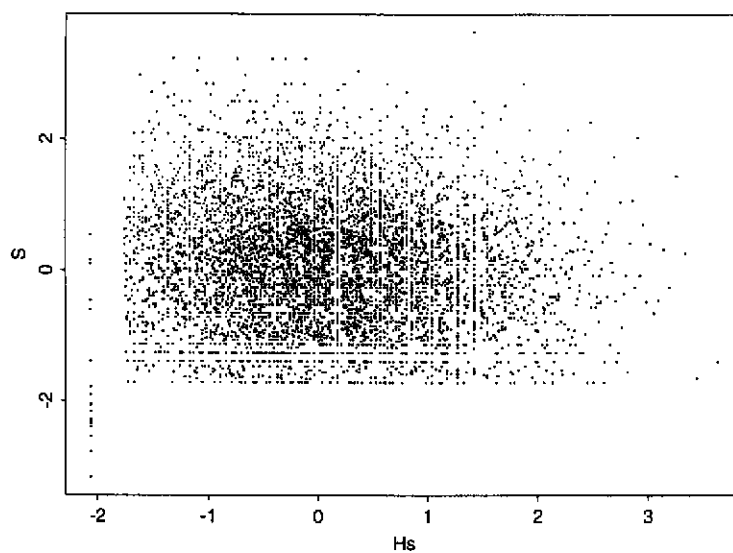
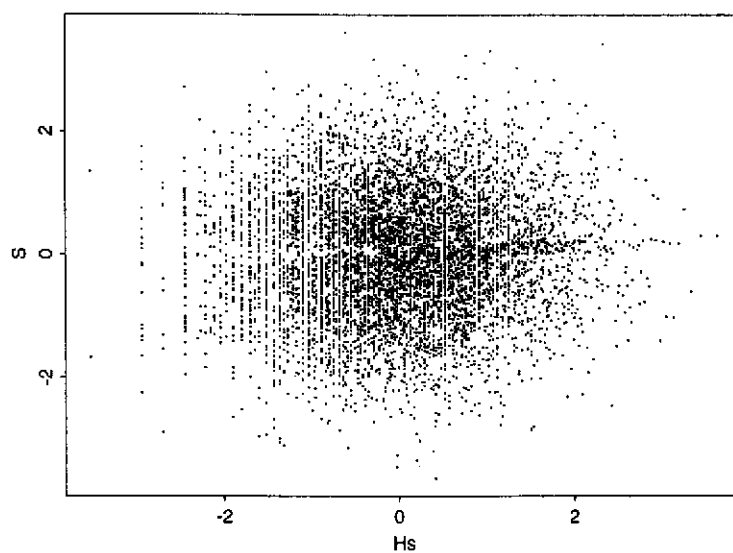
Figure 7.34: Sim2:  $S$  versus  $H_S$  (plotted on the Gaussian scale).Figure 7.35: Sim3:  $S$  versus  $H_S$  (plotted on the Gaussian scale).

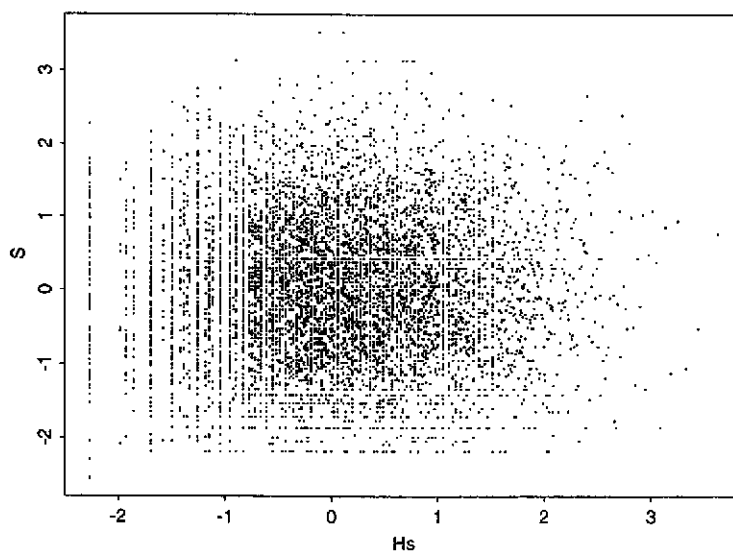
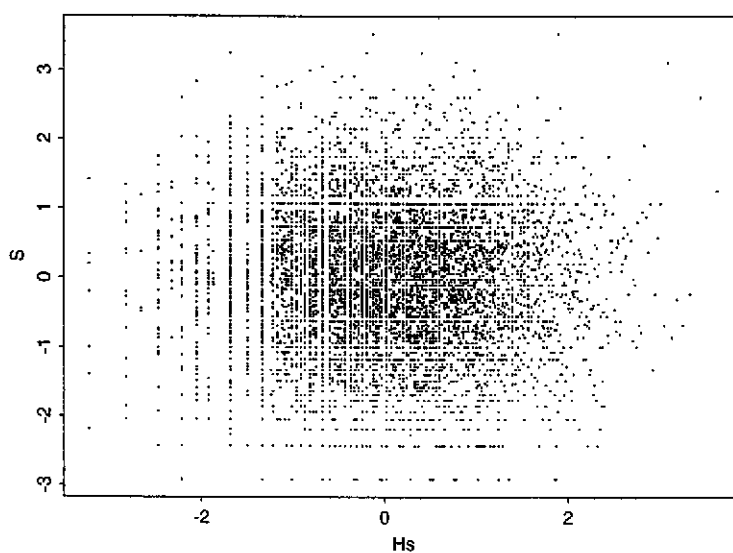
Figure 7.36: Sim4:  $S$  versus  $H_S$  (plotted on the Gaussian scale).Figure 7.37: Sim5:  $S$  versus  $H_S$  (plotted on the Gaussian scale).

Figure 7.38: Sim1: Mean and Variance of  $S$  (on the Gaussian scale) versus threshold for  $H_S$  (on the Gaussian scale). Dotted lines give 95% confidence interval.

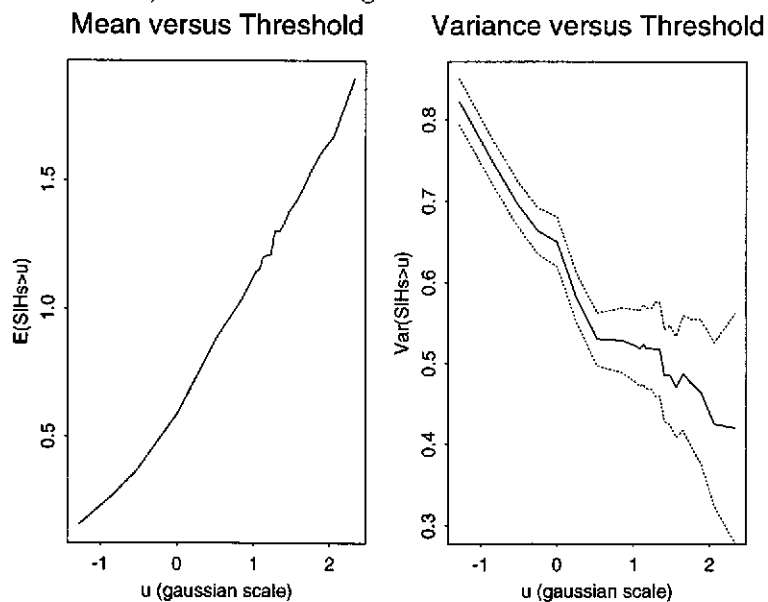


Figure 7.39: Sim2: Mean and Variance of  $S$  (plotted on the Gaussian scale) versus threshold for  $H_S$  (on the Gaussian scale). Dotted lines give 95% confidence interval.

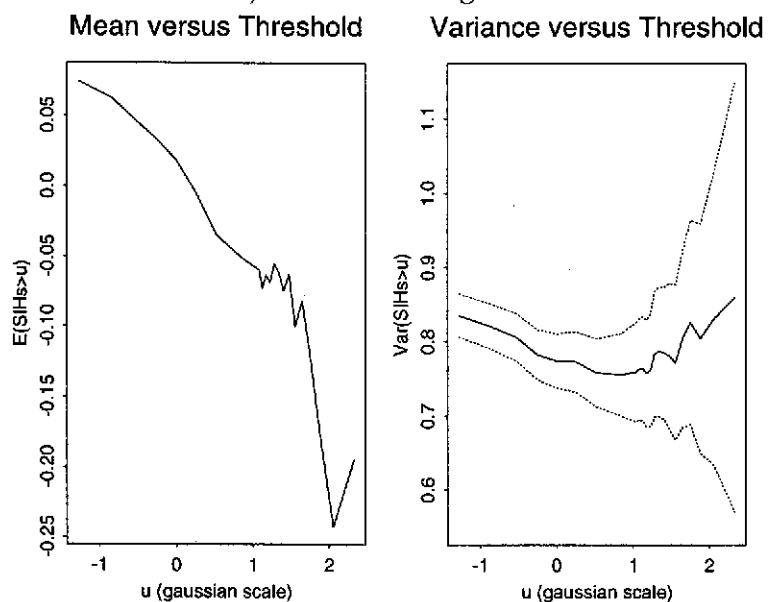


Figure 7.40: Sim3: Mean and Variance of  $S$  (plotted on the Gaussian scale) versus threshold for  $H_S$  (on the Gaussian scale). Dotted lines give 95% confidence interval.

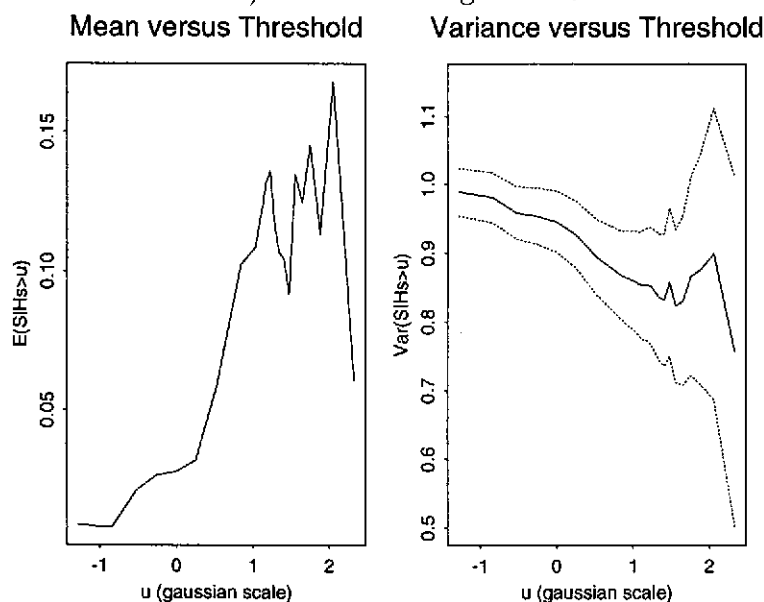


Figure 7.41: Sim4: Mean and Variance of  $S$  (plotted on the Gaussian scale) versus threshold for  $H_S$  (on the Gaussian scale). Dotted lines give 95% confidence interval.

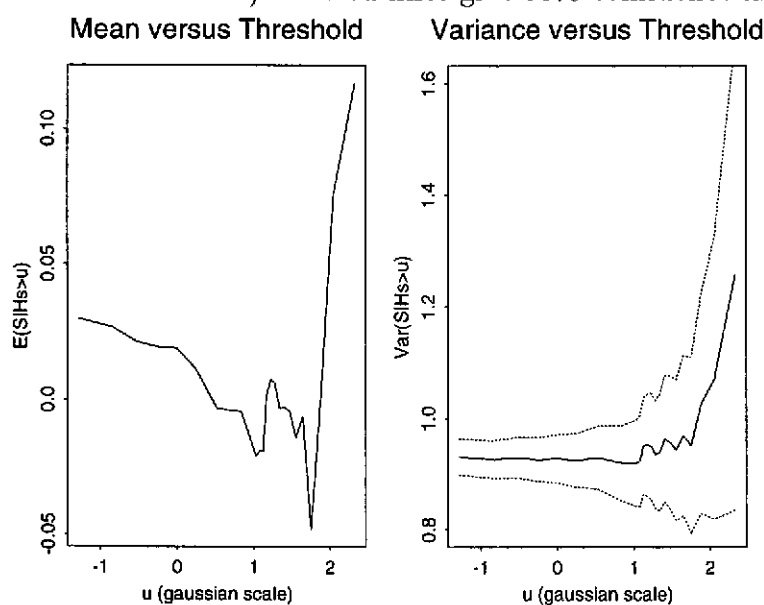


Figure 7.42: Sim5: Mean and Variance of  $S$  (plotted on the Gaussian scale) versus threshold for  $H_S$  (on the Gaussian scale). Dotted lines give 95% confidence interval.

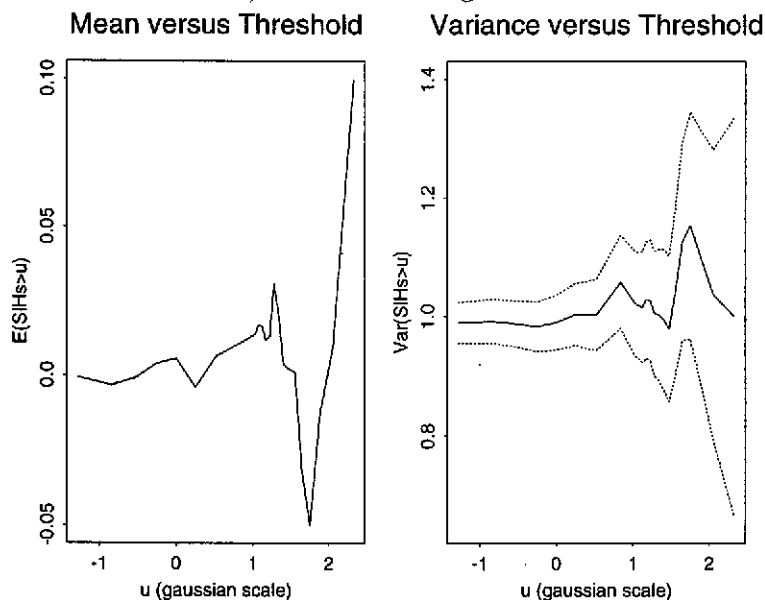


Figure 7.43: Sim1:  $S$  versus  $H_S$  for the original data and the data simulated from the fitted regression.

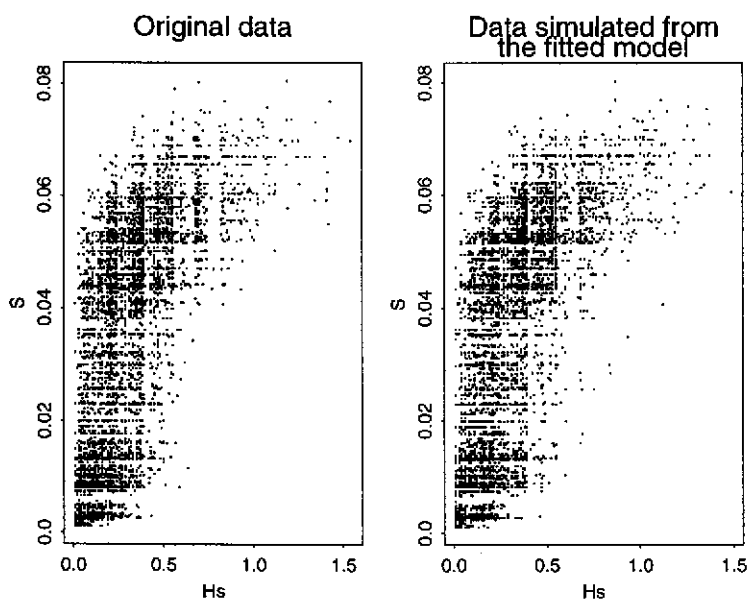


Figure 7.44: Sim2:  $S$  versus  $H_S$  for the original data and the data simulated from the fitted regression.

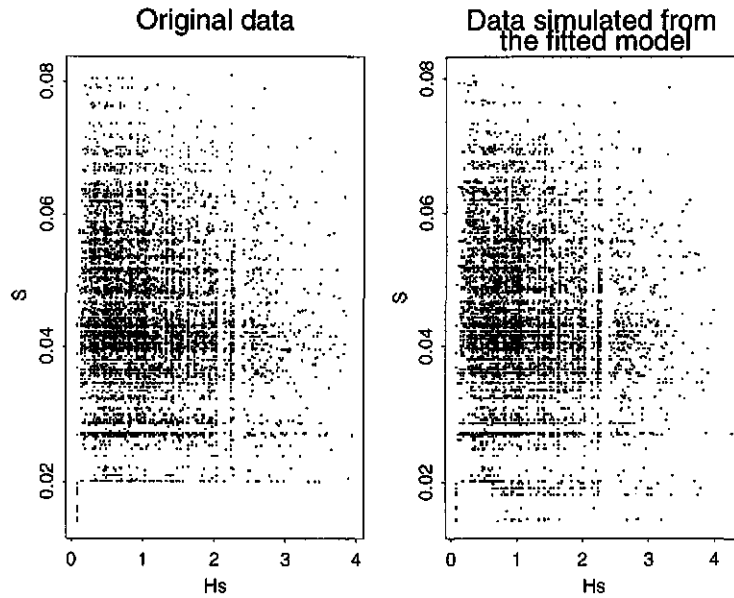


Figure 7.45: Sim3:  $S$  versus  $H_S$  for the original data and the data simulated from the fitted regression.

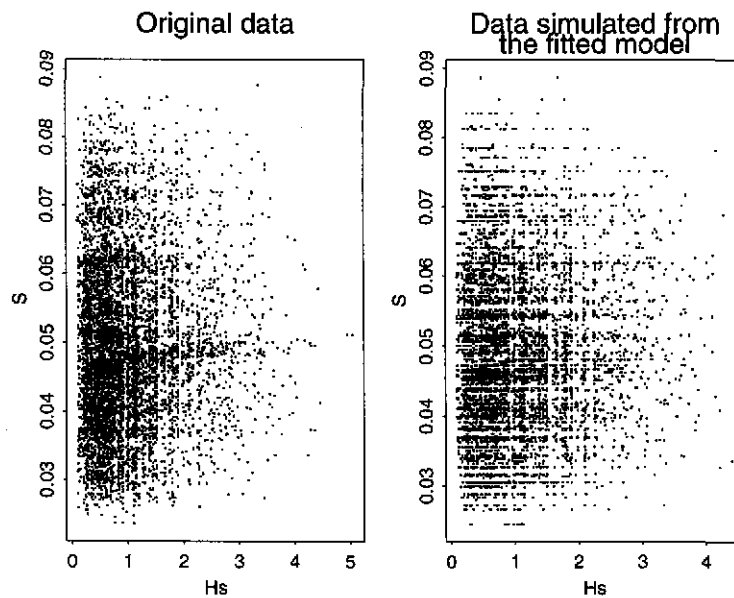


Figure 7.46: Sim4:  $S$  versus  $H_S$  for the original data and the data simulated from the fitted regression.

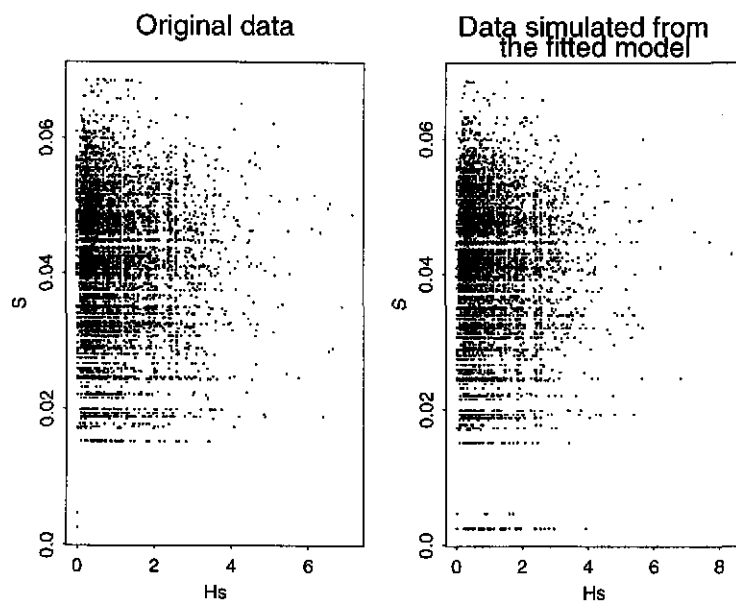
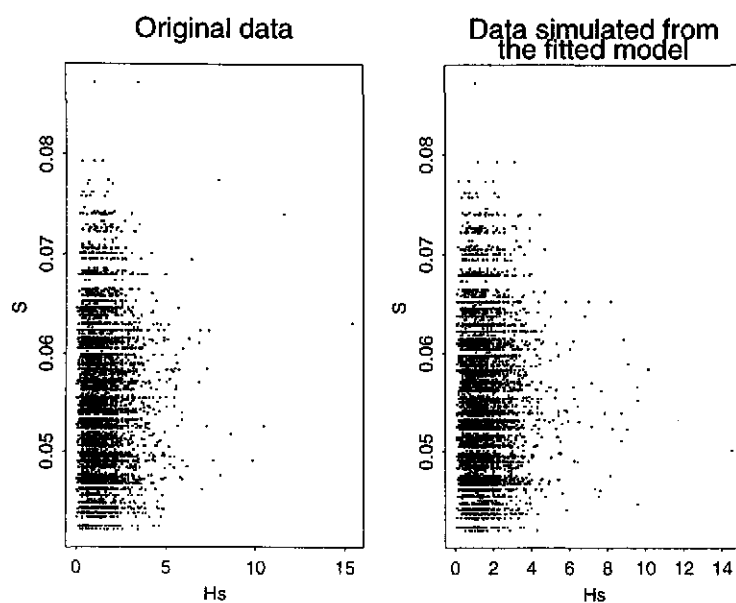


Figure 7.47: Sim5:  $S$  versus  $H_S$  for the original data and the data simulated from the fitted regression.





# Chapter 8

## Simultaneous Extremes of $(SWL, H_S)$

In this chapter we focus on the estimation of the joint probability

$$\Pr\{SWL > x, H_S > y\}.$$

Probabilities of this form, thought of as a function of  $x$  and  $y$ , are termed the *joint survivor function* of the joint distribution of  $(SWL, H_S)$ . Here we are particularly interested in finding all the possible combinations of  $(x, y)$  such that the joint survivor function is a small fixed probability, i.e. extrapolation from the sample is required. We present these combinations as curves, which correspond to contours of equal joint survivor function. These contours are the main output of the standard approach of the current implementation of JPM (see Section 1.2) and are often used for initial design calculations. The refined version of current implementation uses this information to derive the probability of failure.

In Sections 8.1 and 8.2 we present the contours of the estimated joint survivor function for Sim1-Sim5 for cases where

- both the marginal distributions are known, and
- no knowledge of the marginal distributions is accounted for,

respectively. Throughout these sections, contours are shown corresponding to 5, 10, 50, 100 and 1000 year return periods (i.e. for each point  $(x, y)$  on the associated contour curve, the probability of the event  $\{SWL > x, H_S > y\}$  is such that this event occurs on average once in the specified return period). Such contours are shown for

1. the fitted joint distribution model, and
2. the joint distribution of the actual simulation model used to generate the Sim data sets.

Before we consider the estimated joint survivor function contour plots, we outline the possible forms that these contour curves are to be expected to take. For generality, here we consider arbitrary variables  $(X, Y)$ .

### Limit values

The limits of the joint survivor function as either  $x \rightarrow -\infty$  with  $y$  fixed, or  $y \rightarrow -\infty$  with  $x$  fixed, are important special cases as

$$\begin{aligned}\lim_{x \rightarrow -\infty} \Pr\{X > x, Y > y\} &= \Pr\{Y > y\} \\ \lim_{y \rightarrow -\infty} \Pr\{X > x, Y > y\} &= \Pr\{X > x\},\end{aligned}$$

i.e. the limit values are the marginal exceedance probabilities.

### Complete positive dependence

When the variables follow complete positive dependence, the joint survivor function simplifies as

$$\Pr\{X > x, Y > y\} = \min(\Pr\{X > x\}, \Pr\{Y > y\}).$$

In addition, if  $X$  and  $Y$  have the same marginal distribution, i.e.  $\Pr\{X > x\} = \Pr\{Y > x\}$  for all  $x$ , then  $X = Y$  always.

### Independence

When the variables are independent, the joint survivor function simplifies as

$$\Pr\{X > x, Y > y\} = \Pr\{X > x\} \Pr\{Y > y\}.$$

These three features are helpful in assessing the contour curves of the joint survivor function as:

- limit values give marginal return level/return period combinations;
- for complete positive dependence, the  $T$  year contour consists of the values of  $(x, y)$  which give

$$\min(\Pr\{X > x\}, \Pr\{Y > y\}) = \frac{1}{N_{obs}T},$$

where  $N_{obs}$  is the number of observations per year. Defining  $x_T$  and  $y_T$  by

$$\Pr\{X > x_T\} = \Pr\{Y > y_T\} = \frac{1}{N_{obs}T},$$

i.e. they are the marginal  $T$  year return levels for the two variables, we have that the contour takes the form:

$$\{(x, y) : y = y_T \text{ for } x < x_T, \text{ and } x = x_T \text{ for } y < y_T\}.$$

This is just two perpendicular lines at the marginal  $T$  year return levels for  $X$  and  $Y$ . For practical purposes, it is sufficient to consider only the intersection point for these two lines, i.e.  $(x_T, y_T)$ .

- for independence the contour of equal joint survivor function is simple to obtain. It is not possible to give a general description of the form of contour shape as it is influenced by the form of the marginal distributions of the variables.

## 8.1 Marginal distributions known

In this section we treat the marginal distributions as known. The situation is not unrealistic as often we are able to incorporate additional knowledge about the marginal variables into the JPM. A consequence of including this extra information is that, in this section, the only unknown feature of the joint distribution of the sea condition variables is the dependence structure. This allows a better comparison of our proposed dependence models with the current methods.

We incorporate the extra information through use of the joint density  $f_{\mathbf{X}}$  using the

1. known marginal distribution for each element of  $\mathbf{X}$ ,
2. estimated dependence structure (i.e. as estimated in Chapter 7).

This joint density estimate is modified from the full fitted form to have the same marginal densities as those used to simulate the data. From this estimated joint density the associated joint survivor function,  $\Pr\{SWL > x, H_S > y\}$  is evaluated by integration over the region  $\{SWL > x, H_S > y\}$ .

In practice, had contours of the joint survivor function already been estimated before incorporating the knowledge of the marginal distribution then the modification to the joint survivor function contours is simply obtained by re-calibrating the marginal scales of the previous estimate. For example, changing the 100 year marginal return level from the estimated value to the known value. Consequently, estimated contours of equal joint survivor function should agree exactly with the contours from the simulation model at the limits ( $x \rightarrow -\infty$  and also  $y \rightarrow -\infty$ ) of the curves.

Unfortunately, in this study some inconsistency arose in the evaluation of these known marginals so that the values used in the current implementation were slightly incorrect in

a few cases. The reason for this was a change in the handling of small wave heights which the removal of resulted in extra observations being generated in some cases (lengthening the tail of  $H_S$ ). Nevertheless this error does not substantially detract from the inter-comparisons.

Figures 8.1-8.8 show contours of equal joint survivor function estimates from the fitted model and derived from the simulation model. Any significant discrepancy between the two sets of contours would show that either

1. the statistical estimation, using the correct dependence model, is poor, or
2. the fitted families of dependence models are not sufficiently general to fit these data well.

We discuss the fits for each data set in turn before drawing general conclusions.

**Sim1** The two sets of curves, shown in Figure 8.1, exhibit excellent agreement.

**Sim2** The two sets of curves, shown in Figure 8.2, also exhibit an excellent agreement.

**Sim3** Here we have plots for  $(Surge, H_S)$  and  $(SWL, H_S)$  in Figures 8.3 and 8.4 respectively. The contours again seem well reproduced by the fitted model. Some discrepancies occur for  $(SWL, H_S)$ , due primarily to the fact that as we have not modified the  $SWL$  marginal distribution to follow the simulation model (which is complex as it arises from the combination of independent tide and surge).

**Sim4** Here we have plots for two different fitted dependence structures: in Figure 8.5 the threshold bivariate normal model is used, in Figure 8.6 the mixture of bivariate normals model is considered. In both cases the fitted statistical dependence models under-estimate the contour curves. For the threshold model the contours are further from the contours given by the simulation model than for the mixture of bivariate normals model. This is particularly obvious at the more extreme contours. For these data the diagnostic plots suggested the variables could reasonably be taken as completely dependent. From Figures 8.5 and 8.6 we see that a very close agreement with the simulation model is given by perpendicular lines – corresponding to complete dependence, and that complete dependence is a better model than either of the fitted models.

**Sim5** Here we have the same two figures as given for Sim4. We see that the threshold model averages the two forms of dependence that occur in the simulation model, the compromise leading to a poor fit (see Figure 8.7). In contrast, the mixture of bivariate normals gives an excellent fit. Note that here, although the dependence

is strong, taking the variables to be completely dependent would be a substantial over-estimate.

Once the marginal features have been corrected for, the main source of error in estimating contours of equal joint survivor function arises from not having a sufficiently flexible parametric dependence model. The bivariate normal (and threshold fitted version) were fine for Sim1-Sim3 when this was the correct family of dependence structures, but were poor for both Sim4 and Sim5. On the other hand, the mixture of two bivariate normals (which includes the bivariate normal as a special case) gives good fits in Sim4, when it is not the correct form, as well as for Sim5, when it is the correct family. Note also that differences that have been observed between the contours of the estimated and simulation models occurred for combinations  $(x, y)$  where  $x > \max SWL$  and  $y > \max H_S$ , and so were due to long range joint extrapolations.

Figure 8.1: Sim1:  $H_S$ - $SWL$  curves of equal joint survivor probability expressed in return periods (in years) when the marginal distributions are known

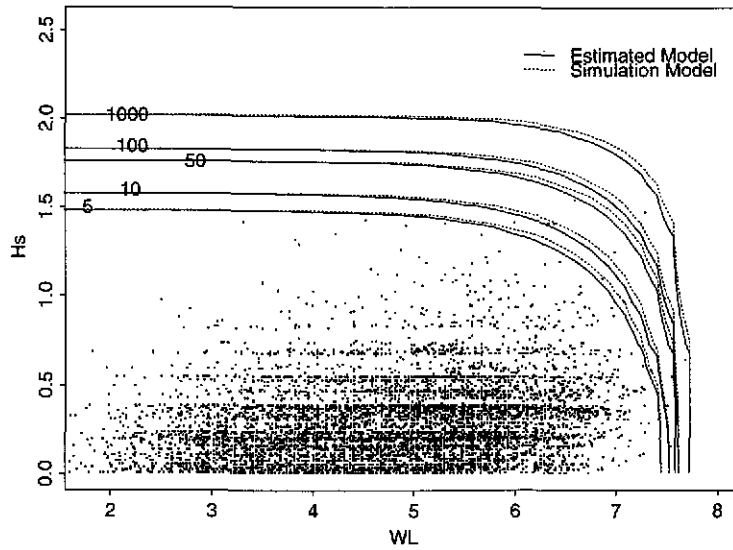


Figure 8.2: Sim2:  $H_S$ - $SWL$  curves of equal joint survivor probability expressed in return periods (in years) when the marginal distributions are known

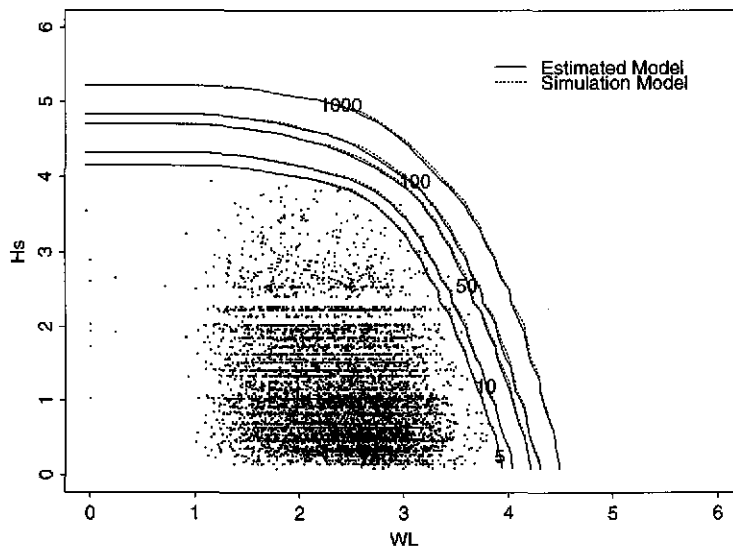


Figure 8.3: Sim3:  $H_S$ -Surge curves of equal joint survivor probability expressed in return periods (in years) when the marginal distributions are known

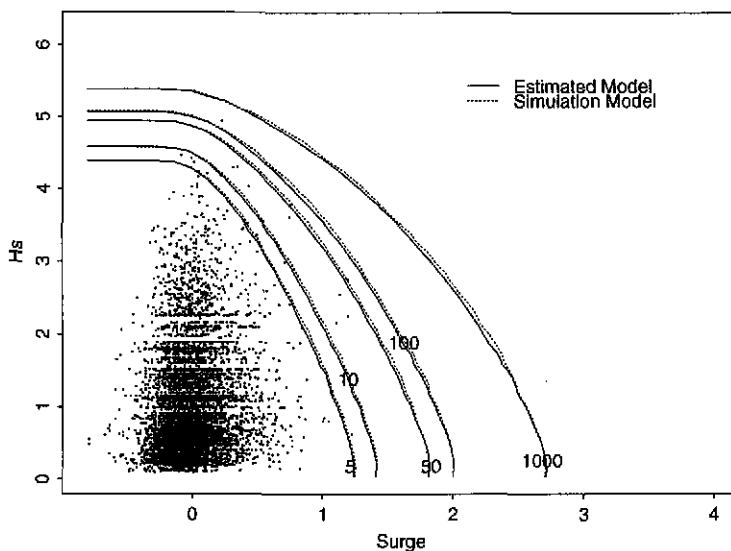


Figure 8.4: Sim3:  $H_S$ -SWL curves of equal joint survivor probability expressed in return periods (in years) when the marginal distributions are known

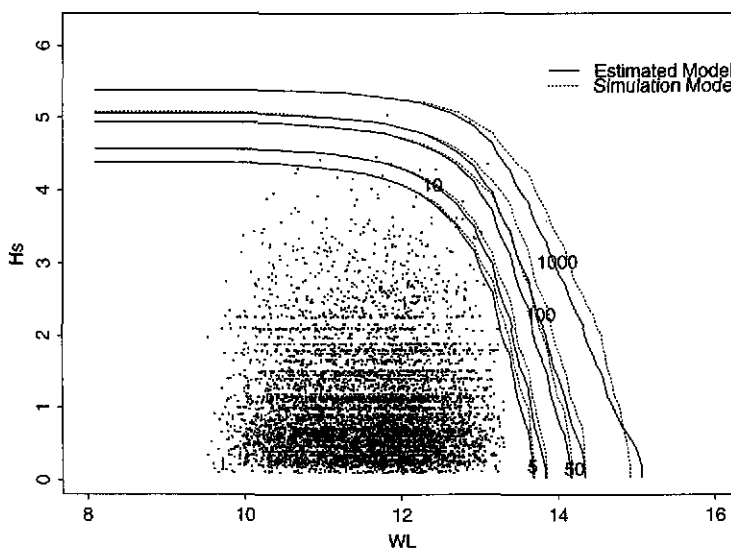


Figure 8.5: Sim4:  $H_S$ - $SWL$  curves of equal joint survivor probability expressed in return periods (in years) when the marginal distributions are known. Here the dependence model is the fitted bivariate normal threshold model

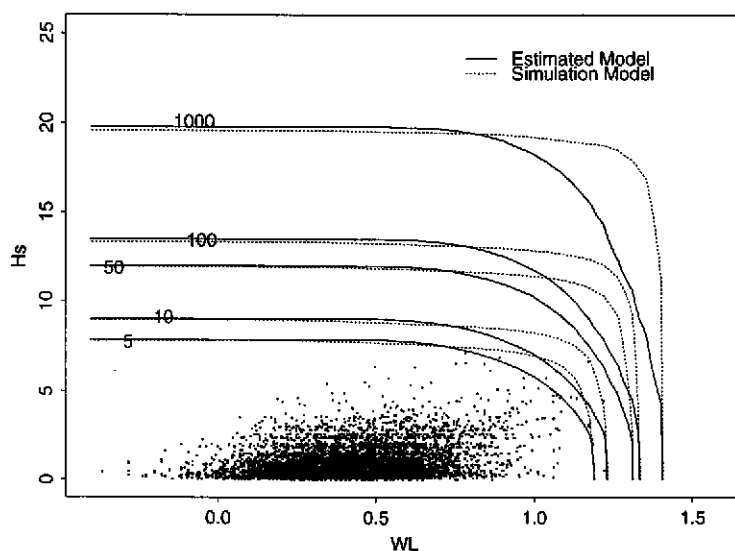


Figure 8.6: Sim4:  $H_S$ - $SWL$  curves of equal joint survivor probability expressed in return periods (in years) when the marginal distributions are known. Here the dependence model is the fitted mixture of bivariate normals model

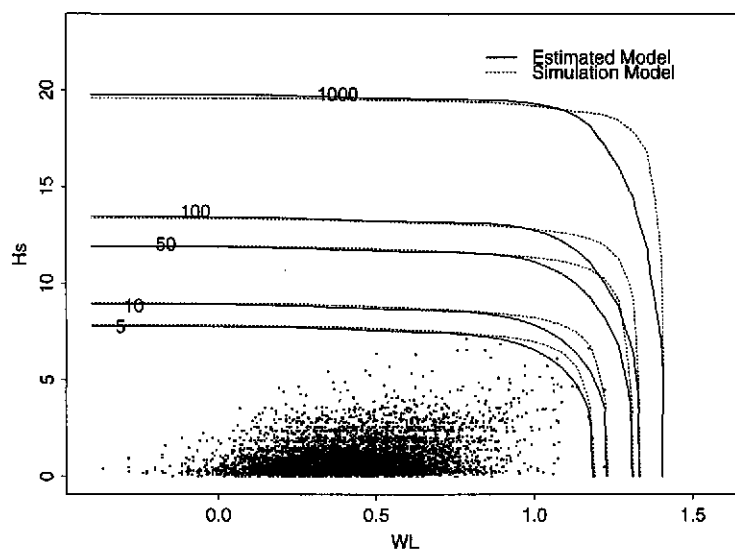


Figure 8.7: Sim5:  $H_S$ - $SWL$  curves of equal joint survivor probability expressed in return periods (in years) when the marginal distributions are known. Here the dependence model is the fitted bivariate normal threshold model

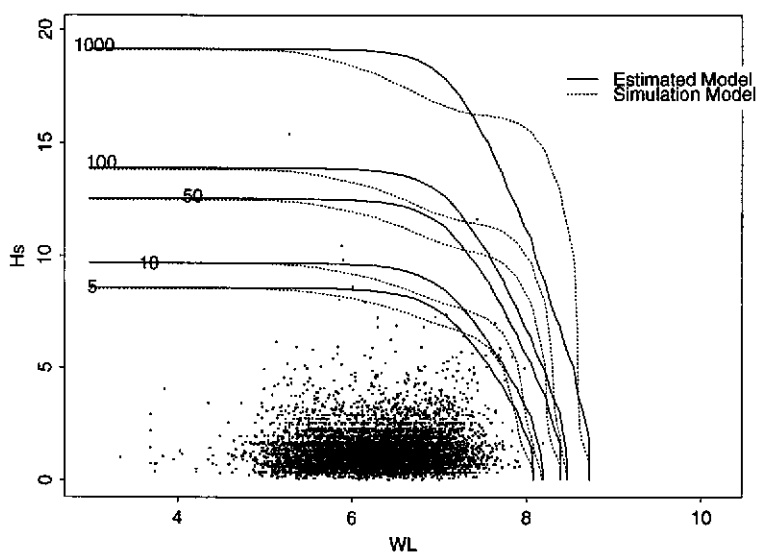
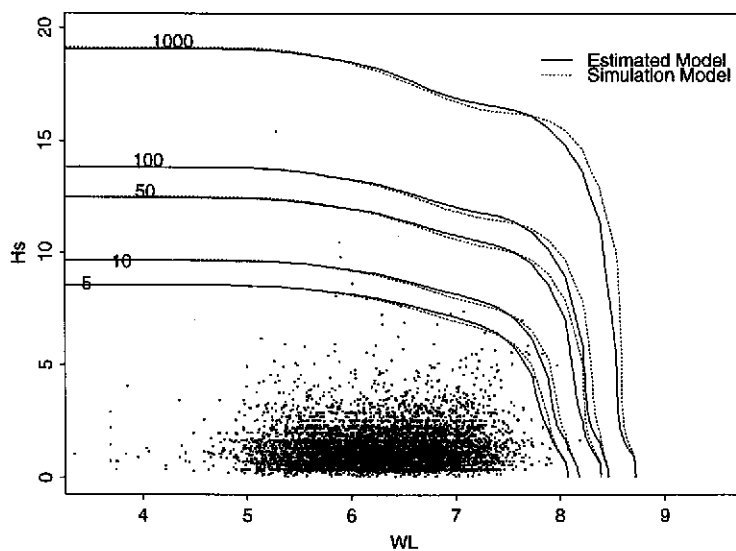


Figure 8.8: Sim5:  $H_S$ - $SWL$  curves of equal joint survivor probability expressed in return periods (in years) when the marginal distributions are known. Here the dependence model is the fitted mixture of bivariate normals model



### 8.1.1 Comparison with current implementation

HR have modified their estimates of the joint survivor function contours to incorporate the extra marginal knowledge by manual modification of the marginal scales. Results have been given for return periods of 1, 10, 100 and 1000 years. For comparison with the plots in Figures 8.1-8.8, we show only the 10 and 1000 year contour values; these are tabulated in Tables 8.1-8.5 and given in Figures 8.9-8.12.

The comparison with the simulation model values and the fitted model are given below:

**Sim1** Comparison is not directly possible here as HR have separately estimated the joint survivor function for waves from two direction sectors. For direction sector  $0^\circ \leq \theta \leq 110^\circ$ , the 10 year and 1000 year contours lie just above the respective contours for the simulation model, whereas for direction sector  $110^\circ < \theta < 360^\circ$  they lie much below. As the first sector is slightly more likely, and the one most likely to produce the extreme combinations, this provides a good estimate.

**Sim2** The HR contour estimates agree very well with the simulation and fitted model contours.

**Sim3** The HR contours significantly over-estimate the ( $SWL, H_S$ ) contours as given by both the simulation and fitted model. Some element of this over-estimation is due to the inconsistency in the known marginal distributions for  $H_S$ , with the same marginal being used for the simulation and fitted models but slightly larger values provided to HR for use.

**Sim4** The HR contours seem poor in this case. The strong form of dependence in the simulated data has not been captured, and the contours have been badly underestimated. For the 1000 year contour, it is worrying that the error is so large in the HR estimated contour within the range of the  $SWL$  data. Specifically, the contour decreases rapidly in the  $H_S$  value. This feature was not observed in either of the statistically fitted models, or for the other four Sim data analyses.

**Sim5** The HR estimated contours appear to be good for low return periods but significantly under-estimate for high return periods.

In two cases the HR implementation of current methods has produced a good estimate of the dependence structure of extreme  $SWL$  and  $H_S$  combinations. In three other cases the estimates are poor, one in which there is a slight over-estimation (which would lead to conservative design), and two cases of substantial under-estimation (leading to under-design).

Figure 8.9: Sim2:  $H_S$ - $SWL$  curves of equal joint survivor probability expressed in return periods (in years) when the marginal distributions are known. Curves shown are 10 and 1000 year return period for Estimated model, Simulation model and HR estimates

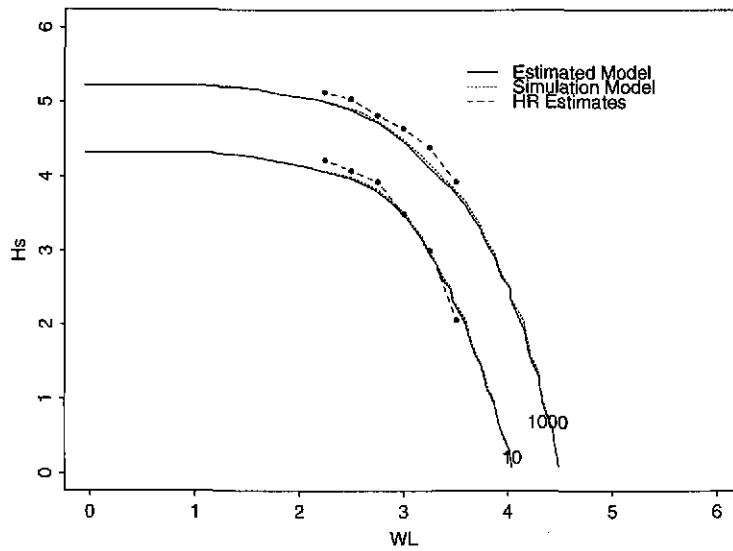


Figure 8.10: Sim3:  $H_S$ - $SWL$  curves of equal joint survivor probability expressed in return periods (in years) when the marginal distributions are known. Curves shown are 10 and 1000 year return period for Estimated model, Simulation model and HR estimates

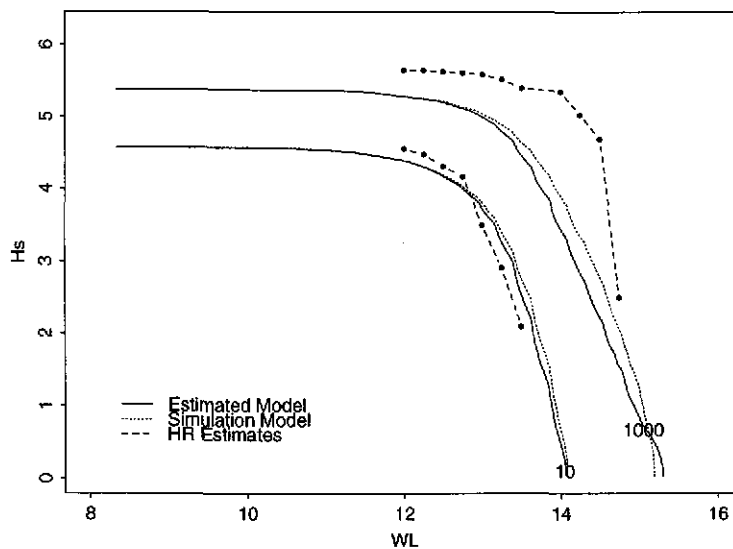


Figure 8.11: Sim4:  $H_S$ - $SWL$  curves of equal joint survivor probability expressed in return periods (in years) when the marginal distributions are known. Curves shown are 10 and 1000 year return period for Estimated model (Mixture Model), Simulation model and HR estimates

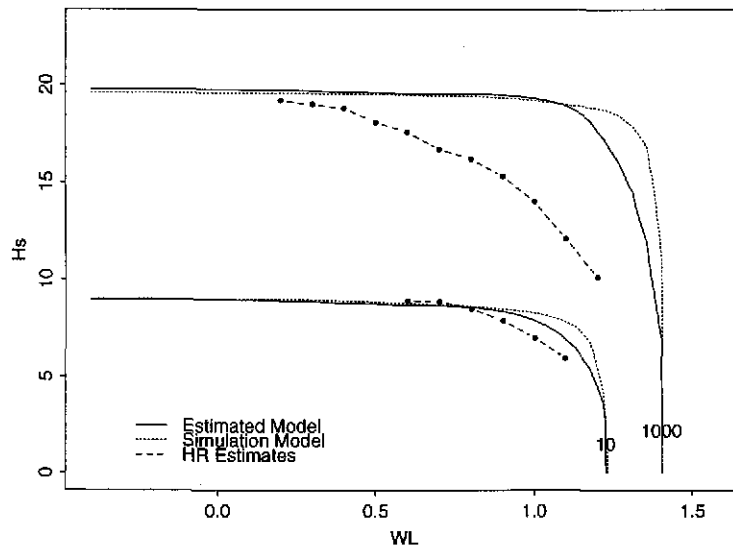
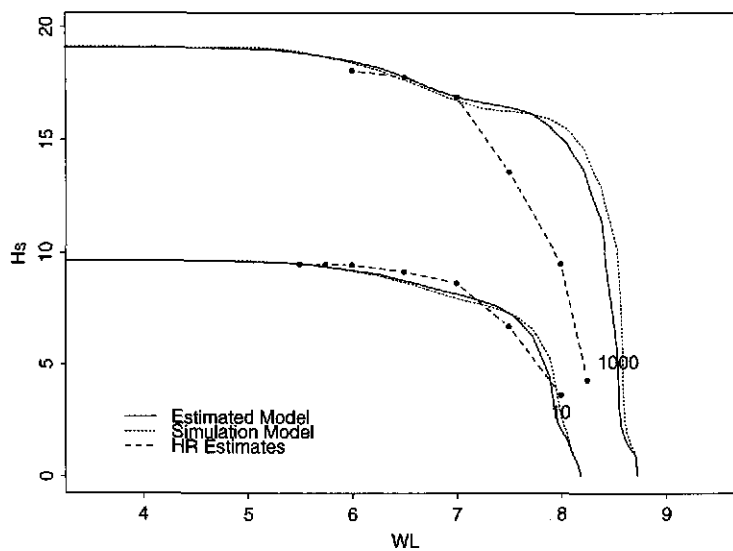


Figure 8.12: Sim5:  $H_S$ - $SWL$  curves of equal joint survivor probability expressed in return periods (in years) when the marginal distributions are known. Curves shown are 10 and 1000 year return period for Estimated model (Mixture Model), Simulation model and HR estimates



$SWL$	10 year $H_S$		1000 year $H_S$	
	$(0^\circ \leq \theta \leq 110^\circ)$	$(110^\circ < \theta \leq 360^\circ)$	$(0^\circ \leq \theta \leq 110^\circ)$	$(110^\circ < \theta < 360^\circ)$
6.00	–	1.11	–	1.49
6.25	1.52	1.08	2.04	1.46
6.50	1.43	1.01	2.02	1.43
6.75	1.32	0.95	2.00	1.41
7.00	1.16	0.86	1.94	1.37
7.25	0.94	0.67	1.82	1.28
7.50	–	–	1.48	1.09

Table 8.1: HR estimates of points on the 10 and 1000 year contours of the joint survivor function of  $(SWL, H_S)$  for Sim1: separate estimates conditional on the wave direction,  $\theta$ , satisfying  $0^\circ \leq \theta \leq 110^\circ$  and  $110^\circ < \theta < 360^\circ$ .

$SWL$	10 year $H_S$	1000 year $H_S$
2.25	4.22	5.13
2.50	4.08	5.04
2.75	3.93	4.83
3.00	3.50	4.65
3.25	3.00	4.39
3.50	2.06	3.93
3.75	–	3.15
4.00	–	2.45

Table 8.2: HR estimates of points on the 10 and 1000 year contours of the joint survivor function of  $(SWL, H_S)$  for Sim2, when the marginal distributions are known.

$SWL$	10 year $H_S$	1000 year $H_S$
12.00	4.56	5.65
12.25	4.48	5.65
12.50	4.31	5.63
12.75	4.17	5.61
13.00	3.50	5.59
13.25	2.91	5.52
13.50	2.10	5.40
14.00	–	5.35
14.25	–	5.03
14.50	–	4.69
14.75	–	2.50

Table 8.3: HR estimates of points on the 10 and 1000 year contours of the joint survivor function of  $(SWL, H_S)$  for Sim3, when the marginal distributions are known.

$SWL$	10 year $H_S$	1000 year $H_S$
0.2	–	19.2
0.3	–	19.0
0.4	–	18.8
0.5	–	18.1
0.6	8.90	17.6
0.7	8.85	16.7
0.8	8.47	16.2
0.9	7.86	15.3
1.0	6.98	14.0
1.1	5.92	12.1
1.2	–	10.1

Table 8.4: HR estimates of points on the 10 and 1000 year contours of the joint survivor function of  $(SWL, H_S)$  for Sim4, when the marginal distributions are known.

$SWL$	10 year $H_S$	1000 year $H_S$
5.50	9.51	–
5.75	9.50	–
6.00	9.48	18.1
6.50	9.18	17.8
7.00	8.66	16.9
7.50	6.68	13.6
8.00	3.60	9.5
8.25	–	4.3

Table 8.5: HR estimates of points on the 10 and 1000 year contours of the joint survivor function of  $(SWL, H_S)$  for Sim5, when the marginal distributions are known.

## 8.2 Marginal distributions unknown

Figures 8.13-8.20 show contours of equal joint survivor function from the fitted model and derived from the simulation model. If the statistical model we have used to describe the sea conditions fits well then these contours should be in good agreement. Discrepancies between the two sets of contours show that at least one aspect of the statistical estimate is poor. Possible sources of inadequacies of the fit are:

1. Poor marginal fits: the statistical family is correct each time (except for Sim3  $SWL$ ), but a poor fit results from a poor fit of the GPD to the upper tail (details of these fits are discussed in Chapter 6).
2. Poor dependence structure fits: the statistical family of fitted dependence models is not always that from which the data were simulated, but even when it is, the estimated parameters may be poor. This feature was studied in isolation in Section 8.1 where the marginal distributions were treated as known, but contributes here when the marginal distributions are also unknown.

We discuss the fits for each data set in turn before drawing general conclusions.

**Sim1** The two sets of curves (shown in Figure 8.13) exhibit good agreement. The only obvious small difference is in the extrapolation of the  $H_S$  variable, with the fitted model over-estimating marginal return levels.

**Sim2** The two sets of curves (shown in Figure 8.14) exhibit moderate agreement. The most obvious differences stem from poor marginal estimates (for each variable the

fitted model under-estimates return levels). The basic shape of the contour curves seems reasonable, corresponding to the good fit of the dependence structure found in Section 8.1. For these data the fitted model is from the same dependence model family as used to generate the data.

**Sim3** Here we have plots for  $(Surge, H_S)$  and  $(SWL, H_S)$  in Figures 8.15 and 8.16 respectively. The basic shape of the contours again seems fine, following from the good estimation of dependence in Section 8.1, but the return levels for *Surge* and *SWL* are under-estimated, whereas the  $H_S$  return levels are over-estimated.

**Sim4** Here we have plots for the two different fitted dependence structures: in Figure 8.17 the bivariate normal threshold model is used, whereas in Figure 8.18 the mixture of bivariate normals model is considered. In each case the same marginal distribution fits are used, so differences between these figures are due to differences in the fitted dependence structure. In Section 8.1 we found that the mixture model fitted much the better. That is still apparent here despite the marginal return levels being under-estimated for each margin (most notably for  $H_S$  which has the contrived longer tail here). The dependence features are best considered by comparing the shape of the contour curves in the region of greatest curvature. Most notable is that in Figure 8.17 this part of the curve is further from the true form derived from the simulation model than in Figure 8.18. This is particularly obvious at the most extreme contours. The general shape of the contour of the fitted model in Figure 8.18 seems to represent the dependence well (recall that the simulation model here had a stronger form of dependence in the extreme values than any of the models we are fitting).

**Sim5** Here we have the same two figures as given for Sim4. The most striking feature of these figures is the very poor estimate of return levels for  $H_S$ , with the tail being substantially over-estimated (although within the uncertainty of the estimates it is not statistically significantly different). The likely reason for this over-estimation can be seen in the figures, as the data show that the 300 year return level occurred by chance in the sample (corresponding to a 10 year sample). For *SWL*, return levels are slightly under-estimated. This large distortion of the marginal features makes dependence aspects of the fit hard to assess.

In conclusion we have found that the main source of error in estimating contours of equal joint survivor function is from marginal estimation (a feature largely outside the remit of this current project). If no additional information were available, then relative to the marginal estimation uncertainties, the dependence modelling proposed here for

$(SWL, H_S)$  seems reasonably good. Qualitatively, what this means is that to estimate such contours it seems reasonable to recommend that we need

- More than 10 years of data for each of the marginal variables;
- Simultaneous observational data for  $(SWL, H_S)$  covering a 10 year period,

to be able to estimate 100 year contours and beyond with any confidence.

In practice, simultaneous observational data are difficult to obtain for longer than 10 year periods, but separate information on  $SWL$  and  $H_S$  is available based on longer time periods of data. As the marginal and dependence estimation has been separated into a two stage procedure, additional marginal data can easily be incorporated into the JPM. This marginal information may take the form of

- extra data for the site: for example when  $H_S$  is hindcast for a longer period,
- an estimate of the distribution for the variable obtained from a larger scale analysis: for example estimates of  $SWL$  extremes produced by a spatial analysis as in Dixon and Tawn (1994, 1995).

This correction for marginal features is particularly important for  $SWL$  as a direct analysis, using a period of less than 18.61 years, is likely to produce poor extrapolations as features of the nodal cycle of the tide are ignored. Incorporating extra marginal information overcomes such potential weaknesses. In Section 8.1 we showed how such information can be incorporated into the analysis to give improved contour curves.

Finally we compare the estimates given by the approach developed here with those obtained by the current methods implemented by HR. There are two differences between the HR methods and ours:

- marginal models and estimation techniques,
- dependence estimation.

Thus in addition to the differences found in Section 8.1, where the marginal distribution were treated as known, here we have additional differences due to marginal uncertainty.

Figure 8.13: Sim1:  $H_S$ - $SWL$  curves of equal joint survivor probability expressed in return periods (in years)

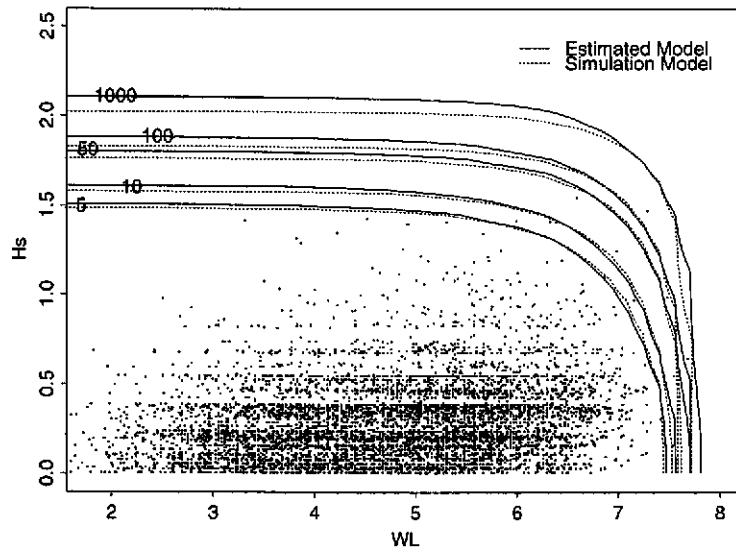


Figure 8.14: Sim2:  $H_S$ - $SWL$  curves of equal joint survivor probability expressed in return periods (in years)

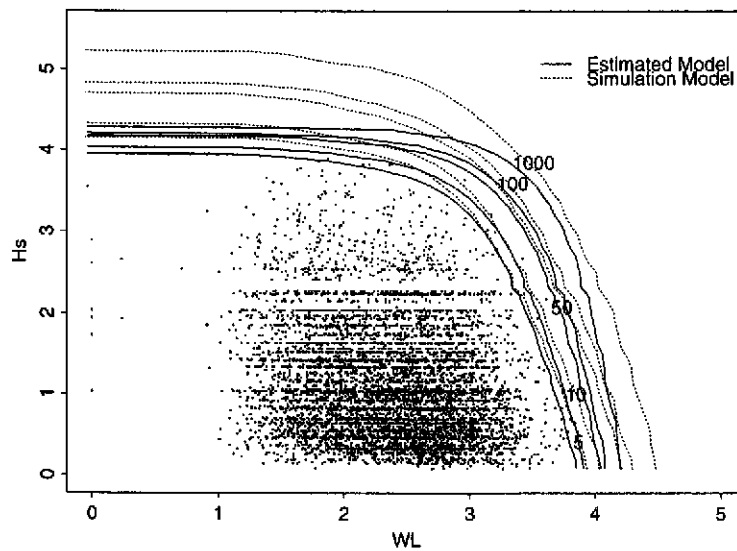


Figure 8.15: Sim3:  $H_S$ -Surge curves of equal joint survivor probability expressed in return periods (in years)

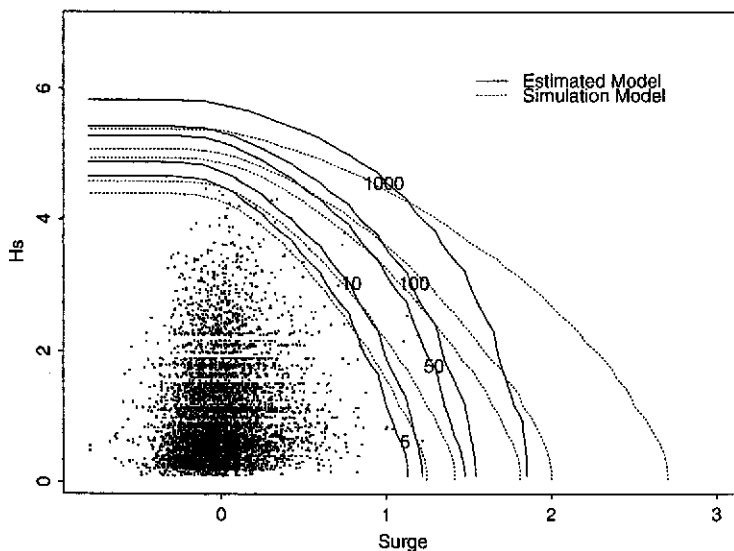


Figure 8.16: Sim3:  $H_S$ -SWL curves of equal joint survivor probability expressed in return periods (in years)

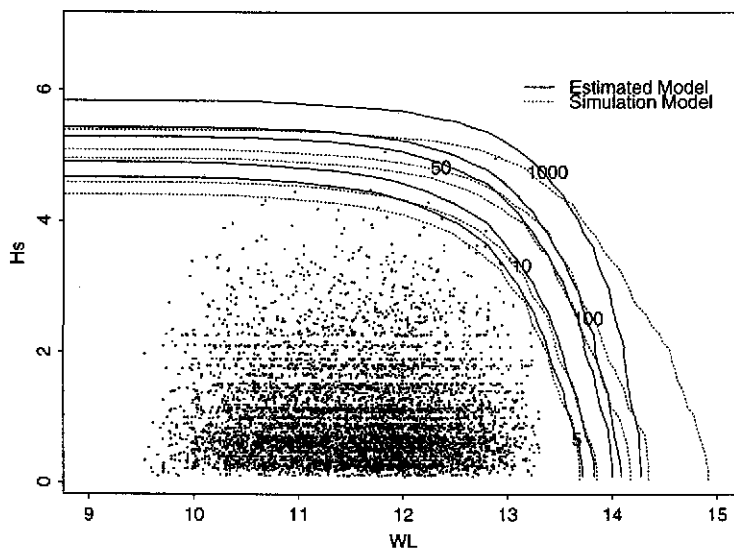


Figure 8.17: Sim4:  $H_S$ - $SWL$  curves of equal joint survivor probability expressed in return periods (in years) for the fitted bivariate normal threshold model

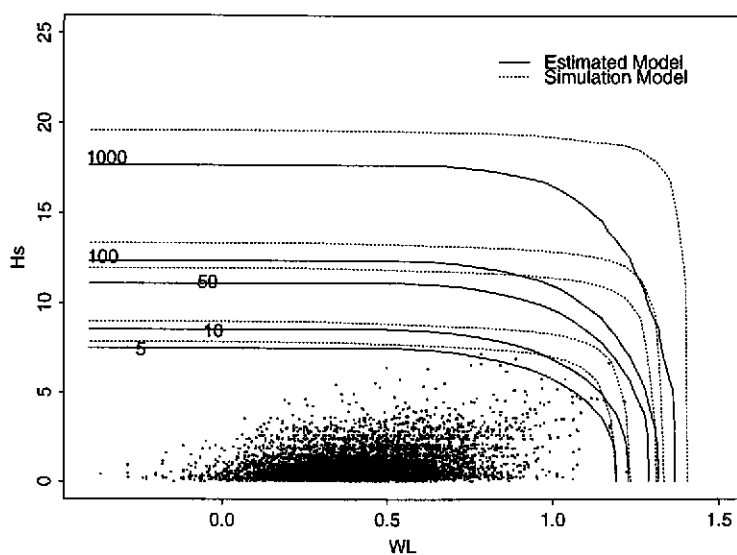


Figure 8.18: Sim4:  $H_S$ - $SWL$  curves of equal joint survivor probability expressed in return periods (in years) for the fitted mixture of bivariate normals model

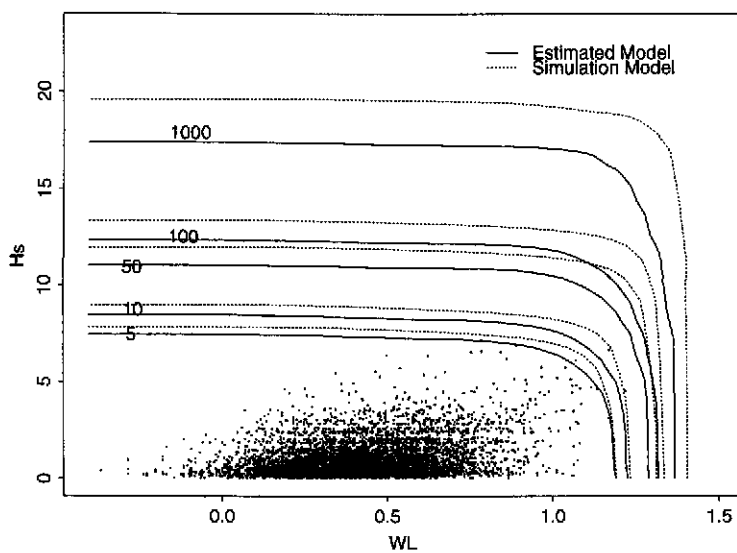


Figure 8.19: Sim5:  $H_S$ - $SWL$  curves of equal joint survivor probability expressed in return periods (in years) for the fitted bivariate normal threshold model

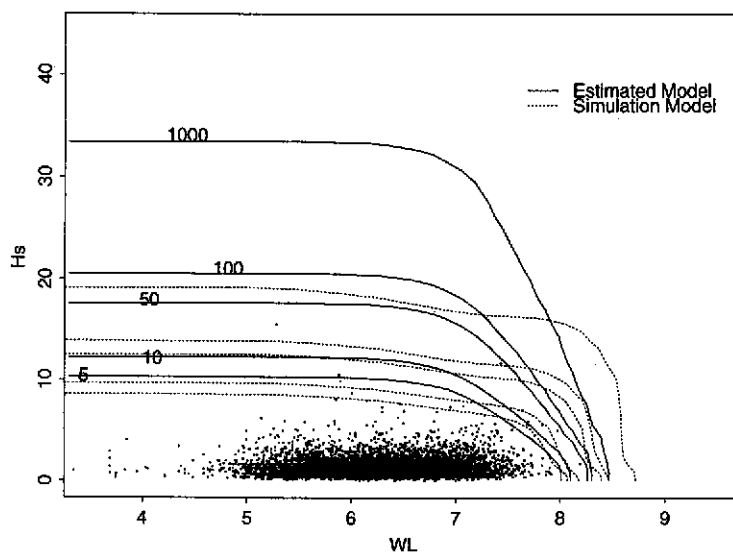
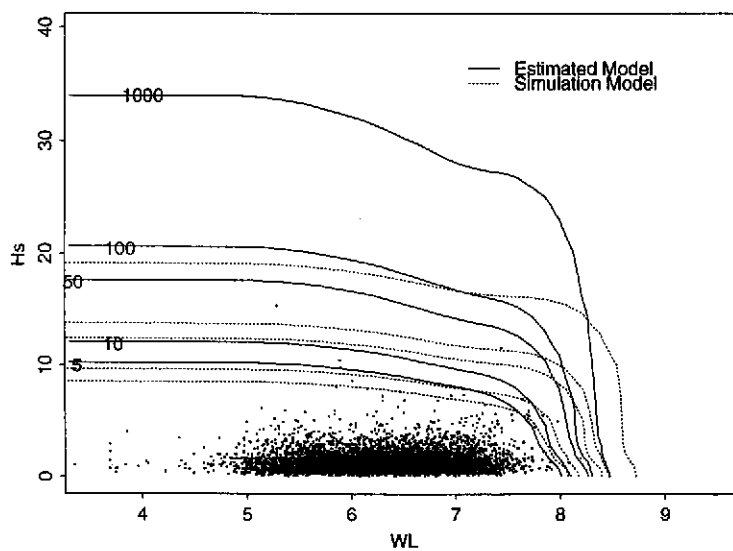


Figure 8.20: Sim5:  $H_S$ - $SWL$  curves of equal joint survivor probability expressed in return periods (in years) for the fitted mixture of bivariate normals model



### 8.2.1 Comparison with current implementation

HR have implemented the current methodology for estimating the joint survivor function, and produced contours of equal value of this function for return periods of 1, 10, and 20 years. For comparison with the plots in Figures 8.13-8.20 we only give the 10 year contour values, these are tabulated in Tables 8.6–8.10. For larger return periods the differences in the marginal extrapolation methods dominate, so such comparisons are outside the remit of this project. The estimation of marginal distributions and dependence structure by HR uses different methods to those described in this report (for details see Hawkes and Hague, 1994). The comparison with the simulation model values and the fitted model described above for this contour curve are given below:

- Sim1** Comparison is not directly possible here as HR have separately estimated the joint survivor function for waves from two direction sectors (these direction sectors do not exactly tie in with those used to simulate the data). Despite the distribution of  $SWL$  being in a conditional form, dependent on  $\theta$ , the estimated marginal distribution of  $SWL$  is found to agree very well with the simulation model.
- Sim2** The HR contour estimates give return levels for  $H_S$  which over-estimate to the same degree as our estimated model under-estimates in Figure 8.14. For  $SWL$  the HR estimates are similar to our marginal return level estimates. The dependence features are well captured.
- Sim3** Here the HR contour estimates give return levels for  $H_S$  which substantially over-estimate (our estimates, given in Figure 8.15, also over-estimate but to a lesser extent), and are similar to our estimates for  $SWL$ . The dependence features seem to be adequately captured.
- Sim4** Here the HR contour is good at this return period. In Section 8.1 the strong form of dependence for these data was not captured by the HR approach, so we know that this good estimate is not sustained for larger return periods. Also the marginal return levels for  $H_S$  at higher return periods are under-estimated. The  $SWL$  marginal distribution seems to fit well.
- Sim5** Again the HR contour is adequate at this return period. However, from Section 8.1 we know that the strong form of dependence has not been captured (the curvature of the contour is not sufficiently peaked). The  $H_S$  return levels have been under-estimated (with the estimated marginal 10 year level the same as the simulation model 5 year level) but is still – better than our estimate (given in Figure 8.19) which is an over-estimate (corresponding to the simulation model 50 year level). The  $SWL$  marginal distribution seems to be well fitted.

<i>SWL</i>	<i>H<sub>S</sub></i>	
	$(0^\circ \leq \theta \leq 190^\circ)$	$(190^\circ < \theta \leq 270^\circ)$
4.0	1.82	1.25
4.5	1.82	1.24
5.0	1.80	1.23
5.5	1.77	1.22
6.0	1.69	1.17
6.5	1.52	1.09
6.75	1.41	–
7.0	1.23	0.97
7.25	–	0.88
7.5	0.68	0.73

Table 8.6: HR estimates of points on the 10 year contour of the joint survivor function for Sim1: separate estimates conditional on the wave direction,  $\theta$ , satisfying  $0^\circ \leq \theta \leq 190^\circ$  and  $190^\circ < \theta \leq 270^\circ$ .

<i>SWL</i>	1.50	1.75	2.00	2.25	2.50	2.75	3.00	3.25	3.50	3.75
<i>H<sub>S</sub></i>	4.61	4.57	4.45	4.28	4.06	3.79	3.48	3.01	2.17	0.98

Table 8.7: HR estimates of points on the 10 year contour of the joint survivor function for Sim2.

<i>SWL</i>	11.00	11.50	12.00	12.25	12.50	12.75	13.00
<i>H<sub>S</sub></i>	5.25	5.19	5.00	4.87	4.70	4.38	3.61

Table 8.8: HR estimates of points on the 10 year contour of the joint survivor function for Sim3.

$SWL$	0.4	0.5	0.6	0.7	0.8	0.9	1.0	1.1	1.2
$H_S$	7.42	7.34	7.27	7.23	7.15	6.88	6.48	5.86	4.14

Table 8.9: HR estimates of points on the 10 year contour of the joint survivor function for Sim4.

$SWL$	6.00	6.50	6.75	7.00	7.25	7.50	8.00
$H_S$	8.52	8.20	8.03	7.62	7.13	6.56	3.77

Table 8.10: HR estimates of points on the 10 year contour of the joint survivor function for Sim5.

## **Part III**

# **Applications to the Estimation of the Probability of Failure for an Existing Design**



## Chapter 9

# Analysis of Overtopping Discharge Rates

The methodology developed in the first two parts of this report can be applied to any design problem. In this chapter we examine an application where the mode of failure is an extreme overtopping discharge rate, and the analysis is required for an existing design. We focus on the problem of estimating return levels of extreme overtopping discharge rates, which can be rephrased in terms of estimating the probability that the overtopping discharge rate exceeds some critical level.

In this chapter we consider five application sites (corresponding to the five simulated data sets, *Sim1–Sim5*). For each hypothetical site, the overtopping discharge rate,  $Q_C$ , is given by equation (1.1.1), with the sea-wall design characteristics  $(a_1, a_2, v)$  given in Table 9.1. This specification of the problem may be unrealistic, as the sea condition data are offshore data (as the waves have been hindcast), whereas the overtopping discharge rate, equation (1.1.1), presumes the waves to be as measured at the sea-wall. As a result a small number of high wave heights, with very low steepness, tend to dominate the overtopping results. On the other hand, the analysis is primarily to

- illustrate the application of the JPM to a design problem;
- enable a comparison between the SVM and JPM;
- enable comparison between the methods developed in this report and methods currently implemented, such as the two different levels of analysis described in Section 1.2.

In this chapter we first describe special features of the methods as applied to overtopping discharge rates (Section 9.1), before applying these methods to the simulated data. A benefit of using simulated data for the sea condition data is that we can derive the

associated distribution of extreme overtopping rates exactly, thus simplifying the comparisons between the methods. To clarify our presentation of results, we focus on the estimation of the 100 year overtopping discharge rate, giving estimates and comparisons for each data set, from Sim1 in Section 9.2 to Sim5 in Section 9.6. Finally in Section 9.8, for completeness, we give estimates for the 10 and 50 year overtopping discharge rates for each of these simulated data sets.

Simulated data	$a_1$	$a_2$	$v$
Sim1	0.0192	46.96	8.5
Sim2	0.0192	46.96	5.0
Sim3	0.0192	46.96	14.5
Sim4	0.0192	46.96	2.5
Sim5	0.0192	46.96	9.0

Table 9.1: Information on the structural design for the simulated data. Here the sea-wall is a simple sloping wall with a 1:4 slope,  $a_1$  and  $a_2$  dimensionless constants and  $v$  is the crest elevation in metres (relative to ODN except for Sim3 and Sim5 which are relative to Chart Datum). See equation (1.1.1) for details of how these design parameters influence overtopping discharge rates.

## 9.1 Background Methods

We apply five different methods of analysis of extreme overtopping discharge rates,

- two applications of the structure variable method,
- three levels of application of the joint probability method.

First we outline special features of these methods in their application to the specific problem of estimating extremes of overtopping discharge rates,  $Q_C$ .

### SVM applied to $Q_C$

The standard SVM, as described in Section 2.1, is applied directly to the structure variable,  $Q_C$  the overtopping discharge rate. The results were derived by applying the GPD threshold model to a range of thresholds (corresponding to upper quantiles over the range 90 – 99.5%).

**SVM applied to  $\log Q_C$** 

The SVM is applied indirectly, by statistically analysing a transformed structure variable,  $\log Q_C$ , and extrapolation. The return level estimates on the  $Q_C$  scale are given by taking the exponential of the estimates on the  $\log Q_C$  scale. The results were derived by applying the GPD threshold model to a range of thresholds (corresponding to upper quantiles over the range 90 – 99.5%).

Of the two SVM, this is the closest in spirit to the general approach HR use for univariate extrapolation to estimate return levels. We have applied our methods in a routine approach, whereas in practical studies subjective choice, such as threshold choice, and assessment of fit, would be carefully taken. The HR approach requires a greater number of *choices* to be made, which protects against physically unrealistic extrapolations, but potentially may force the extrapolation to be inconsistent with the extremal data. The HR estimates for these Sim data sets will be given in the HR report which describes the practical implementation of the methods.

This all acts as a note of warning not to extrapolate without at least assessing the sensitivity to the aspects of the model that are subjectively chosen, and evaluating the estimation uncertainty.

**JPM applied using statistical model**

The joint distribution of  $(SWL, H_S, T_Z)$  is given by the joint distribution of  $(SWL, H_S, S)$  through the joint distribution of  $(SWL, H_S)$  and the conditional distribution of  $S|H_S$  (due to the conditional independence of  $S$  and  $SWL$  given  $H_S$ ). The estimate of the joint distribution of  $(SWL, H_S)$  is given in Chapter 6 and Section 7.1, whereas the estimated conditional distribution of  $S|H_S$  is given in Section 7.2. We have applied two versions of this method, based on

- the fully estimated joint distribution of  $(SWL, H_S, S)$ ,
- the joint distribution of  $(SWL, H_S, S)$  estimated with the marginal distributions of  $SWL$  and  $H_S$  taken to be known.

In each case the results are obtained using the general methodology described in Section 2.2.

**Current implementation of JPM: basic method**

This method corresponds to the basic method described in Section 1.2. The estimated joint survivor function values for  $(SWL, H_S)$  are given in Chapter 8. HR repeated the analysis in each application using two different constant wave steepness values: one being

$S = 0.06$  (common to all analyses), and the other a value derived for each individual data set. Two versions of this method have been applied; these are

- estimates of 1, 10, 100 and 1000 year return levels of overtopping discharge rates based on the estimated joint survivor function of  $(SWL, H_S)$  with the marginal distributions of  $SWL$  and  $H_S$  taken to be known,
- estimates of 1, 10 and 20 year return levels for overtopping discharge rates based on the fully estimated joint survivor function of  $(SWL, H_S)$ .

### Current implementation of JPM: refined method

This method corresponds to the refined method described in Section 1.2, in which the exact failure region (with respect to  $H_S$  and  $SWL$ , but not with respect to  $T_Z$  as steepness is treated as fixed) is used. Here the joint density of  $(SWL, H_S)$  is derived from the estimated joint survivor function given in the basic method (i.e. from the estimates given in Chapter 8) by suitable differencing over a grid (interval lengths of 0.5m). In each application a value of constant wave steepness is used (here  $S = 0.06$  and a value derived from the data). This choice was made for consistency with the basic method, but is not always made in current 'risk analysis' studies. This method has only been applied to Sim2, where two levels of implementation were undertaken:

- estimates based on the estimated joint density of  $(SWL, H_S)$  with known marginal distribution,
- estimates based on the exact joint distribution of  $(SWL, H_S)$ .

## 9.2 Application to Sim1

For this hypothetical site, the five largest overtopping discharge rates, and the associated combinations of  $(SWL, H_S, T_Z)$ , from a hypothetical 10 year period are given in Table 9.2. It is seen that the largest observed rate is an order of magnitude greater than the next largest values. This has a significant impact on extrapolations applied directly to the  $Q_C$  data, producing massively over-estimated return levels. The estimate is not shown in Figure 9.1 which illustrates the other estimates of the 100 year overtopping discharge rate. The target return levels for  $Q_C$ , from the simulation model, are given in Table 9.3. The other estimates are discussed below:

**SVM** the estimated level is shown against the threshold for the SVM applied to  $\log Q_C$ .

The level is under-estimated for thresholds below the 96% quantile, but above this threshold level the return level is well estimated.

**JPM statistical model** the estimate is a slight over-estimate of the level (giving the actual 140 year level). Here the statistical model is based on estimated marginal distributions. Known marginal distributions are not used because of the directionality.

**JPM current implementation** estimates of the 100 year level are given for two direction sectors only, so direct comparison is not possible for these data. Here we report only estimates obtained using known marginal distribution for  $H_S$  and  $SWL$ . For the  $0^\circ \leq \theta < 110^\circ$  direction sector, HR take  $S = 0.06$  which gives the estimated 100 year overtopping discharge rate of 0.016 (corresponding to the actual 30 year rate). Also for the  $110^\circ < \theta < 360^\circ$  direction sector HR take  $S = 0.025$  obtaining the 100 year overtopping rate of 0.019 (corresponding to the actual 40 year rate).

For this site each of the methods appear to produce equally acceptable estimates (with the exclusion of the SVM to  $Q_C$ ). This is not too surprising as

1. for this site, the estimated joint survivor function given by the statistical model and current implementation seems adequately estimated,
2. the dependence between ( $SWL, H_S$ ) is moderately strong, so the error in the failure region of the current implementation is not large, and
3. the variation of  $S$  given  $H_S$  is large, is relatively small, so taking this value as fixed is a reasonable approximation.

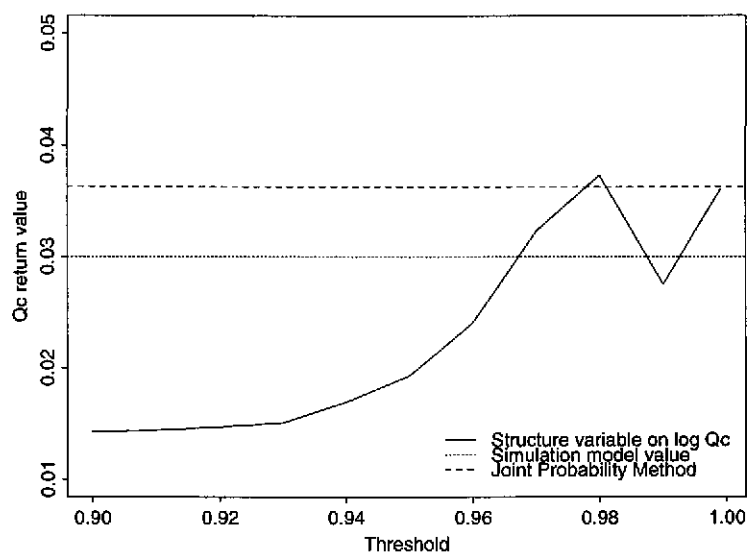
$SWL$	$H_S$	$T_Z$	$Q_C$
7.28	1.47	3.66	0.01676
7.48	0.99	3.10	0.00397
6.59	1.54	3.76	0.00237
6.98	1.25	3.45	0.00221
6.31	0.59	6.82	0.00142

Table 9.2: The largest five sea condition values for Sim1 in terms of the structure function, overtopping discharge rate  $Q_C$  given by equation (1.1.1). Here  $SWL$  is in terms of metres relative to ODN,  $H_S$  is in metres, and  $T_Z$  in secs. Overtopping discharge rate,  $Q_C$ , is in  $\text{metre}^3/\text{sec}/\text{metre}$ .

Return period (years)	Return level $Q_C$	Return period (years)	Return level $Q_C$
5	0.0040	100	0.0300
10	0.0075	200	0.0455
20	0.0127	300	0.0533
30	0.0161	400	0.0632
40	0.0192	500	0.0694
50	0.0213	600	0.0727
60	0.0232	700	0.0782
70	0.0251	800	0.0829
80	0.0270	900	0.0856
90	0.0288	1000	0.0874

Table 9.3: Sim1: Return levels for  $Q_C$  (in  $\text{metre}^3/\text{sec}/\text{metre}$ ) from simulation model.

Figure 9.1: Sim1  $Q_C$  100 year return value for the SVM applied to  $\log Q_C$  and the JPM based on the bivariate normal dependence model for  $(SWL, H_S)$ . The threshold axis is related to applications of the SVM



## 9.3 Application to Sim2

For this hypothetical site, the five largest overtopping discharge rates, and the associated combinations of  $(SWL, H_S, T_Z)$ , are given in Table 9.4. As the largest observed  $Q_C$  rates are consistent with the other large levels, we can apply the SVM to  $Q_C$  directly, but also apply the SVM to the  $\log Q_C$  data. The target return levels for  $Q_C$  for the simulation model are given in Table 9.5. Estimates of the 100 year overtopping discharge rate are shown in Figure 9.2. Additionally, we have estimates from current implementation at the basic and refined levels of application. All these estimates are discussed below:

**SVM** the estimated level is shown against the threshold for the SVM applied to  $Q_C$  and to  $\log Q_C$ . For  $Q_C$ , the level is grossly over-estimated for all thresholds up to the 99% quantile. Alternatively, for  $\log Q_C$ , levels are consistently under-estimated for all thresholds (giving the actual 25 year rate).

**JPM statistical model** the estimate given for the statistical model very slightly over-estimates the rate (giving the actual 140 year rate). Here, the statistical model is based on estimated marginal distributions.

**JPM current implementation: basic method** If the standard value of  $S = 0.06$  is taken then the estimated 100 year value is 0.56 (corresponding to a value less than the actual 5 year rate). In contrast, taking  $S = 0.03$  (determined from the Sim2 data) the estimate is increased to 1.5 (the actual 35 year rate). Here, the known marginal distributions are used.

**JPM current implementation: refined method** Using  $S = 0.06$  the refined method gave equally poor estimates. However taking  $S = 0.03$  leads to a slight over-estimate (corresponding approximately to the actual 200 year rate).

Of all the methods applied to the data, only the JPM statistical model and the JPM current implementation (with  $S$  specially chosen) appear to produce acceptable estimates. Possible reasons for this poor performance of the other estimators are that

1. the negative correlation of  $(SWL, H_S)$  means that the basic method of current implementation is likely to under-estimate.
2. the high variability of  $S$  for large values of  $H_S$  means that estimates based on fixing  $S$  at some value, a feature of all currently implemented methods, will give biased estimates.

For this hypothetical site we compare the importance of each of the above features.

- For the current implementation the refined method gives a higher overtopping discharge rate than the basic method, as it includes a wider range of loading conditions which contribute to the failure region. There is a degree of coarseness in the refined method due to the coarseness of the grid used for converting the estimated joint survivor function into a joint density function. More refinement would be possible, but is time-consuming, since it relies on manual interpolation of return periods from the estimated contours of joint survivor functions. This stage of the refined method is made more difficult when the known marginal distributions are used, since the marginal axes are a non-linear transformation of marginal axes when the marginal distribution is estimated.

A feature of the coarseness is that the refined method will tend to overestimate overtopping (if  $S$  is really a constant value), because central values of wave height and water level are used for each 'cell', whereas the probability density function is concentrated towards the lower corners of the cell. This feature is seen in the above estimates.

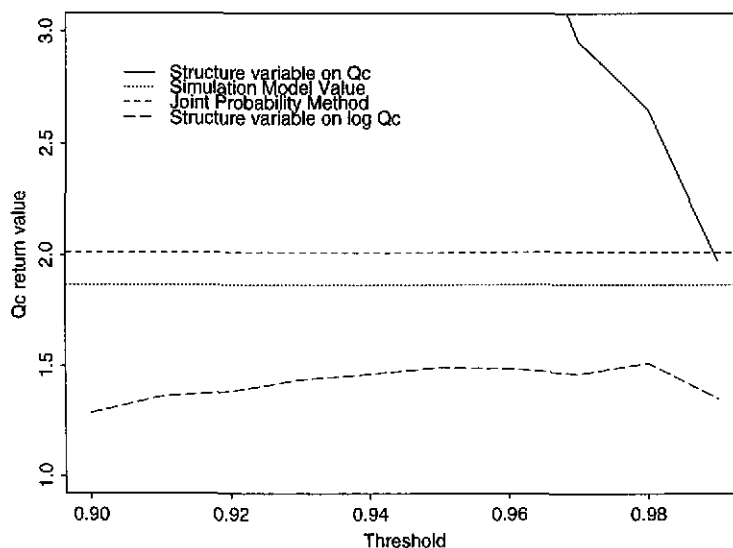
$SWL$	$H_S$	$T_Z$	$Q_C$
2.38	3.34	10.31	1.1465
2.18	3.22	9.28	1.0920
2.46	3.42	10.44	0.939
1.88	3.89	11.00	0.9314
3.26	3.64	7.65	0.8798

Table 9.4: The largest five sea condition values for Sim2 in terms of the structure function, overtopping discharge rate  $Q_C$  given by equation (1.1.1). Here  $SWL$  is in terms of metres relative to ODN,  $H_S$  is in metres, and  $T_Z$  in secs. Overtopping discharge rate,  $Q_C$ , is in  $\text{metre}^3/\text{sec}/\text{metre}$ .

Return period (years)	Return level $Q_C$	Return period (years)	Return level $Q_C$
5	0.9476	100	1.8673
10	1.1516	200	2.1462
20	1.3640	300	2.3205
30	1.4881	400	2.4042
40	1.5745	500	2.4703
50	1.6308	600	2.5544
60	1.6991	700	2.6169
70	1.7613	800	2.7049
80	1.8036	900	2.7498
90	1.8357	1000	2.7517

Table 9.5: Sim2: Return levels for  $Q_C$  (in  $\text{metre}^3/\text{sec}/\text{metre}$ ) from simulation model.

Figure 9.2: Sim2  $Q_C$  100 year return value for the SVM applied to  $Q_C$  and  $\log Q_C$  and the JPM based on the bivariate normal dependence model for  $(SWL, H_S)$ . The threshold axis is related to applications of the SVM



## 9.4 Application to Sim3

For this hypothetical site the five largest overtopping discharge rates, and the associated combinations of  $(SWL, H_S, T_Z)$ , are given in Table 9.6, and the target return levels for  $Q_C$ , from the simulation model, are given in Table 9.7. The largest two observed overtopping discharge rates are twice the size of the fourth and fifth largest observations, which leads to the SVM based on the  $Q_C$  data producing a long estimated tail resulting in over-estimated return levels. The 100 year overtopping discharge rate estimates are shown in Figure 9.3, these are discussed below:

**SVM** the estimated level is shown against the threshold for the SVM applied to  $Q_C$  and  $\log Q_C$ . The level is badly over-estimated for  $Q_C$  for all thresholds, and slightly over-estimated for  $\log Q_C$  data.

**JPM statistical model** the estimate is very good (the estimated value is the actual 90 year rate). Here, the statistical model is based on estimated marginal distributions.

**JPM current implementation** For  $S = 0.06$  the estimate of the 100 year rate is 1.86 (corresponding to the actual 25 year rate), whereas for the derived value of  $S = 0.048$  the estimated 100 year rate is 2.3 (corresponding to the actual 70 year rate). Here, the known marginal distributions were used.

With the exclusion of the SVM applied to  $Q_C$ , the methods agree to a reasonable degree. In comparing these methods we should note that:

1. For the current implementation, known marginal distribution have been used whereas for the statistical model estimated marginal distribution were used;
2. The estimated joint survivor function is slightly over-estimated in the current implementation but not in the statistical model. This should lead to over-estimated overtopping discharge rates using the current implementation;
3. The failure region used in the current implementation (basic method) always leads to under-estimation of overtopping discharge rates;
4. The omission, in the current implementation, of the large variation of  $S$ , given that  $H_S$  is large, leads to under-estimation.

These features seem to have balanced each other for these data to produce an acceptable estimate for the current implementation of the JPM.

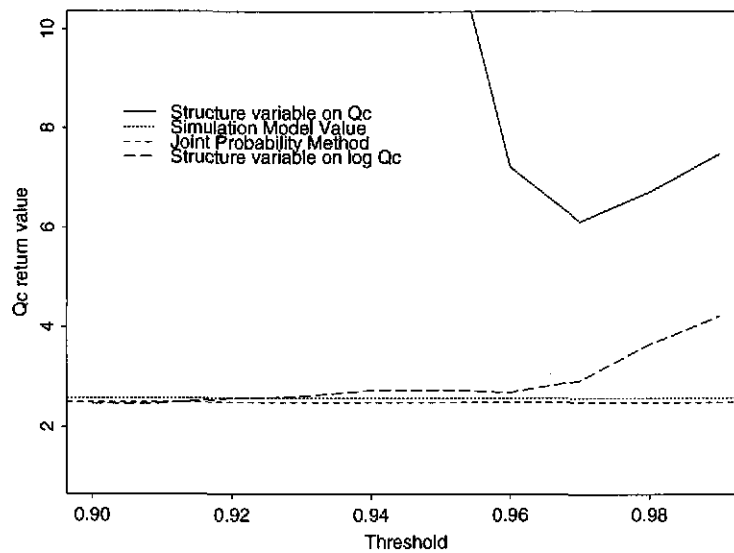
$SWL$	$H_S$	$T_Z$	$Q_C$
13.11	4.37	8.57	2.20413
12.88	4.95	7.92	1.8589
12.45	4.30	8.70	1.2745
12.78	3.62	7.76	0.9231
11.83	5.05	7.99	0.8149

Table 9.6: The largest five sea condition values for Sim3 in terms of the structure function, overtopping discharge rate  $Q_C$  given by equation (1.1.1). Here  $SWL$  is in terms of metres relative to ODN,  $H_S$  is in metres, and  $T_Z$  in secs. Overtopping discharge rate,  $Q_C$ , is in  $\text{metre}^3/\text{sec}/\text{metre}$ .

Return period (years)	Return level $Q_C$	Return period (years)	Return level $Q_C$
5	1.1171	100	2.5782
10	1.4094	200	2.9652
20	1.7253	300	3.3309
30	1.9158	400	3.6324
40	2.0449	500	4.1264
50	2.1698	600	4.5034
60	2.2977	700	4.5779
70	2.3685	800	5.4004
80	2.4291	900	5.5087
90	2.4986	1000	5.7691

Table 9.7: Sim3: Return levels for  $Q_C$  (in  $\text{metre}^3/\text{sec}/\text{metre}$ ) from simulation model.

Figure 9.3: Sim3  $Q_C$  100 year return value for the SVM applied to  $Q_C$  and  $\log Q_C$  and the JPM based on the bivariate normal dependence model for  $(SWL, H_S)$ . The threshold axis is related to applications of the SVM



## 9.5 Application to Sim4

For this hypothetical site the five largest overtopping discharge rates, and the associated combinations of  $(SWL, H_S, T_Z)$ , are given in Table 9.8, and the target return levels for  $Q_C$ , from the simulation model, are given in Table 9.9. Relative to the previous hypothetical sites (Tables 9.2, 9.4 and 9.6) the overtopping discharge rates are much larger. This feature is due to the extreme wave height and wave period data being much larger. Here, variations in  $SWL$  are largely unimportant in affecting the overtopping rate. Correspondingly, the dependence between  $(SWL, H_S)$  is also unimportant. This is disappointing as these data have strong dependence for  $(SWL, H_S)$  which is generally poorly estimated). This hypothetical site has exceptionally large waves, for two reasons

1. the data on which this hypothetical site was based is Christchurch, which has large offshore waves,
2. we chose to lengthen the tail of the wave height variable (for overtopping studies this was clearly an inappropriate choice).

The simulated waves are completely unrealistic as inshore waves, so the resulting overtopping given by equation (1.1.1) is quite false. Nevertheless, as an assessment of performance under varying conditions, the comparison still has value. The 100 year overtopping discharge rate estimates are shown in Figures 9.4 and 9.5, these are discussed below:

**SVM** the estimated level is shown against the threshold for the SVM applied to  $Q_C$  and  $\log Q_C$ . The level is badly over-estimated for  $Q_C$  at thresholds less than the 98% quantile and under-estimated for higher thresholds. No stability with threshold is seen, so this method is poor. For  $\log Q_C$  data, the estimates are stable with respect to threshold but under-estimate badly, (the estimated rate corresponds to actual 10 year rate).

**JPM statistical model** Four estimates are given here:

- an estimate based on the threshold bivariate normal dependence model for  $(SWL, H_S)$  with estimated marginal distributions (shown in Figure 9.4),
- an estimate based on the threshold bivariate normal dependence model for  $(SWL, H_S)$  with known marginal distributions (shown in Figure 9.4),
- an estimate based on the mixture of bivariate normals dependence model for  $(SWL, H_S)$  with estimated marginal distributions (shown in Figure 9.5),
- an estimate based on the mixture of bivariate normals dependence model for  $(SWL, H_S)$  with known marginal distributions (shown in Figure 9.5).

Three features emerge from considering these figures:

1. all four estimates are reasonable by comparison with the SVM. When the marginal distributions are estimated, the actual return period of the estimated rate is 200 years, whereas when the known marginal distributions are used, the return period of the estimate is 400 years;
2. the choice of dependence model makes almost no difference here (this was explained above from an intuitive standpoint, the estimates here confirm this);
3. the use of known marginal distributions has made the estimates worse than the estimates based on unknown marginal distribution. This is counter-intuitive, but results from the  $T_Z$  variable dominating this extrapolation with this component of the model unaffected by treating the distributions of  $H_S$  and  $SWL$  as known. Hence, any error in its modelling (i.e. the modelling of  $S|H_S$  and  $H_S$ ) outweighs other aspects of the joint distribution model. Recall, this is the site for which a false relationship between  $S$  and  $H_S$  was found in Section 7.2.

**JPM current implementation** For  $S = 0.06$  the estimate of the 100 year rate is 15.0 (corresponding to the actual 18 year rate), whereas for  $S = 0.04$  (derived from the data) the estimate is 20.8 (corresponding to the 45 year rate). Here, the known marginal distributions were used. Holding  $S$  constant has been beneficial, as the sensitivity to  $T_Z$  has been reduced.

For these data, in Section 7.1.2 we identified that without being overly conservative ( $SWL, H_S$ ) could be taken to be completely dependent. However increasing the dependence makes the JPM statistical model estimate worse. In contrast for the JPM current implementation, with  $S = 0.04$ , with these variables taken to be completely dependent the actual 100 year rate is estimated almost perfectly.

Detailed comparison of methods is unjustified here. Again the JPM (at all levels of implementation) seems to be preferable to the SVM.

$SWL$	$H_S$	$T_Z$	$Q_C$
1.17	6.64	12.13	8.003
0.50	6.38	14.75	7.924
0.75	6.54	12.15	6.444
0.89	6.89	11.22	6.413
0.97	5.75	12.24	6.053

Table 9.8: The largest five sea condition values for Sim4 in terms of the structure function, overtopping discharge rate  $Q_C$  given by equation (1.1.1). Here  $SWL$  is in terms of metres relative to ODN,  $H_S$  is in metres, and  $T_Z$  in secs. Overtopping discharge rate,  $Q_C$ , is in  $\text{metre}^3/\text{sec}/\text{metre}$ .

Return period (years)	Return level $Q_C$	Return period (years)	Return level $Q_C$
5	8.6723	100	27.1627
10	11.7261	200	33.5968
20	15.5245	300	35.9757
30	17.8495	400	38.0409
40	19.9222	500	40.8586
50	21.6399	600	44.3648
60	23.0572	700	46.2059
70	24.3832	800	47.9264
80	25.6450	900	48.3332
90	26.3787	1000	48.8283

Table 9.9: Sim4: Return levels for  $Q_C$  (in  $\text{metre}^3/\text{sec}/\text{metre}$ ) from simulation model.

Figure 9.4: Sim4  $Q_C$  100 year return value for the SVM applied to  $Q_C$  and  $\log Q_C$  and the JPM based on the bivariate normal dependence model for  $(SWL, H_S)$  with estimated and known marginal parameters. The threshold axis is related to applications of the SVM

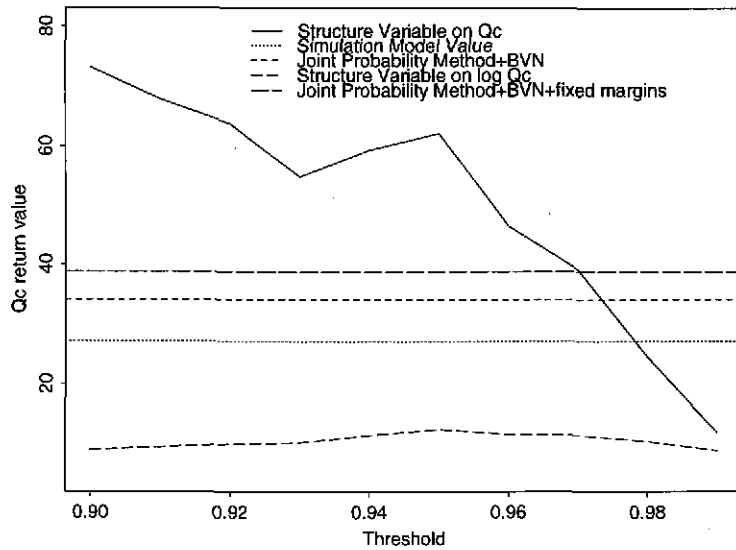
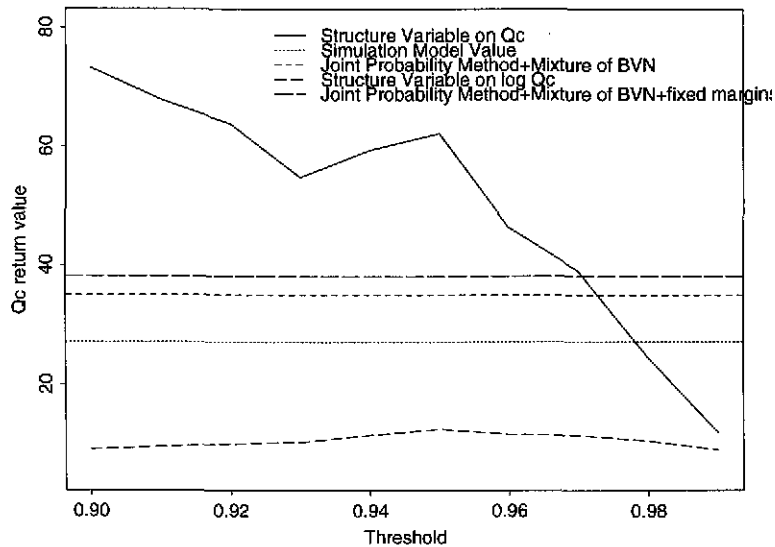


Figure 9.5: Sim4  $Q_C$  100 year return value for the SVM applied to  $Q_C$  and  $\log Q_C$  and the JPM based on the mixture of bivariate normals dependence model for  $(SWL, H_S)$  with estimated and known marginal parameters. The threshold axis is related to applications of the SVM



## 9.6 Application to Sim5

For this hypothetical site, the five largest overtopping discharge rates, and the associated combinations of  $(SWL, H_S, T_Z)$ , are given in Table 9.10, and the target return levels for  $Q_C$ , from the simulation model, are given in Table 9.11. The large overtopping discharge rates for Sim5 are similar to those for Sim4 (see Table 9.8). This feature is again due to the long tail of the extreme wave height distribution. This results in variations in  $SWL$  being largely unimportant in determining the overtopping rate. The dependence between  $(SWL, H_S)$  is also unimportant. The simulated wave data, although consistent with data at Dowsing, represent offshore waves, and are unrealistic as inshore waves, so the resulting overtopping, given by equation (1.1.1), is dominated by their values. This reduces the value of the comparison at this site, as the care given to modelling dependence between  $(SWL, H_S)$  in Chapters 7 and 8 is not exploited when  $(H_S, T_Z)$  dominate the variation in  $Q_C$  values. The 100 year overtopping discharge rate estimates are shown in Figures 9.6 and 9.7; these are discussed below:

**SVM** the estimated level is shown against the threshold for the SVM applied to  $Q_C$  and  $\log Q_C$ . The level is badly over-estimated for  $Q_C$ , with the degree of over-estimation reduced for larger thresholds. No stability with threshold is seen, so this method is poor. For  $\log Q_C$  data, the estimates are stable with respect to threshold, but under-estimate the rate (corresponding to the 50 year rate).

**JPM statistical model** Four estimates are given here:

- an estimate based on the threshold bivariate normal dependence model for  $(SWL, H_S)$  with estimated marginal distributions (shown in Figure 9.6),
- an estimate based on the threshold bivariate normal dependence model for  $(SWL, H_S)$  with known marginal distributions (shown in Figure 9.6),
- an estimate based on the mixture of bivariate normals dependence model for  $(SWL, H_S)$  with estimated marginal distributions (shown in Figure 9.7),
- an estimate based on the mixture of bivariate normals dependence model for  $(SWL, H_S)$  with known marginal distributions (shown in Figure 9.7).

Three features emerge from considering these figures:

1. The use of known marginal distributions has improved the estimates, as the  $H_S$  upper tail was badly over-estimated which led to over-estimated overtopping return levels;
2. The choice of dependence model makes some difference here, with the mixture of bivariate normals producing the best estimates;

3. All four estimates are reasonable by comparison with the SVM applied to  $Q_C$ . By comparison with the SVM applied to  $\log Q_C$ , only the known marginal distributions cases are better. For known marginal distribution, with either dependence model, the JPM statistical model estimate is very good.

**JPM current implementation** For  $S = 0.06$  the estimate of the 100 year level is 10.32 (corresponding to the actual 20 year level), whereas for  $S = 0.05$  (derived from the data) the estimate is 15.1 (corresponding to the actual 45 year rate). Here, the known marginal distributions were used.

The statistical modelling used in the JPM gives the best estimates here. As  $H_S$  dominates the overtopping discharge rate distribution, the choice of dependence model has only a small influence, with the most critical component of the JPM being accurate estimation of the marginal distribution of  $H_S$ . Again, the JPM performs better than the SVM.

$SWL$	$H_S$	$T_Z$	$Q_C$
5.89	10.48	11.31	6.236
7.64	7.02	9.87	5.982
5.90	9.83	11.34	5.680
6.01	8.63	10.34	3.845
6.47	7.64	9.99	3.650

Table 9.10: The largest five sea condition values for Sim5 in terms of the structure function, overtopping discharge rate  $Q_C$  given by equation (1.1.1). Here  $SWL$  is in terms of metres relative to ODN,  $H_S$  is in metres, and  $T_Z$  in secs. Overtopping discharge rate,  $Q_C$ , is in  $\text{metre}^3/\text{sec}/\text{metre}$ .

Return period (years)	Return level $Q_C$	Return period (years)	Return level $Q_C$
5	5.9903	100	19.4855
10	8.2648	200	23.8109
20	11.0693	300	26.7994
30	12.9900	400	29.5869
40	14.4488	500	30.7396
50	15.6470	600	32.4526
60	16.6410	700	33.5968
70	17.4921	800	34.3186
80	18.2494	900	35.7950
90	18.9181	1000	37.4294

Table 9.11: Sim5: Return levels for  $Q_C$  (in metre<sup>3</sup>/sec/metre) from simulation model.

Figure 9.6: Sim5  $Q_C$  100 year return value for the SVM applied to  $Q_C$  and  $\log Q_C$  and the JPM based on the bivariate normal dependence model for  $(SWL, H_S)$  with estimated and known marginal parameters. The threshold axis is related to applications of the SVM

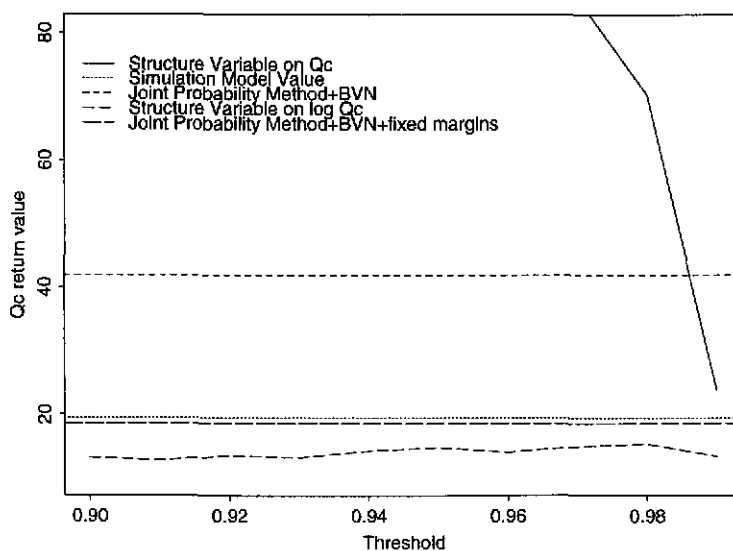
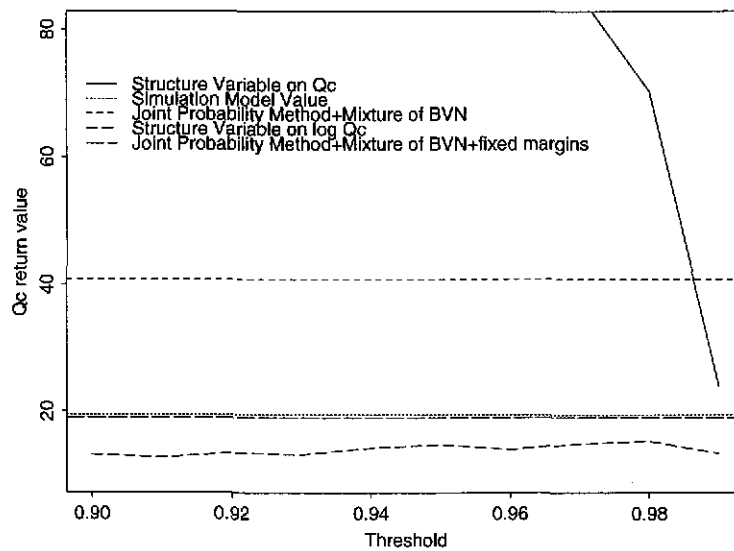


Figure 9.7: Sim5  $Q_C$  100 year return value for the SVM applied to  $Q_C$  and  $\log Q_C$  and the JPM based on the mixture of bivariate normals dependence model for  $(SWL, H_S)$  with estimated and known marginal parameters. The threshold axis is related to applications of the SVM



## 9.7 Comment on Current Implementation Results

The estimates of extreme overtopping rate given by the basic method of the current implementation of the JPM for the 100 year level were found to be under-estimates in Sections 9.2 – 9.6. Here we briefly look to see if this under-estimation is consistent over data sets. In Table 9.12 we give the actual return period for the levels predicted by the basic method to be the 100 and 1000 year levels. Two return periods are given for each data set, corresponding to estimates with  $S = 0.06$  and with a fixed value for  $S$  derived for each data set. For these hypothetical sites, the typical level of protection offered by a design to the 100 year rate would actually be approximately 25 years (if  $S = 0.06$  is used), or more realistically 45 years (when  $S$  is derived from the data). This is a reasonably consistent bias. The estimates for the 1000 year level show that this degree of under-estimation is similar for other return levels, although is not as consistently observed over the data sets. This suggests that a rough re-calibration rule is to double the estimated return period of return levels estimated using the current implementation (basic method).

To give some measure of the performance of the current implementation relative to the JPM statistical model we also summarise estimates for the JPM statistical model. For Sim1-Sim5 the actual return period of the overtopping level estimated to have a 100 year return period are 140, 140, 90, 200 (400) and 1000 (85) respectively (where the numbers in brackets are estimates obtained using the known marginal distributions). These estimates are not directly comparable with those from the current implementation as here the known marginal distributions have not been used. For Sim1-Sim3 the performance of the JPM statistical model is better than the current implementation. Sim4 and Sim5 are completely unrealistic data sets, particularly in relation to the structure function, hence comparison is essentially meaningless. For completeness the methods compare as follows: for Sim4 the current implementation is best, yet this is in contrast to the estimates in Chapter 8, so is totally due to the modelling of  $S$ ; and for Sim5, when we are comparing like with like, i.e. 85 v 45 year return periods the JPM statistical model appears best.

## 9.8 Other Figures

For completeness, we also give the estimated return levels for return periods of 10 and 50 years. Generally these values, shown in Figures 9.8-9.21, show the same features identified for the 100 year level of overtopping discharge rate.

The comparisons so far have excluded estimates for the JPM applied using the basic current implementation with estimated marginals. Table 9.13 gives estimated 10 year  $Q_C$  values based on the current implementation of the JPM. We see there is a reason-

Site	$S = 0.06$		Derived $S$	
	100 year	1000 year	100 year	1000 year
Sim1	45	750	40	550
Sim2	< 5	5	35	250
Sim3	25	2000	70	2000
Sim4	25	150	45	480
Sim5	20	100	45	350

Table 9.12: Actual return period of design levels estimated by the current implementation (basic level) of the JPM: for  $S = 0.06$  and when  $S$  is derived from the data. For Sim1 these results correspond to the dominant direction. Owing to the dominance of wave period for Sim4 and Sim5 these estimates should be largely ignored.

ably consistent pattern of improvement in the estimated levels when the known marginal distribution are used.

site	$S = 0.06$		Derived $S$		actual values
	estimated	known	estimated	known	
Sim1	0.005	0.003	0.0035/0.0117	0.0021/0.0043	0.0075
Sim2	0.298	0.347	0.97	1.06	1.151
Sim3	0.902	0.763	1.22	1.05	1.48
Sim4	3.95	6.37	5.9	9.3	11.7
Sim5	3.88	3.75	4.7	6.5	8.3

Table 9.13: Estimated 10 year return levels for  $Q_C$  obtained using estimated and known marginals via the current implementation (basic level) of the JPM. For Sim1 ( $S = 0.06$ ) these results correspond to the dominant direction, whereas for derived  $S$  each direction sector is given.

Figure 9.8: Sim1  $Q_C$  10 year return value for the SVM applied to  $\log Q_C$  and the JPM based on the bivariate normal dependence model for  $(SWL, H_S)$ . The threshold axis is related to applications of the SVM

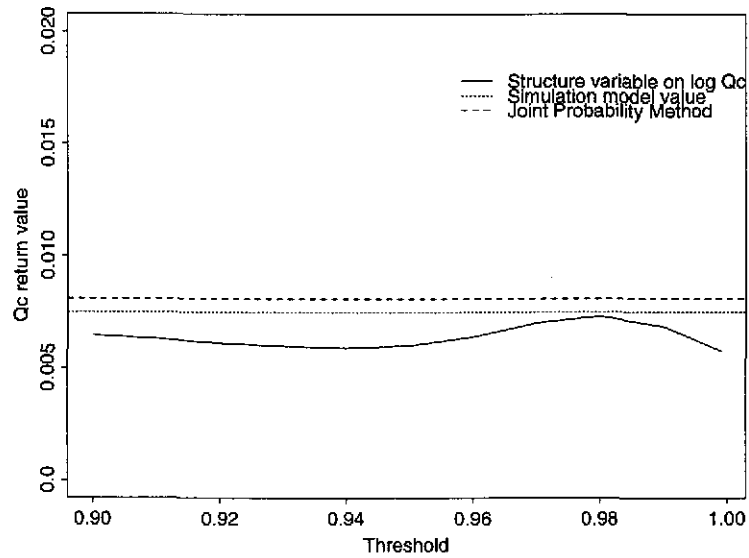


Figure 9.9: Sim1  $Q_C$  50 year return value for the SVM applied to  $\log Q_C$  and the JPM based on the bivariate normal dependence model for  $(SWL, H_S)$ . The threshold axis is related to applications of the SVM

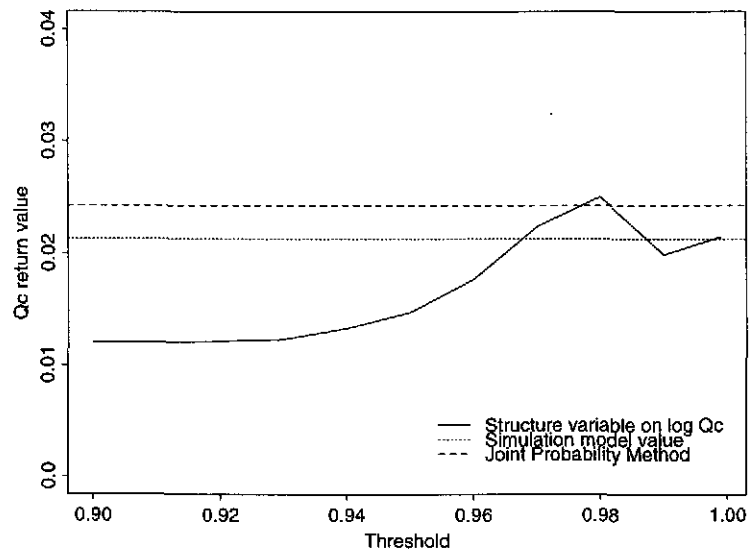


Figure 9.10: Sim2  $Q_C$  10 year return value for the SVM applied to  $Q_C$  and  $\log Q_C$  and the JPM based on the bivariate normal dependence model for  $(SWL, H_S)$ . The threshold axis is related to applications of the SVM

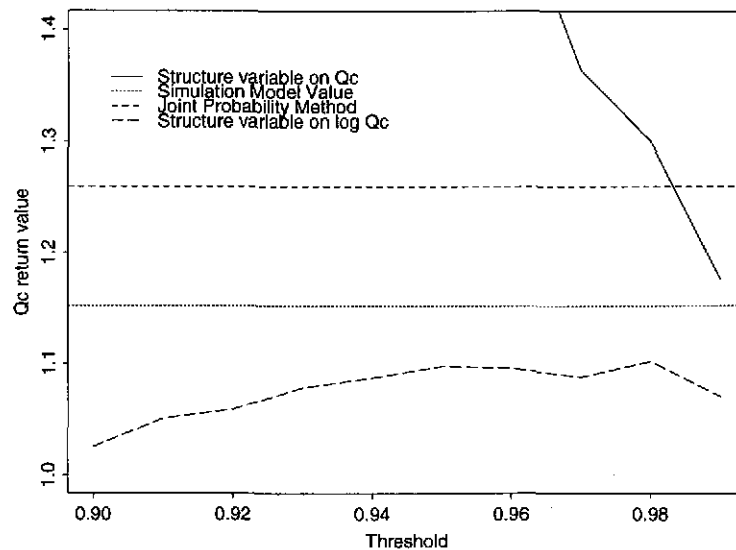


Figure 9.11: Sim2  $Q_C$  50 year return value for the SVM applied to  $Q_C$  and  $\log Q_C$  and the JPM based on the bivariate normal dependence model for  $(SWL, H_S)$ . The threshold axis is related to applications of the SVM

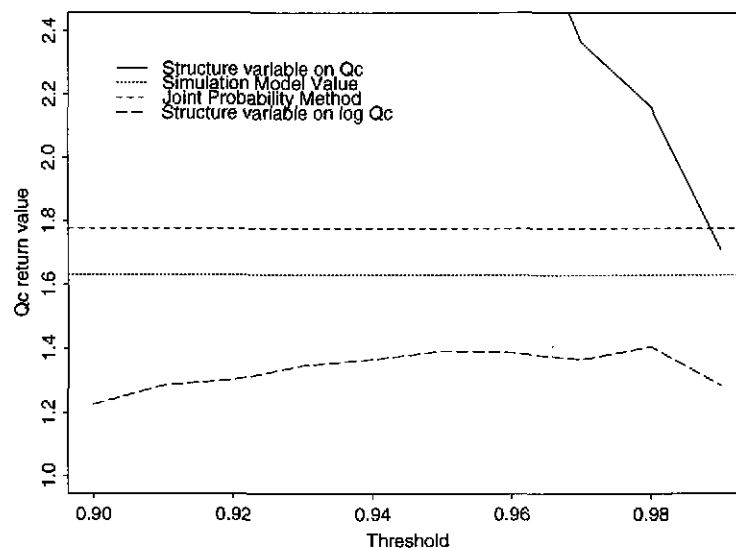


Figure 9.12: Sim3  $Q_C$  10 year return value for the SVM applied to  $Q_C$  and  $\log Q_C$  and the JPM based on the bivariate normal dependence model for  $(SWL, H_S)$ . The threshold axis is related to applications of the SVM

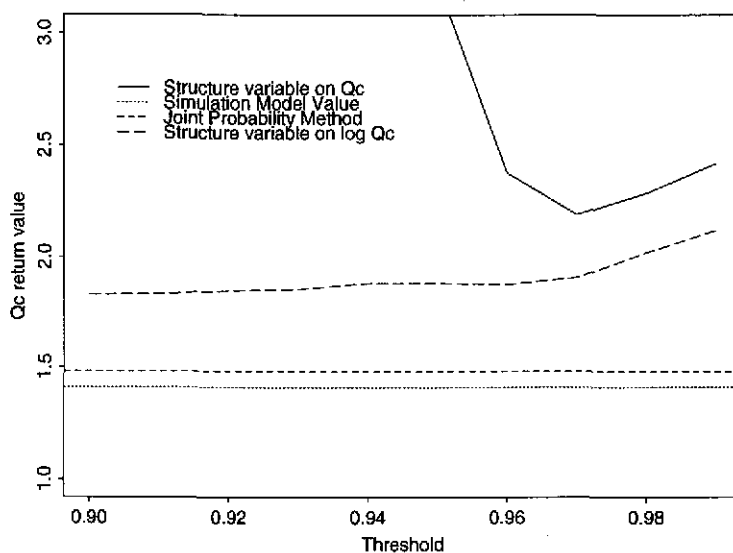


Figure 9.13: Sim3  $Q_C$  50 year return value for the SVM applied to  $Q_C$  and  $\log Q_C$  and the JPM based on the bivariate normal dependence model for  $(SWL, H_S)$ . The threshold axis is related to applications of the SVM

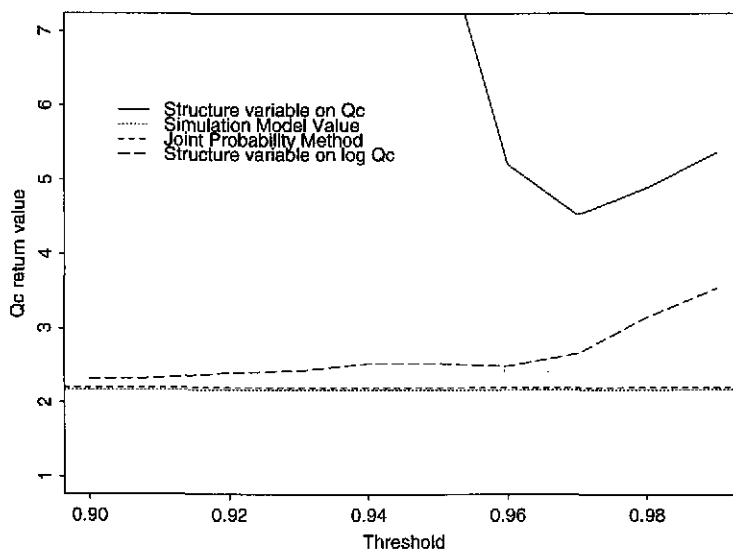


Figure 9.14: Sim4  $Q_C$  10 year return value for the SVM applied to  $Q_C$  and  $\log Q_C$  and the JPM based on the bivariate normal dependence model for  $(SWL, H_S)$  with estimated and known marginal parameters. The threshold axis is related to applications of the SVM

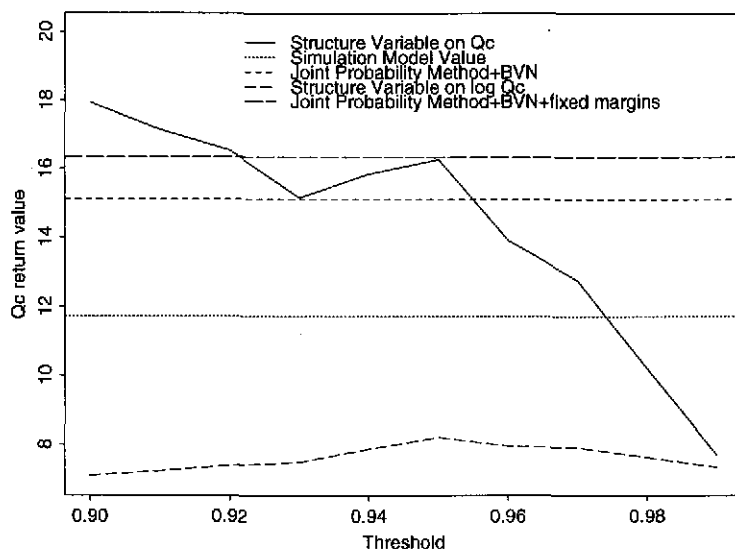


Figure 9.15: Sim4  $Q_C$  10 year return value for the SVM applied to  $Q_C$  and  $\log Q_C$  and the JPM based on the mixture of bivariate normals dependence model for  $(SWL, H_S)$  with estimated and known marginal parameters. The threshold axis is related to applications of the SVM

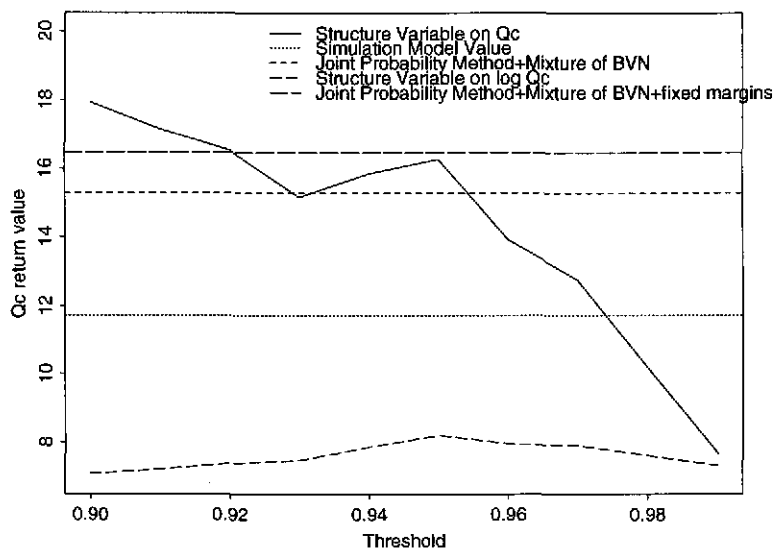


Figure 9.16: Sim4  $Q_C$  50 year return value for the SVM applied to  $Q_C$  and  $\log Q_C$  and the JPM based on the bivariate normal dependence model for  $(SWL, H_S)$  with estimated and known marginal parameters. The threshold axis is related to applications of the SVM

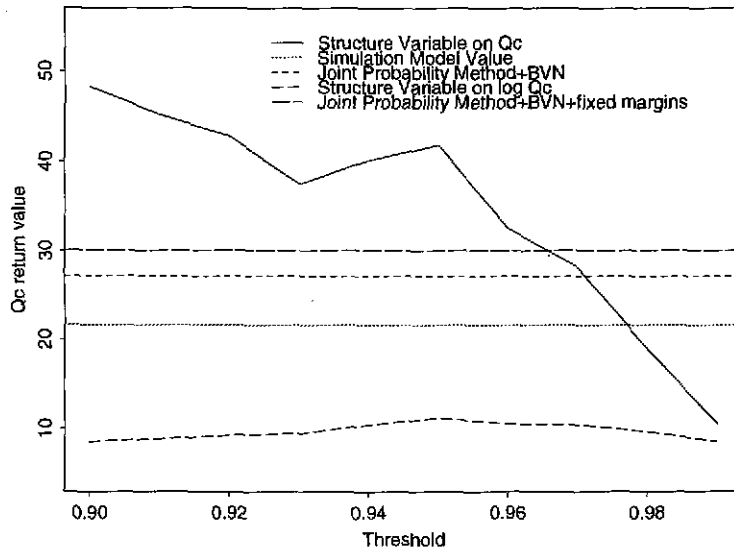


Figure 9.17: Sim4  $Q_C$  50 year return value for the SVM applied to  $Q_C$  and  $\log Q_C$  and the JPM based on the mixture of bivariate normals dependence model for  $(SWL, H_S)$  with estimated and known marginal parameters. The threshold axis is related to applications of the SVM

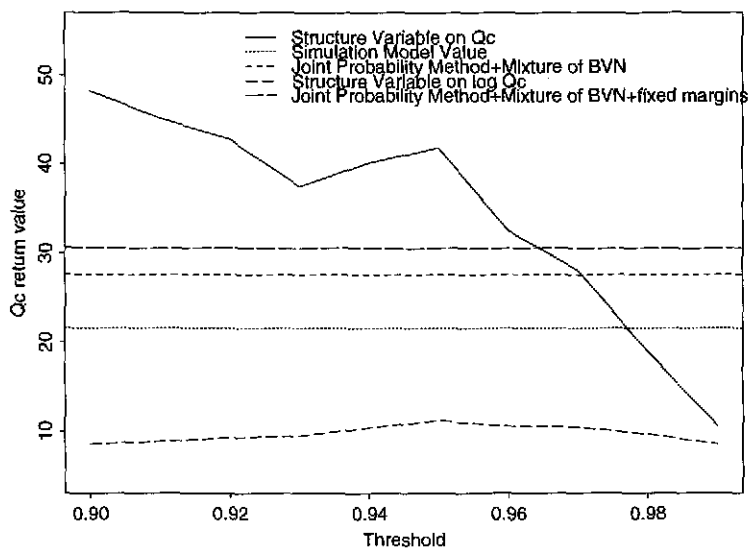


Figure 9.18: Sim5  $Q_C$  10 year return value for the SVM applied to  $Q_C$  and  $\log Q_C$  and the JPM based on the bivariate normal dependence model for  $(SWL, H_S)$  with estimated and known marginal parameters. The threshold axis is related to applications of the SVM

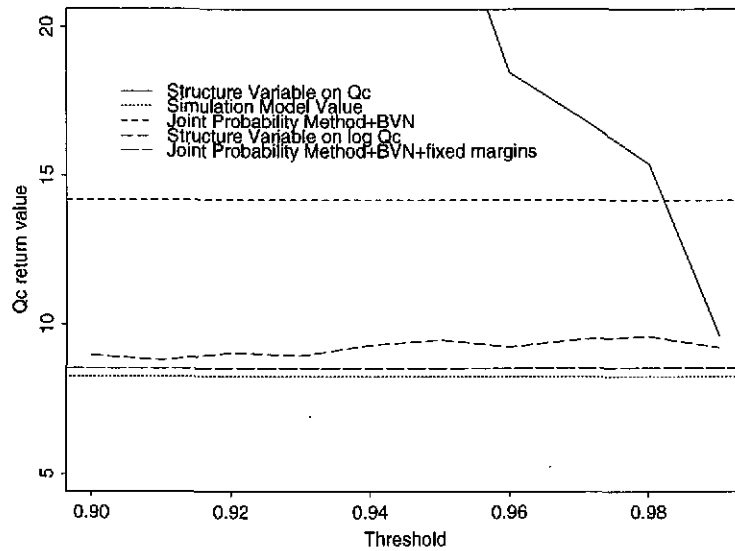


Figure 9.19: Sim5  $Q_C$  10 year return value for the SVM applied to  $Q_C$  and  $\log Q_C$  and the JPM based on the mixture of bivariate normals dependence model for  $(SWL, H_S)$  with estimated and known marginal parameters. The threshold axis is related to applications of the SVM

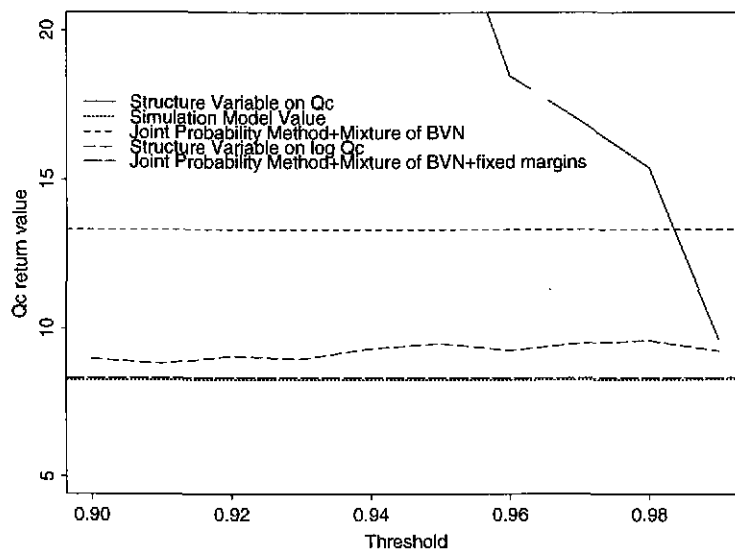


Figure 9.20: Sim5  $Q_C$  50 year return value for the SVM applied to  $Q_C$  and  $\log Q_C$  and the JPM based on the bivariate normal dependence model for  $(SWL, H_S)$  with estimated and known marginal parameters. The threshold axis is related to applications of the SVM

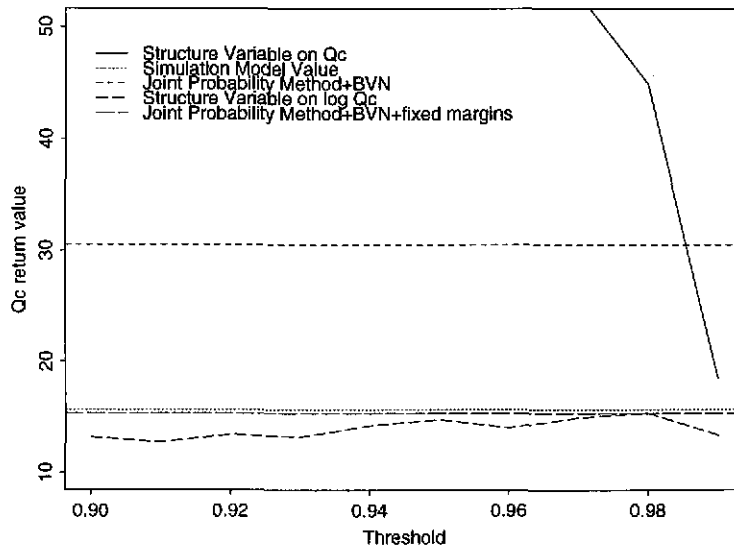
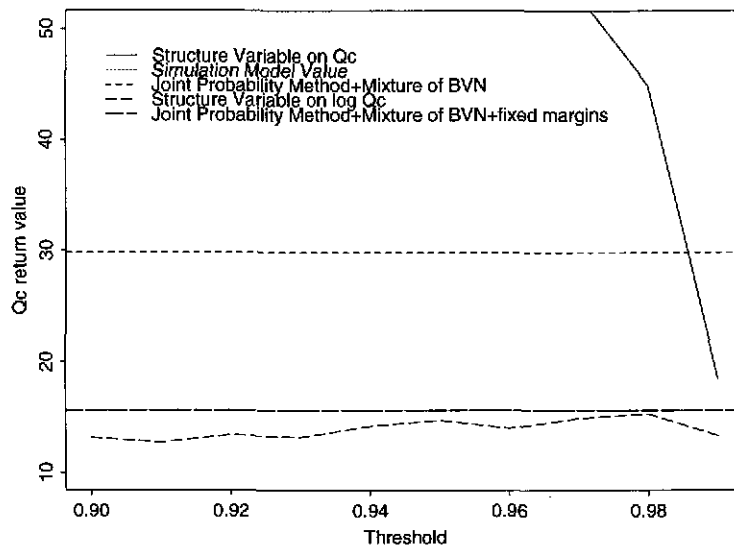


Figure 9.21: Sim5  $Q_C$  50 year return value for the SVM applied to  $Q_C$  and  $\log Q_C$  and the JPM based on the mixture of bivariate normals dependence model for  $(SWL, H_S)$  with estimated and known marginal parameters. The threshold axis is related to applications of the SVM





# Chapter 10

## Comparisons and Conclusions

In this report we have developed new statistical models and procedures for joint probability methods applied to design problems where the environmental variables which cause failures are extreme sea conditions.

The new statistical methods developed in Part I involve:

- Extreme value models for the marginal variables of  $H_S$  and  $SWL$ .
- A range of dependence models for  $(SWL, H_S)$ , which enable flexible modelling of different dependence structures between these variables.
- A technique for explaining variations in  $T_Z$  through wave steepness and associated  $H_S$  values.
- An objective modelling procedure and diagnostic tests allowing aspects of the modelling assumptions to be checked.
- A move towards a model-based method for extrapolations, rather than the current methods which rely in part on subjective extrapolation by eye.
- Statistical models that enable probabilities for events of interest to be evaluated. The main technique for this is through simulation of a series of pseudo sea condition data. Two options were developed: a continuous time simulation of the conditions at high water levels and direct simulation of extreme events.

Together, these techniques provide a general/flexible framework for addressing the problem of evaluating the probability of failure of a structure.

The applications of the joint distribution fits in Part II show that:

- The statistical models have sufficient flexibility to capture the features of the joint distribution of sea conditions which produce extreme loading conditions for a range of observational and simulated data sets.

- The proposed methods appear to perform better than current methods in estimating the joint extremes of  $(SWL, H_S)$  and the behaviour of  $S$  for extreme waves.
- Dependence modelling of  $(SWL, H_S)$  appears to be less important than marginal modelling. Methods for including extra marginal distribution were discussed and illustrated.

The illustration of the techniques to the problem of estimating extreme overtopping discharge rates in Part III of the report revealed:

- In general, the newly developed joint probability methods are better than structure variable methods. This was not the case with existing methods as the JPM, unlike the SVM, ignored variation in  $T_Z$ .
- Currently implemented versions of the JPM, aimed at calculating the joint survivor functions with given return periods, tend to under-estimate overtopping discharge rates. The main reason for this under-estimation is the exclusion of variation of  $S$  in the analysis. By selecting an appropriate fixed value for  $S$  the impact of this is reduced.
- The simplification of the failure region for  $(SWL, H_S)$  causes relatively little contribution to any under-estimation (typically the return period of an overtopping level is over-estimated by a factor of 1.5-2.0, which may be important in some applications). Conversely, the refined version of the current implementation, which re-uses results from the basic method to produce a better estimate of overtopping, has potential for some over-estimation due to the methods used to evaluate the probability of failing in a rectangular region.
- The importance of careful marginal modelling. This feature proved particularly important in this study, as the wave heights and periods dominated the extrapolations of overtopping discharge rates. This was probably due to the use of 'offshore' wave conditions as if they were 'inshore' waves, so that they were often unrealistically large.
- The need for future comparisons of the methods, based on a range of carefully implemented design problems.

# Chapter 11

## References

- Alcock, G.A. (1984). *Parameterising Extreme Still Water Levels and Waves in Design Level Studies*. Report no. 183, Institute of Oceanographic Sciences.
- Carter, D.J.T. and Challenor, P.G. (1981). *Estimating Return Values of Wave Height*. Report no 116. Institute of Oceanographic Sciences.
- Coles, S.G. and Tawn, J.A. (1994). Statistical methods for multivariate extremes: an application to structural design (with discussion). *Appl. Statist.*, **43**, 1–48.
- Davison, A.C. and Smith, R.L. (1990). Models for exceedances over high thresholds (with discussion). *J. Roy. Statist. Soc., B*, **52**, 393–442.
- Dixon, M.J. and Tawn, J.A. (1994). *Estimates of Extreme Sea-Levels at the UK A-Class Sites: Site-by-Site analyses*. Internal Document no. **65**, Proudman Oceanographic Laboratory.
- Dixon, M.J. and Tawn, J.A. (1995). *Extreme Sea-Levels at the UK A-Class Sites: Optimal Site-by-Site Analyses for the East Coast*. Internal Document no. **72**, Proudman Oceanographic Laboratory.
- Flather, R. A. (1987). Estimates of extreme conditions of tide and surge using a numerical model of the north-west European continental shelf. *Est. Coast. Shelf. Sci.*, **24**, 69–93.
- Hawkes, P. and Hague, R. (1994). *Validation of Joint Probability Methods for Large Waves and High Water Levels*, Report SR **347**, HR Wallingford.
- Hydraulics Research Station (1980). Design of seawalls allowing for wave overtopping. *HRS Report 924*, HR Wallingford.
- Leadbetter, M.R., Lindgren, G. and Rootzen, H. (1983). *Extremes and Related Properties of Random Sequences and Series*. New York: Springer.
- Ledford, A.W. and Tawn, J.A. (1996). Statistics for near independence in multivariate extreme values. *Biometrika*, **83**, 169–187.
- Pickands, J. (1975). Statistical inference using extreme order statistics. *Ann. Statist.*, **3**, 119–131.

- Prandle, D. and Wolf, J. (1978). The interaction of surge and tide in the North Sea and River Thames. *Geophys. J. R. Astr. Soc.*, **55**, 203–216.
- Smith, R.L. (1989). Extreme value analysis of environmental time series: an application to trend detection in ground-level ozone (with discussion), *Statist. Sci.*, **4**, 367–393.
- Tawn, J.A. (1992). Estimating probabilities of extreme sea-levels, *Appl. Statist.*, **41**, 77–93.

# Appendix A

## Background information

### A.1 Joint Distributions

Consider the situation where there is a  $d$ -dimensional vector of random variables,  $\mathbf{X} = (X_1, \dots, X_d)$ . For continuous random variables the extension of the probability density function for a single variable to the vector variable case is the joint probability density function,  $f_{\mathbf{X}}(x_1, \dots, x_d)$ , which satisfies the following properties:

- $f_{\mathbf{X}}(x_1, \dots, x_d) = f_{\mathbf{X}}(\mathbf{x}) \geq 0$  for all  $\mathbf{x} = (x_1, \dots, x_d)$ .
- The  $d$ -fold ( $d$ -dimensional) integral

$$\int_{-\infty}^{\infty} \dots \int_{-\infty}^{\infty} f_{\mathbf{X}}(\mathbf{x}) dx_1 \dots dx_d = \int_{-\infty}^{\infty} \dots \int_{-\infty}^{\infty} f_{\mathbf{X}}(\mathbf{x}) d\mathbf{x} = 1.$$

- The probability of some event,  $E$  say, is given by

$$\Pr\{\mathbf{X} \in E\} = \int_E f_{\mathbf{X}}(\mathbf{x}) d\mathbf{x}.$$

The probability density function of the separate variables, known as the **marginal variables**, can be derived from the joint probability density function by summing the joint density over the other variables. For example, for variable  $X_i$ , this is given by the  $(d-1)$ -fold integral

$$f_{X_i}(x_i) = \int_{-\infty}^{\infty} \dots \int_{-\infty}^{\infty} f_{\mathbf{X}}(\mathbf{x}) dx_1 \dots dx_{i-1} dx_{i+1} \dots dx_d, \text{ for } i = 1, \dots, d.$$

That is, marginal distributions are obtained by summing over all the possibilities of the other random variables. Similarly, by summing over a set of the random variables, the joint probability density function of the subset of the remaining variables is obtained, i.e. the joint density function of  $(X_{i+1}, \dots, X_d)$  is given by

$$f_{\mathbf{X}}(x_{i+1}, \dots, x_d) = \int_{-\infty}^{\infty} \dots \int_{-\infty}^{\infty} f_{\mathbf{X}}(\mathbf{x}) dx_1 \dots dx_i.$$

An important concept for joint probability problems is that of **conditional probability**. The conditional probability of an event occurring given another event is known to have occurred arises frequently when working with dependent random variables. The conditional probability of event  $E_2$  given  $E_1$  is known to have occurred is defined by

$$\Pr\{\mathbf{X} \in E_2 | \mathbf{X} \in E_1\} = \frac{\Pr\{\mathbf{X} \in E\}}{\Pr\{\mathbf{X} \in E_1\}},$$

where  $E = E_1 \cap E_2$  is the intersection of events  $E_1$  and  $E_2$ . Similarly, the conditional probability density function for  $(X_1, \dots, X_i)$  given  $(X_{i+1} = x_{i+1}, \dots, X_d = x_d)$ , is given by

$$\frac{f_{\mathbf{X}}(\mathbf{x})}{f_{(X_{i+1}, \dots, X_d)}(x_{i+1}, \dots, x_d)}$$

where the denominator is the joint probability density function of  $(X_{i+1}, \dots, X_d)$ .

All the information about the variation of the vector of random variables is contained in the joint probability density function. Summaries of this function are helpful in comparing different distributions, so summary statistics are often evaluated. The most common summaries are the marginal mean and variance of each individual variable and, as measures of dependence between the variables, the *covariance* and *correlation* between each pair of variables.

Correlation and covariance are measures of linear dependence between two variables. Let  $f(x_i, x_j)$  denote the joint probability density function for the pair  $(X_i, X_j)$ . Let  $\mu_i$  and  $\sigma_i^2$  denote the marginal mean and variance of variable  $i$ , then  $\text{Cov}(X_i, X_j)$ , the covariance of  $(X_i, X_j)$ , is given by

$$\text{Cov}(X_i, X_j) = \int_{-\infty}^{\infty} \int_{-\infty}^{\infty} (x_i - \mu_i)(x_j - \mu_j) f(x_i, x_j) dx_i dx_j,$$

and the correlation between these two variables is given by

$$\text{Correlation}(X_i, X_j) = \frac{\text{Cov}(X_i, X_j)}{\sigma_i \sigma_j}.$$

The correlation,  $\rho$ , is a non-dimensional quantity always lying in the range  $-1 \leq \rho \leq 1$ . When  $\rho = 0$  there is no linear dependence between the variables; when  $\rho > 0$  there is a positive linear association between the variables, with large values in each variable (and small values in each variable) coinciding more often than if there were no relationship between the variables; and when  $\rho < 0$  there is a negative linear association between the variables, with large values in one variable coinciding with small values in the other variable, and vice-versa, more often than if there were no relationship between the variables.

## A.2 The Normal Distribution

In this section we give the distribution and properties of a univariate normal distribution (i.e. one dimensional variable) and a multivariate normal distribution (i.e. a vector of univariate normal random variables).

### A.2.1 Univariate Normal Distribution

The probability density function of a normal random variable  $Y$  is given by

$$f(y) = \frac{1}{(2\pi)^{1/2}\sigma} \exp\left\{-\frac{(y-\mu)^2}{2\sigma^2}\right\}, \text{ for all } -\infty < y < \infty$$

where  $\sigma > 0$ . The expectation of the variable is  $\mu$  and the variance is  $\sigma^2$ , hence the standard notation  $Y \sim N(\mu, \sigma^2)$ . The distribution function for this random variable cannot be evaluated analytically, but symbolically is expressed as

$$\begin{aligned} \Pr\{Y \leq y\} &= \int_{-\infty}^y \frac{1}{(2\pi)^{1/2}\sigma} \exp\left\{-\frac{s^2}{2\sigma^2}\right\} ds, \\ &= \Phi[(y-\mu)/\sigma]. \end{aligned}$$

When  $\mu = 0$  and  $\sigma = 1$  then the distribution is said to be in standard form, i.e.  $Y \sim N(0, 1)$ . To transform  $Y \sim N(\mu, \sigma^2)$  to  $Z \sim N(0, 1)$  we use the relationship

$$Z = \frac{Y - \mu}{\sigma}.$$

### A.2.2 Multivariate Normal Distribution

First we give results for  $\mathbf{Z} = (Z_1, \dots, Z_d)$ , a random variable which follows a multivariate normal distribution with standard normal marginal distributions, i.e. each marginal distribution is  $Z_i \sim N(0, 1)$ . It follows that  $\mathbf{Z}$  has joint density function

$$f_{\mathbf{Z}}(\mathbf{z}) = \phi(\mathbf{z}) = \frac{1}{(2\pi)^{d/2}(\det(\Sigma))^{1/2}} \exp\left\{-\frac{1}{2}\mathbf{z}^T \Sigma^{-1} \mathbf{z}\right\},$$

where the range of  $z_i$ , for  $i = 1, \dots, d$ , is  $-\infty < z_i < \infty$ . Here  $\det(\Sigma)$  is the determinant of the  $d \times d$  matrix  $\Sigma$ , termed the variance-covariance matrix,

$$\Sigma = \begin{pmatrix} \sigma_{11} & \dots & \dots & \sigma_{1d} \\ \dots & \dots & \sigma_{ij} & \dots \\ \dots & \sigma_{ji} & \dots & \dots \\ \sigma_{d1} & \dots & \dots & \sigma_{dd} \end{pmatrix}$$

with  $(i, j)$ th element corresponding to the pairwise covariance of variables  $Z_i$  and  $Z_j$ . Thus, as

$$\rho_{ij} = \text{Correlation}(Z_i, Z_j) = \frac{\text{Cov}(Z_i, Z_j)}{(\text{Var}(Z_i)\text{Var}(Z_j))^{1/2}} = \sigma_{ij},$$

we have

$$\Sigma = \begin{pmatrix} 1 & \dots & \dots & \rho_{1d} \\ \dots & \dots & \rho_{ij} & \dots \\ \dots & \rho_{ji} & \dots & \dots \\ \rho_{d1} & \dots & \dots & 1 \end{pmatrix},$$

where  $\rho_{ij}$  is the correlation of  $Z_i$  and  $Z_j$ . Therefore, the diagonal of  $\Sigma$  is a series of entries of ones and the matrix is symmetric.

To illustrate the notation, we now give this joint density in the bivariate case:

$$f_{Z_1, Z_2}(z_1, z_2) = \phi(z_1, z_2) = \frac{1}{2\pi(1 - \rho^2)^{1/2}} \exp \left\{ -\frac{1}{2(1 - \rho^2)}(z_1^2 - 2\rho z_1 z_2 + z_2^2) \right\}, \quad (\text{A.2.1})$$

where  $-\infty < (z_1, z_2) < \infty$ . Here  $\rho = \rho_{12} = \rho_{21}$ , with  $-1 \leq \rho \leq 1$ , is the correlation between  $Z_1$  and  $Z_2$ , so in terms of  $\Sigma$ ,

$$\Sigma = \begin{pmatrix} 1 & \rho \\ \rho & 1 \end{pmatrix}$$

and

$$\Sigma^{-1} = \frac{1}{(1 - \rho^2)} \begin{pmatrix} 1 & -\rho \\ -\rho & 1 \end{pmatrix}.$$

**Property 1:** An important special case is when  $\rho = 0$ , i.e. no correlation. Then

$$f_{Z_1, Z_2}(z_1, z_2) = \frac{1}{2\pi} \exp \left\{ -\frac{1}{2}(z_1^2 + z_2^2) \right\} = f_{Z_1}(z_1)f_{Z_2}(z_2),$$

so  $(Z_1, Z_2)$  are independent.

**Property 2:** The marginal density of  $Z_1 \sim N(0, 1)$ . This result follows from

$$f_{Z_1}(z_1) = \int_{-\infty}^{\infty} f_{Z_1, Z_2}(z_1, z_2) dz_2.$$

**Property 3:** The density of  $Z_1|Z_2 = z_2$  is

$$\frac{1}{(2\pi(1 - \rho^2))^{1/2}} \exp \left\{ -\frac{1}{2(1 - \rho^2)}(z_1 - \rho z_2)^2 \right\}$$

so that  $Z_1|Z_2 = z_2 \sim N(\rho z_2, (1 - \rho^2))$ . The result follows from

$$f_{Z_1|Z_2=z_2}(z_1|z_2) = \frac{f_{Z_1, Z_2}(z_1, z_2)}{f_{Z_2}(z_2)}.$$

Now consider the more general situation where  $\mathbf{Y} = (Y_1, \dots, Y_d)$ , a random variable which follows a multivariate normal distribution with marginal distributions being  $Y_i \sim N(\mu_i, \sigma_i^2)$  for  $i = 1, \dots, d$ . It follows that  $\mathbf{Y}$  has joint density function

$$f_{\mathbf{Y}}(\mathbf{y}) = \frac{1}{(2\pi)^{d/2}(\det(\Sigma))^{1/2}} \exp \left\{ -\frac{1}{2}(\mathbf{y} - \boldsymbol{\mu})^T \Sigma^{-1}(\mathbf{y} - \boldsymbol{\mu}) \right\},$$

with  $y_i : -\infty < y_i < \infty$  for  $i = 1, \dots, d$ . Here  $\boldsymbol{\mu} = (\mu_1, \dots, \mu_d)^T$  and  $\Sigma$  is the variance-covariance matrix with  $(i, j)$ th element corresponding to the pairwise covariance of variables  $Y_i$  and  $Y_j$ . Thus, as

$$\rho_{ij} = \text{Corr}(Y_i, Y_j) = \frac{\text{Cov}(Y_i, Y_j)}{(\text{Var}(Y_i)\text{Var}(Y_j))^{1/2}} = \sigma_{ij}/(\sigma_i\sigma_j),$$

we have

$$\Sigma = \begin{pmatrix} \sigma_1^2 & \dots & \dots & \sigma_1\sigma_d\rho_{1d} \\ \dots & \dots & \sigma_i\sigma_j\rho_{ij} & \dots \\ \dots & \sigma_i\sigma_j\rho_{ji} & \dots & \dots \\ \sigma_1\sigma_d\rho_{d1} & \dots & \dots & \sigma_d^2 \end{pmatrix},$$

where  $\rho_{ij}$  is the correlation of  $Y_i$  and  $Y_j$ . To illustrate the notation we again give this joint density in the bivariate case:

$$f_{\mathbf{Y}}(\mathbf{y}) = c \exp \left\{ -\frac{1}{2(1-\rho^2)} \left( \left( \frac{y_1 - \mu_1}{\sigma_1} \right)^2 - 2\rho \left( \frac{y_1 - \mu_1}{\sigma_1} \right) \left( \frac{y_2 - \mu_2}{\sigma_2} \right) + \left( \frac{y_2 - \mu_2}{\sigma_2} \right)^2 \right) \right\},$$

with

$$c = \frac{1}{2\pi\sigma_1\sigma_2(1-\rho^2)^{1/2}}$$

and  $-\infty < (y_1, y_2) < \infty$ . Here  $\rho = \rho_{12} = \rho_{21}$  is the correlation between  $Y_1$  and  $Y_2$ . Now,

$$Y_1 | (Y_2 = y_2) \sim N\left(\mu_1 + \frac{\sigma_1}{\sigma_2}\rho(y_2 - \mu_2), \sigma_1^2(1-\rho^2)\right).$$

We often denote the distribution of  $\mathbf{Y}$  by

$$\mathbf{Y} \sim \text{MVN}_d(\boldsymbol{\mu}, \Sigma)$$

where  $\boldsymbol{\mu} = (\mu_1, \dots, \mu_d)^T$  is the vector of mean values of  $\mathbf{Y}$ , and  $\Sigma$  is the variance-covariance matrix of  $\mathbf{Y}$ . Note  $\text{MVN}_d$  denotes multivariate normal distribution of  $d$ -dimensions. When  $d = 2$  the notation is often simplified to

$$\mathbf{Y} \sim \text{BVN}(\boldsymbol{\mu}, \Sigma).$$

### A.3 The Probability Integral Transform

In studying dependence between variables, it helps to have all the variables following the same marginal distribution, as then marginal and dependence properties of the statistical models can be easily separated. However, in any problem the random variables cannot be expected to follow the same distribution, so some transformation is required before such an assumption can be made. In this section we give the transformation necessary to transform a random variable,  $Y$ , with distribution function,  $F(y)$ , to a random variable,  $T$ , with distribution function  $G(t)$ . The approach we use is the probability integral transform, which is a standard general approach to transformation of random variables. The transformation we use is

$$T = G^{-1}(F(Y)), \quad (\text{A.3.1})$$

where  $G^{-1}$  denotes the inverse of the function  $G$ . The transformed random variable  $T$  has distribution function  $G$ , since:

$$\begin{aligned} \Pr\{T \leq t\} &= \Pr\{G^{-1}(F(Y)) \leq t\} \\ &= \Pr\{F(Y) \leq G(t)\} \\ &= \Pr\{Y \leq F^{-1}[G(t)]\} \\ &= F(F^{-1}[G(t)]) \text{ as the distribution function of } Y \text{ is } F \\ &= G(t). \end{aligned}$$

### A.4 Likelihoods for Dependence Models

Here we give the likelihood function which is required in fitting the dependence models for significant wave height and still water level. The likelihood is the probability of the data for a given set of parameter values, regarded as a function of the parameters. As the data are independent pairs, the likelihood is a product of the likelihood contributions for the separate data pairs, hence we give only the likelihood contribution of a typical pair.

Throughout, we use the notation  $(X_1, X_2)$  to denote the pair of still water level and significant wave height variables in the original space, and  $(X_1^*, X_2^*)$  to denote these variables after each variable has been transformed to follow a standard Normal random variable, i.e. using equation (A.3.1) in Section A.3. We denote the distribution function of a univariate standard Normal random variable by  $\Phi(z)$ , i.e.

$$\Pr(X_1^* \leq z) = \Pr(X_2^* \leq z) = \Phi(z).$$

Similarly we let  $\Phi(z_1, z_2)$  denote the joint distribution of bivariate Normal variables, i.e. if  $(X_1^*, X_2^*)$  follow a bivariate Normal distribution, with joint density given by equation (A.2.1), then

$$\Pr(X_1^* \leq z_1, X_2^* \leq z_2) = \Phi(z_1, z_2).$$

### A.4.1 Bivariate Normal Model

The likelihood contribution for the observation  $(x_1^*, x_2^*)$  is

$$\frac{\partial^2 \Phi(x_1^*, x_2^*)}{\partial x_1^* \partial x_2^*} = \phi(x_1^*, x_2^*)$$

where  $\phi(x_1^*, x_2^*)$  is the joint density function of the bivariate Normal distribution with standard marginal distributions.

### A.4.2 Bivariate Normal Threshold Model

Under the threshold model described in Section 4.2.1, we have a full model for the joint distribution of observations having both variables above suitable thresholds, but otherwise have an incomplete model. As a consequence, points which have one or both marginal variable values below the respective threshold are censored at the threshold. Here we consider two cases, the first where the observations are of standard Normal random variables, i.e. observations of  $(X_1^*, X_2^*)$ , with thresholds  $(u_1^*, u_2^*)$ , and the second where  $(X_1, X_2)$  are observed, these being taken to have GPD marginals above thresholds  $(u_1, u_2)$ .

#### Normal Marginals

For an observation  $(x_1^*, x_2^*)$ , the likelihood can take one of four forms depending on whether the two thresholds are exceeded or not:

- If  $x_1^* \leq u_1^*$  and  $x_2^* \leq u_2^*$  then the likelihood contribution is

$$\Phi(u_1^*, u_2^*);$$

- If  $x_1^* > u_1^*$  and  $x_2^* \leq u_2^*$  then the likelihood contribution is

$$\frac{\partial \Phi(x_1^*, u_2^*)}{\partial x_1^*};$$

- If  $x_1^* \leq u_1^*$  and  $x_2^* > u_2^*$  then the likelihood contribution is

$$\frac{\partial \Phi(u_1^*, x_2^*)}{\partial x_2^*};$$

- If  $x_1^* > u_1^*$  and  $x_2^* > u_2^*$  then the likelihood contribution is

$$\phi(x_1^*, x_2^*).$$

### Original Marginals with GPD Tails

Consider  $X_i$  ( $i = 1, 2$ ) to be modelled by a GPD over suitable thresholds  $u_i$  ( $i = 1, 2$ ), so that the distribution function of  $X_i$  is taken to be

$$F_{X_i}(x_i) = 1 - \lambda_i \{1 + \xi_i(x_i - u_i)/\sigma_i\}_+^{-1/\xi_i}, \text{ for } x_i > u_i,$$

where  $\lambda_i = \Pr(X_i > u_i)$ , and  $\sigma_i > 0$ . Then for  $x_i > u_i$ , the marginal variables are transformed to normality through the probability integral transform (A.3.1), giving

$$X_i^* = \Phi^{-1}(F_{X_i}(X_i)) \text{ for } i = 1, 2,$$

and in particular,

$$u_i^* = \Phi^{-1}(F_{X_i}(u_i)) \text{ for } i = 1, 2,$$

represent the thresholds mapped onto the normal scale. For an observation  $(x_1, x_2)$  the likelihood can take one of four forms depending on whether the two thresholds are exceeded or not:

- If  $x_1 \leq u_1$  and  $x_2 \leq u_2$  then the likelihood contribution is

$$\Phi(u_1^*, u_2^*);$$

- If  $x_1 > u_1$  and  $x_2 \leq u_2$  then the likelihood contribution is

$$\frac{\partial \Phi(x_1^*, u_2^*)}{\partial x_1^*} \frac{dx_1^*}{dx_1},$$

- If  $x_1 \leq u_1$  and  $x_2 > u_2$  then the likelihood contribution is

$$\frac{\partial \Phi(u_1^*, x_2^*)}{\partial x_2^*} \frac{dx_2^*}{dx_2},$$

- If  $x_1 > u_1$  and  $x_2 > u_2$  then the likelihood contribution is

$$\phi(x_1^*, x_2^*) \frac{dx_1^*}{dx_1} \frac{dx_2^*}{dx_2}.$$

In the above expressions, for  $i = 1, 2$ ,

$$\frac{dx_i^*}{dx_i} = \frac{\lambda_i}{\phi(x_i^*)\sigma_i} \{1 + \xi_i(x_i - u_i)/\sigma_i\}_+^{-1-1/\xi_i}.$$

### A.4.3 Mixture of Bivariate Normals

Here the variables are taken to be modelled by standard Normal marginal random variables, but with dependence structure which arises from the mixture of two bivariate normal random variables. For the construction, we take  $\mathbf{T} = (T_1, T_2)$  to be a mixture of two bivariate normal random variables. We first construct the joint distribution function of  $\mathbf{T}$  and then, via marginal transformation of  $\mathbf{T}$ , obtain the joint distribution of  $\mathbf{T}^* = (T_1^*, T_2^*)$ , where the marginal distributions are standard normal random variables.

The vector random variable  $\mathbf{T}$  is defined by:

$$\mathbf{T} = \epsilon \mathbf{Z}_1 + (1 - \epsilon) \mathbf{Z}_2$$

i.e.

$$T_j = \epsilon Z_{1j} + (1 - \epsilon) Z_{2j} \text{ for } j = 1, 2$$

where

1.  $\epsilon = 0$  with probability  $1 - p_M$ , and  $\epsilon = 1$  with probability  $p_M$ ;
2.  $\mathbf{Z}_1 \sim \text{BVN}(\boldsymbol{\mu}_1, \Sigma_1)$  where  $\boldsymbol{\mu}_1 = (\mu_{11}, \mu_{12})$  and

$$\Sigma_1 = \begin{pmatrix} \sigma_{11}^2 & \rho_1 \sigma_{11} \sigma_{12} \\ \rho_1 \sigma_{11} \sigma_{12} & \sigma_{12}^2 \end{pmatrix};$$

3.  $\mathbf{Z}_2 \sim \text{BVN}(\boldsymbol{\mu}_2, \Sigma_2)$  where  $\boldsymbol{\mu}_2 = (\mu_{21}, \mu_{22})$  and

$$\Sigma_2 = \begin{pmatrix} \sigma_{21}^2 & \rho_2 \sigma_{21} \sigma_{22} \\ \rho_2 \sigma_{21} \sigma_{22} & \sigma_{22}^2 \end{pmatrix}.$$

It follows that the joint density function,  $f_{\mathbf{T}}$ , of  $\mathbf{T}$  is

$$f_{\mathbf{T}}(\mathbf{t}) = p_M f_{\mathbf{Z}_1}(\mathbf{t}) + (1 - p_M) f_{\mathbf{Z}_2}(\mathbf{t})$$

where  $f_{\mathbf{Z}_1}$  and  $f_{\mathbf{Z}_2}$  are the joint densities of  $\mathbf{Z}_1$  and  $\mathbf{Z}_2$  respectively.

We now derive the marginal distribution of  $T_j$  ( $j = 1, 2$ ). As

$$\Pr\{T_j \leq t\} = F_{T_j}(t) = p_M \Phi\left(\frac{t - \mu_{1j}}{\sigma_{1j}}\right) + (1 - p_M) \Phi\left(\frac{t - \mu_{2j}}{\sigma_{2j}}\right),$$

it follows that

$$T_j^* = \Phi^{-1}(F_{T_j}(T_j)) \text{ for } j = 1, 2$$

are standard normal random variables.

For likelihood calculations we now give the joint density of  $\mathbf{T}^* = (T_1^*, T_2^*)$ :

$$f_{\mathbf{T}^*}(\mathbf{t}^*) = \{f_{\mathbf{Z}_1}(t_1(t_1^*), t_2(t_2^*))p + f_{\mathbf{Z}_2}(t_1(t_1^*), t_2(t_2^*)) (1-p)\} \frac{\phi(t_1^*)\phi(t_2^*)}{f_{T_1}(t_1(t_1^*))f_{T_2}(t_2(t_2^*))}$$

where  $t_j(t_j^*) = F_{T_j}^{-1}(\Phi(t_j^*))$ .

In practice this statistical model is over-parametrised for statistical purposes. To avoid parameter redundancy we take

$$\boldsymbol{\mu}_1 = 0, \sigma_{11} = 1 \text{ and } \sigma_{12} = 1.$$

# List of Figures

3.1	Joint density contours for the bivariate logistic dependence structure when the marginal distributions are standard normal, i.e. $Z_i = \Phi^{-1}(\exp(-1/X_i))$ for $X_i$ a unit Fréchet variable and $i = 1, 2$ . The dependence parameter $\alpha = 1, 0.9, 0.8, 0.7, 0.5, 0.3$ . . . . .	38
3.2	Joint density contours for the bivariate normal dependence structure when the marginal distributions are standard normal, i.e. $Z_i = \Phi^{-1}(\exp(-1/X_i))$ for $X_i$ a unit Fréchet variable and $i = 1, 2$ . The dependence parameter $\rho = -0.5, -0.2, 0.0, 0.2, 0.5, 0.8$ . . . . .	39
4.1	Estimation of the distribution function of $T_Z$ at Christchurch: estimates from the empirical distribution of $T_Z$ , constant $S$ and independence of $(H_S, S)$ . . . . .	55
5.1	Cardiff observational data and Sim1 data: $H_S$ vs SWL . . . . .	78
5.2	Cardiff observational data and Sim1 data: $H_S$ vs $T_Z$ . . . . .	78
5.3	Cardiff observational data and Sim1 data: SWL vs $T_Z$ . . . . .	79
5.4	Cardiff observational data and Sim1 data: $H_S$ vs $\theta$ . . . . .	79
5.5	Cardiff observational data and Sim1 data: $T_Z$ vs $\theta$ . . . . .	80
5.6	Cardiff observational data: $H_S$ vs Surge . . . . .	80
5.7	Dover observational data and Sim2 data: $H_S$ vs SWL . . . . .	81
5.8	Dover observational data and Sim2 data: $H_S$ vs $T_Z$ . . . . .	81
5.9	Dover observational data and Sim3 data: SWL vs $T_Z$ . . . . .	82
5.10	Dover observational data: $H_S$ vs Surge . . . . .	82
5.11	North Wales observational data and Sim3 data: $H_S$ vs SWL . . . . .	83
5.12	North Wales observational data and Sim3 data: $H_S$ vs $T_Z$ . . . . .	83
5.13	North Wales observational data and Sim3 data: SWL vs $T_Z$ . . . . .	84
5.14	North Wales observational data and Sim3 data: $H_S$ vs Surge . . . . .	84
5.15	Christchurch observational data and Sim4 data: $H_S$ vs SWL . . . . .	85
5.16	Christchurch observational data and Sim4 data: $H_S$ vs $T_Z$ . . . . .	85
5.17	Christchurch observational data and Sim4 data: SWL vs $T_Z$ . . . . .	86

5.18	Christchurch observational data: $H_S$ vs Surge . . . . .	86
5.19	Dowsing observational data and Sim5 data: $H_S$ vs SWL . . . . .	87
5.20	Dowsing observational data and Sim5 data: $H_S$ vs $T_Z$ . . . . .	87
5.21	Dowsing observational data and Sim5 data: SWL vs $T_Z$ . . . . .	88
5.22	Dowsing observational data: $H_S$ vs Surge . . . . .	88
6.1	GPD shape parameter estimates versus the empirical distribution function calculated in $u$ for SWL data at Cardiff and Christchurch. Dots denote maximum likelihood estimates. Lines denote lower and upper bounds of the 95% confidence intervals. . . . .	91
6.2	GPD shape parameter estimates versus the empirical distribution function calculated in $u$ for SWL data at Dowsing and Shoreham. Dots denote maximum likelihood estimates. Lines denote lower and upper bounds of the 95% confidence intervals. . . . .	92
6.3	GPD shape parameter estimates versus the empirical distribution function calculated in $u$ for SWL data at North Wales and Dover. Dots denote maximum likelihood estimates. Lines denote lower and upper bounds of the 95% confidence intervals. . . . .	93
6.4	Probability and quantile plots for the GPD fitted to SWL data at Cardiff and North Wales. Also shown in each plot is the $x = y$ line. . . . .	94
6.5	GPD shape parameter estimates versus the empirical distribution function calculated in $u$ for Surge level data at Cardiff and Christchurch. Dots de- note maximum likelihood estimates. Lines denote lower and upper bounds of the 95% confidence intervals. . . . .	97
6.6	GPD shape parameter estimates versus the empirical distribution function calculated in $u$ for Surge level data at Dowsing and Shoreham. Dots denote maximum likelihood estimates. Lines denote lower and upper bounds of the 95% confidence intervals. . . . .	98
6.7	GPD shape parameter estimates versus the empirical distribution function calculated in $u$ for Surge level data at North Wales and Dover. Dots denote maximum likelihood estimates. Lines denote lower and upper bounds of the 95% confidence intervals. . . . .	99
6.8	Probability and quantile plots for the GPD fitted to Surge level data at Cardiff and Christchurch. Also shown in each plot is the $x = y$ line. . . . .	100
6.9	Probability and quantile plots for the Weibull distribution fitted to $H_S$ observations at Cardiff and Christchurch. Also shown in each plot is the $x = y$ line. . . . .	105

6.10	Probability and quantile plots for the Weibull distribution fitted to $H_S$ observations at Dowsing and Shoreham. Also shown in each plot is the $x = y$ line. . . . .	106
6.11	Probability and quantile plots for the Weibull distribution fitted to $H_S$ observations at North Wales and Dover. Also shown in each plot is the $x = y$ line. . . . .	107
6.12	Probability and quantile plots for the Truncated Weibull distribution fitted to $H_S$ exceedances at Cardiff and Christchurch. Also shown in each plot is the $x = y$ line. . . . .	108
6.13	Probability and quantile plots for the Truncated Weibull distribution fitted to $H_S$ exceedances at Dowsing and Shoreham. Also shown in each plot is the $x = y$ line. . . . .	109
6.14	Probability and quantile plots for the Truncated Weibull distribution fitted to $H_S$ exceedances at North Wales and Dover. Also shown in each plot is the $x = y$ line. . . . .	110
6.15	Probability and quantile plots for the GPD fitted to $H_S$ exceedances at Cardiff and Christchurch. Also shown in each plot is the $x = y$ line. . . . .	111
6.16	Probability and quantile plots for the GPD fitted to $H_S$ exceedances at Dowsing and Shoreham. Also shown in each plot is the $x = y$ line. . . . .	112
6.17	Probability and quantile plots for the GPD fitted to $H_S$ exceedances at North Wales and Dover. Also shown in each plot is the $x = y$ line. . . . .	113
6.18	Cardiff: Estimates of two extreme quantiles under the Weibull and the GPD models versus the empirical distribution function calculated in $u$ . . .	114
6.19	Christchurch: Estimates of two extreme quantiles under the Weibull and the GPD models versus the empirical distribution function calculated in $u$ . . .	115
6.20	Dowsing: Estimates of two extreme quantiles under the Weibull and the GPD models versus the empirical distribution function calculated in $u$ . . .	116
6.21	Shoreham: Estimates of two extreme quantiles under the Weibull and the GPD models versus the empirical distribution function calculated in $u$ . . .	117
6.22	North Wales: Estimates of two extreme quantiles under the Weibull and the GPD models versus the empirical distribution function calculated in $u$ . . .	118
6.23	Dover: Estimates of two extreme quantiles under the Weibull and the GPD models versus the empirical distribution function calculated in $u$ . . . . .	119
6.24	Histogram of Steepness at various sites. . . . .	122
6.25	Histogram of measured steepness at Morecambe, Boygrift and Lyme. . . . .	123
6.26	Histogram of Wave Direction at various sites. . . . .	125

- 7.1 Correlation function,  $\rho_u$ , between  $(H_S, SWL)$  versus the threshold (in probability of non-exceedance) for the different sites . . . . . 130
- 7.2 Correlation function,  $\rho_u$ , between  $(H_S, Surge)$  versus the threshold (in probability of non-exceedance) for the different sites . . . . . 130
- 7.3 Cardiff: Correlation function,  $\rho_u$ , between  $(H_S, SWL)$  versus the threshold (in probability of non-exceedance) separately for  $\theta < 190^\circ$  and  $\theta > 190^\circ$  . . 131
- 7.4 Cardiff: Correlation function,  $\rho_u$ , between  $(H_S, Surge)$  versus the threshold (in probability of non-exceedance) separately for  $\theta < 190^\circ$  and  $\theta > 190^\circ$  . . 131
- 7.5 Christchurch: Estimated correlation function,  $\rho_u$ , between  $(H_S, SWL)$  and  $(H_S, Surge)$  versus the threshold (in probability of non-exceedance) for the fitted mixture of bivariate normals and the threshold bivariate normal . . . 133
- 7.6 Dowsing: Estimated correlation function,  $\rho_u$ , between  $(H_S, SWL)$  and  $(H_S, Surge)$  versus the threshold (in probability of non-exceedance) for the fitted mixture of bivariate normals and the threshold bivariate normal . 133
- 7.7 Dover: Correlation function,  $\rho_u$ , between  $(H_S, SWL)$  and  $(H_S, Surge)$  versus the threshold (in probability of non-exceedance) for the fitted mixture of bivariate normals and the threshold bivariate normal . . . . . 134
- 7.8 North Wales: Estimated correlation function,  $\rho_u$ , between  $(H_S, SWL)$  and  $(H_S, Surge)$  versus the threshold (in probability of non-exceedance) for the fitted mixture of bivariate normals and the threshold bivariate normal . . . 134
- 7.9 Cardiff: Correlation function,  $\rho_u$ , between  $(H_S, SWL)$  and  $(H_S, Surge)$  versus the threshold (in probability of non-exceedance) for the fitted mixture of bivariate normals and the threshold bivariate normal . . . . . 135
- 7.10 Shoreham: Estimated correlation function,  $\rho_u$ , between  $(H_S, SWL)$  and  $(H_S, Surge)$  versus the threshold (in probability of non-exceedance) for the fitted mixture of bivariate normals and the threshold bivariate normal . 135
- 7.11 Sim1: Diagnostic test for the form of the dependence in the extremes of  $H_S$ - $SWL$ . The solid line is the test statistic and the dotted line its pointwise 95% confidence interval. . . . . 138
- 7.12 Sim2: Diagnostic test for the form of the dependence in the extremes of  $H_S$ - $SWL$ . The solid line is the test statistic and the dotted line its pointwise 95% confidence interval. . . . . 138
- 7.13 Sim3: Diagnostic test for the form of the dependence in the extremes of  $H_S$ - $SWL$ . The solid line is the test statistic and the dotted line its pointwise 95% confidence interval. . . . . 139

7.14	Sim4: Diagnostic test for the form of the dependence in the extremes of $H_S$ - $SWL$ . The solid line is the test statistic and the dotted line its pointwise 95% confidence interval. . . . .	139
7.15	Sim5: Diagnostic test for the form of the dependence in the extremes of $H_S$ - $SWL$ . The solid line is the test statistic and the dotted line its pointwise 95% confidence interval. . . . .	141
7.16	Correlation function, $\rho_u$ , between $(H_S, SWL)$ versus the threshold (in probability of non-exceedance) for the different simulated data sets. . . . .	142
7.17	Sim3: Correlation function, $\rho_u$ , between $(H_S, SWL)$ and $(H_S, Surge)$ versus the threshold (in probability of non-exceedance) . . . . .	142
7.18	Sim4: Correlation function, $\rho_u$ , between $(H_S, SWL)$ versus the threshold (in probability of non-exceedance) for the fitted mixture of bivariate normals and the threshold bivariate normal . . . . .	143
7.19	Sim5: Correlation function, $\rho_u$ , between $(H_S, SWL)$ versus the threshold (in probability of non-exceedance) for the fitted mixture of bivariate normals and the threshold bivariate normal . . . . .	143
7.20	Sim1 $H_S$ - $SWL$ joint density contours: the contours of joint density value 0.01, 0.001, 0.0001, 0.00001 are shown. The estimated model is the bivariate normal model. . . . .	144
7.21	Sim2 $H_S$ - $SWL$ joint density contours: the contours of joint density value 0.01, 0.001, 0.0001, 0.00001 are shown. The estimated model is the bivariate normal model. . . . .	144
7.22	Sim3 $H_S$ -Surge joint density contours: the contours of joint density value 0.01, 0.001, 0.0001, 0.00001 are shown. The estimated model is the bivariate normal model. . . . .	145
7.23	Sim3 $H_S$ - $SWL$ joint density contours: the contours of joint density value 0.01, 0.001, 0.0001, 0.00001 are shown. The estimated model is the bivariate normal model. . . . .	145
7.24	Sim4 $H_S$ - $SWL$ joint density contours: the contours of joint density value 0.01, 0.001, 0.0001, 0.00001 are shown. The estimated model is the threshold bivariate normal model. . . . .	146
7.25	Sim4 $H_S$ - $SWL$ joint density contours: the contours of joint density value 0.01, 0.001, 0.0001, 0.00001 are shown. The estimated model is the mixture of bivariate normals model. . . . .	146
7.26	Sim5 $H_S$ - $SWL$ joint density contours: the contours of joint density value 0.01, 0.001, 0.0001, 0.00001 are shown. The estimated model is the threshold bivariate normal model. . . . .	147

7.27	Sim5 $H_S$ - $SWL$ joint density contours: the contours of joint density value 0.01, 0.001, 0.0001, 0.00001 are shown. The estimated model is the mixture of bivariate normals model. . . . .	147
7.28	Sim1: $S$ versus $H_S$ and regression curve (plotted on the original scale). . .	150
7.29	Sim2: $S$ versus $H_S$ and regression curve (plotted on the original scale). . .	150
7.30	Sim3: $S$ versus $H_S$ and regression curve (plotted on the original scale). . .	151
7.31	Sim4: $S$ versus $H_S$ and regression curve (plotted on the original scale). . .	151
7.32	Sim5: $S$ versus $H_S$ and regression curve (plotted on the original scale). . .	152
7.33	Sim1: $S$ versus $H_S$ (plotted on the Gaussian scale). . . . .	152
7.34	Sim2: $S$ versus $H_S$ (plotted on the Gaussian scale). . . . .	153
7.35	Sim3: $S$ versus $H_S$ (plotted on the Gaussian scale). . . . .	153
7.36	Sim4: $S$ versus $H_S$ (plotted on the Gaussian scale). . . . .	154
7.37	Sim5: $S$ versus $H_S$ (plotted on the Gaussian scale). . . . .	154
7.38	Sim1: Mean and Variance of $S$ (on the Gaussian scale) versus threshold for $H_S$ (on the Gaussian scale). Dotted lines give 95% confidence interval. .	155
7.39	Sim2: Mean and Variance of $S$ (plotted on the Gaussian scale) versus threshold for $H_S$ (on the Gaussian scale). Dotted lines give 95% confidence interval. . . . .	155
7.40	Sim3: Mean and Variance of $S$ (plotted on the Gaussian scale) versus threshold for $H_S$ (on the Gaussian scale). Dotted lines give 95% confidence interval. . . . .	156
7.41	Sim4: Mean and Variance of $S$ (plotted on the Gaussian scale) versus threshold for $H_S$ (on the Gaussian scale). Dotted lines give 95% confidence interval. . . . .	156
7.42	Sim5: Mean and Variance of $S$ (plotted on the Gaussian scale) versus threshold for $H_S$ (on the Gaussian scale). Dotted lines give 95% confidence interval. . . . .	157
7.43	Sim1: $S$ versus $H_S$ for the original data and the data simulated from the fitted regression. . . . .	157
7.44	Sim2: $S$ versus $H_S$ for the original data and the data simulated from the fitted regression. . . . .	158
7.45	Sim3: $S$ versus $H_S$ for the original data and the data simulated from the fitted regression. . . . .	158
7.46	Sim4: $S$ versus $H_S$ for the original data and the data simulated from the fitted regression. . . . .	159
7.47	Sim5: $S$ versus $H_S$ for the original data and the data simulated from the fitted regression. . . . .	159

- 8.1 Sim1:  $H_S$ - $SWL$  curves of equal joint survivor probability expressed in return periods (in years) when the marginal distributions are known . . . . 166
- 8.2 Sim2:  $H_S$ - $SWL$  curves of equal joint survivor probability expressed in return periods (in years) when the marginal distributions are known . . . . 166
- 8.3 Sim3:  $H_S$ - $Surge$  curves of equal joint survivor probability expressed in return periods (in years) when the marginal distributions are known . . . . 167
- 8.4 Sim3:  $H_S$ - $SWL$  curves of equal joint survivor probability expressed in return periods (in years) when the marginal distributions are known . . . . 167
- 8.5 Sim4:  $H_S$ - $SWL$  curves of equal joint survivor probability expressed in return periods (in years) when the marginal distributions are known. Here the dependence model is the fitted bivariate normal threshold model . . . . 168
- 8.6 Sim4:  $H_S$ - $SWL$  curves of equal joint survivor probability expressed in return periods (in years) when the marginal distributions are known. Here the dependence model is the fitted mixture of bivariate normals model . . 168
- 8.7 Sim5:  $H_S$ - $SWL$  curves of equal joint survivor probability expressed in return periods (in years) when the marginal distributions are known. Here the dependence model is the fitted bivariate normal threshold model . . . . 169
- 8.8 Sim5:  $H_S$ - $SWL$  curves of equal joint survivor probability expressed in return periods (in years) when the marginal distributions are known. Here the dependence model is the fitted mixture of bivariate normals model . . 169
- 8.9 Sim2:  $H_S$ - $SWL$  curves of equal joint survivor probability expressed in return periods (in years) when the marginal distributions are known. Curves shown are 10 and 1000 year return period for Estimated model, Simulation model and HR estimates . . . . . 171
- 8.10 Sim3: $H_S$ - $SWL$  curves of equal joint survivor probability expressed in return periods (in years) when the marginal distributions are known. Curves shown are 10 and 1000 year return period for Estimated model, Simulation model and HR estimates . . . . . 171
- 8.11 Sim4:  $H_S$ - $SWL$  curves of equal joint survivor probability expressed in return periods (in years) when the marginal distributions are known. Curves shown are 10 and 1000 year return period for Estimated model (Mixture Model), Simulation model and HR estimates . . . . . 172
- 8.12 Sim5:  $H_S$ - $SWL$  curves of equal joint survivor probability expressed in return periods (in years) when the marginal distributions are known. Curves shown are 10 and 1000 year return period for Estimated model (Mixture Model), Simulation model and HR estimates . . . . . 172

8.13	Sim1: $H_S$ - $SWL$ curves of equal joint survivor probability expressed in return periods (in years) . . . . .	178
8.14	Sim2: $H_S$ - $SWL$ curves of equal joint survivor probability expressed in return periods (in years) . . . . .	178
8.15	Sim3: $H_S$ - $Surge$ curves of equal joint survivor probability expressed in return periods (in years) . . . . .	179
8.16	Sim3: $H_S$ - $SWL$ curves of equal joint survivor probability expressed in return periods (in years) . . . . .	179
8.17	Sim4: $H_S$ - $SWL$ curves of equal joint survivor probability expressed in return periods (in years) for the fitted bivariate normal threshold model . .	180
8.18	Sim4: $H_S$ - $SWL$ curves of equal joint survivor probability expressed in return periods (in years) for the fitted mixture of bivariate normals model .	180
8.19	Sim5: $H_S$ - $SWL$ curves of equal joint survivor probability expressed in return periods (in years) for the fitted bivariate normal threshold model . .	181
8.20	Sim5: $H_S$ - $SWL$ curves of equal joint survivor probability expressed in return periods (in years) for the fitted mixture of bivariate normals model .	181
9.1	Sim1 $Q_C$ 100 year return value for the SVM applied to $\log Q_C$ and the JPM based on the bivariate normal dependence model for $(SWL, H_S)$ . The threshold axis is related to applications of the SVM . . . . .	192
9.2	Sim2 $Q_C$ 100 year return value for the SVM applied to $Q_C$ and $\log Q_C$ and the JPM based on the bivariate normal dependence model for $(SWL, H_S)$ . The threshold axis is related to applications of the SVM . . . . .	195
9.3	Sim3 $Q_C$ 100 year return value for the SVM applied to $Q_C$ and $\log Q_C$ and the JPM based on the bivariate normal dependence model for $(SWL, H_S)$ . The threshold axis is related to applications of the SVM . . . . .	198
9.4	Sim4 $Q_C$ 100 year return value for the SVM applied to $Q_C$ and $\log Q_C$ and the JPM based on the bivariate normal dependence model for $(SWL, H_S)$ with estimated and known marginal parameters. The threshold axis is related to applications of the SVM . . . . .	202
9.5	Sim4 $Q_C$ 100 year return value for the SVM applied to $Q_C$ and $\log Q_C$ and the JPM based on the mixture of bivariate normals dependence model for $(SWL, H_S)$ with estimated and known marginal parameters. The threshold axis is related to applications of the SVM . . . . .	202
9.6	Sim5 $Q_C$ 100 year return value for the SVM applied to $Q_C$ and $\log Q_C$ and the JPM based on the bivariate normal dependence model for $(SWL, H_S)$ with estimated and known marginal parameters. The threshold axis is related to applications of the SVM . . . . .	205

- 9.7 Sim5  $Q_C$  100 year return value for the SVM applied to  $Q_C$  and  $\log Q_C$  and the JPM based on the mixture of bivariate normals dependence model for  $(SWL, H_S)$  with estimated and known marginal parameters. The threshold axis is related to applications of the SVM . . . . . 206
- 9.8 Sim1  $Q_C$  10 year return value for the SVM applied to  $\log Q_C$  and the JPM based on the bivariate normal dependence model for  $(SWL, H_S)$ . The threshold axis is related to applications of the SVM . . . . . 209
- 9.9 Sim1  $Q_C$  50 year return value for the SVM applied to  $\log Q_C$  and the JPM based on the bivariate normal dependence model for  $(SWL, H_S)$ . The threshold axis is related to applications of the SVM . . . . . 209
- 9.10 Sim2  $Q_C$  10 year return value for the SVM applied to  $Q_C$  and  $\log Q_C$  and the JPM based on the bivariate normal dependence model for  $(SWL, H_S)$ . The threshold axis is related to applications of the SVM . . . . . 210
- 9.11 Sim2  $Q_C$  50 year return value for the SVM applied to  $Q_C$  and  $\log Q_C$  and the JPM based on the bivariate normal dependence model for  $(SWL, H_S)$ . The threshold axis is related to applications of the SVM . . . . . 210
- 9.12 Sim3  $Q_C$  10 year return value for the SVM applied to  $Q_C$  and  $\log Q_C$  and the JPM based on the bivariate normal dependence model for  $(SWL, H_S)$ . The threshold axis is related to applications of the SVM . . . . . 211
- 9.13 Sim3  $Q_C$  50 year return value for the SVM applied to  $Q_C$  and  $\log Q_C$  and the JPM based on the bivariate normal dependence model for  $(SWL, H_S)$ . The threshold axis is related to applications of the SVM . . . . . 211
- 9.14 Sim4  $Q_C$  10 year return value for the SVM applied to  $Q_C$  and  $\log Q_C$  and the JPM based on the bivariate normal dependence model for  $(SWL, H_S)$  with estimated and known marginal parameters. The threshold axis is related to applications of the SVM . . . . . 212
- 9.15 Sim4  $Q_C$  10 year return value for the SVM applied to  $Q_C$  and  $\log Q_C$  and the JPM based on the mixture of bivariate normals dependence model for  $(SWL, H_S)$  with estimated and known marginal parameters. The threshold axis is related to applications of the SVM . . . . . 212
- 9.16 Sim4  $Q_C$  50 year return value for the SVM applied to  $Q_C$  and  $\log Q_C$  and the JPM based on the bivariate normal dependence model for  $(SWL, H_S)$  with estimated and known marginal parameters. The threshold axis is related to applications of the SVM . . . . . 213

- 9.17 Sim4  $Q_C$  50 year return value for the SVM applied to  $Q_C$  and  $\log Q_C$  and the JPM based on the mixture of bivariate normals dependence model for  $(SWL, H_S)$  with estimated and known marginal parameters. The threshold axis is related to applications of the SVM . . . . . 213
- 9.18 Sim5  $Q_C$  10 year return value for the SVM applied to  $Q_C$  and  $\log Q_C$  and the JPM based on the bivariate normal dependence model for  $(SWL, H_S)$  with estimated and known marginal parameters. The threshold axis is related to applications of the SVM . . . . . 214
- 9.19 Sim5  $Q_C$  10 year return value for the SVM applied to  $Q_C$  and  $\log Q_C$  and the JPM based on the mixture of bivariate normals dependence model for  $(SWL, H_S)$  with estimated and known marginal parameters. The threshold axis is related to applications of the SVM . . . . . 214
- 9.20 Sim5  $Q_C$  50 year return value for the SVM applied to  $Q_C$  and  $\log Q_C$  and the JPM based on the bivariate normal dependence model for  $(SWL, H_S)$  with estimated and known marginal parameters. The threshold axis is related to applications of the SVM . . . . . 215
- 9.21 Sim5  $Q_C$  50 year return value for the SVM applied to  $Q_C$  and  $\log Q_C$  and the JPM based on the mixture of bivariate normals dependence model for  $(SWL, H_S)$  with estimated and known marginal parameters. The threshold axis is related to applications of the SVM . . . . . 215

# List of Tables

4.1	Results from simulating 10000 samples of size 6000 from a Weibull distribution with known parameters $a = 0$ , $b = 1$ and $c = 1.2$ . . . . .	49
4.2	Results from simulating 10000 samples of size 6000 from a Weibull distribution with known parameters $a = 0$ , $b = 1$ and $c = 1.5$ . . . . .	49
4.3	Results from simulating 10000 samples of size 6000 from a Weibull distribution with known parameters $a = 0$ , $b = 1$ and $c = 1.7$ . . . . .	49
4.4	Results from simulating 10000 samples of size 6000 from a Weibull distribution with known parameters $a = 0$ , $b = 1$ and $c = 0.7$ . . . . .	50
5.1	Information about the observational data sites: SWL – still water level, Waves – significant wave height, wave period, wave direction. . . . .	70
5.2	Differences in the statistical models for the simulated data sets Sim1-Sim5. . . . .	75
6.1	Maximum likelihood estimates of the parameters of the GPD fitted to <i>SWL</i> data at observation sites (standard errors in parentheses). . . . .	90
6.2	Maximum likelihood estimates of the parameters of the GPD fitted to <i>SWL</i> simulated for the synthetic data sets (standard errors in parentheses). . . . .	95
6.3	Maximum likelihood estimates of the parameters of the GPD fitted to Surge level data at various sites (standard errors in parentheses). . . . .	96
6.4	Maximum likelihood estimates of the parameters of the GPD fitted to simulated Surge level data (standard errors in parentheses). . . . .	101
6.5	Maximum likelihood estimates of the parameters of the Weibull distribution fitted to $H_S$ observations at various sites (standard errors in parentheses). . . . .	103
6.6	Maximum likelihood estimates of the parameters of the Truncated Weibull distribution fitted to $H_S$ exceedances at various sites (standard errors in parentheses). . . . .	104
6.7	Maximum likelihood estimates of the parameters of the GPD fitted to $H_S$ exceedances at various sites (standard errors in parentheses). . . . .	104

6.8	Maximum likelihood estimates of the parameters of the GPD fitted to simulated $H_S$ threshold exceedances for the synthetic data sets (standard errors in parentheses). . . . .	120
7.1	Parameter estimates for the mixture of bivariate normals applied to observational $(H_S, SWL)$ data. . . . .	132
7.2	Parameter estimates for the mixture of bivariate normals applied to observational $(H_S, Surge)$ data. . . . .	132
7.3	Parameter estimates for the mixture of bivariate normals applied to the simulated $(H_S, SWL)$ data and for Sim3* to $(H_S, Surge)$ . . . . .	141
7.4	Parameter estimates for the linear regression of $S^*$ on $H_S^*$ applied above a threshold $u$ (on the Gaussian scale). Standard errors are given in parentheses. For Sim4 and Sim5 the value of $u$ used in the regression model is $u = 0$ . . . . .	149
8.1	HR estimates of points on the 10 and 1000 year contours of the joint survivor function of $(SWL, H_S)$ for Sim1: separate estimates conditional on the wave direction, $\theta$ , satisfying $0^\circ \leq \theta \leq 110^\circ$ and $110^\circ < \theta < 360^\circ$ . . . . .	173
8.2	HR estimates of points on the 10 and 1000 year contours of the joint survivor function of $(SWL, H_S)$ for Sim2, when the marginal distributions are known. . . . .	173
8.3	HR estimates of points on the 10 and 1000 year contours of the joint survivor function of $(SWL, H_S)$ for Sim3, when the marginal distributions are known. . . . .	174
8.4	HR estimates of points on the 10 and 1000 year contours of the joint survivor function of $(SWL, H_S)$ for Sim4, when the marginal distributions are known. . . . .	174
8.5	HR estimates of points on the 10 and 1000 year contours of the joint survivor function of $(SWL, H_S)$ for Sim5, when the marginal distributions are known. . . . .	175
8.6	HR estimates of points on the 10 year contour of the joint survivor function for Sim1: separate estimates conditional on the wave direction, $\theta$ , satisfying $0^\circ \leq \theta \leq 190^\circ$ and $190^\circ < \theta \leq 270^\circ$ . . . . .	183
8.7	HR estimates of points on the 10 year contour of the joint survivor function for Sim2. . . . .	183
8.8	HR estimates of points on the 10 year contour of the joint survivor function for Sim3. . . . .	183

8.9	HR estimates of points on the 10 year contour of the joint survivor function for Sim4. . . . .	184
8.10	HR estimates of points on the 10 year contour of the joint survivor function for Sim5. . . . .	184
9.1	Information on the structural design for the simulated data. Here the sea-wall is a simple sloping wall with a 1:4 slope, $a_1$ and $a_2$ dimensionless constants and $v$ is the crest elevation in metres (relative to ODN except for Sim3 and Sim5 which are relative to Chart Datum). See equation (1.1.1) for details of how these design parameters influence overtopping discharge rates. . . . .	188
9.2	The largest five sea condition values for Sim1 in terms of the structure function, overtopping discharge rate $Q_C$ given by equation (1.1.1). Here $SWL$ is in terms of metres relative to ODN, $H_S$ is in metres, and $T_Z$ in secs. Overtopping discharge rate, $Q_C$ , is in $\text{metre}^3/\text{sec}/\text{metre}$ . . . . .	191
9.3	Sim1: Return levels for $Q_C$ (in $\text{metre}^3/\text{sec}/\text{metre}$ ) from simulation model. .	192
9.4	The largest five sea condition values for Sim2 in terms of the structure function, overtopping discharge rate $Q_C$ given by equation (1.1.1). Here $SWL$ is in terms of metres relative to ODN, $H_S$ is in metres, and $T_Z$ in secs. Overtopping discharge rate, $Q_C$ , is in $\text{metre}^3/\text{sec}/\text{metre}$ . . . . .	194
9.5	Sim2: Return levels for $Q_C$ (in $\text{metre}^3/\text{sec}/\text{metre}$ ) from simulation model. .	195
9.6	The largest five sea condition values for Sim3 in terms of the structure function, overtopping discharge rate $Q_C$ given by equation (1.1.1). Here $SWL$ is in terms of metres relative to ODN, $H_S$ is in metres, and $T_Z$ in secs. Overtopping discharge rate, $Q_C$ , is in $\text{metre}^3/\text{sec}/\text{metre}$ . . . . .	197
9.7	Sim3: Return levels for $Q_C$ (in $\text{metre}^3/\text{sec}/\text{metre}$ ) from simulation model. .	197
9.8	The largest five sea condition values for Sim4 in terms of the structure function, overtopping discharge rate $Q_C$ given by equation (1.1.1). Here $SWL$ is in terms of metres relative to ODN, $H_S$ is in metres, and $T_Z$ in secs. Overtopping discharge rate, $Q_C$ , is in $\text{metre}^3/\text{sec}/\text{metre}$ . . . . .	201
9.9	Sim4: Return levels for $Q_C$ (in $\text{metre}^3/\text{sec}/\text{metre}$ ) from simulation model. .	201
9.10	The largest five sea condition values for Sim5 in terms of the structure function, overtopping discharge rate $Q_C$ given by equation (1.1.1). Here $SWL$ is in terms of metres relative to ODN, $H_S$ is in metres, and $T_Z$ in secs. Overtopping discharge rate, $Q_C$ , is in $\text{metre}^3/\text{sec}/\text{metre}$ . . . . .	204
9.11	Sim5: Return levels for $Q_C$ (in $\text{metre}^3/\text{sec}/\text{metre}$ ) from simulation model. .	205

- 9.12 Actual return period of design levels estimated by the current implementation (basic level) of the JPM: for  $S = 0.06$  and when  $S$  is derived from the data. For Sim1 these results correspond to the dominant direction. Owing to the dominance of wave period for Sim4 and Sim5 these estimates should be largely ignored. . . . . 208
- 9.13 Estimated 10 year return levels for  $Q_C$  obtained using estimated and known marginals via the current implementation (basic level) of the JPM. For Sim1 ( $S = 0.06$ ) these results correspond to the dominant direction, whereas for derived  $S$  each direction sector is given. . . . . 208